Cape Peninsula
University of Technology

ADVANCED OXIDATION PROCESS USING OZONE/HETEROGENEOUS CATALYSIS FOR THE DEGRADATION OF PHENOLIC COMPOUNDS (CHLOROPHENOLS) IN AQUEOUS SYSTEM

by

OPUTU OGHENEOCHUKO UTIEYIN

Dissertation submitted in partial fulfilment of the requirements for the degree

Doctor of Philosophy: **Chemistry**

in the Faculty of **Applied Sciences**

at the Cape Peninsula University of Technology

Supervisor: **Professor Fatoki OS**

Cape Town
Date submitted (October 2016)

DECLARATION

I, Ogheneochuko, Utieyin Oputu, declare that the contents of this dissertation/thesis represent my own unaided work, and that the dissertation/thesis has not previously been submitted for academic examination towards any qualification. Furthermore, it represents my own opinions and not necessarily those of the Cape Peninsula University of Technology.

Signed **Date**

ABSTRACT

The use of ozone as an advanced oxidation process is gathering wide spread attention with the major limitation to its application being its cost of operation and design considerations. While the general approach of most researches is to buttress the already known fact of the efficacy of the process, little attention is given to studying the by-products of ozone reactions with organics. The aims of this study were to investigate the efficacy of the ozonation process for removing recalcitrant phenolics: phenol, 2-chlorophenol (2CP), 4-chlorophenol (4CP) and 2,4-dichloropheno (2,4DCP) from aqueous medium with a view of understanding various reaction pathways of the process and identifying possible intermediates and residual compounds using liquid chromatography-mass spectrometry (LC-MS). The choice of the selected chlorophenols would also elucidate the role of the positioning of the chlorine atoms in determining reaction rates, pathways and subsequent mechanisms and by-products. Sequel to this, oxy-hydroxy iron in β-phase (β-FeOOH, akaganite) and various β-FeOOH bonded composites on support metal oxides (Al_2O_3, NiO and TiO_2) were prepared via hetero-junction joining, and explored as a possible promoter to improve the efficiency of the ozonation process. Apparent first order reaction rates constants of tested phenolics was in the order 2,4-DCP > 2-CP > Phenol > 4-CP, irrespective of the tested pH. The individual rates however increased with increasing pH. The position 4 chlorine atom was found to be least susceptible to hydroxylative dechlorination. Catechol intermediate and pathway was identified as the major degradation pathway for phenol and 2-CP, while 4-chlorocatechol pathways were more important for 4-CP and 2,4-DCP. The formation of polymeric dimers and trimers by all compounds was pronounced at alkaline pH. Heterogeneous catalytic ozonation using β-FeOOH reduced ozonation time for 4-CP by 32%. Mechanism for β-FeOOH/ozone catalysis showed that the catalyst suffered reductive dissolution in acidic pH and the kinetics of 4-CP removal using the catalyst was best described using a two stage kinetic model. The first stage was attributed to heterogeneous catalysis of ozone breakdown on β-FeOOH surface generating faster reacting radicals, while the second stage was due to homogeneous catalysis by reduced Fe^{2+} ions in solution. β-FeOOH stabilized on NiO at a 5% ratio exhibited superior catalytic property compared to the other tested composites. Characterization by high-resolution transmission electron microscopy (HRTEM) affirmed a β-FeOOH-NiO bonded interfaced composite which was stable as a

catalyst over four (4) recycle runs. The mechanism of operation of the composite was via an increased ozone breakdown to radicals as monitored via photoluminescence experiments. The composite material produced satisfactory results when tested on real wastewater samples. Results from this study contribute to the current understanding on reaction mechanisms for ozone with phenols and chlorophenols, for the first time monitoring time captured intermediates via liquid chromatography-mass spectrometric method, which preserves the integrity of reaction intermediates. Also this study proposes heterogeneous catalysts; β-FeOOH and β-FeOOH bonded composites as possible improvements for simple ozone based water purification systems.

ACKNOWLEDGEMENTS

I wish to thank:

- Fatoki Olalekan Siyanbola, its rare to find such an accommodating supervisor ever so willing to follow research wherever it goes.
- Ximba Bhekumusa Jubulani, who patiently listened to me even when I knew absolutely nothing.
- Jonnalagadda, SB, who made sure things were kept simple.
- Adekola Folahan, your time spend in designing a working plan did not go to waste.
- Wicht Merril, your early decisions on instrumentation is not forgotten.
- Hugo Victor, 'Its research, just bite the bullet', he said; and now comes the end.
- Marshall Lona, from orders to working protocols, she had all things covered.
- Kucich Daniella, who made sure I got any laboratory help I needed.
- Chowdhury Mahabubur Fahaad, research is a strange thing. Friends are often needed to point out facts that are right there before your eyes.
- Nyamayaro Kudzi, protocols are easy to follow if you are brilliant. Making your own protocols and following them requires a spark of genius.
- Kamanda, Sosthene and Awongo Aliwa, two hard working students who stirred up motivation, synthesizing compounds through weekends and holidays.
- Kok David, your knowledge and experience on the LC-MS is difficult to overlook.
- Zide Dorcas, who kept the organic structures flowing and the coffee mug full.
- Chansa Jenny, behind a pretty thesis is a pretty face. Your proficiency at COD measurements is baffling.
- Olatunji Olatunde Stephen, this thesis is based on your writing plan.
- Olujimi Olarenwaji Olusoji, simple words of encouragements mean a lot.
- My Mother Oputu Margaret Boyowa, your prayers were eventually answered.
- My siblings, Oputu Akpevweoghene Alero, Oputu Otaokpakovwe Eyefujirin, Oputu Oghenenyerhovwo Sisanwunmi and Oputu Eguonor Omamuli. I am eternally grateful for your support and confidence.
- My dear friend, Aghoghovia Onoriode Philip, who was excellent company when research was down.
- To many others too numerous to mention, laboratory colleagues, station mates, friends, bishops pointing at f7 and rooks holding down the back ranks, I thank you all.

DEDICATION

To my dad Senior Apostle Israel Ejaeta Oputu

RSC Advances

PAPER

View Article Online
View Journal | View Issue

Cite this: *RSC Adv.*, 2015, **5**, 59513

A novel β-FeOOH/NiO composite material as a potential catalyst for catalytic ozonation degradation of 4-chlorophenol†

Ogheneochuko Oputu[a] Mahabubur Chowdhury,*[b] Kudzanai Nyamayaro,[a] Franscious Cummings,[c] Veruscha Fester[a] and Olalekan Fatoki[b]

In this study we report on the organic linker mediated fabrication and catalytic activity of a novel β-FeOOH/NiO composite material for the first time. Four-chlorophenol (4-CP) was used as a target molecule to evaluate the catalytic activity of the composite material in ozonation reactions. Three different β-FeOOH loadings, labelled 2, 5 and 10% β-FeOOH/NiO composites were prepared. The 5% β-FeOOH/NiO composite material showed the highest activity in the composite structure. XRD, FTIR and TEM were used to characterise the composite structure. Evidence of a chemically bonded interface between β-FeOOH and NiO was apparent from the FTIR and TEM results. Adsorption of 4-CP on the catalyst surface was found to be negligible. First order reaction kinetics were used to describe the 4-CP degradation behaviour and the rate constants increased with increasing initial pH of the solution. No detectable amount of both Fe and Ni leaching into the solution was observed at a pH range of 10–2.3. After 20 min of the ozonation reaction, 85% of 4-CP was removed by the heterogeneous system as opposed to 47% by ozonation alone. The developed composite material exhibited good recyclability as the catalytic activity of the material could be recovered by calcination after use. A maximum of 66% of COD was removed just after 50 min of the catalytic ozonation reaction. The enhanced catalytic activity of the composite material was due to higher generation of OH˙ which was supported by photoluminescence (PL) experiments.

Received 16th May 2015
Accepted 2nd July 2015

DOI: 10.1039/c5ra09177b

www.rsc.org/advances

1. Introduction

The use of ozone as a chemical oxidant for organics in water has gathered wide spread research interest due to its stronger oxidizing power when compared to the more common chlorination and its avoidance of chlorinated by-products such as chloromethanes. The industrial application of ozone for large-scale water treatment still faces certain problems; ozone oxidation is selective, and requires being produced *in situ via* an expensive process. Also, recent work has shown that ozonation in the presence of bromine produces brominated by-products.[1] The conversion of ozone to unselective OH˙ gives better results for oxidation of organics, as the oxidizing power of OH˙ is higher than that of ozone. Research projects have therefore been geared towards the efficient conversion of ozone to OH˙ for application in water purification processes. Methods for achieving this objective includes, UV based break down of ozone to OH˙, application of ozone under high pH conditions, combining ozone with hydrogen peroxide and application of ozone in the presence of transition metal ions such as Fe^{2+} and Mn^{2+} to produce OH˙. While the application of metal ions and peroxide introduces unrecoverable reagents consumed in the reaction process, the use of UV for ozone breakdown incurs additional cost to the water purification process. The use of heterogeneous catalyst offers an advantage over aforementioned processes, in that the ozone breakdown to OH˙ is *via* surface reaction mechanisms and therefore the catalyst can be recovered and recycled. Various metal oxides and metal oxides on metal oxide-supports surfaces such as; TiO_2, MnO_2, Al_2O_3, $Cu–Al_2O_3$, $Cu–TiO_2$, $Ru–CeO_2$, VO/TiO_2, VO–silica gel, $TiO_2–Al_2O_3$, $ZnAl_2O_4$ and Fe_2O_3/Al_2O_3 have been used to break down ozone to generate OH˙.[2–5]

Iron is an earth abundant material and has been recommended as a catalyst amongst many others. Many reports have been published that used iron based catalyst in ozonation process to remove various organic compounds, *i.e.* phenol, aniline, carboxylic acids, chlorobenzene, chlorophenols, dyes or natural organic matter.[6–10] Very little attention has been given towards iron oxy hydroxide materials despite their low toxicity and cheap and simple synthesis procedure. Catalytic properties

[a]Department of Chemistry, Cape Peninsula University of Technology, Republic of South Africa

[b]Flow Process Research Centre, Cape Peninsula University of Technology, Republic of South Africa. E-mail: chowdhurym@cput.ac.za

[c]Electron Microscope Unit, University of the Western Cape, Republic of South Africa

† Electronic supplementary information (ESI) available. See DOI: 10.1039/c5ra09177b

JOURNAL OF ENVIRONMENTAL SCIENCES 35 (2015) 83–90

Available online at www.sciencedirect.com

ScienceDirect

www.journals.elsevier.com/journal-of-environmental-sciences

JOURNAL OF ENVIRONMENTAL SCIENCES
www.jesc.ac.cn

Catalytic activities of ultra-small β-FeOOH nanorods in ozonation of 4-chlorophenol

Ogheneochuko Oputu[1], *Mahabubur Chowdhury*[2,*], *Kudzanai Nyamayaro*[1], *Olalekan Fatoki*[1], *Veruscha Fester*[2]

1. *Department of Chemistry, Cape Peninsula University of Technology, South Africa*
2. *Flow Process and Rheology Centre, Cape Peninsula University of Technology, South Africa*

ARTICLE INFO

Article history:
Received 25 November 2014
Revised 6 February 2015
Accepted 27 February 2015
Available online 15 June 2015

Keywords:
Ultra-small β-FeOOH
Heterogeneous–homogeneous catalysis
Catalytic ozonation
Waste water treatment

ABSTRACT

We report the catalytic properties of ultra-small β-FeOOH nanorods in ozonation of 4-chlorophenol (4-CP). XRD, TEM, EDS, SAED, FTIR and BET were used to characterize the prepared material. Interaction between O_3 and β-FeOOH was evident from the FTIR spectra. The removal efficiency of 4-CP was significantly enhanced in the presence of β-FeOOH compared to ozone alone. Removal efficiency of 99% and 67% was achieved after 40 min in the presence of combined ozone and catalyst and ozone only, respectively. Increasing catalyst load increased COD removal efficiency. Maximum COD removal of 97% was achieved using a catalyst load of 0.1 g/100 mL of 4-CP solution. Initial 4-CP concentration was not found to be rate limiting below 2×10^{-3} mol/L. The catalytic properties of the material during ozonation process were found to be pronounced at lower initial pH of 3.5. Two stage first order kinetics was applied to describe the kinetic behavior of the nanorods at low pH. The first stage of catalytic ozonation was attributed to the heterogeneous surface breakdown of O_3 by β-FeOOH, while the second stage was attributed to homogeneous catalysis initiated by reductive dissolution of β-FeOOH at low pH.

Introduction

Oxidation processes such as biological, chemical and physical are major steps during water treatment. In theory, chemical oxidation processes overcome some of the drawbacks of the physical and biological processes; however, as reported in several researches, they do not bring about complete mineralization of water pollutants (Kasprzyk-Hordern et al., 2003). Wide application of ozone as a chemical oxidant to mineralize organic compounds can be found in the literature (Zhao et al., 2008; Wen et al., 2012; Gonçalves et al., 2012; Marques et al., 2013). Catalytic ozonation is speculated to be a promising method for being environment friendly and its high effectiveness (Ma et al., 2014). Catalytic ozonation using metal oxides and metal oxides on metal oxide-supports, such as TiO_2, MnO_2, Al_2O_3, Cu-Al_2O_3, Cu–TiO_2, Ru–CeO_2, VO/TiO_2, VO-silica gel, TiO_2–Al_2O_3 and Fe_2O_3/Al_2O_3, have been reported (Kasprzyk-Hordern et al., 2003; Qi et al., 2013). However, very little attention has been given toward iron oxy hydroxide materials despite their low toxicity and cost as well as the simple synthesis procedure. Catalytic properties of FeOOH based materials, such as α-FeOOH (Park et al., 2004) and γ-FeOOH (Chou and Huang, 1999), have been reported before in the presence of H_2O_2 (Nie et al., 2014). Catalytic ozonation of nitrobenzene has been reported using α-FeOOH and β-FeOOH. Application of β-FeOOH/Al_2O_3 was reported in the degradation of pharmaceuticals (Yang et al., 2010) and also the inhibition of bromate formation (Nie et al., 2014). In both

* *Corresponding author*. E-mail: chowdhurym@cput.ac.za (Mahabubur Chowdhury).

http://dx.doi.org/10.1016/j.jes.2015.02.013
1001-0742/

Current citations: 6

Water Treatment Technologies: Principles, Applications, Successes and Limitations of Bioremediation, Membrane Bioreactor and the Advanced Oxidation Processes

Ogheneochuko U. Oputu[1], Olushola S. Ayanda[2*], Olalekan O. Fatoki[1], Cecilia O. Akintayo[2], Emmanuel G. Olumayede[2], and Olusola Solomon Amodu[3]

[1]Department of Chemistry, Faculty of Applied Sciences, Cape Peninsula University of Technology, P.O. Box 962, Cape Town, South Africa

[2]Environmental and Nanoscience Research, Department of Industrial Chemistry, Federal University Oye Ekiti, P.M.B 373, Oye Ekiti, Ekiti State, Nigeria

[3]Department of Chemical Engineering, Lagos State Polytechnic, P.M.B 21606, Ikorodu, Lagos, Nigeria

[*]**Corresponding author:** *Olushola S. Ayanda, Environmental and Nanoscience Research, Department of Industrial Chemistry, Federal University Oye Ekiti, P.M.B 373, Oye Ekiti, Ekiti State, Nigeria, Tel.: +2348054642362; E-mail: osayanda@gmail.com

Abstract

The release and accumulation of organic and inorganic pollutants in the environment by natural and anthropogenic sources have led to serious environmental problems; this subsequently results to adverse effects on human health and wildlife. Therefore, to prevent the harmful effects of environmental contaminants, the development of newer and/or combined technologies for the remediation of contaminated water and wastewaters has been of great importance. This book presents bioremediation, membrane bioreactor and the Advanced Oxidation Processes (AOPs) as other forms of water and wastewater treatment technologies. Bioremediation and membrane bioreactor are ecofriendly, effective and cheap methods of detoxification. The AOPs have also emerged as a set of versatile water and wastewater treatment techniques. AOPs have been widely applied for the removal of a wide range of contaminants including pharmaceuticals, dyes, surfactants, pesticides, herbicides, disinfection by-products, endocrine disrupting chemicals etc. However, there are still ongoing investigation on the impact of the oxidants used, nanoparticles/catalysts, and resultant metabolites on human health and the environment.

Keywords: Advanced Oxidation Processes, Bioremediation, catalysis, nanotechnology, phytoremediation, membrane bioreactor, sonolysis

Introduction

In the last three decades, concerns about environmental pollution have increased around

ACADEMIC OUTPUTS OF RESEARCH REPORTED IN THIS THESIS

Published papers

OPUTU, O., CHOWDHURY, M., NYAMAYARO, K., FATOKI, O. & FESTER, V. 2015. Catalytic activities of ultra-small β-FeOOH nanorods in ozonation of 4-chlorophenol. *Journal of Environmental Sciences,* 35**,** 83-90.

OPUTU, O., CHOWDHURY, M., NYAMAYARO, K., CUMMINGS, F., FESTER, V. & FATOKI, O. 2015. A novel β-FeOOH/NiO composite material as a potential catalyst for catalytic ozonation degradation of 4-chlorophenol. *RSC Advances,* 5**,** 59513-59521.

Books

OPUTU, O. U., AYANDA, O. S., FATOKI, O. S., AKINTAYO, C. O., OLUMAYEDE, E. G. & AMODU, O. S. 2015. Water Treatment Technologies: Principles, Applications, Successes and Limitations of Bioremediation, Membrane Bioreactor and the Advanced Oxidation Processes. *In:* AYANDA, O. S. (ed.). OMICS ebooks group.

Oral Presentations

FATOKI, O. S., OPUTU, O. U. Novel β-FeOOH/NiO composite as possible catalyst in ozonation of organics: An advanced oxidation process (AOP). 7th Society of Environmental Toxicology and Chemistry (SETAC) Africa Conference, Langebaan, South Africa. 5-7 October, 2015.

FATOKI, O. S., OPUTU, O. U. Akaganite (β-FeOOH) promoted heterogeneous-homogeneous catalytic ozonation of 4-chlorophenol. PITTCON Confrence and Exposition, Pensylvenia, USA. 9-12 March 2015.

Poster Presentations

OPUTU, O., CHOWDHURY, M., NYAMAYARO, K., CUMMINGS, F., FESTER, V. & FATOKI, O. Novel β-FeOOH/NiO composite material as potential catalyst for

ozonation of organics. 7th Society of Environmental Toxicology and Chemistry (SETAC) Africa Conference, Langebaan, South Africa. 5-7 October, 2015.

TABLE OF CONTENTS

DECLARATION ..... **II**

ABSTRACT ..... **III**

ACKNOWLEDGEMENTS ..... **V**

DEDICATION ..... **VI**

RESEARCH ARTICLE 1 ..... **VII**

RESEARCH ARTICLE 2 ..... **VIII**

PUBLISHED E-BOOK ..... **IX**

ACADEMIC OUTPUTS OF RESEARCH REPORTED IN THIS THESIS ..... **X**

TABLE OF CONTENTS ..... **XII**

CHAPTER ONE **1**

1. INTRODCUTION **1**

1.1. BACKGROUND 1

1.2. PROBLEM STATEMENTS 4

1.3. PURPOSE STATEMENT 5

1.4. OBJECTIVES OF THE RESEARCH 5

1.4.1. Main Objectives 5

1.4.2. Specific Objectives 5

1.5. SIGNIFICANCE OF THE RESEARCH 6

1.6. LIMITATIONS OF THE STUDY 6

1.7. INSTRUMENT EMPLOYED 6

1.7.1. Data Analysis and Findings 7

CHAPTER TWO **8**

2. LITERATURE REVIEW **8**

2.1. PHENOLS AND CHLOROPHENOLS 8

2.1.1. Phenol 8

2.1.2. 2-chlorophenol 9
2.1.3. 4-chlorophenol 9
2.1.4. 2,4-dichlorophenol 9
2.1.5. Summary on the phenols 10
2.2. WATER TREATMENT TECHNOLOGIES: A BRIEF OVERVIEW 10
2.3. THE ADVANCED OXIDATION PROCESS 15
2.3.1. Homogeneous AOPs without energy 19
2.3.1.1. Ozonation in alkaline medium 19
2.3.1.2 Oxidation using hydrogen peroxide 21
2.3.1.3 Fenton and Fenton-like processes 22
2. 3. 1. 4 Ozone/H_2O_2 (peroxone) process 24
2.3.2. Homogeneous AOPs using UV 25
2.3.2.1 UV/Ozone 26
2.3.2.2 UV/ H_2O_2 26
2.3.2.3 UV/Fenton process (Fe^{2+}/UV/ H_2O_2) 27
2.3.3. Homogeneous AOP using ultrasound (Sonolysis) 29
2.3.4. Homogeneous process using solar energy 31
2.3.5. Wet oxidation process using thermal energy 32
2.3.6. Oxidation using microwave energy 33
2.3.7. Heterogeneous catalytic oxidation 35
2.3.7.1 Heterogeneous photo-catalysis 36
2.3.7.2. Heterogeneous wet oxidation 38
2.3.7.3 Heterogeneous catalysis at ambient conditions 41
2.3.8. Iron (Fe) as heterogeneous catalyst in ambient air oxidation (ozonation and Fenton reactions) 42
2.3.9. Summarizing the AOPs 44
2.4. TECHNIQUES APPLIED IN THIS STUDY 45
2.4.1. Transmission electron microscopy (TEM) 45
2.4.2. Infra-red spectroscopy 45
2.4.3. X-ray diffractometry 46
2.4.4. High Pressure Liquid Chromatography-Time of Flight (TOF)-Mass Spectrometry 47

CHAPTER 3 51

3. METHODOLOGY 51

3.1. CALIBRATION OF OZONE GENERATOR 51
3.1.1. Determination of ozone mass transfer to aqueous phase 52
3.2. HPLC DETERMINATION OF CHLOROPHENOLS 53
3.2.1. Chemicals 53
3.2.2. HPLC instrumentation and chromatographic conditions 53
3.3. LCMS DETERMINATION OF CHLOROPHENOLS 54
3.4. PREPARATION OF B-FEOOH 55
3.5. PREPARATION OF FEOOH NANO MATERIAL COMPOSITES 56
3.6. CHARACTERIZATION OF NANOMATERIAL: FTIR, TEM AND XRD 56
3.7. EXPERIMENTAL 56
3.7.1. Determination of ozonation reaction rates 56
3.7.2. Heterogeneous catalysis: Determination of catalytic property of β-FeOOH and composites 57
3.7.3. Determination of Chemical Oxygen Demand (COD) 57
3.7.4. Determination of Hydroxy radicals by coumarin experiments 58
3.7.5. Sampling of wastewater 58

CHAPTER 4 60

4. RESULTS AND DISCUSSION 60
4.1. OPTIMIZATION OF OZONATION SET-UP 60
4.1.1. Calibration of ozone generator 60
4.1.2. Evaluation of reactor mass-transfer efficiency of reactor 60
4.1.3. Optimizing gas flow and substrate concentration 62
4.1.4. Optimization of quenching agent for ozone 63
4.2. CHARACTERIZATION OF B-FEOOH, NIO AND B-FEOOH-NIO COMPOSITE 65
4.3. EFFECT OF PH ON KINETICS AND INTERMEDIATES OF PHENOL AND CHLOROPHENOLS OZONATION 70
4.3.1. Effect of pH on kinetics 70
4.3.2. Effect of pH on intermediates 77
4.3.2.1 Intermediates of phenol ozonation 78
4.3.2.2 Intermediates of 2-chlorophenol ozonation 95
4.3.2.3 Intermediates of 4-chlorophenol ozonation 105
4.3.2.4. Intermediates of 2,4-dichlorophenol ozonation 116
4.4. HETEROGENEOUS CATALYSIS OF 4-CHLOROPHENOL OZONATION BY B-FEOOH 129
4.4.1. Effect of initial pH on the degradation efficiency of 4-CP 130

4.4.2. Effect of β-FeOOH dose on degradation efficiency of 4-chlorophenol 133
4.4.3. Effect of 4-chlorophenol concentration 136
4.5. HETEROGENEOUS CATALYSIS OF 4-CHLOROPHENOL OZONATION USING B-FEOOH-NIO COMPOSITE 137
4.5.1. 7-Hydroxycoumarin (7HC) and tert-butanol testing 141
4.5.2. Recovery and reuse of catalyst 145
4.6. TESTING OF COMPOSITE ON WASTEWATER 147
5. CONCLUSION AND RECOMMENDATION 151
5.1. CONCLUSION 151
5.2. RECOMMENDATION 153
6. BIBLIOGRAPHY/REFERENCES 154
7. APPENDIX 170

LIST OF FIGURES

Figure 2.1: Circular clarifier with visible surface skimmer. Courtesy CoCT Wastewater treatment works. 13
Figure 2.2: Ozone gas bubbled into water columns in a water treatment plant. 14
Figure 2.3: Schematic presentation of the advanced oxidation process adapted from Oputu et al. (2015c). Abbreviations: O_3 ozonation; H_2O_2 peroxide; AC activated carbon; UV ultraviolet; TiO_2 titanium oxide; WO wet oxidation; WPO wet peroxide oxidation; SCWO supercritical wet oxidation..... 18
Figure 2.4: X-ray diffracted pair. X-ray 1, reinforced by X-ray 2. 47
Figure 2.5: Schematic illustration of Agilent ion source and TOF tube 48
Figure 3.1: Ozonation set up 51
Figure 3.2: Reactor setup for preparation of β-FeOOH 55
Figure 4.1: Effect of oxygen flow rate on reactor ozone concentration and time 61
Figure 4.2: Effect of operating temperature on reactor ozone concentration 62
Figure 4.3 Effect of flow rate on phenol ozonation 63
Figure 4.4 (a) UV absorption patterns of bovine catalase at different concentrations (b) ozone quenching tests using varying concentrations of bovine catalase..... 64
Figure 4.5 (a) ozone quenching test using varying concentration of sodium thiosulphate (b) ozone quenching test at varying ration of ozonated solution and sodium thiosulphate (0.0005 M) 65
Figure 4.6: FTIR spectrum of β-FeOOH, NiO, 2%, 5% and 10% β-FeOOH –NiO composite 66
Figure 4.7: XRD spectrum of β-FeOOH, NiO, 2 %, 5 % and 10 % β-FeOOH –NiO composite 67
Figure 4.8: Bright field electron transmission images of (a) β- FeOOH and (b) NiO at 10 nm Inset: SAED showing diffraction planes 68
Figure 4.9 (a) Bright-field TEM micrograph of 2 % FeOOH-NiO, (b) corresponding EDS spectrum of area of interest, (c) Bright-field TEM micrograph of 5% FeOOH-NiO, (d) corresponding EDS spectrum 69
Figure 4.10: (a) TEM image of composite, (b) HRTEM image with characteristic d-spacing 69
Figure 4.11: (a) Dark-field scanning TEM (STEM) micrograph of the 5 wt% Fe-NiO, (b) area of interest in the yellow window was used to correct for sample drift. (c) extracted elemental maps. 70

Figure 4.12: Pseudo first order plots for ozonation of phenol and varying pH (2.5, 4, 7, 10) 72
Figure 4.13: Pseudo first order plots for ozonation of 2-chorophenol and varying pH (2.5, 4, 7, 10) 72
Figure 4.14: Pseudo first order plots for ozonation of 4-chorophenol and varying pH (2.5, 4, 7, 10) 73
Figure 4.15: Pseudo first order plots for ozonation of 2,4-dichlorphenol at varying pH (2.5, 4, 7 and 10) 73
Figure 4.16: Logarithmic plot of total apparent rate versus starting pH of solution 77
Figure 4.17: (a) DAD [280 nm] and (b) TIC chromatograms of phenol (C_6H_6O) RT = 17.897 min 79
Figure 4.18: DAD and TIC chromatograms for hydroquinone ($C_6H_6O_2$) RT = 8.707 min 79
Figure 4.19: DAD and TIC chromatograms for resorcinol ($C_6H_6O_2$) RT= 11.963 min 79
Figure 4.20: DAD and TIC chromatograms for catechol ($C_6H_6O_2$) RT= 13.867 min 80
Figure 4.21: DAD and TIC chromatograms for benzoquinone ($C_6H_4O_2$) RT = 12.973 min . 80
Figure 4.22: DAD and TIC chromatogram of 2,5-dihydroxybenzoquinone ($C_6H_6O_4$) RT = 10.187 min 80
Figure 4.23: Proposed scheme for phenol degradation based on results from this study. Structures in parentheses are assumed/inferred from literature. 94
Figure 4.24: Representative chromatogram for 2-chlorophenol RT= 21.493 95
Figure 4.25: DAD (280 nm) chromatogram for 2-chlorophenol ozonation in acidic media (pH 3) t=20mins 96
Figure 4.26: DAD (280 nm) chromatogram for 2-chlorophenol ozonation without pH control t=20mins 96
Figure 4.27: DAD (280 nm) chromatogram for 2-chlorophenol ozonation in alkaline media (pH 10) t=20mins 96
Figure 4.28: DAD (280 nm) chromatogram for 2-chlorophenol ozonation constant alkaline media (pH 10) t=20mins 97
Figure 4.29: Novel break down products for ozonation of 2-chlorophenol identified my LC-MS 101
Figure 4.30: Proposed scheme for 2-chlorophenol degradation based on results from this study 104
Figure 4.31: Representative chromatogram of 4-chlorophenol (RT=22,287). Top DAD. Bottom TIC. 105

Figure 4.32: Total ion chromatogram (TIC) for 4-chlorophenol ozonation in acidic medium. Starting pH 3.5, t=20 minutes 106
Figure 4.33 Total ion chromatogram (TIC) for 4-chlorophenol ozonation at dissolution pH 6 t=20 minutes..... 106
Figure 4.34: Total ion chromatogram (TIC) for 4-chlorophenol ozonation in alkaline medium. Starting pH 10, t=20 minutes 106
Figure 4.35 Total ion chromatogram (TIC) for 4-chlorophenol ozonation with pH held constant at pH 10. Time =20 minutes 107
Figure 4.36: Residual compounds of 4-chlorophenol degradation 112
Figure 4.37: Proposed scheme for 4-chlorophenol degradation based on results from this study..... 115
Figure 4.38: Representative DAD and TIC chromatogram for 2,4-dichlorophenol at the start of each experiment. RT= 21.680 minutes. 116
Figure 4.39: DAD (280 nm) and TIC chromatogram for 2,4-dichlorophenol at t= 10 minutes in acidic media. pH 3 117
Figure 4.40: DAD (280 nm) and TIC chromatogram for 2,4-dichlorophenol at t= 10 minutes without pH control..... 117
Figure 4.41: DAD (280 nm) and TIC chromatogram for 2,4-dichlorophenol at t= 10 minutes in alkaline medium. pH 10. 118
Figure 4.42: DAD (280 nm) and TIC chromatogram for 2,4-dichlorophenol at t= 10 minutes. pH held constant in alkaline medium (pH 10)..... 118
Figure 4.43: Residual compounds of 2,4-dichlorophenol degradation..... 124
Figure 4.44: Proposed scheme for 2,4-dichlorophenol degradation based on results from this study. Compounds in parenthesis are inferred based on reactions 128
Figure 4.45: Degradation efficiency of 4-chlorophenol (4-CP) by catalytic ozonation (catalyst dose 0.01 %, 4-CP = $2x10^{-3}$M)..... 130
Figure 4.46: Effect of β-FeOOH on rate of 4-chlorophenol degradation 131
Figure 4.47: Two stage reaction kinetics of β-FeOOH at low pH 3.5..... 132
Figure 4.48: Fe-ions in solution in β -FeOOH experiment at low pH 3.5..... 133
Figure 4.49: (a) 4-CP removal efficiency at increasing catalyst load, (b) COD removal ratio at different catalyst load..... 134
Figure 4.50: (a) Concentration of Fe-ions in solution at increasing β-FeOOH dose, (b) Pseudo first order rate plots for 4-chlorophenol at increasing β-FeOOH dose. 136

Figure 4.51: (a) Kinetic study under different 4-chlorpphenol concentrations and (b) dependence of rate constants (k) on initial 4-chlorophenol concentrations 137
Figure 4.52: Degradation rate (in bold) of 4-chlorophenol by ozonation in the presence of TiO_2 and β-FeOOH supported on TiO2..... 138
Figure 4.53: Degradation rate (in bold) of 4-chlorophenol by ozonation in the presence of Al_2O_3 and β-FeOOH supported on Al_2O_3. 139
Figure 4.54: Degradation rate (in bold) of 4-chlorophenol by ozonation in the presence of NiO and β-FeOOH supported on NiO. 140
Figure 4.55 (a) Photoluminescence changes observed during reaction in the presence of composite, (b) 7-hydroxycoumarin produced during the reactions. 142
Figure 4.56: Role of hydroxyl radicals on the degradation of 4-chlorophenol 143
Figure 4.57: Fe and Ni ions in solution during heterogeneous catalysis using β-FeOOH-NiO 145
Figure 4.58 (a) Settling rate of β-FeOOH and β-FeOOH-NiO composite over a 10 hour period, (b) reactor conditions after 10 hours post 4-chlorophenol ozonation. 146
Figure 4.59: Percentage 4-chlorophenol removal using recycled composite..... 147
Figure 4.60: COD removal from untreated wastewater from Company 1 by catalysed and uncatalyzed ozonation (inset: picture of raw and ozone treated wastewater). Left: corresponding COD removal rates by both processes..... 149
Figure 4.61: COD removal from onsite-treated-wastewater from Company 1 by catalysed and uncatalyzed ozonation. Left: corresponding COD removal rates by both processes 149
Figure 4.62: COD removal from wastewater from Company 2 by catalysed and uncatalyzed ozonation (inset: picture of raw and ozone treated wastewater). Left: corresponding COD removal rates by both processes 150
Figure 4.63: COD removal from municipal industrial water collected from Company 1 by catalysed and uncatalyzed ozonation. Left: corresponding COD removal rates by both processes..... 150

LIST OF TABLES

Table 2.1: Water treatment classes (Dore, 2014)..... 11
Table 3.1: Chromatographic parameters for quantification of phenols 54
Table 3.2: LCMS parameters for identification of intermediates..... 55
Table 4.1: Ozone concentrations as a function of oxygen flow rate..... 60
Table 4.2: Showing variation of ozone (mg/L) in reactor with time (minutes) at different oxygen flow rates (mL/min). Temperature 20^{o}C..... 61
Table 4.3: Ozone concentration at 293K and 300K at different flow rates..... 62
Table 4.4: Apparent rate constants for ozonation of phenol and chlorophenols at varying pH 76
Table 4.5: Intermediates of phenol ozonation at varying pH as followed by LCMS 81
Table 4.6: Other intermediates reported during oxidation of phenol. In bold are intermediates also identified in this study..... 92
Table 4.7: Intermediates for 2-chlorophenol ozonation at varying pH as followed by LCMS 98
Table 4.8: Intermediates reported during ozonation of 2-chlorophenol. In bold are intermediates also identified in this study..... 102
Table 4.9: Intermediates for 4-chlorophenol ozonation at varying pH as followed by LCMS 108
Table 4.10: Intermediates reported during ozonation of 4-chlorophenol. In bold are intermediates also identified in this study..... 113
Table 4.11: Intermediates for 2,4-dichlorophenol ozonation at varying pH as followed by LCMS 119
Table 4.12: Intermediates reported during ozonation/oxidation of 2,4-dichlorophenol. In bold are intermediates also identified in this study..... 125
Table 4.13: Effect of pH on contribution of B-FeOOH to kinetic of 4-chlorophenol degradation 132
Table 4.14: Apparent rate constants for catalytic ozonation processes. Rates in min^{-1} 140
Table 4.15: Physicochemical character of sampled wastewater and municipal industrial water.* Not determined onsite..... 149

LIST OF STRUCTURES

Structure 1: Phenol 83
Structure 2: Catechol 83
Structure 3: Acrylic acid 83
Structure 4: cyclohexadieneone 84
Structure 5: 2,5-cyclohexadieneone 84
Structure 6: phenol radical ion 84
Structure 7: cyclohexadieneone radical ion 84
Structure 8: 2,5-cyclohexadieneone radical ion 84
Structure 9: 2-Acetylfuran 85
Structure 10: 1-(3-furyl)ethanone 85
Structure 11: Catechol radical 85
Structure 12: Resorcinol 85
Structure 13: Hydroquinone 85
Structure 14: o,o-biphenol 86
Structure 15: p-phenoxyphenol 86
Structure 16: o,p-biphenol 86
Structure 17: p,p-biphenol 86
Structure 18: o-phenoxyphenol 86
Structure 19: 3-(3-phenoxyphenoxy)phenol 87
Structure 20: 4-(4-phenoxyphenoxy)phenol 87
Structure 21: Pyruvic acid 87
Structure 22: 2,3-dioxypropanoic acid 87
Structure 23: Malonic acid 87
Structure 24: Tartronic acid 87
Structure 25: 1,4-dioxo-2-butene 88
Structure 26: 4-oxo-2-butenoic acid 88
Structure 27: Fumaric acid 88
Structure 28: Maleic acid 88
Structure 29: Malic acid 88
Structure 30: Tartaric acid 88
Structure 31: Pyrone 89
Structure 32: 4-hydroxy-2-pentendioic acid 89
Structure 33: 2,3-dihydroxy-1,4-benzoquinone 89

Structure 34: 4,5-dihydroxy-1,2-benzoquinone 89
Structure 35: 2,6-dihydroxybenzoquinone 89
Structure 36: 3,6-dihydroxy-1,2-benzoquinone 89
Structure 37: muconic acid 90
Structure 38: 2,3-dihydroxyhydroquinone 90
Structure 39: 2,5-dihydroxyhydroquinone 90
Structure 40: 2,6-dihydroxyhydroquinone 90
Structure 41: 3-hydroxy-1,2-benzoquinone 90
Structure 42: 4-hydroxy-1,2-benzoquinone 90
Structure 43: 2-hydroxy-1,4-benzoquinone 90
Structure 44: 2-chlorophenol 99
Structure 45: 2,3dioxopropanoic acid 99
Structure 46: chlorohydroquinone 100
Structure 47: chlorocatechol 100
Structure 48: 2,2'-3,3'-biphenyldiol 100
Structure 49: 4,4'-dichloro-3,3'-biphenyldiol 100
Structure 50: 4-chlorophenol 110
Structure 51: 4-chlorocatechol 110
Structure 52: 4-chloro-3-(4-chlorophenoxy)phenol 111
Structure 53: 5,5'-dichloro-2,2'-biphenyldiol 111
Structure 54: 4-chloro-3-(4-chloro-3-(4-chlorophenoxy)phenol 112
Structure 55: 5,5',6''-trichloro-[1,1':4',1''-terphenyl]-2,2'3''-triol 112
Structure 56: 2,4-dichlorophenol 120
Structure 57: 2,4-dichlororesorcinol 120
Structure 58: 4,6-dichlororesorcinol 120
Structure 59: 3,5-dichlorocatechol 120
Structure 60: 4,4'6,6'-tetra-o-o'biphenol 121
Structure 61: 2,4-dichloro-6-(2,4-dichlorophenoxy)phenol 121
Structure 62: 3-chlorocatechol 122
Structure 63: 4-chlorocatechol 122
Structure 64: trichlorotrihydroxybiphenyl 123
Structure 65: 3',5,5'-trichloro-2,2'-3-biphenyltriol 123
Structure 66: 5-chloro-3-(2,4-dichlorophenoxy)benzene-1,2-diol 123
Structure 67: 4-chloro-2,6-bis(2,4-dichlorophenoxy)phenol 124

Structure 68: maleic anhydride 124

APPENDICES

Appendix 7.A: Intermediates of phenol ozonation at varying pH as followed by LCMS t= 40 mins and t=60 mins 170
Appendix 7.B: EIC of Catechol $C_6H_6O_2$ produced upon ozonation of phenol..... 172
Appendix 7.C: EIC of isomer of Catechol $C_6H_6O_2$ produced upon ozonation of phenol.... 172
Appendix 7.D: EIC of one of two dimerised compounds of phenol ozonation in alkaline medium $C_{12}H_{10}O_2$ 172
Appendix 7.E: EIC of second dimerization compound of phenol ozonation $C_{12}H_{10}O_2$..... 173
Appendix 7.F: EIC of trimer $C_{18}H_{14}O_3$ produced upon alkaline ozonation of phenol..... 173
Appendix 7.G: EIC of acrylic acid $C_3H_4O_2$ (compound 21) produced upon ozonation of phenol 173
Appendix 7.H: EIC of pyruvic acid $C_3H_4O_3$ (compound 17) produced upon ozonation of phenol 173
Appendix 7.I: Extracted chromatograms showing two hydroxylation products of 2CP ozonation $C_6H_5ClO_2$ presented as compound 43 and compound 44. 174
Appendix 7.J: Mass spectrum of first hydroxylation product of 2-chlorophenol $C_6H_5ClO_2$. 174
Appendix 7.K: Mass spectrum of second hydroxylation product of 2-chlorophenol ozonation $C_6H_5ClO_2$ 174
Appendix 7.L: Mass spectrum of catechol $C_6H_6O_2$ produced upon hydroxylation of 2-chlorophenol..... 175
Appendix 7.M: Mass spectrum of quinone produced from catechol $C_6H_4O_2$..... 175
Appendix 7.N: Mass spectrum of dimerization compound of 2-chlorophenol $C_{12}H_8Cl_2O_2$. 175
Appendix 7.O: Mass spectrum of 4-chlorophenol showing isotope distributions C_6H_5ClO 176
Appendix 7.P: Mass spectrum of single hydroxylation product of 4-chlorophenol ozonation $C_6H_5ClO_2$ 176
Appendix 7.Q: Mass spectrum of dimerised product of 4-chlorophenol ozonation $C_{12}H_8Cl_2O_2$ 176
Appendix 7.R: Mass spectrum of trimerised product of 4-chlorophenol ozonation $C_{18}H_{11}Cl_3O_3$ 177
Appendix 7.S: Mass spectrum of 2,4-dichlorophenol showing isotope spacing used for identification $C_6H_4Cl_2O$ 177
Appendix 7.T: Mass spectrum of hydroxylation product on ozonation of 2,4-dichlorophenol $C_6H_4Cl_2O_2$..... 177

Appendix 7.U: Mass spectrum of first dimerization product of 2,4-dichlorophenol ozonation $C_{12}H_6Cl_4O_2$ 178
Appendix 7.V: Mass spectrum of second dimerization product of 2,4-dichlorophenol ozonation $C_{12}H_7Cl_3O_3$ 178
Appendix 7.W: Mass spectrum of dechlorination product of 2,4-dichlorophenol ozonation $C_6H_5ClO_2$ 178

CHAPTER ONE

1. INTRODCUTION

1.1. Background

In the last three decades, concern about environmental pollution has increased around the world. This has resulted in the promulgation of more restrictive environmental laws. With the development of more advanced analytical techniques for the identification and quantification of pollutants, the tendency is to continue expanding those restrictions to protect the environment, in particular, the regulation of toxic substances, mutagens and carcinogenic precursors and carcinogenic substances. Especially important are the regulations placed on water from water purification plants, industrial and municipal wastewater/sewage treatment plants.

While the water purification plants serve to purify surface and groundwater for drinking applications, the wastewater and sewage plants treat wastewater from industrial sources and sewage sludge before releasing the treated water into the environment or into recycle lines for reuse. In the City of Cape Town, as with many other cities in developed countries, these recycled water are used for non-drinking applications. The paper-pulp industry in Cape Town utilizes 70% of the recycled treated wastewater and this reduces the pressure on ground water sources for paper production.

In recent years, there has been an increased concern about the quality of water discharged from industrial/sewage plants and even from water purification plants as certain recalcitrant xenobiotic organic compounds have been detected in surface water, groundwater streams and in drinking water. A vast number of pharmaceuticals and endocrine disrupting chemicals (EDCs) have been detected in effluents from sewage treatment plants (Andreozzi et al., 2003, José et al., 2010), surface water (Castiglioni et al., 2004, Brown et al., 2006) and less frequently in drinking water (Stackelberg et al., 2007). These pharmaceuticals range from simple antibiotics to anticonvulsants, beta-blockers, cytostatic drugs and x-ray contrasting medium (Wang et al., 2011, Focazio et al., 2008). The intrinsic design of these chemicals prevents their attack by the microbes used in the biological treatment of municipal sewage and, therefore, they persist in the effluent during discharge of treated wastewater. Natural waters and treated wastewater represent the most significant exposure pathways for EDCs to biota as they are only partially removed by wastewater treatment processes (Daughton and Ternes, 1999). The presence of

surfactants used for the manufacture of detergents, pesticides and cosmetics have also been reported in treated effluents and receiving waters (Wensing et al., 2005). Xenobiotic end products such as dyes (Correia et al., 1994), pesticides, herbicides and insecticides (Gilliom et al., 1999), and other precursor chemicals such as nitro- and chloro- benzenes have also been detected in water samples (Cortés et al., 2000, Mallevialle, 1975).

From the foregoing, it is apparent that the present conventional techniques such as flocculation, coagulation, adsorption on activated carbon, biological treatment and membrane processes for the purification of drinking water and the treatment of wastewater are ineffective for removal of certain recalcitrant organics from water (Gültekin and Ince, 2007). One major disadvantage of some of these techniques is the concentration of pollutant on a secondary medium or in solution and hence the generation of sludge which is more concentrated and far more acutely toxic than the individual pollutant. The proper disposal of this secondary generated pollutant therefore offers another problem. At present, membrane waste sludge containing several stabilized xenobiotic compounds is being emptied into sewers and surface waters where they pose further environmental threat (Erickson, 2002, Tambosi et al., 2009). Also, while adsorption on activated carbon shows promise for removal of organics, reports on application in real wastewater revealed that adsorption for certain organics was reduced by as much as 1000 times when compared to results from laboratory scale experiments (Fukuhara et al., 2006). Coupled with this disadvantage is the fact that the reuse of activated carbon is limited to a specific number of cycles and the generated spent carbon requires proper disposal treatment (Choi et al., 2005). Biological degradation and photo-degradation are one of the major technologies applied for removal of toxic chemicals such as chlorinated phenols, aromatics and pesticides (Oller et al., 2010). However, in the context of removal described by The European Commission Joint Centre (EC, 2003), these conventional technologies have been regarded as unsatisfactory for treatment of industrial wastewater since many of the organics present are resistant to biological treatment. Many of the toxic organics have been reported to inhibit the proper respiratory activity of the microorganisms in these biological treatment plants and thus render them inactive (Sadik et al., 2004). Arguably, some of these techniques such as adsorption when carried out in the biosorption mode utilize inexpensive adsorbents and as such the reduction in running cost may become a long run

advantage. However, there is still no report of a break-through material capable of total pollutant removal from wastewater.

The use of chemical treatment for the removal of toxic organics in water and wastewater has become an alternative to conventional treatment technologies. Especially important are those based on the use of ozone, hydrogen peroxide and the advanced oxidation processes (AOP) also referred to as the advanced oxidation technologies (AOT). These techniques are based on rapid oxidation of organics (in aqueous medium) using radicals such as hydroxyl or persulphate and have been reported to bring about complete mineralization of toxic xenobiotic organics frequently detected in water/waste water and the mortality of disease causing pathogens (Yasar et al., 2007). Several workers have reported the use of advanced oxidation processes for removal of pharmaceuticals (Klavarioti et al., 2009, Méndez-Arriaga et al., 2009), endocrine disruptors (Olmez-Hanci et al., 2010), pesticides (Ballesteros Martín et al., 2009, Abdessalem et al., 2010), surfactants (Bandala et al., 2008) and a wide range of other industrial toxic chemicals such as phenols (Pimentel et al., 2008, Lachheb et al., 2008), humic acids and benzene derivatives (Ji et al., 2009, Ayoub et al., 2010, Ikematsu et al., 2004) commonly detected in surface, ground and wastewaters. These techniques are superior to the conventional chlorination of water as they can be optimized to also oxidize disinfection by-products such as the halomethanes and haloacetic acids associated with chlorination of water (Chin and Bérubé, 2005). Since the end product of complete mineralization is the production of carbon dioxide and water, the advanced oxidation processes therefore offer another significant advantage in avoiding the production of a secondary pollutant encountered when using other conventional techniques.

Furthermore, the AOP's have been applied to several real waste scenarios such as dye effluents from dye industry (Feng et al., 2010), pulp mill effluents high in phenolics (Jamil et al., 2011, Catalkaya and Kargi, 2007), land fill leachates (Cortez et al., 2011, Sun et al., 2009) drinking water (Rahman et al., 2010b, Rahman et al., 2010a) and have shown better treatment efficiency when compared with conventional processes. Combined with other techniques, the AOPs have also been used as pre-, or post-treatment unit operations as part of a multiple barrier approach for water purification (Feng et al., 2010, Mandal et al., 2010, Grafias et al., 2010). The possible application of AOP's in hybrid water treatment process based on

adsorption and catalytic wet air oxidation has also been reported (Julcour Lebigue et al., 2010).

1.2. Problem Statements

The contamination of surface and groundwater by poorly treated effluents from point sources such as industrial, pharmaceutical, leachate and sewage treatment plants is well established in literature. This has been attributed to the failure of the existing conventional treatment technologies to remove certain recalcitrant/persistent pollutants that have been identified in effluents from treatment plants. These pollutants are regarded as a threat to environmental safety and public health as they range from disinfection by-products to toxic chemicals, which are established mutagens and carcinogens.

The continuous release of such waters into the environment may constitute a long-term potential risk for aquatic and terrestrial organisms. The situation is pressing in countries such as South Africa and other developed cities such as USA, Germany and UK where there is a reliance on treated wastewater collected from the aforementioned sources to supplement for non-drinking applications such as irrigation and industrial use. This has formed an important component for both wastewater management and water resource management in these countries. The most significant restraint to the reuse of wastewater is the potential risk to public health when these wastewaters carrying pollutants are recycled into municipal water supply or used to recharge aquifer streams. A report by the Department of Water Affairs (DWAF) stated that the level of compliance of some wastewater/water treatment works in the city of Cape Town is as low as 52% (DWAF., 2004, CoCT., 2006, CoCT., 2007).

While there is a worldwide effort to achieve 100% removal of pollutants, it is obvious that the existing technologies currently in operation are not capable of completely removing certain xenobiotic compounds, and more advanced systems are required. It is, therefore, imperative to research and develop cost effective tertiary treatment methods capable of efficiently removing recalcitrant xenobiotic pollutants in wastewater/water. The advanced oxidation processes present a set of versatile techniques capable of mineralizing organic pollutants present in waste water by rapid oxidation using in-situ generated radicals, and as such has been the subject of recent research in water/wastewater treatment technology (Gerrity et al., 2010,

Jeong et al., 2010a, Jeong et al., 2010b, Razavi et al., 2011, Pálfi et al., 2011, Mandal et al., 2010, Pham et al., 2010, Jamil et al., 2011, Cortez et al., 2011) They are also readily incorporated into conventional treatment processes as shown by several reports (Ballesteros Martín et al., 2009, Ballesteros Martín et al., 2008, Mandal et al., 2010, Grafias et al., 2010, Feng et al., 2010)

1.3. Purpose Statement

Treatment of water and wastewater using conventional technologies is largely regarded as inefficient for removal of several identified recalcitrant organics in water. At present, there are still limitations to the use of the promising 'advanced oxidation processes'. The mechanisms of elimination using these methods, and intermediates thereof during the treatment/pre-treatment of organics in water/wastewater have not been fully understood. With the array of heterogeneous catalysts combination and the development of sophisticated monitoring technologies, there is potential for the development of the advanced oxidation processes to produce cleaner effluents after water treatment.

With the heavy reliance on wastewater re-use for non drinking application in South Africa, it is imperative to research/develop technologies, especially the advanced oxidation process for the treatment of these wastewater streams.

1.4. Objectives of the Research

1.4.1. Main Objectives

The main objective of the study is to investigate the possibility of advanced oxidation processes for the degradation of phenols (phenol, 2-chlorophenol, 4-chlorophenol, 2,4-dichlorophenol and 2,4,6-trichlorophenol) commonly found in wastewater.

1.4.2. Specific Objectives

- ✓ Create a method for the determination of candidate phenolic compounds in water using High performance liquid chromatography (HPLC).
- ✓ Design conditions for the oxidation of the candidate phenols using ozonation process.
- ✓ Develop methods for monitoring oxidation intermediates using HPLC, and HPLC-MS
- ✓ Investigate the effect of heterogeneous catalyst on the ozonation process for the candidate phenols.

- ✓ Develop degradation pathways for the ozonation of phenol and target chlorophenols.
- ✓ Compare the degree of degradation of candidate phenol by both catalysed and unanalysed oxidation processes and determine which of the two processes is better.

1.5. Significance of the Research

This research aimed at presenting information regarding the ozonation kinetic and intermediates of phenol and chlorophenol. Such information is necessary when assessing the routes, end product and overall efficiency/acceptability of the ozonation process. The study explored the development of heterogeneous catalyst for ozonation reaction, testing developed catalyst on laboratory prepared samples and wastewater from industry. The success of proposed catalyst would play an important role in catalyst development in the field of heterogeneous ozonation and possible application in wastewater remediation.

1.6. Limitations of the study

This study did not aim at developing pilot ozonation plants for wastewater treatment.

1.7. Instrument Employed

- Ozone generator from Ecological Technology (Eco Tech 1000) with oxygen gas 99.999 % from Air Liquide.
- Waters HPLC model for quantification of phenols and intermediates
- Agilent 6230 LC-MS-TOF for real-time identification of phenol, intermediates and end-products
- COD analysers for monitoring mineralization of phenols
- Analytical balance
- Hana 1000 pH meter with working electrodes
- UV-Vis spectrophotometer for determination of ozone and peroxide during the calibration of the ozone generator and also for the determination of residual ozone after AOP.
- Waters Symmetry C8 reverse phase HPLC column
- Phillips 3830 X-ray diffractometer (XRD)
- Tecnai TF20 thermionic transmission electron microscope (TEM)

- Perkin Elmer 1000 series Fourier Transform Infrared (FTIR) spectrometer

1.7.1. Data Analysis and Findings

Results on kinetic data are presented based on appropriate kinetic models and plots. Discussions are presented in a systematic manner, engaging relevant literature where necessary. Results from this study have been published in reputable journals.

CHAPTER TWO

2. LITERATURE REVIEW

2.1. Phenols and Chlorophenols

Phenol and its nineteen possible chlorinated derivatives are EPA environmental priority pollutants, which enter the environment via various sources related to their use. General purpose uses for these compounds range from monomers in plastic production (for example phenol to bisphenol-A), to herbicidal and insecticidal uses. The chlorophenols possess a strong medicinal taste and smell and are undesired products of processes such as chlorination of water and bleaching of wood pulp during paper production (Fatoki and Opeolu, 2009, Michałowicz and Duda, 2007).

2.1.1. Phenol

The isolation of phenols was achieved in the early eighteenth century and its structure was verified in 1842 (Hugo, 1977). In the petrochemical, pharmaceutical, plastic and pesticide chemical industries phenol is used as a raw material (Xiao et al., 2006). In 2005, Chemical Marketing Reporter highlighted the major uses of phenol to be the production of bisphenol-A and of phenolic resins (CMR, 2005). The same communication underlined other uses, which include production of caprolactam, aniline, alkyl-phenols and xylenols. Phenol has also been reported to be used as a unselective slimicide (Budavari et al., 1989), a disinfectant and antiseptic (McDonnell and Russell, 1999) and recently has been investigated as a topical anaesthesia (Ball, 2015).

Phenol is EPA priority pollutant number 65 and has been detected in air, water and ground samples. Release into the air has been reported to be the consequence of industrial combustion processes (Jay and Stieglitz, 1995, Moreira dos Santos et al., 2004), tobacco cigarette smoke (Pistonesi et al., 2006), leakages from storage tanks and residential wood burning. Phenol also finds its way into water bodies as effluent from many manufacturing industries as highlighted in early reports (Goerlitz et al., 1985, Parkhurst et al., 1979). These industries mainly use phenol containing compounds in their formulations for disinfectants and health care products (Budavari et al., 1989). Natural sources of phenol include decomposition of animal waste and organic waste. Accidental point source discharges of phenol has shown that phenol contamination via this means can be quickly contained due to the rapid rate of biodegradation of phenol (Xing et al., 1994).

2.1.2. 2-chlorophenol

The US environmental protection agency lists 2-Chlorophenol as priority pollutant number 24 (USEPA, 2016). 2-Chlorophenol has been used as biocides (Hoppin et al., 1998) as an antiseptic agent (Shehata et al., 2012), and a starting compound to produce higher chlorophenols and phenolic resins (Krijgsheld and van der Gen, 1986). 2-Chlorophenols can be found in water, air and soil. The presence of 2-chlorophenol in air can be attributed to its high volatility-it is the only chlorophenol that is liquid at room temperature- which is the major dispersal mechanism into the environment (Scow and et al., 1982). 2-Chlorophenol is released into the air chiefly as vapour produced during chlorophenol and chlorophenol products manufacture (Scow and et al., 1982). The foremost point source of water pollution by 2-chlorophenol is via Industrial waste discharge (Krijgsheld and van der Gen, 1986). Early reports have identified 2-chlorophenol in leachate from municipal landfill sites, highlighting landfills as a potential source of organic dissemination into surface and groundwater (Brown and Donnelly, 1988).

2.1.3. 4-chlorophenol

4-chlorophenol has been used as biocides and as an antiseptic (Hoppin et al., 1998, Shehata et al., 2012). It is also applied as a disinfectant for homes, hospitals and farm uses. Additional uses include production of higher chlorinated phenols, synthesis of dyes and drugs, denaturant for alcohol and selective solvent in refining of mineral oils (Krijgsheld and van der Gen, 1986). The major sources of 4-chlorophenol into the environment are industrial waste discharges and chlorination of water containing phenolic products (Czaplicka 2004). Early reports have identified 4-chlrophenol in effluents from bleaching of pulp. More recently, 4-chlorophenol has been detected in surface water in Europe (Faludi et al., 2015) and a dam tributaries in South Africa (Olorundare et al., 2015).

2.1.4. 2,4-dichlorophenol

2,4-Dichlorophenol is EPA priority pollutant number 31 and is generally used for mothproofing and as a miticide, pesticide and herbicide. 2,4-Dichlrophenol enters the environment via discharge and burning of chlorinated wastes. There have also being reports of 2,4-dichlorophenol emissions during combustion of municipal solid waste, coal and herbicides (Gomez et al., 1988, Junk et al., 1986, Öberg et al., 1989). Water pollution by industrial waste discharge is another major source of 2,4-

dichlrophenol into the aquatic system (Krijgsheld and van der Gen, 1986). Natural formation of 2,4-dichlrophenol from de novo synthesis by fungi was postulated by (Hoekstra et al., 1999).

2,4-dichlorophenol has been detected in effluent released from industries that manufacture photographic equipment and supplies, iron, electrical components, steel, pharmaceuticals, and organic chemicals, plastics and from paper pulp and paperboard mills (Paasivirta et al., 1985). Breakdown of pesticides and chlorinated phenolics have being hypothesized to be the main reason for 2,4-dichlrophenol build up in runoffs from farms and leachates from landfill sites, respectively (Brown and Donnelly, 1988).

2.1.5. Summary on the phenols

Wide spread use of phenols and the chlorophenols have led to their release into various aquatic environments either as accidental discharges or from wastewater treatment plants. A recent study conducted by our research group in The City of Cape Town identified several priority phenols, phthalate esters and other endocrine disruptors in influents - and in some cases - effluents from wastewater treatment plants (Olujimi et al., 2012). As highlighted in that report, the release of chlorophenols, and other organics into surface water streams is due to the poor efficiency of the wastewater treatment plants to remove these organics from influent water. It has therefore become imperative to develop/apply new techniques capable of removing these recalcitrant organics from water.

2.2. Water treatment technologies: A brief overview

There exist a vast array of methods for treating water and wastewater, each with its advantages and drawbacks. A typical Wikipedia search itemizes 97 differing methods that have been applied at one time or another in the pursuit of differing levels of purified water (Wikipedia, 2016). These methods range from simple physical treatment processes such as sedimentation, flocculation, filtration (sand and screen filters), and clarifiers to more specialized techniques such as the American Petroleum Institute's (API) oil-water separator, chemical methods (such as Fenton process) and membrane processes (membrane bioreactors and membrane distillation). Others include techniques based on advanced oxidation using UV (AOP) and those based on nano-technology. While most of these techniques are

well established in their applications others, such as the advanced oxidations based on ozone are still in their budding stage as evidenced from the amount of researches currently devoted to their study. Due to the diversity of the existing water treatment techniques, a unified method for their classification is non-existent. While some authors may classify the techniques based on their principle of operation (i.e. Physical, Chemical, Biological, etc.), others may chose to classify them based on their degree of efficiency or the class of water they are capable of treating. For this review, the method of classification adopted is based on the recent classification system proposed by Dore (2014). The six-class system proposed by the author classifies treatment technologies based on the number/kind of contaminant removed by the process itself, the measured standard acceptable water being that treated by chlorination (Class 1). The six classes summarily presented in Table 2.1 categorizes water treatments themselves and not the final water quality or water source and as such may be used for assessing potential/possible long-term health risks from the application of a class of techniques.

Table 2.1: Water treatment classes (Dore, 2014)

Class	Typical treatment technology	Contaminants removed
Class 1	Chlorination	Water disinfection; removal of most pathogens
Class 2	High rate clarification and filtration	Disinfection plus suspended solid removal
Class 3	Ultra Violet	Class 2 plus removal of protozoa
Class 4	Ozonation	Class 3 plus removal of dissolved organic matter (no DPB a precursors)
Class 5a	Activated carbon powered or granula carbon	Class 3 plus removal of geosmin and other taste and odour compounds. DPB[s], Volatile Organic Compounds. Endocrine disruptors, micro-pollutants, pesticides, pharmaceuticals and personal care products
Class 5b	Advanced oxidation process	Class 5a plus higher efficacy of removal of chemicals and other micro-pollutants (e.g. pesticides, pharmaceuticals, taste and odour concerns)
Class 6	Reverse Osmosis or distillation	Class 5 plus removal of salinity

DPB stands for " disinfection by-products."

Class 1 treatment technologies are simply for disinfection and removal of pathogens and are typically used as follow up to physical processes such as flocculation,

clarification and filtration. This method of treatment is sufficient for ground water sources, which are low in suspended solids but are inadequate for surface water sources, which would require primary clarification before disinfection. The drawback of this class of treatment facilities is that they do not remove protozoa – especially of the *Cryptosporidium* family - from treated water and lead to production of disinfection by products (DBPs) such as the trihalomethanes (THMs), nitrosamines and haloacetic acids (HAAs). An early failure of Class 1 treatment technologies, - and especially chlorination - was a reported outbreak of dermatitis (31 cases) in the United States, where patients were exposed to residual (free) chlorine as high as 27 mg/L in municipal water supply (Michael and St. Louis, 1988). Patients displayed symptoms varying from urticarial rashes, skin burning and change in hair colour to green. The reports by the authors identified other pathogens, such as *G. lamblia* as culprit in several of the water related disease outbreak as a result of unintentional consumption of water in swimming pools even when chlorination had been maintained at adequate levels (Michael and St. Louis, 1988). Another report on water borne outbreaks due to excessive exposure to accumulated chloramines in water, which persist as disinfection by-products of nitrogenous compounds such as perspiration, saliva and urine led to respiratory problems for swimmers in recreational facilities (Jonathan et al., 2008). This further highlighted the disadvantages of the Class 1 chlorination technology and underscores the need for improved water treatment techniques especially adequate to treat chlorine resistant microbes.

Class 2 treatment techniques which include clarification and filtration is applied to surface waters to remove suspended solids before disinfection in order to avoid disinfection by products (DBPs), which frequently occur during chlorination of water containing humus, suspended solids or other organics. Such facilities however would not remove chemically resistant protozoa. Figure 2.1 illustrates circular clarifiers with visible surface skimmers operated by the City of Cape Town Municipality. The skimmers slowly rotate round the clarifier skimming floating material, which is then trapped above a fenced enclosure. By introducing this step before disinfection, the entire process aims to reduce the risk of DBPs present in treated water. The class-2 clarification processes include techniques such as coagulation and flocculation, sedimentation and flotation, and filtration process. Coagulation processes promote the aggregation of small particles into larger particles that can be subsequently removed by sedimentation and/or filtration.

Coagulation process is comprised of three sequential steps. These steps include coagulant formation, particle destabilization and particle aggregation. Coagulant formation and particle destabilization are promoted in a rapid-mixing stage where treatment chemicals are added to cause destabilization. Particle aggregation is then promoted in a flocculation stage where inter-particle collisions create larger particles amenable to separation from the treated water. Sedimentation and flotation on the other hand are solid-liquid gravity separation processes. Sedimentation promotes gravity settling of solid particles to the bottom of a water column where accumulated solids are removed. Flotation processes introduce gas bubbles into the water attached to the solid particles and create bubble-solid agglomerates that float to the top of the water column where accumulated solids are removed. Both sedimentation and coagulation are generally used in combination to remove floc particles and improve subsequent filtration. Filtration process is relied on in most water treatment facilities for the removal of suspended particulate matter present in a water body or agglomerated by any of the earlier discussed processes. Common particulates removed are clay, silt, precipitated natural organic matter (NOM), metal salts and microorganisms from disinfection. The filtration process is credited with the specified removal of enteroviruses and *Giardia lambia*. Consequently, the process is considered an integral part of overall water disinfection process. The most common types of filters are granular media filters such as sand, crushed anthracite coal, garnet, ilmenite, and granular activated carbon (GAC).

Figure 2.1: Circular clarifier with visible surface skimmer. Courtesy CoCT Wastewater treatment works.

Class 3 and Class 4 techniques utilize ultra violet light and ozone, respectively and are capable of removing – in addition to pathogens and suspended solids - protozoa and dissolved organic matter, respectively. Ever since its inception in Nice, France in 1906, ozonation has been in use in several countries in Europe. Due to its higher oxidizing power compared to chlorine, ozone is capable of removing certain recalcitrant organics (e.g. phenols, pesticides and some detergents) and protozoa not removed by chlorine disinfection. This technology also avoids the production of DBPs and is therefore generally accepted as superior to the chlorination techniques. Currently, there are over 3000 large-scale municipal plants worldwide using ozone for water treatment, with the main limitation to its application being its production cost. Ozone gas is applied as a short-lived disinfectant produced in-situ in water treatment plants as shown in Figure 2.2. Despite its higher cost of operation compare to chlorination, there is growing interest in ozonation technology due to public concerns of DBPs in water. Another challenge to the use of ozonation is that unlike chlorine, it does not provide any residual disinfection after its application. This means that reticulating bacterial growth becomes an important factor when water is held for prolonged period before use.

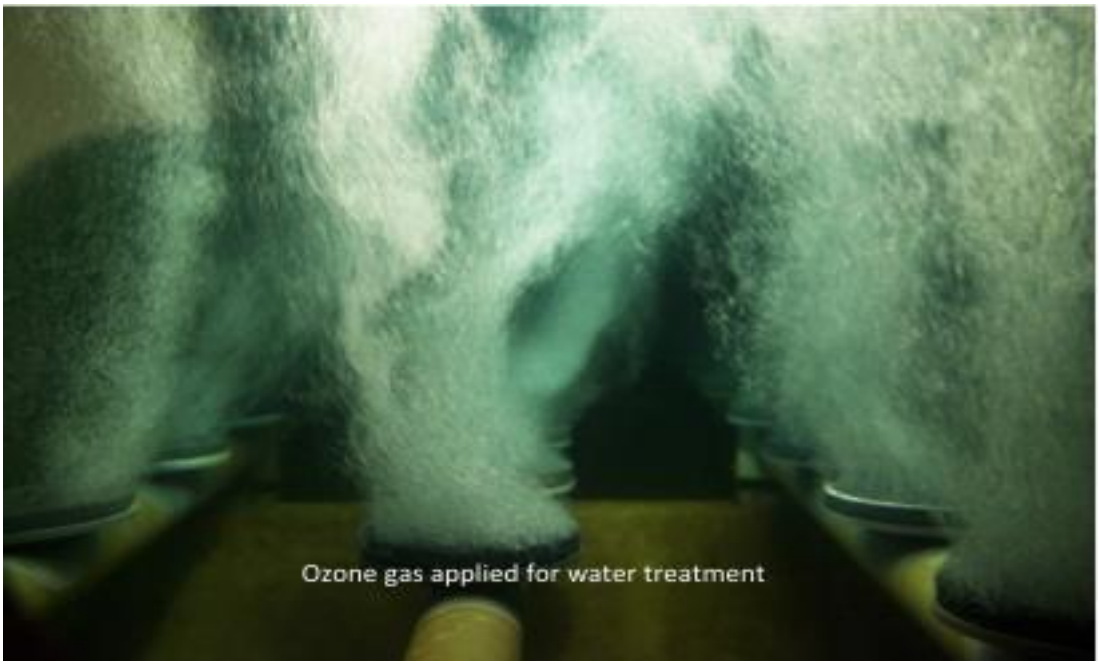

Figure 2.2: Ozone gas bubbled into water columns in a water treatment plant.

Class 5 treatment techniques (activated carbon and advanced oxidation processes AOP) are capable of removing odour, taste, volatile and recalcitrant organics ranging from pesticides, pharmaceuticals, DBPs and other personal care products

(PCPs). The use of granular activated carbon (GAC) – Class 5a- has been implemented in many large water treatment plants in Europe (Dussert and Van Stone, 2000) and its efficacy for removing all sorts of contaminants has been further confirmed (Rodriguez-Mozaz et al., 2004). The current industrial use of advanced oxidation process (Class 5b) involves the use of ozone in combination with UV-light. A detailed review on the developing field of advanced oxidation processes is presented in the following section. Reverse osmosis, nano-filtration and distillation (Class 6) techniques remove all target compounds of Class 5 techniques and also salinity from water. While such technology is highly desired, several workers have highlighted that its development and wide application would be greatly hindered by its operational cost (Dore, 2005, Fritzmann et al., 2007, Karagiannis and Soldatos, 2008). Based on the classification system described thus far, a higher treatment class indicates a greater removal of contaminants and by implication, incurs a higher cost.

The water treatment process in South Africa is based on the use of chlorine as the disinfectant. Dams and rivers serve as major intake sources for water into treatment plants. Influent water is firstly pre-treated by chlorination to inactivate disease-causing pathogens followed by mixing, coagulation and flocculation. After sedimentation and filtration, the clean water is then chlorinated again to kill remaining germs and the treated water is pumped to reservoir tanks from where it is transferred to consumers. While several municipalities are aware of the threat of trihalomethanes in chlorinated water, the choice of using chlorine is anchored on the residual disinfectant effect it posses. Also, the perceived absence of organic compounds in the influent waters lessens the risks of formation of disinfectant by-products (DBPs). With the recent detection of several phenolics, phthalates, and pharmaceuticals in surface waters within South Africa, there is a renewed interest in identifying and developing alternate technologies for treatment of water within the countries catchment areas.

2.3. The advanced oxidation process

AOPs were defined in 1987 by Glaze as "near ambient temperature and pressure treatment processes which involve the generation of hydroxyl radicals in sufficient quantities to effect water purification" (Glaze et al., 1987). Hydroxyl radical is traditionally thought to be the active species responsible for the destruction of pollutants. In the light of recent evidence, this definition may require a revision as

several publications have reported the use of other radicals such as sulphate and azide radical generated in-situ for the degradation of organic pollutants in wastewater radical (An et al., 2010, Sun et al., 2009, Yang et al., 2009, Chowdhury et al., 2015b). The use of the AOPs also referred to as the advanced oxidation technologies (AOTs) have been reported to bring about complete mineralization of toxic xenobiotic organics frequently detected in water and wastewater. AOPs have also been successfully applied to the removal of disease causing pathogens in water (Yasar et al., 2007). Several workers have reported the use of AOPs for removal of pharmaceuticals (Klavarioti et al., 2009, Méndez-Arriaga et al., 2009), endocrine disruptors (Olmez-Hanci et al., 2010), pesticides (Abdessalem et al., 2010, Ballesteros Martín et al., 2008, Ballesteros Martín et al., 2009), surfactants (Bandala et al., 2009) and a wide range of other industrial toxicants such as phenols (Kim and Ihm, 2011, Pimentel et al., 2008), humic acids and benzene derivatives (Ayoub et al., 2010, Ikematsu et al., 2004) commonly detected in surface, ground and wastewaters. These techniques are superior to the conventional chlorination of water as they can be optimized to also oxidize disinfection by-products such as the halomethanes and haloacetic acids associated with chlorination of water (Chin and Bérubé, 2005). Since the end products of complete mineralization are carbon dioxide and water, the AOPs offer another significant advantage in avoiding the production of a secondary pollutant encountered when using other conventional techniques. Furthermore, the AOPs have been applied to several real waste scenarios such as dye effluents from dye industry (Feng et al., 2010), pulp mill effluents high in phenolics (Catalkaya and Kargi, 2007, Jamil et al., 2011), land fill leachates (Cortez et al., 2011) and drinking water (Rahman et al., 2010a, Rahman et al., 2010b). These have shown better treatment efficiency when compared with conventional processes. In combined mode with other techniques, they have also been used as pre-treatment or post-treatment unit operations as part of the multiple barrier approach for water purification (Feng et al., 2010, Grafias et al., 2010, Mandal et al., 2010). The possible application of AOPs in hybrid water treatment process based on adsorption and catalytic wet air oxidation has recently been proposed (Julcour Lebigue et al., 2010).

Although the AOPs use different reagent systems, which include photochemical degradation processes (UV/O_3, UV/H_2O_2), photo-catalysis (TiO_2/UV, photo-Fenton), and chemical oxidation processes (O_3, O_3/H_2O_2, H_2O_2/Fe^{2+}, H_2O_2/Fe^{3+}), they all produce hydroxyl radicals ($OH^{\bullet}$), which are highly reactive and non-selective

(Rosenfeldt et al., 2007, Skoumal et al., 2006). Sulphate radicals ($SO_4^{\bullet}$) produced using oxone is more selective than hydroxyl radical (Sun et al., 2009)

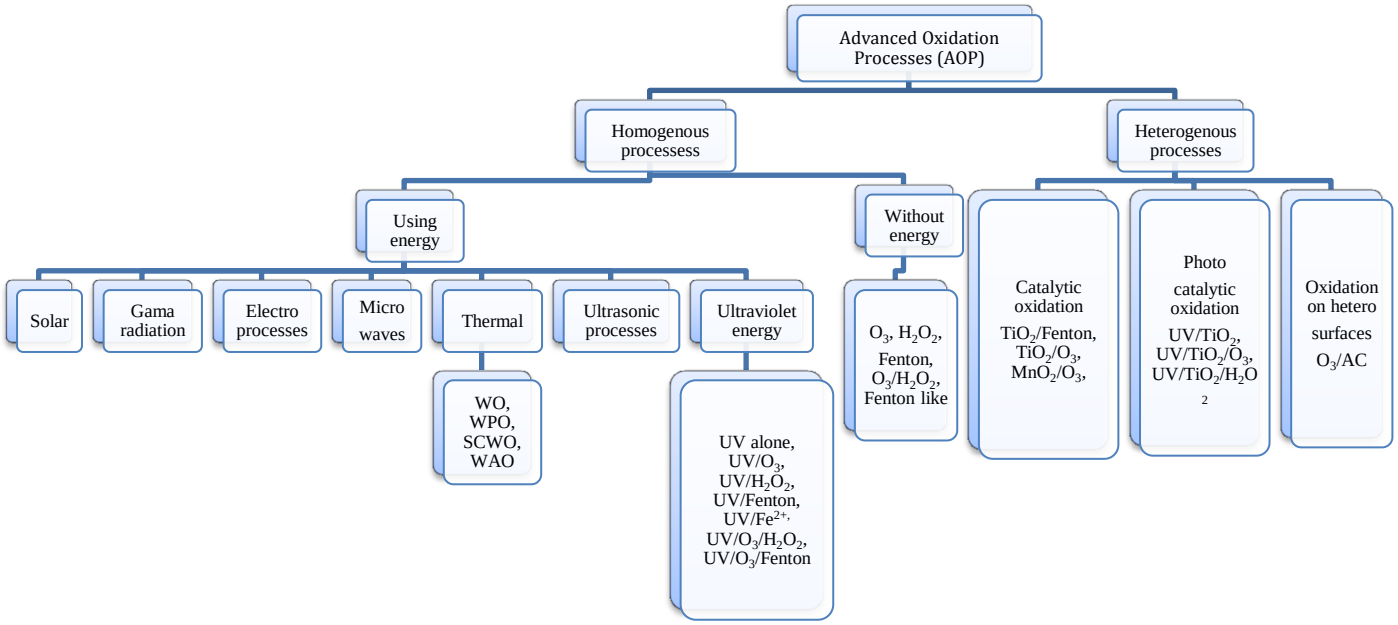

Figure 2.3: Schematic presentation of the advanced oxidation process adapted from Oputu et al. (2015c). Abbreviations: O_3 ozonation; H_2O_2 peroxide; AC activated carbon; UV ultraviolet; TiO_2 titanium oxide; WO wet oxidation; WPO wet peroxide oxidation; SCWO supercritical wet oxidation. O_3 = ozone, H_2O_2 = hydrogen peroxide, TiO_2 = titanium dioxide.

These AOPs, summarized in Figure 2.3, may be classified as homogeneous or heterogeneous. The major distinguishing factor between these two broad classes is the absence of a solid phase catalyst or promoter in the homogeneous process. In homogeneous processes, reagents such as H_2O_2, soluble O_3 and/or aqueous metals are used to generate OH radicals in aqueous phase for oxidizing dissolved organics. Energy sources such as solar, microwave, thermal and others presented in Figure 2.3 are not considered as a separate phase from the aqueous medium. On the other hand, heterogeneous processes utilize a solid catalyst phase or surface upon which radicals are generated. The generation of radicals by UV generated holes on TiO_2 solids dispersed in an aqueous medium is a typical example. Others such as O_3 break down on solid metal oxides may be specifically regarded as catalytic processes and are broadly classified under heterogeneous processes. Homogeneous processes can be further subdivided into processes that are driven by external energy and processes that do not operate on external energy sources. These energy sources include UV light, solar energy, electrochemical, ultrasonic (sonolysis), microwave, thermal and gamma radiation.

For the purpose of this review, a discussion on the various homogeneous AOPs is presented in full as the interpretation of data obtained in this study is based on some knowledge of overlap between the processes.

2.3.1. Homogeneous AOPs without energy

2.3.1.1.Ozonation in alkaline medium

Ozone is unstable in aqueous medium, decomposing spontaneously by a complex mechanism that involves the generation of hydroxyl radicals. The degradation of organic compounds occurs through the action of O_3 itself as well as through the radicals generated in alkaline medium. The scheme for the radical generation has been extensively argued (Hoigné, 1997). Hoigné showed that ozone decomposition in aqueous solution proceeds via the formation of hydroxyl radicals as shown in Equation 2.1-Equation 2.8. In the reaction mechanism, hydroxyl ion (OH^-) has the role of initiator.

Equation 2.1

$$OH^- + O_3 \longrightarrow O_2 + HO_2^-$$

Equation 2.2

$$HO_2^- + H^+ \rightleftharpoons H_2O_2\ (acidic\ medium)$$

Equation 2.3

$$HO_2^- + O_3 \longrightarrow HO_2^{\bullet} + O_3^{-\bullet}$$

Equation 2.4

$$HO_2^{\bullet} \leftrightharpoons H^+ + O_2^{-\bullet}$$

Equation 2.5

$$O_2^{-\bullet} + O_3 \longrightarrow O_2 + O_3^{-\bullet}$$

Equation 2.6

$$O_3^{-\bullet} + H^+ \longrightarrow HO_3^{\bullet}$$

Equation 2.7

$$HO_3^{\bullet} \longrightarrow HO^{\bullet} + O_2$$

Equation 2.8

$$HO^{\bullet} + O_3 \longrightarrow HO_2^{\bullet} + O_2$$

The mechanism also elucidates the role exerted by H_2O_2 since it is formed during the decomposition of ozone as shown in Equation 2.2. It is therefore clear that the addition of H_2O_2 to O_3 aqueous solution would enhance the O_3 decomposition, with the formation of OH radicals. This forms the basis for the use of another process based on O_3 and H_2O_2: the peroxone process (O_3/H_2O_2). A less complex scheme for decomposition of O_3 to radicals was proposed by Alaton et al. (2002), which summarily generate two moles of hydroxyl radicals and a mole of oxygen from the reaction between ozone, hydroxyl ions and a proton. The use of ozonation has been extensively applied for the decomposition of organics in water and wastewater. The effluents from pulp and paper industry contain a number of toxic compounds especially phenols and its chlorinated derivatives. The paper making process utilizes a large amount of water and their effluents laden with xenobiotic organics are directly discharged into surface water streams, posing deleterious effects to aquatic

life. Catalkaya and Kargi (2007) utilized ozonation process as a pre-treatment operation for effluents from a pulp mill in Turkey. The method was regarded as effective for the removal of colour from the effluent. Chelme-Ayala et al. (2010) employed the ozonation process for the treatment of pesticides present in a membrane concentrate from a membrane plant in Alberta, Canada. The workers recorded removal efficiency of 87% for bromoxynil and 63% for trifluralin from the concentrates. A good number of articles published on the application of ozonation for the treatment of various organics in wastewater can be found in the literature (Consejo et al., 2005, Dombi et al., 2002, Schröder and Meesters, 2005, Wu et al., 2004). The major limitation to the use of O_3 for water treatment lies with the operational cost of the process itself. O_3 is an unstable gas with a lifetime spanning only a few minutes when in water. It therefore has to be produced in-situ when required. Also, its application requires well-designed gas-liquid contacting devices to bring about effective mass transfer of O_3 from the gas phase to liquid phase.

2.3.1.2 Oxidation using hydrogen peroxide

Oxidation by peroxide (H_2O_2) alone is not regarded as an AOP because H_2O_2 is not a radical. Hydrogen peroxide is stable in water and oxidation is based on the intrinsic oxidative power of the peroxide molecule being a natural oxidizing agent. However, in practical applications, H_2O_2 undergoes solar photolysis, providing radicals in a way similar to UV photolysis of H_2O_2 and as such the participation of the $OH^{\bullet}$ during H_2O_2 oxidation cannot be ruled out. The process of H_2O_2 breakdown without a catalyst is slow and has been largely regarded as ineffective for the treatment of organics in wastewater. In a study by Coca et al. (2007), peroxide alone added to brown coloured molasses obtained from a fermentation factory in Spain, did not bring about any change in colour of the wastewater even after 18 hours of contact. Continued stepwise addition of peroxide (0.02 M) up until 23 hours also did not lead to a significant change in the brown colour of the syrupy wastewater. The use of UV combined separately with chlorine and H_2O_2 as a novel AOP for the treatment of trichloroethylene in drinking water was evaluated by. *Wang et al. (2012)*. In their study, the rate of trichloroethylene decay by UV, UV/chlorine and UV/H_2O_2 at different pH values were studied and compared. They reported that the UV/chlorine process was more efficient than the UV/H_2O_2 process at pH 5, but in the neutral and alkaline pH range, the UV/H_2O_2 process became more efficient. An earlier article published by Prado and Esplugas (1999) had shown that the formation

of hydroxyl radical by hydrogen peroxide in the absence of UV light was only favourable at high pH. They reported the effect of varying pH on the oxidation of atrazine (a pesticide) by H_2O_2. At pH 4.8 and 6.8, atrazine removal of 4% and 9% (respectively) was observed over a 24-hour period. However, at higher basic pH (11.4), a 100% removal of the pesticide was achieved within 180 minutes. The mechanism of generation of the radicals suspected to be involved in the oxidation process at high pH has however not been investigated.

In another study, Yasar and co-workers in Pakistan studied the use of H_2O_2 (a well known disinfectant) for the immobilization of pathogens in industrial effluents (Yasar et al., 2007). Results obtained under optimized oxidant dose of 170 mg/L showed that the oxidant was capable of removing 99% of the pathogens present in the wastewater. As a drawback to its use the authors highlighted that pathogens immobilized by H_2O_2 were reactivated after an incubation period, which varied depending on the reaction condition. This problem was overcome when H_2O_2 was used in combination with other processes such as UV and O_3.

Bases on the findings of the referenced literature, we may infer that the use of H_2O_2 for water treatment is significantly affected by pH and only effective at alkaline pH. Also, when applied as a disinfectant for living cells (pathogens), colony regrowth is only suppressed when H_2O_2 is used in conjunction with other processes. Another disadvantage of this process is the presence of residual peroxide, which may require further attention after the water treatment itself. Some other researchers have reported the use of peroxide as an oxidant for organics (Ikematsu et al., 2004, Ledakowicz et al., 2006).

2.3.1.3 Fenton and Fenton-like processes

More than a century ago, H. J. Fenton described the oxidation power of H_2O_2 on certain organic molecules in which OH radicals are produced from H_2O_2 in the presence of Fe (II) as catalyst. Later on, a reaction mechanism was proposed by Walling and is illustrated by equations 9-11 (Walling, 1975).

Equation 2.9

$$Fe^{2+} + H_2O_2 \longrightarrow Fe^{3+} + OH^- + OH^{\bullet}$$

Equation 2.10

$$Fe^{3+} + H_2O_2 \longrightarrow Fe^{2+} + H^+ + HOO^{\bullet}$$

Equation 2.11

$$Fe^{2+} + OH^{\bullet} \longrightarrow Fe^{3+} + OH^-$$

The renewed interest of researchers for this classical reactive system is today underscored by a significant number of investigations devoted to its application in wastewater treatment. Due to its simplicity (requiring neither special apparatus nor reactants), the Fenton process is one of the most widely applied and researched processes for treatment of recalcitrant compounds. Mandal *et al.* investigated the use of Fenton reagent for the degradation of wastewater collected from industrial effluent plants in India (Mandal et al., 2010). They investigated the effect of operating variables such as pH, temperature, peroxide and Fe (II) dose for the reduction of chemical oxygen demand (COD) in the wastewater sample. The Fenton process requires strict pH control and several published data places optimum pH for the process in the range: 2.5 - 3.5. The authors observed that at optimized conditions of pH 3, Fe (II) 6 mg/L, and peroxide dose of 220 mg/L, the COD removal after 30 min was 90%. Extending the time to 24 hours only increased the COD removal by an additional 5%. It was therefore suggested that the process be used in combination with biological treatments for total removal of organics in the wastewater, as it was ineffective for low concentrations of the organic substances in their study. Chen *et al.* also utilized the Fenton process for the degradation of model pollutant (salicylic acid) in aqueous solution. Salicylic acid removal efficiency under optimized conditions was 96% after 150 min, and COD reduction was 80%. As shown by the results, the Fenton process was effective for the degradation of salicylic acid. The complete mineralization was however not as efficient as the degradation of the pollutant (Chen et al., 2010). Several other reports concerned with the application of Fenton process for the amelioration of organics in wastewater abound in the literature (Faouzi et al., 2006, Sun et al., 2008, Tambosi et al., 2009). All processes which involve the use of Fe^{3+} ions (either as hydroxyl complexes or as oxalate complexes) or oxidizing metals such as manganese (as permanganate) are referred to as Fenton-like processes. Especially important amongst them is the ferrioxalate complex, which has a strong absorption at wavelengths above 400 nm and therefore undergoes reactions that can be photo-catalysed by visible light. The photo degradation of hydroxyl and oxalate complexes of Fe (III) generate Fe^{2+} ions

which catalyses the decomposition of H_2O_2 to OH radicals. Equation 2.12 - Equation 2.16 shows the participation of Fe as oxalate in the production of hydroxyl radical.

Equation 2.12

$$Fe(OH)^{2+} + hv \longrightarrow Fe^{2+} + OH^{\bullet}$$

Equation 2.13

$$Fe(C_2O_4) + H_2O_2 \longrightarrow Fe\,(C_2O_4)^{+} + OH^{\bullet} + OH^{-}$$

Equation 2.14

$$Fe(C_2O_4)_3^{3-} + hv \longrightarrow Fe^{2+} + 2{C_2O_4}^{2-} + {C_2O_4}^{-\bullet}$$

Equation 2.15

$$Fe(C_2O_4)_3^{3-} + {C_2O_4}^{-\bullet} \longrightarrow Fe^{2+} + 3{C_2O_4}^{2-} + 2CO_2$$

Equation 2.16

$${C_2O_4}^{-\bullet} \longrightarrow CO_2 + CO_2^{-\bullet}$$

Additionally, other free radicals and active species are generated as shown by Equation 16. A significant advantage of the Fenton-like process is the avoidance of Fe^{3+} sludge associated with the classical Fenton process.

2. 3. 1. 4 Ozone/H_2O_2 (peroxone) process

H_2O_2 in an aqueous solution is partially dissociated to hydro-peroxide ion (HO_2^-), which reacts with ozone giving rise to a series of chain reactions involving OH radicals (Al Momani, 2007). Equation 2.17 and Equation 2.18 illustrate the direct attack of O_3 by H_2O_2 and hydro-peroxide ion to give OH radicals and HO_2 radicals, respectively (Al Momani, 2007). The efficiency of the peroxone process is based on the generation of these radicals.

Equation 2.17

$$H_2O_2 + 2O_3 \longrightarrow 2OH^{\bullet} + 3O_2$$

Equation 2.18

$$HO_2^- + O_3 \longrightarrow HO_2^{\bullet} + O_3^{\bullet}$$

The hydro-peroxide ion produced by the decomposition of H_2O_2 reversibly recombines with hydrogen ions in solution to give H_2O_2 (Equation 2.19)

Equation 2.19

$$HO_2^- + H^+ \rightleftharpoons H_2O_2$$

Indeed the decomposition of ozone at high pH also produces the hydro-peroxide ion, which reversibly produces peroxide as shown by Equation 2.2. The external addition of H_2O_2 to aqueous solution of ozone would therefore enhance the decomposition of ozone to give OH radicals according to the Le' Chatelier principle. The influence of pH is also evident since in the ozone decomposition mechanism the active species is the conjugate base OH_2^- whose concentration is strictly dependent on pH. An increase in pH and addition of H_2O_2 to an aqueous solution of ozone would thus result in higher hydroxyl radical production and the attainment of a higher steady state concentration of OH in the radical chain decomposition process. It is worthy to note that the adoption of this AOP does not bring about a significant change in the apparatus or industrial reactor since it is only necessary to add an H_2O_2 dosing system. Cortez and co-workers applied the peroxone system for the treatment of landfill leachates in Portugal with the aim of increasing the biodegradability of the treated leachate in a combined chemical/biological process (Cortez et al., 2011). While both ozonation and peroxone process significantly improved the biochemical and chemical oxygen demand ratios (BOD/COD), implying improved biodegradability, the peroxone process presented higher ratios and hence higher biodegradability of the treated leachates. The application of one process over the other would therefore depend on the running cost of chemicals weighed against the desired quality of effluent required for subsequent biological treatment. The use of ozone in combination with H_2O_2 has been widely accepted to increase the generation of the non-selective $OH^{\bullet}$ during ozonation, leading to improved elimination of refractory organic compounds (Rahman et al., 2010b, Coca et al., 2005, Sánchez-Polo et al., 2007).

2.3.2. Homogeneous AOPs using UV

Homogeneous AOPs using UV radiation are generally applied for the degradation of compounds that adsorb UV radiation. These are usually dyes and aromatic

hydrocarbons capable of absorbing UV energy. As previously mentioned, the UV is not considered a separate phase from the aqueous medium to which it is applied.

2.3.2.1 UV/Ozone

Advanced oxidation processes using ozone and UV proceeds via the photolysis of aqueous ozone to produce hydroxyl radicals as shown by the reaction presented in Equation 2.20 - Equation 2.21. The aqueous solution is irradiated with UV light at a wavelength of 254 nm for ozone absorption. At this wavelength, the extinction coefficient of ozone is 177 times greater than that of peroxide.

Equation 2.20

$$H_2O + O_3 + UV \rightarrow 2OH^{\cdot} + O_2$$

Equation 2.21

$$2OH^{\cdot} \longrightarrow H_2O_2$$

This method has been used for the degradation of phenol at (Catorceno et al., 2010). Results were compared with processes run without the use of UV radiation. The comparison showed the effect of UV radiation on the oxidation process. The UV/O_3 process was capable of 99.2% removal of dissolved organic carbon as compared to O_3 alone (58.2%). Some researchers have equally applied this method for the degradation of carbamazepine, clofibric acid, diazepam and diclofenac, and monitored the degradation products by liquid chromatography-mass spectrometry (LC-MS) (José et al., 2010). They reported a complete removal (100%) of these recalcitrant pharmaceuticals (except for diazepam) under simultaneous ozonation and UV photolysis. Haloacetic acid and trihalomethanes are a major group of disinfection by-products and have been identified as carcinogens. The UV/O_3 was reported to have been suitable for the mineralization of trichloro- and dichloroacetic acids, which are classical haloacetic acids, produced during disinfection of water by chlorination (Wang et al., 2009b).

2.3.2.2 UV/ H_2O_2

The use of UV to bring about photolysis of hydrogen peroxide has also been adopted for the treatment of wastewater contaminated with a wide range of organics. This process entails the photolytic symmetrical splitting of a molecule of

peroxide to give two hydroxyl radicals as shown by Equation 2.22. Typical UV absorption of H_2O_2 is at 257 nm.

Equation 2.22

$$H_2O_2 + UV \longrightarrow 2OH^{\cdot}$$

UV/H_2O_2 system can totally mineralize any organic compound reducing it to CO_2 and water. However, in real-life scenarios, such a drastic process is not necessary. The toxicity of oxidation products is not a problem since they are easily biodegraded (Vogelpohl, 2007). The major drawback of this process is the smaller extinction coefficient of H_2O_2, which is 18.6 $M^{-1}cm^{-1}$ at 257 nm, thus only a relatively small fraction of the incident UV light is exploited for AOP. Nevertheless, several studies have been carried out to optimize this process for purification of water. This is justified by the relative ease of handling H_2O_2 and the cost of chemicals. The use of UV/H_2O_2 for the detoxification of raw textile wastewater prior to biological treatment with dehydrogenase has been reported (Ledakowicz et al., 2001). The decrease in inhibitory effect from 30% when UV was used alone to 26% for UV/ H_2O_2 was attributed to the synergistic effect of the combined treatment. The raw wastewater inhibited the enzyme activity by 47%. They concluded that the AOP was an effective method for detoxification of textile wastewater. The positive impact has been demonstrated by a significant decrease of inhibitory action of microbial growth on activated sludge during subsequent biodegradation. Kestioglu et al. (2005) applied the UV/H_2O_2 process for the treatment of raw effluent from an olive mill treatment plant in Turkey. They obtained effluent possessed a low pH (<2), a high COD (10 240 mg/L) and a high total phenol content (975 mg/L). Treatment periods of 400 and 1440 minutes reduced the COD to 3060 and 3650 mg/L, respectively. The total phenol for optimized peroxide dose was also reduced to 22 and 10 mg/L, respectively, accounting for 99% of COD and phenol removal. The use of this method as an AOP for treating contaminant in wastewater has also been reported in other studies (Benitez et al., 2000a, Cañizares et al., 2008, Sauer et al., 2006, Thiruvenkatachari et al., 2007).

2.3.2.3 UV/Fenton process (Fe^{2+}/UV/ H_2O_2)

The rate of degradation of an organic pollutant with Fenton and Fenton like reagents is strongly accelerated by irradiation with UV-Vis light (Çatalkaya and Sengül, 2006,

Prato-Garcia et al., 2009). This is an extension of the Fenton process, which takes advantage of energy derived from photons in UV-Vis irradiation at wavelength values higher than 300 nm. In these conditions, the photolysis of iron (III) hydroxide complex that is the product of Fenton process (Equation 2.11), allows for the regeneration of Fe^{2+}as given by Equation 2.23.

Equation 2.23

$$Fe(OH)^{2+} \overset{h\nu}{\rightarrow} Fe^{2+} + OH^{\bullet}$$

In this scheme using UV radiation, Fe^{2+} acts as a real catalyst as it is regenerated and recycled during the production of radicals after reaction with H_2O_2. Another advantage of this process is the reduction in the formation of Fe^{3+} sludge, which is associated with the conventional Fenton process. Despite the great deal of work devoted by researchers to these processes, scanty indications have been found about their industrial application. This is not surprising since the application of the Fenton processes requires strict pH control. Generally, pH range between 2.5 and 3.0 are regarded as the best for this system. Huang et al. (2008) studied the oxidation of dye-reactive black-B using the UV/Fenton process and compared the results with experiments run for the Fenton and an electro-Fenton process. UV light source was from a UV-A lamp, wavelength 365 nm, and dye concentration was 10,000 mg/L. Optimum pH for the process was established as 2.5 and mineralization was found to be 98%. The synergistic effect of the UV light was apparent when compared to the Fenton process, which brought about a 78% mineralization. They also identified two degradation intermediates i.e. oxalic acid and formic acid. While the process readily mineralized the formic acid, the oxalic acid intermediate was more resistant to the chemical treatment.

The degradation mechanism of carbofuran (2, 3-dihydro-2, 2-dimethylbenzofuran-7-ylmethylcarbamate), a frequently used carbamate derivative pesticide considered a priority pollutant, using the UV/Fenton process, was reported by Javier Benitez and co-workers (2002). The carbamate concentration was 4.52 x 10^{-4} M, temperature 20^{o}C and pH 3. At H_2O_2 and Fe^{2+} concentrations 50 x 10^{4} and 5 x 10^{-4} M, respectively, the process brought about a complete mineralization of carbofuran in 5 minutes, with a rate constant 30 times higher than a similar experiment conducted in the absence of UV radiation. The authors concluded that the synergic effect observed in the photo-Fenton system was due to the generation of OH radicals in

several reactions and to the catalytic character of the Fenton's reaction in the presence of UV radiation. Other relevant discussions on the use of this process are well presented in the literature (Kusvuran and Erbatur, 2004, Liou et al., 2003, Muñoz et al., 2006, Saritha et al., 2007).

2.3.3. Homogeneous AOP using ultrasound (Sonolysis)

The formation of OH radicals when ultrasounds are used is due to high temperature and pressure conditions that are reached inside the bubbles generated by the ultrasounds. The process is based on the 'hot-spot' theory (localized generation of extreme conditions of temperature and pressure). According to the theory, sonolysis causes liquid cavitation giving rise to high-energy bubbles, which collapse generating radicals. In the case of reactions where the controlling mechanism is the radical attack, the use of hydrogen peroxide and ozone enhances the degradation due to generation of additional free radicals. Generally, this type of AOP reduces cost since no radiation is needed, and can be readily combined with other methods. Sonolysis has been reported to be safe, sludge free and without the generation of secondary pollutant. It has the ability to penetrate cloudy waters and presents better energy conservation schemes. Despite its advantages, there are technical and economic challenges limiting the scale-up and adoption of this technology for industrial wastewater treatment. The technology necessary is still in its budding stage, and not well developed as other options.

The reactions that occur in the presence of ozone and ultrasound (represented as '))))') are shown in Equations 24-31 (He et al., 2007, Mark et al., 1998)

Equation 2.24

$$H_2O \overset{)))}{\rightarrow} H^{\bullet} + OH^{\bullet}$$

Equation 2.25

$$O_3 \overset{)))}{\rightarrow} O_2 + O$$

Equation 2.26

$$O + H_2O \longrightarrow 2OH^{\bullet}$$

Equation 2.27

$$O_3 + OH^{\bullet} \longrightarrow O_2 + HO_2^{\bullet}$$

Equation 2.28

$$O_2 + H^{\bullet} \longrightarrow HO_2^{\bullet}$$

Equation 2.29

$$O_3 + HO_2^{\bullet} \longrightarrow 2O_2 + OH^{\bullet}$$

Equation 2.30

$$OH^{\bullet} + OH^{\bullet} \longrightarrow H_2O_2$$

Equation 2.31

$$HO_2^{\bullet} + OH^{\bullet} \longrightarrow H_2O + O_2$$

He et al. (2008) used this ultrasound method to achieve effective degradation of p-aminophenol, an intermediate in the production of paracetamol. For an initial p-aminophenol concentration of 10 mmol/L, a degradation efficiency of 99% was achieved within 30 min. Mineralization of the p-aminophenol was 77% at this time. Ozone dose was at 5.3 g/h at 25^{o}C with a pH of 11 and an ultrasonic energy density of 0.3 W/mL. It was observed that the degradation was influenced by the pH, temperature and ozone dose, but unaffected by an increase in energy density per unit volume of the ultrasound energy. By combining ultrasounds and H_2O_2, it was possible to achieve the formation of free radicals in gaseous phase of the cavitation bubbles formed during the sonication. Proposed mechanism for the production of free radicals was given by Shemer and Narkis (2005) and is shown in Equation 2.32 - Equation 2.34.

Equation 2.32

$$H_2O_2 \overset{)))}{\rightarrow} OH^{\bullet} + OH^{\bullet}$$

Equation 2.33

$$H_2O_2 + O_2 \overset{)))}{\rightarrow} 2HO_2^{\bullet}$$

Equation 2.34

$$H_2O_2 + OH^{\bullet} \longrightarrow HO_2^{\bullet} + H_2O$$

2.3.4. Homogeneous process using solar energy

The current trend in energy management is to develop technologies that run on renewable energies. Especially important in this regard are those that run on the universally abundant solar energy. The radiant energy from the sun consists of a wide band of energized photons capable of generating hydroxyl radicals via the photolysis of peroxide in a manner similar to the use of UV-Vis light source. The non-selective radical generated then degrades the organics pollutant. Muruganandham and Swaminathan (2007) investigated solar energy as energy source to drive the photolytic cleavage of H_2O_2 and Fenton process was by far the de-colorization of reactive yellow-14 (dye). Heterogeneous and homogeneous experiments were carried out under sunny conditions in borosilicate glass tubes with solar irradiation in open-air condition. Solar intensity was measured every 30 minutes using a LT Lutron LX-10/A (digital Lux meter) and the average light intensity over the duration of the experiment was calculated. They reported that the use of solar irradiation in the presence of H_2O_2 enhanced the de-colorization of the dye solution resulting in an increase in the percentage removal from 12.7% for peroxide alone to 71.2% in solar-peroxide experiments. The reaction has been more favourable at lower pH. The percentage removal of the dye using the Fenton process in the presence of solar energy also rose from 73.7% to 80.3%. In another experiment using solar energy and TiO_2, the dye removal after 80 minutes was 82.1%. In a solar/TiO_2 process, TiO_2 utilizes UV part of the solar spectrum (wavelength shorter than 380 nm) to produce e- and h^+ (positive holes). The highly oxidative h^+ (E^o = 2.7 eV) directly reacts with the surface adsorbed dye molecule or directly oxidizes the organic compounds via formation of OH radical. Studies on the effect of solar light intensity on the de-colorization showed that an increase of the solar light intensity from 700 to 1250 Lux increases the decolourization from 73.2% to 91.25, 85.3 to 93.4% and 28.7 to 42.1% for solar/TiO_2, solar/H_2O_2/Fe^{2+} and solar/H_2O_2 processes, respectively. The enhancement of removal was attributed to increase in hydroxyl radical production. Light intensity determines the amount of photons adsorbed by the catalyst. With the increase in the solar power, the catalyst absorbs more photons and produces more hydroxyl radicals. While the heterogeneous process produces a lightly lower removal percentage compared to the homogenous process, the possibility of catalyst recovery and reuse makes the heterogeneous process more attracted compared to the homogeneous Fenton process. Moreover, the presence of residual Fe – ions in treated solutions using the

Fenton process would require additional ion exchange removal systems, incurring additional operational cost.

Sun and co-workers also applied the solar/Fenton process for removal of *p*-nitroaniline from aqueous (Sun et al., 2008). Solar experiments were carried out on sunny days in water cooled double glass cylindrical jacket reactors. The results for degradation of *p*-nitroaniline in water showed that *p*-nitroaniline is hardly decomposed by solar/H_2O_2. However, in both Fenton and solar/Fenton process, *p*-nitroaniline could be degraded effectively with degradation efficiency of 91 % and 99 %, respectively. The low removal of the process is in line with reports by Muruganandham and Swaminathan and would suggest that solar energy alone does not generate sufficient radicals from H_2O_2 breakdown to effect water treatment (Muruganandham and Swaminathan, 2007). In view of the problems with homogeneous process, possible interest in research would be to develop heterogeneous catalyst with solar energy harnessing potential superior to TiO_2 with an interest in harnessing the abundant energy in visible light.

2.3.5. Wet oxidation process using thermal energy

The wet oxidation (WO) also referred to as wet-air oxidation (WAO) or subcritical oxidation process is another effective method extensively used in industrial oxidation to treat hazardous waste and heavily polluted effluents. The process was pioneered by Strehlenert in 1911(Kusvuran et al., 2004). It differs from the rest of the other conventional AOPs not only in terms of operating conditions but also in the concentration of the pollutant present in the wastewater. They are mainly used for concentrated wastewaters in order to allow auto-thermal operation and thus reduction in operating cost. The basic idea of WO is the oxygenation of organic and/or oxidizable inorganic-containing materials in fluid phase to inorganic or smaller molecular organic matter using air or pure oxygen as oxidant at upper temperatures (125-350^{o}C) and pressures (0.5-20 MPa). In WO processes, elevated temperatures and pressure increase the concentration of dissolved oxygen and enhance the contact between molecular oxygen and organic matter Debellefontaine and Foussard (2000) and thus the oxidation rate. Although the degree of oxidation in the process is dependent on the process conditions, retention time and feed composition, WO can treat a variety of organic waste, domestic sludge and even those produced by various branches of industrial activity.

The process can be coupled with a biological treatment facility, and unlike incineration, is not handicapped by a bad ecological image. The technique, however, requires a high first investment capital, but the operating cost is moderate as compared to other AOPs. Variants of this technique are the supercritical water oxidation (SCWO), which operates at T ≥ 375^{o}C and P ≥ 22.1 MPa, and the wet peroxide oxidation (WPO) which substitutes hydrogen peroxide for oxygen as the active oxidant, efficiently reducing the running cost. Hydroxyl radicals are formed when hydrogen peroxide decomposes on heterogeneous surface of the reactor, or on other heterogeneous species present in the reactor. García-Molina et al. (2005) applied the wet peroxide oxidation for the treatment of solutions containing 4-chlorophenol (4-CP) and 2,4-dichlorophenol (2,4-DCP). At the three tested temperatures of 100, 130 and 160^{o}C, the percentage removal of 4-CP was 100% using 2.5 mL and 5 mL of H_2O_2 in 200 mL solution of 4-CP (1000 mg/L). The total mineralization was however not complete as TOC values for 4-CP were as low as 70%. 2,4-DCP was tested at two temperatures (100 and 130^{o}C) owing to its volatility to the gas phase at 160^{o}C. At 5 mL H_2O_2, again a complete removal (100%) was reported with TOC values of 72.1 and 75.5% for the two temperatures, respectively. Lower concentrations of H_2O_2 had TOC values as low as 58.5%. Identified intermediates include phenol, hydroquinone and benzoquinone. Kusvuran and co-workers also employed the WO process for decolourization of a solution of reactive red-120 (azo-dye) in aqueous solution. Reactor operating temperature was varied between 200 and 300^{o}C with a constant temperature of 17 bars. The degradation of the dye was markedly improved by increasing temperature from 200 to 300 ^{o}C. At 250^{o}C and 17 bar, the substrate was completely removed after 20 min treatment. The temperature had the major effect on the reaction rate and the half-life of the organics (Kusvuran et al., 2004).

2.3.6. Oxidation using microwave energy

Microwave technology has emerged as a promising technique based on physical, chemical and biological methods for the treatment of wastewater and waste activated sludge. When applied as an energy source for AOPs, the microwave radiation provides not only a heat source (the thermal effect) but also a specific effect (the non-thermal effect). Marken and co-workers suggested that this effect leads to an enhanced photo-assisted degradation of several substrates (Marken et al., 2000). The non-thermal effect can lead to an increased number of charge on a

metal oxide such ad TiO_2, as well as induce formation of traps that can prolong carrier lifetimes and lead to additional quantities of $OH^{\bullet}$ produced in TiO_2 photo-assisted oxidations in water. This secondary non-thermal effect of microwave on nanoparticles would prove useful in the fields of environmental management and pollution control.

In order to investigate the non-thermal effect of microwave in AOP, Horikoshi and co-workers developed and applied a microwave discharge electrodeless lamp (MDEL) an AOP for the degradation of 0.05 M 2,4-dichlorophenoxyacetic acid (a herbicide: 2,4-D) (Horikoshi et al., 2007). Degradation of the herbicide was monitored spectrophotometrically by the loss of UV absorption at 204 nm and also by reduction in total organic carbon (TOC). Efficiency of the MDEL was compared with those for conventional microwave (MW) energy source and UV lamp (Hg source). The authors observed that microwave discharge electrodeless lamp (MDEL) gave superior results when compared to the conventional UV lamp or the microwave source. The workers identified lamp proximity to substrate solution as an important variable for the reaction process. This is expected since heat transfer from the lamp (thermal effect) would be greatly reduced with increasing distance of the lamp from the reactor setup. TiO_2 was also tested with success as a potential catalyst for sequestering microwave energy generated from the MDEL. The authors went on to propose that the MDEL electrodeless lamp introduced a non-thermal effect into the microwave technique, which would prove to be an attractive innovation when developed for attenuation and disposal of environmental contaminants.

In another experiment utilizing the microwave technique, Wang and co-workers applied the microwave–H_2O_2 AOP for the pre-treatment of sewage sludge obtained from Gaobeidian municipal sludge process plant in Beijing, China (Wang et al., 2009c). The effect of catalase on the efficiency of the process was investigated. Catalase present as a biological component of the sludge is a terminal respiratory enzyme, which attacks H_2O_2, breaking it to molecular O_2 and 2 electrons (Guwy et al., 1998, Guwy et al., 1999). By monitoring the reduction of residual H_2O_2 with increasing temperatures, the workers were able to establish that the activity of the catalyst was significantly reduced above $45^{o}C$. Compared to control experiments, a considerable increase in sludge solubilisation with increasing temperatures was also observed. The degree of sludge solubilisation was strongly affected by H_2O_2 ratios

with increasing amounts of soluble COD and TOC being8 released into the supernatant as H_2O_2 dosing ration increased. Although the AOP (microwave/H_2O_2) was effective for sludge pre-treatment in the study, there were still high concentrations of residual H_2O_2 in the sludge, ranging 436-18773 mg H_2O_2/L. The higher the H_2O_2/TCOD dosing ratio was, the lesser the amount of H_2O_2 that was consumed by the process. The proper evaluation of residual H_2O_2 would therefore prove crucial in the practical application of this AOP.

2.3.7. Heterogeneous catalytic oxidation

In recent years, there has been an enormous amount of research and development in the area of heterogeneous catalytic and photo-catalytic water purification processes due to their effectiveness in degrading and mineralizing recalcitrant organic compounds as well as the possibility of utilizing solar, UV and visible spectrum. Applied catalysts include activated carbon, tempered metals, and metal oxide nanoparticles. Several research projects have been directed at advancing the synthesis and functionality of various sizes and shapes of semi-conductor and metal nanoparticles. The objectives of these projects are mainly to improve the performance and utilization of nanoparticles in various applications, which include the AOPs. While the mechanism of mineralization using activated carbon in AOP is by adsorption on the carbon surface followed by rapid oxidation of concentrated pollutant on the carbon interface, the mechanism for metals and nanoparticles in AOP is by complex photo- or thermal- initiated redox reactions which lead either to direct mineralization of the organics or the generation of free radicals with subsequent mineralization.

Heterogeneous catalyst utilized in AOP may be applied in one of three modes:

(1) As catalyst applied in photo-processes to bring about photo-catalytic degradation of an organic substrate (when used alone with UV light) or with other AOP such as UV/ozonation or UV/Fenton

(2) As hetero-catalyst at elevated temperatures to catalyse wet oxidation processes

(3) As hetero-catalyst at ambient temperatures and pressure to catalyse an optimized AOP such as ozonation, Fenton or peroxone processes.

2.3.7.1 Heterogeneous photo-catalysis

The most common nanoparticle applied as a heterogeneous photo-catalyst in AOP is TiO_2. To this end, a vast number of articles have been devoted to studies of the application of this oxide to various pollutants, and in combination with other processes such as the ozonation and ultrasound-assisted-photolytic processes (Madhavan et al., 2010a, Madhavan et al., 2010b). Others heterogeneous catalyst applied in AOP include: ZnO, SnO_2, Al_2O_3, In_2O_3, ZnS, Fe_2O_3, CeO_2, ZrO_2, SiO_2, CuO, MnO_2 and CdS (Ahmed et al., 2011, Ahmed et al., 2010). While the physical, chemical and catalytic properties of these catalysts vary markedly; the principle of operation as photo-catalysts remains the same. The adsorption of electromagnetic energy (in the UV or visible region) by electrons on the surface of a photo-catalyst brings about an excitation of these surface electrons. When the energy absorbed is greater than the band-gap energy (ΔE), the excited electrons move from the valence-band to the conduction-band. This mechanism generates active species, which promotes redox reactions. The absorption of photons with energy lower than ΔE or longer wavelengths usually causes energy dissipation in the forms of heat.

2.3.7.1.1 Photo-catalytic oxidation

Early applications of photo-catalyst include coating of self-cleaning windows and windshields, and floor-tiles, which have been used in hospitals to reduce the density of colonies of microorganisms in hospital walls and floors. They have also been applied in architectural constructions, producing deodorizing, mold-preventing and self-cleaning surfaces (Heller, 1995). Subsequent application extended poto-catalytic oxidation to water purification for removal of organics in water. The use of UV/TiO_2 for the treatment of dye solutions and other refractory organic pollutants in water has been reported (Sauer et al., 2006, Mascolo et al., 2008, Lachheb et al., 2008). Mascolo and co-workers applied the UV/TiO_2 process for the removal of methyl-*tert*-butyl-ether (MTBE) from (I) laboratory prepared solutions containing MTBE and (II) ground water samples containing MTBE collected from a petrochemical site in Southern Italy. The workers reported that the process was most suitable for the simulated wastewater and recommended that particular care should be taken when extrapolating organic degradation results obtained from synthetic aqueous solutions (Mascolo et al., 2008).

Saritha and co-workers applied the UV/TiO_2 process for the removal of 4-chloro-2-nitrophenol, a USEPA listed pollutant, widely available in bulk drug and pesticide wastes. Under similar operating conditions, results for the UV/TiO_2 process were superior to the UV/H_2O_2, Fenton, peroxide and UV processes. The UV/TiO_2 process brought about an 85% mineralization of the pollutant in 120 minutes. In the absence of TiO_2, UV mineralization was very slow because 4-chloro-2-nitrophenol undergoes light absorptions, which do not contribute to the removal of the compound (Saritha et al., 2007). Due to surface are limitations and poor adsorption capacity of TiO_2 (resulting from its non-porous nature), present research is directed towards incorporating photo-catalysts on porous supports which would absorb target environmental pollutants more efficiently prior to subsequent oxidation by the photo-catalyst (Fatimah et al., 2010, Papoulis et al., 2010, Ökte and Yilmaz, 2009).

In line with this trend, subsequent researches were devoted towards supporting TiO_2 on materials such as montmorillonite (Chen et al., 2011) and sepiolite (Karamanis et al., 2011) with a view of shortening the absorption band gap of TiO_2 and improve its photo-catalytic character. A recent review highlights the roles of titanium and ion-doped titanium oxide on photo-catalytic degradation of pollutants in aqueous solutions (Teh and Mohamed, 2011).

2.3.7.1.2 Photo-catalytic ozonation

According to Tanaka and co-workers, Equations 35-38 may represent the basic mechanism of photo-catalytic ozonation (Tanaka et al., 1996, Tanaka et al., 2000);

Equation 2.35

$$TiO_2 \xrightarrow{h\nu} h^+ + e^-$$

Equation 2.36

$$O_3 + e^- \rightarrow O_3^-$$

Equation 2.37

$$O_3^- \rightarrow O_2 + O^-$$

Equation 2.38

$$H_2O + O^- \rightarrow OH^- + OH^\bullet$$

Even though the actual mechanism may be more complicated as illustrated by earlier research (Ruppert et al., 1994), the principle has been widely applied for the

treatment of environmental pollutants in water (Beltrán et al., 2009, Beltrán et al., 2010). The $UV/TiO_2/O_3$ process was reported to be superior to O_3, UV/O_3, and $UV/TiO_2/O_2$ process for the degradation of neonicotinoid insecticide in water. The synergistic effect of O_3 on TiO_2 was evident at neutral and acidic pH. At basic pH, decomposition of O_3 by reaction with OH^- was the prevailing mechanism for OH radical production (Cernigoj et al., 2007, Rajeswari and Kanmani, 2009). A similar synergistic effect was also reported for the photo-catalytic ozonation of dimethyl phthalate using laboratory prepared TiO_2 (Jing et al., 2011). The rate constant for the $UV/TiO_2/O_3$ process was 2.5 times more than that in $UV/TiO_2/O_2$ (UV/O_3) process. The TOC removal of the photo-catalytic ozonation process increased with increasing ozone dosage and was describe by the Langmuir-Hinshelwood model.

2.3.7.2. Heterogeneous wet oxidation

The application of heterogeneous catalyst to either the wet air oxidation (WAO, subsequently referred to as catalytic wet air oxidation, CWAO) or the wet peroxide (WPO, subsequently referred to as catalytic wet peroxide oxidation, CWPO) AOP (both described in section 2.3.5) have been reported (Arena et al., 2010, Benitez et al., 2011, Yu et al., 2011, Zhan et al., 2010). The application of proper catalysts for CWAO, not only reduces the severity of the reaction conditions but also more easily decomposes even refractory pollutants, thereby reducing capital and operational cost (Larachi, 2005). Heterogeneous catalysts applied in these processes possess high temperature, physical, chemical and mechanical stability. They would also possess a high resistance to attrition over a wide pressure and temperature range.

2.3.7.2.1 Catalytic wet air oxidation

Various heterogeneous catalyst including noble metals, metal oxides and mixed metal oxides have been extensively studied to enhance the efficiency of CWAO. In the three-phase CWAO process, organic pollutants are oxidized by activated O_2 species in the presence of a solid catalyst, forming biodegradable intermediates (such as low molecular weight carboxylic acids), or are mineralized to CO_2, water and associated inorganic salts. Several recently developed heterogeneous catalysts, including transition metal oxides and noble metals deposited on different supports, have shown good catalytic activity in CWAO of organic pollutants present in drinking and wastewater (Levec and Pintar, 2007). The use of mixed metal oxides for CWAO of phenol in water has been reported (Akyurtlu et al., 1998). Batch

experiments were run using varying combinations of copper, zinc and aluminium oxides in an autoclave and a paar reactor. The effect of operating variables such as catalyst loading, catalyst composition, temperature, oxygen partial pressure, initial phenol concentration and stirring speed was reported. The time required for total phenol conversion ranged from half an hour to two hours and was dependent on the experimental conditions. When the reaction between oxygen species and phenol was started from room temperature, the degradation was observed to proceed via two regimes. Firstly, an induction period was observed, after which there was a transition to a much higher activity regime. However, when the phenol was introduced after a preheating period of a solution saturated with oxygen, no induction period was observed.

An overview of the catalytic pattern of homogeneous (Cu^{2+}, Fe^{3+}, Mn^{2+}) and cerium - supported ($CuCeO_x$, $MnCeO_x$) transition metals in the CWAO of phenol has been reported (Arena et al., 2010). Catalyst test were carried out at 150^{o}C and 1.4 MPa using a PTF-lined autoclave containing 0.25 mL, 1000 mg/L phenol and operated in a semi-batch mode. The catalytic homogeneous wet air oxidations were observed to proceed via an unselective autocatalytic free-radical path leading to refractory C1-C2 acids, while the CWAO on heterogeneous ceria gave superior efficiency and was accounted for by the Langmuir-Hinshekwood (L-H) mechanism.

In another study, Yu and co-workers applied Ru supported on γ-Al_2O_3 and Ce/γ-Al_2O_3 for CWAO of isopropyl alcohol, phenol, acetic acid and N,N-dimethylformamide (Yu et al., 2011). The efficiency of the catalyst was observed to increase with increasing temperature. The Ru-Ce/γ-Al_2O_3 catalyst produced superior removal efficiency compared to the Ru-γ-Al_2O_3 for all the substrates studied and the efficiency was ascribed to a better dispersion of the Ru particles on the Ce/γ-Al_2O_3 surface as well as an increase in number of effectively active sites on the cluster-derived catalyst surface. The efficiency of platinum supported on activated carbon and on multi-walled carbon nano-tubes (CNT) as heterogeneous catalyst in CWAO of selected pharmaceuticals was investigated by Benitez and co-workers (Benitez et al., 2011). Supported platinum catalyst has been reported to be highly effective in the oxidation of organic compounds (Garcia et al., 2005, Mikulová et al., 2007). Operating variables such as catalyst type, dose, temperature (120-140^{o}C), and oxygen pressure (20-40 bar) were considered. There was significant enhancement in the removal of the pharmaceuticals using CWAO relative to WAO. Platinum

supported on activated carbon gave greater removal efficiency compared to platinum supported on CNT under the same conditions, reflecting the contribution of adsorption effects in addition to oxidation pathways for the removal of the pharmaceuticals under study.

A recent review by Kim and Ihm summarizes heterogeneous catalysts applied in wet air oxidation systems for the removal of refractory organic pollutants in industrial wastewater (Kim and Ihm, 2011). The review covers earlier application of CWAO to pollutants such as phenol and phenolic compounds, carboxylic acids, dyes, ammonia, and industrial waters. Also discussed in the review are reaction mechanisms and kinetics of CWAO and catalyst deactivation processes. Catalyst metals covered in the review include noble metals such as Ru, Rh, Pd, Ir and Pt as well as oxides of Cr, Mn, Fe, Co, Ni, Cu, Zn, Mo and Ce.

2.3.7.2.2 Catalytic wet peroxide oxidation

The mechanistic pathway for the generation of hydroxyl radicals from the decomposition of hydrogen peroxide proposed by Li *et al* involves the initiation of a chain reaction by the reaction of hydrogen peroxide with homogeneous or heterogeneous species present in the reactor system (Li et al., 1991). According to this suggested pathway, one way of improving the efficiency and yield of hydroxyl radicals, and thus lowering operating cost would be to introduce a heterogeneous catalyst into the reactor system. In view of this, several workers have applied various catalysts to WPO processes. Doocey and Sharratt applied iron-loaded zeolite for the removal of chlorinated phenolic waste from aqueous waste (Doocey and Sharratt, 2004). The efficient use of generated hydroxyl radicals is sustained by selective adsorption of the phenolic waste onto the iron-loaded zeolite followed, by in-situ Fenton oxidation by the hydroxyl radicals on the catalyst surface. This Fenton-type oxidation using iron supported on alumina and activated carbon has also been reported for the CWPO of halogenated organic compounds in ground water (Hofmann et al., 2005). Over the last decade, hydrotalcite-like compounds (HT), otherwise referred to as layered double hydroxide (LDHs) have received increasing attention owing to their diverse application especially in catalysis (Centi and Perathoner, 2008, Debecker et al., 2009). These compounds based on the mineral hydrotalcite have been synthesized and employed as catalyst in WPO processes (Kannan et al., 2005, Wang et al., 2009a). A typical application of hyrotalcites was in a CWPO of phenol by Cu-Ni-Al hydrotalcite where a synergistic

effect using the catalyst in the presence of hydrogen peroxide, brought about a complete (100%) removal of phenol within two hours when the system was operated at 30^{o}C (Zhou et al., 2011). When applied alone, the metal HT and hydrogen peroxide only brought about 15.7% and 39.7% removal of phenol, respectively. The effect of operating variables such as catalyst dose, temperature and oxidant/phenol ratio was also reported.

2.3.7.3 Heterogeneous catalysis at ambient conditions

Materials applied as catalyst at ambient conditions include activated carbon (GAC), metals supported on metal oxide surfaces (TiO_2, Al_2O_3, ZrO_3 and CeO_2, FeOOH, MnO_2, Cu-Al_2O_3, Cu-TiO_2) or supported on activated carbon. The catalyst support serves to increase the surface area of the catalyst, decrease sintering and improve hydrophobicity as well as the thermal and chemical stability of the material (Poyatos et al., 2010). Heterogeneous catalytic ozonation is an AOP in which the oxidative property of ozone is improved by adding solid catalytic materials. The process has been considered a potentially low cost AOP, which has been operated successfully at ambient conditions by several workers and may be relatively easier to apply in a water treatment plant (Ma et al., 2004, Rivera-Utrilla et al., 2008). It has been demonstrated that GAC can enhance ozone transformation into OH radicals (Ma et al., 2004). Electrons in the graphenic layers and basic surface groups on GAC are the main factors responsible for the decomposition of O_3 into $OH^{\bullet}$ (Sánchez-Polo et al., 2005, Sánchez-Polo et al., 2006). These generated hydroxyl radicals are responsible for the oxidation of organics using O_3/GAC process. Besides the catalytic role, GAC also serves as an important adsorbent for the organics being treated and would be effective for the removal of hydrophobic micro-pollutants that cannot be oxidized by ozone. Sanchez-Polo *et al.* applied the O_3/GAC AOP for the treatment of para-chlorobenzoate (pCBA) and compared the efficiency of this process with the conventional homogeneous ozonation in alkaline medium (pH 7 and 9) and peroxone processes (O_3/H_2O_2) (Sánchez-Polo et al., 2007). pCBA was selected for the study because of its low reactivity with O_3 (K_{O3}= 0.15 $M^{-1}s^{-1}$) and slow adsorption kinetics on GAC. Their report showed that the O_3/GAC system was inferior to the homogeneous processes. Radical generation in the heterogeneous system involved the adsorption of ozone onto the activated carbon and its subsequent breakdown to radicals. Since this process requires more than one phase, it is therefore slower compared to the homogeneous system where O_3 and

species such as OH^-, H_2O_2 or soluble metals initiates its breakdown are in the same phase. Despite this disadvantage, the use of heterogeneous catalyst for ozone breakdown is gathering interest. This is because the possibility of catalyst regeneration and reuse out ways the inefficiency of the heterogeneous process. More so, the use of metals in homogeneous process poses another problem as these metals whether toxic or not would require removal after the treatment process.

In a recent study, Oputu and co workers applied FeOOH as potential catalyst for removal of 4-chlorophenol from aqueous medium. While the catalyst showed potential, reducing reaction time by one-third, the possibility of metal leaching was of concern. Further work by the group was centred on supporting the catalyst on support NiO to eliminate the catalyst breakdown and increase possibility of reuse. The uses of catalyst supports have become the trend of heterogeneous catalysis (Oputu et al., 2015b, Oputu et al., 2015a).

2.3.8. Iron (Fe) as heterogeneous catalyst in ambient air oxidation (ozonation and Fenton reactions)

Iron exists in two oxidation states; II and III. Wustite (FeO) and hematite (Fe_2O_3) represent the well-known ores of iron in the II and III states, respectively. The various forms of magnetite (Fe_3O_4) e.g. Fe_4O_5 and Fe_5O_6 contain both Fe in II and III states. Iron oxy-hydroxides are the different forms of FeOOH (α-goethite, β-akaganite, γ-lepidocrocite, and δ-feroxyhte), green dust and schwertmannite. The latter two are complex +II and +III state oxides. Iron oxides and oxy-hydroxides are wide spread in nature, non-toxic, cheap and show catalytic properties. These factors have stirred the interest of researches in investigation of possible uses for iron oxides as catalyst in ambient air oxidation and ozonation reaction. The use of heterogeneous catalyst for Fenton reactions seems misplaced, as Fenton mechanism would inevitably require soluble Fe ions and consequently catalyst loss by dissolution. It is however important to understand the behavior of Fe ions generated from hetero-catalyst in Fenton reactions using hydrogen peroxide in order to understand certain observations in ozonation reactions. To this end, relevant literatures on heterogeneous Fenton processes are added to this section.

Chou and Huang (1999) previously reported goethite as a suitable iron source for Fenton reaction during the degradation of benzoic acid. In the presence of hydrogen peroxide (H_2O_2), radicals are generated due to breakdown of H_2O_2 on active sites on

γ-FeOOH surface. The workers observed an accelerated oxidation of benzoic with a reduction in pH (3.2), leading to a two stage kinetic plot for the reaction data. The increased oxidation of benzoic acid was attributed to the increased generation of hydroxyl radical by homogeneous iron (Fe) ions in solution. The term 'reductive dissolution' was used to describe the dissolution of γ-FeOOH during the degradation reaction.

H_2O_2 and O_3 are oxidizing agents, whose breakdown on metal surface lead to generation of radicals. The substitution of H_2O_2 with O_3 is therefore expected to yield radicals in suitable amounts to effect oxidation of aqueous organics. Park et al. (2004) applied α-FeOOH as catalyst in ambient air ozonation of para-chlorobenzoic acid. Ozone decomposition and further generation of hydroxyl radicals was attributed to reaction of ozone with surface acid sites present on α-FeOOH. The identified sites ($\equiv FeOH_2^+$, $\equiv FeOH$ and $\equiv FeO^-$) were described by the acidity constants and related by Equation 2.39 and Equation 2.40. According to the workers, the respective densities of each of these sites is dependent on pH and ionic reactions are promoted on $\equiv FeO^-$ which predominates at high pH.

Equation 2.39

$$\equiv FeOH_2^+ \leftrightarrow \equiv FeOH + H^+ \quad pK_{a1}^s = 6.4$$

Equation 2.40

$$\equiv FeOH \leftrightarrow \equiv FeO^- + H^+ \; pK_{a2}^s = 9.2$$

Experiments conducted in acidic pH and in the presence of tert-butanol were used to delineate working mechanism and showed that radical reactions were suppressed in the presence of the radical scavenger at pH above 3 and became constant at pH > 5. This implied that only surface radicals which react with adsorbed substrate influenced oxidation rate. Ozone breakdown on the surface of α-FeOOH presumed to play a secondary role at higher pH. The stability of α-FeOOH in ozone breakdown reactions was also supported by Muruganandham and Wu (2007). The workers observed that α-FeOOH was stable in acidic solution and showed recycle schemes up to five times. It must be mentioned here that catalyst load was as high as 30 g/L. A dose, which allows for possible recovery of used catalyst even with catalyst loss. In both studies highlighted, the possible leaching of Fe ions into solution was not investigated and as such, the oxy-hydroxide was assumed to be stable in acidic-oxidizing conditions.

In a recent study, Oputu et al. (2015b) applied nano β-FeOOH as catalyst in ozonation of 4-chlorophenol at a dose of 0.1 g/L. Similarly to findings by Park Park et al. (2004), the catalytic reaction was found to proceed through radical generation with the rate of substrate oxidation suppressed by a radical scavenger. The trend of oxidation of substrate however showed an increase in rate with an increase in pH except in cases when pH was sufficiently low (pH 3) to bring about dissolution of β-FeOOH. Careful monitoring of Fe-ions during the course of oxidation reaction revealed an increase in Fe-ions with decreasing pH. At pH 3, homogeneous reactions in a manner similar to Fenton reaction played a significant role in the oxidation of substrate. The workers also observed a two stage kinetic rate similar to that previously published by Chou and Huang (1999). This novel explanation to the working of oxy-hydroxide highlights the similarity between the Fenton and ozone processes as well as explains the higher catalyst efficiency observed by earlier workers at lower pH.

2.3.9. Summarizing the AOPs

The AOP treatments in some cases have been reported to bring about complete mineralization of xenobiotic organic pollutants in water. AOPs have emerged as versatile technologies for the treatment of contaminated water and wastewater; however, many articles have only reported the efficiency of AOPs without necessarily identifying the reaction intermediates or characterizing the final end products left in solution. It is important to note that the complete removal of a pollutant from matrix may not bring about a cleaner water stream as the end product water may contain more toxic organics which are resistant to the applied AOP. It is therefore recommended that analytical techniques for determinations be combined with other methods to monitor the complete mineralization of pollutants and their intermediates. More work is also needed in the area of catalyst development in photolytic systems with interest being on visible light application, and in developing catalysts capable of operating at near ambient conditions in wet oxidation processes. Also the application of AOP to composite mixture of pollutants requires further study as rates and mechanisms for single and mixed systems would vary markedly. Furthermore, the development and application of catalysts to ozonation processes, which would improve efficiency of the process or limit restrictions from operating variables such as pH, would also be of interest.

Many of the applications of water and wastewater treatment technologies reported to date are usually limited to single modelled pollutants. A few other articles have extended developed methods to real wastewater scenarios. While it is impractical to monitor all the pollutants individually/simultaneously in a real wastewater, it is important to study the effect these technologies have on groups of chemicals, which are found together in real contaminated water and wastewater systems.

2.4. Techniques applied in this study

2.4.1. Transmission electron microscopy (TEM)

Electron microscopy techniques use a beam of accelerated electrons as a source of illumination as against visible light photons used in light microscopes. Since the wavelength of electrons are 100, 000 times shorter than that of the photons present in visible light, electron microscopes can produce images with a magnification 5,000 times better than that of visible light. In a transmission electron microscope (TEM), high voltage electrons typically accelerated from a tungsten anode at +100eKv (with respect to the cathode) is focused on and transmitted through an ultra-thin film of sample. Electron beams emerging from the sample convey information about the structure of the sample (Cowley, 1995). High-resolution transmission electron microscopy (HRTEM) is a variant of the simple TEM with a hardware correction for spherical aberration experienced in TEM (Kirkland, 2010). The evolution of HRTEM has allowed for the determining of position of atoms within materials and crystals, emphasizing the usefulness of HRTEM in nano-technological research.

2.4.2. Infra-red spectroscopy

Infrared spectroscopy (IR) exploits the fact that molecules absorb specific frequencies from the electromagnetic spectrum (EMS) that are characteristic of their structure. The absorbed frequencies are directly proportional to vibrational energies and dependent on Hooke's law (Equation 2.41). Where v, c, k, and μ is vibrational frequency, speed of light, force/spring constant and reduced mass of bonding atoms, respectively. Factors which influence the exact IR absorption band of a covalent bond are the shape of molecular potential energy surface, mass of absorbing atoms and associated vibrational coupling (Badger, 1934).

Equation 2.41

$$v = \frac{1}{2\pi c}\sqrt{\frac{k}{\mu}}$$

Equation 2.42

$$\mu = \frac{m_A m_B}{m_A + m_B}$$

When a sample interacts with infrared light, selected IR vibrational frequencies are absorbed. Examination of transmitted light reveals how much energy is absorbed at each frequency. The technique is commonly used for analysis of samples containing covalent bonds (non-metals). IR spectroscopy finds application in this study as the vibrational frequencies of metals when bonded to non-metals (e.g. in metal oxides) occur in the near IR region of the EMS. Previous researches have identified IR vibrational frequencies of Fe-O bond: 850 - 680 cm^{-1} (Chowdhury et al., 2015a, Pal et al., 1999), Ni-O bond: 425 cm-1 (Bahari Molla Mahaleh et al., 2008), Zn-O bond: 472 cm-1 (Hong et al., 2009, Li and Cao, 2011).

2.4.3. X-ray diffractometry

X-ray diffraction is used for determination of crystal structure and phase identification and internal crystal atom arrangement. Its application in material science is based on the principle that diffraction beams generated from a solid surface is directly related to the crystal surface of the material. At an atomic scale, diffraction patterns appear as a series of peaks whose spacing and intensities are related to the size of the structure and concentration of the atoms in the structure, respectively. The K series ($K_{\alpha 1}$, $K_{\alpha 2}$ K_{β}) are the most important lines used for x-ray analysis as lower energy x-rays are easily absorbed by materials. When a filtered beam (monochromatic beam) of x-rays interact with the electron clouds of surface atoms, constructive and destructive refracted rays are produced. Constructive waves produced due to 'in-phase' diffracted x-rays, which are integral numbers of wavelength (n) of the source x-rays are captured by a detector for structural interpretation. Figure 2.4 illustrates a pair of x-rays incident on a periodically aligned plane of atoms P_0P_0, P_1P_1 and P_2P_2.

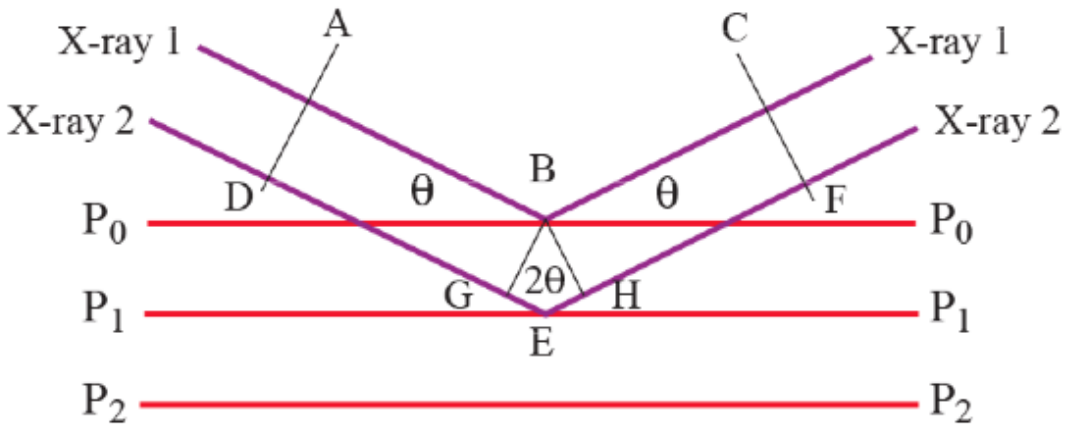

Figure 2.4: X-ray diffracted pair. X-ray 1, reinforced by X-ray 2.

For incident x-ray 1 angle θ represents the angle of diffraction on plane P_0P_0. An in-phase x-ray 2 produces a diffracted x-ray, which amplifies x-ray 1.

Both rays are related by the double triangle GBHE in Figure 2.4 with an angle 2θ. Bragg and Bragg (1913) proposed that diffraction could be considered discontinuous reflectance whose integer wavelengths are related to the surface line spacing by Equation 2.43, where n, λ, d and θ are integers, x-ray wavelength, distance between parallel atomic planes and angle of incident/diffraction, respectively (Atkins and De Paula, 2006).

Equation 2.43

$$n\lambda = 2dSin\theta$$

In its applications, the x-ray mapping of atomic planes are used to identify phases and determine structure in material science. X-ray diffraction patterns of prepared materials are matched in the database presented by the Joint Committee on Powder Diffraction Standards (JCPDS) (File, 1967).

2.4.4. High Pressure Liquid Chromatography-Time of Flight (TOF)-Mass Spectrometry

High-pressure liquid chromatography (HPLC) is an analytical technique used to separate, identify and quantify components in a mixture. It relies on pumps to pass a pressurized liquid solvent containing the sample matrix through a column filled with

a solid adsorbent material. Ever since the construction of the first HPLC system at Yale University in 1964 (Mortimer, 1967), the technique has evolved in versatility and has currently overtaken gas chromatography (GC) since it is not limited to volatiles and thermally stables compounds. HPLC is the technique of choice for analysis of phenol and chlorinated phenols as the derivatization step required as a pre-treatment step in GC analysis is avoided.

A time of flight-mass analyser (TOF-MA) Figure 2.5, separates ions generated at the ion-source according to their mass-to-charge ratio (m/z) based on their time of flight in a flight tube. The flight route of ions is shown in green. When combined with a HPLC system, a TOF-MA ionises molecules (by chemical ionisation CI, electron spray ionisation ESI, atmospheric gas pressure ionisation API), which are separated on the HPLC and determines masses based on their time of flight.

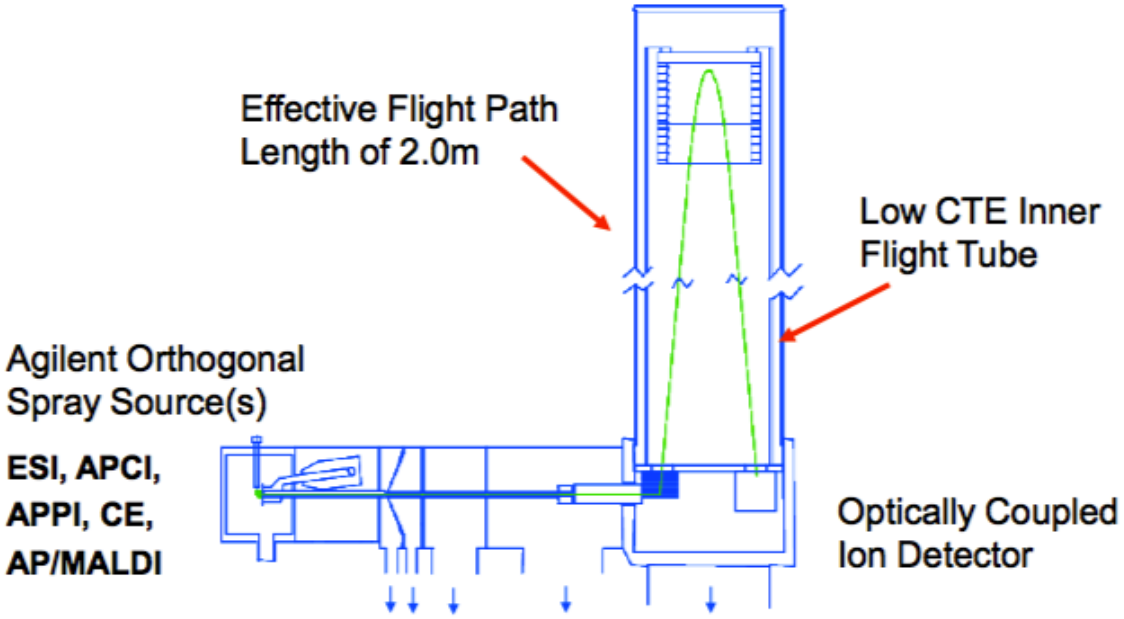

Figure 2.5: Schematic illustration of Agilent ion source and TOF tube. Courtesy Agilent (2014)

Equation 2.44 gives the kinetic energy of ions leaving the ion-source of a MA. Where *eV*, *m* and *v* are kinetic energy (in electron volts), mass of the ion and velocity of the ion respectively.

Equation 2.44

$$Kinetic\ energy = eV = \frac{1}{2}\, mv^2$$

Velocity (*v*) in Equation 2.44 is rated to the length of the tube (*L*) and the time spent by the ion to reach the detector (*t*), by Equation 2.45.

Equation 2.45

$$v = \frac{L}{t}$$

Equation 2.46 (Equation 2.44 + Equation 2.45) shows that the time of flight of an ion is proportional to the square root of the mass and/or mass is proportional to t^2.

Equation 2.46

$$t = L\sqrt{\frac{1}{2}\frac{m}{eV}}$$

The use of a simple HPLC system coupled with a diode array detector (DAD) or UV-Vis detector is a common practice amongst researchers studying the oxidation of organics by AOP (García-Molina et al., 2005, Benitez et al., 2000a, Saritha et al., 2007, Pimentel et al., 2008, Prato-Garcia et al., 2009, Razavi et al., 2011, Dombi et al., 2002, Abdessalem et al., 2010). In principle, compounds are identified on an HPLC-DAD or HPLC-UV-Vis based on their retention times (RTs) on an analytical column with the DAD or UV-Vis serving for quantification. This technique is suitable for identifying known compounds (including the starting substrate). In a typical AOP involving radicals, there exist multiple reaction pathways leading to various products/by-products with identical polarities and therefore RTs, which would overlap with those of known standards identified on a UV-Vis or DAD. Without further spectrum analysis, overlap compounds are indistinguishable. The HPLC-MS and GC-MS techniques provide information about the m/z of an identified compound and can be used to predict more accurate reaction pathways. Also, transient and recalcitrant organics generated during oxidation of an organic by an AOP can be identified. The HPLC-MS technique was recently used for accurate identification of intermediates and time-decay reaction pathway for methyl-orange and per-sulphate radical (Chowdhury et al., 2015b). Razavi et al. (2011) used the HPLC-MS technique for identifying breakdown products upon treating cholesterol lowering statin pharmaceuticals (luvastatin, lovastatin, pravastatin and simvastatin) with radio-pulse generated hydroxyl radicals.

The GC-MS technique has being previously applied for identification of oxidation products for phenol (Huang and Shu, 1995), 2-chlorophenol (Hirvonen et al., 2000, Sung and Huang, 2007), 4-chlorophenol (Hirvonen et al., 2000), nitrobenzene (Zhao et al., 2008). In these studies, various derivatization and reducing steps were applied as unit operations before final analysis. These steps compromise the integrity of samples and make it practically impossible to identify short-lived transient compounds; further underscoring the advantage of the HPLC-MS over the GC-MS technique for identification of non-volatiles produced in aqueous oxidation reactions.

CHAPTER 3

3. METHODOLOGY

3.1. Calibration of ozone generator

Ozone generator supplied by Ecological Technology (Eco Tech, South Africa) was used as ozone source. Oxygen gas (99.999%) was supplied by Air Liquide supplied, South Africa. Oxygen flow to the ozone generator was regulated using a mass flow meter (Bronkhrst M33). Ozone generator was calibrated by determining the ozone dose/minute produced by the generator at varying oxygen flow rates of 5 mL/minute – 50 mL/minute. Ozone was measured by the standard iodometric titrations previously applied in literature (Chou and Chang, 2007). A schematic presentation of the experimental set up is given in Figure 3.1 below.

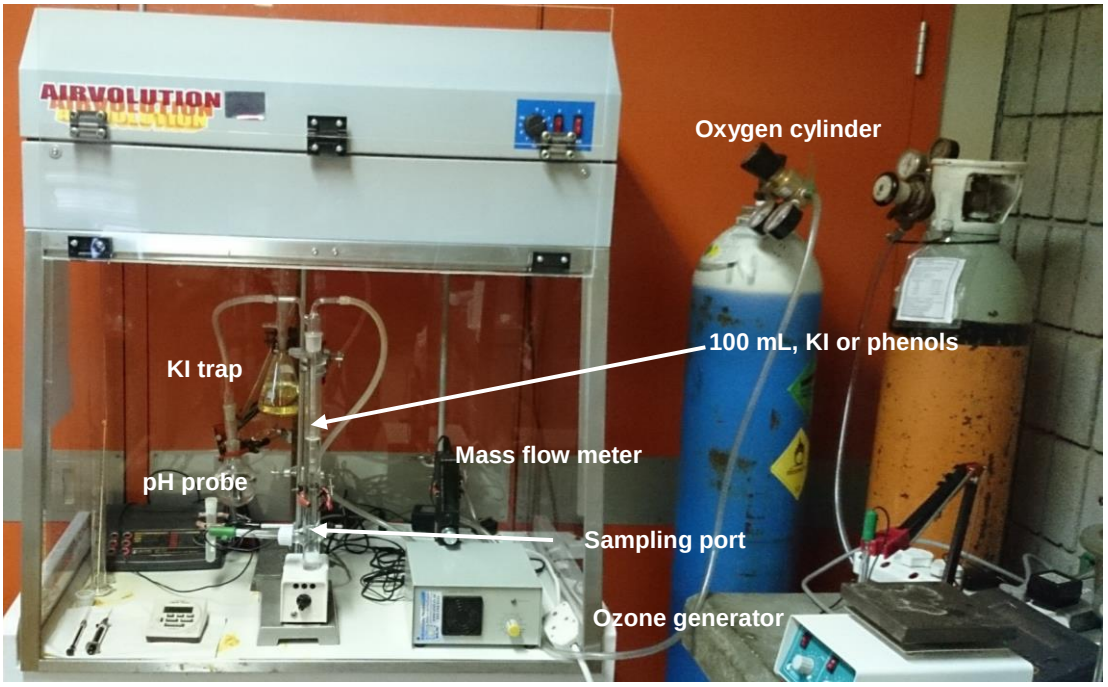

Figure 3.1: Ozonation set up

For a typical measurement, O_2 gas at fixed flow rate (held my a mass flow meter) was passed through the O_3 generator and the O_3 gas was trapped in 100 mL, 2% potassium iodide (KI) placed in the reactor. The Gas flow into the reactor was held constant for exactly 20 minutes.

Equation 3.1

$$O_3 + 2I^- + H_2O \rightarrow O_2 + I_2 + 2OH^-$$

Equation 3.2

$$I_2 + 2S_2O_3^{2-} \rightarrow 2I^- + S_4O_6^{2-}$$

Ozone solubility even in 2% KI is temperature sensitive. Therefore, all measurements and subsequent use of the ozone generator/reactor set-up was done at constant temperature 293K. O_3/O_2 composition in the gas feed was determined by calculating the amount of each gas flowing through the reactor per minute. The quotients thus represent the percentage ozone in the gas feed.

Based on equation 1 and 2 above, the O_3 concentration is equivalent to I_2 concentration and thus equation 3 holds:

Equation 3.3

$$\boldsymbol{C_{O_3} = C_{I_2} = \frac{C_{S_2O_3^{2-}}\, x\, V_{S_2O_3^{2-}}}{2\, V_{I_2}}}$$

The concentration of ozone (mg/L), dose (mg/min) and gas phase concentration (%) was thus determined by taking into account ozone molecular mass, dose time/volume and oxygen gas moles (at varying volumes), respectively.

Moles of oxygen in gas feed were calculated according to Equation 3.4, where P is 1 atm, V is oxygen flow rate, R is gas constant 0.0821 (L. atm K^{-1} mol^{-1}) and T is experimental temperature conditions held constant at 293K.

Equation 3.4

$$n_{O_2} = \frac{PV}{RT}$$

3.1.1. Determination of ozone mass transfer to aqueous phase

Ozone mass transfer from gas to aqueous media was evaluated by monitoring the aqueous ozone concentration as a function of time. For these experiments, ozone gas was bubbled into 100mL milli-Q water and aliquots were drawn at regular intervals for ozone quantification. Ozone in aliquots was determined using the indigo method proposed by Bader and Hoigné (1981). The method involves reacting ozone with a given amount of a buffered solution of the dye (potassium indigo trisulfonate), followed by determination of absorbance of unreacted dye at 600 nm. Ozone calibration standards were prepared from solutions whose ozone concentration was

determined by iodometry. The results of the indigo method were therefore based on the classical iodometric titrations using standard thiosulphate solution.

3.2. HPLC determination of Chlorophenols

A high performance liquid chromatographic method was developed based on the EPA Method 604 Phenols (Waters, 1996) for the simultaneous determination of phenol, four chlorophenols (2-chlorophenol, 4-chlorophenol, 2,4-dichlorophenol and 2,4,6-trichlorophenol) and four intermediate products (catechol, resorcinol, benzoquinone, and hydroquinone) in aqueous solutions. Standard stock solutions of 500 mg/L were prepared by dissolving 500 mg of phenol, chlorophenol and intermediates in 1 L of milliQ water. Calibration standards were prepared by serial dilutions of stock solutions in the range 0.5 mg/L -100 mg/L. The HPLC was calibrated using prepared standard solutions. In the determination of phenols in ozonated solutions, exactly 1 mL of ozonated solution was drawn from the glass reactor using a gas tight glass syringe and transferred into a 10 mL volumetric flask. One millilitre of sodium thiosulphate (0.0005 M) was added to quench further reactions with ozone before making up to the mark with milliQ water. Samples were then analysed by HPLC without any further pre-treatment. For LCMS analysis, the quenching step was excluded in order to prevent contributions of thiosulphate to reaction by-products.

3.2.1. Chemicals

Phenols were obtained from the following sources: phenol (99.5%), 2-chlorophenol (99%), 4-chlorophenol (99%), 2,4-dichlorophenol (99%), 2,4,6-trichlorophenol (98), hydroquinone (99%), Resorcinol (99%), Catechol (98%), Benzoquinone (98%), HPLC and LCMS grade acetonitrile were obtained from Sigma Aldrich, South Africa. Mixed standard solution of phenols and intermediates were prepared by weighing accurate amounts of each salt in milli-Q water (18 Ω). Calibration standards were prepared by further dilution of mixed standards.

3.2.2. HPLC instrumentation and chromatographic conditions

High performance liquid chromatographic separation of phenols was achieved using a Waters Chromatograph equipped with a Waters 1525 binary HPLC pump, Waters 2487 dual λ absorbance detector, Waters 2707 auto-sampler and running on the

Breeze software. The optimized gradient program used for elution and quantification the target compounds is shown in Table 3.1.

Table 3.1: Chromatographic parameters for quantification of phenols

Chromatograph	Waters		
Detector	UV		
Column	Waters Symmetry C8 15mm, 3.9mm 5µ		
Injection volume	20 µL		
Mobile phase	A: water		
	B: Acetonitrile		
Flow-rate	1 mL/min		
Gradient elution	Time (mins)	%A	%B
	0	85	15
	25	0	100
	28	0	100
	30	85	15
Temperature	26 ^{o}C		
Data Collection	Breeze software version 2		

3.3. LCMS determination of Chlorophenols

Oxidation breakdown products of phenols were separated and identified using a liquid chromatograph coupled to a mass spectrometer (Agilent 6230 TOF LC-MS). The Agilent 1260 infinity series used comprised a binary pump, an auto-sampler and an 1100 diode array detector (DAD). Operating program was Mass Hunter software version 3.0. Mobile phase were water (0.1 % formic acid) and acetonitrile (0.1 % formic acid). Ionization of phenol(s) intermediates was by electron spray (ESI) nebulized over a drying gas at 350 °C (nitrogen) and ions were captured in the negative mode. The optimized gradient program used for elution and identification of intermediates on the LC-MS is shown in Table 3.2. A flow rate of 0.4 mL/min was used for 2,4-dichlorophenol, while 0.3 mL/min was used for phenol, 2-chlorophenol and 4-chlorophenol.

Table 3.2: LCMS parameters for identification of intermediates

Chromatograph	Agilent 6230 TOF LC/MS		
Detector	Agilent DAD 1100		
Column	Waters Symmetry C8 15mm, 3.9mm 5µ		
Injection volume	5 µL		
Mobile phase	A: water (1% formic acid)		
	B: Acetonitrile (1% formic acid)		
Flow-rate	0.3 mL/min		
Gradient elution	Time (mins)	%A	%B
	0	85	15
	35	0	100
	47	0	100
	50	85	15
Temperature	26 ^{o}C		
Data Collection	Mass Hunter		

3.4. Preparation of β-FeOOH

β-FeOOH was prepared by hydrothermal synthesis from $FeCl_3$ in Teflon-lined steel reactor. For a typical batch preparation, 0.05 M $FeCl_3$ was prepared using equimolar mixture of n-butanol and water. 130 mL of this mixture was transferred into the reactor (capacity 200 mL). The pH of the mixture was adjusted from 3.5 to 10.0 using NH_4OH. The reactor was then sealed and the mixture incubated at 100^{o}C for 6 hours. Slurry of β-FeOOH was recovered from the reactor, washed copiously with distilled water, centrifuged and air-dried in a watch glass over night. The stainless steel reactor used for the synthesis is presented in Figure 3.2.

Figure 3.2: Reactor setup for preparation of β-FeOOH

3.5. Preparation of FeOOH nano material composites

β-FeOOH was bonded on nano material supports using a similar method previously reported in literature (Rawal et al., 2009, Chowdhury et al., 2015a). Chemically bonded interface between NiO particles, with an average diameter of 50 nm, and β-FeOOH were formed using an organic binder. Three different mol % loading of β-FeOOH (2, 5 and 10%) on NiO was prepared. For a typical synthesis of 5 mol % β-FeOOH and 95 mol % NiO, (labelled as 5 % β-FeOOH/NiO) a calculated amount of β-FeOOH was suspended in 30 mL of ethanol. 10 mL of 0.1 M maleic acid was added to the mixture. In a separate beaker 1g of NiO was dispersed in 30 mL ethanol. The two mixtures were stirred for 4h separately. After 4h the NiO mixture was added to the β-FeOOH mixture and stirred for 16h. The mixture was centrifuged, washed several times and dried overnight in air at 60 ^{o}C. The dried powder was annealed at 250 ^{o}C for 4h in an oven under air to decompose the organic components. Finally the annealed samples were treated under 9W UV light for 4h to remove any residual organic on the surface of the catalyst.

3.6. Characterization of nanomaterial: FTIR, TEM and XRD

The crystal structures of the synthesized products were determined using a Phillips PW 3830/40 x-ray generator with Cu-Kα radiation (Philips, Netherland). The surface morphology of the synthesized materials was studied using a Tecnai TF20 thermionic TEM (Switzerland), equipped with a LaB6 filament and a Gatan GIF energy filter. Images were captured at 200 keV in bright field mode and dark field mode. Selected area electron diffraction (SAED) patterns were obtained using the smallest area aperture available. Infrared spectra were collected with a Perkin Elmer 1000 series FTIR spectrometer in the range 4000 - 200 cm^{-1} in a KBr pellet. Specific surface area and pore diameter was determined by nitrogen adsorption-desorption isotherm at liquid nitrogen temperature (77K) using a Micrometrics - TriStar 3000 instrument (USA). The samples were degassed at 35^{o}C for 24 hours prior to the measurements.

3.7. Experimental

3.7.1. Determination of ozonation reaction rates

Ozonation rates of phenol and desired chlorophenols: 2-Chlorophenol (2CP), 4-chlorphenol (4CP), 2,4-dichlorophenol (24DCP) and 2,4,6-trichlorophenol were determined by treating organic substrate set at $2x10^{-3}$ M with ozone at 10 mL/min

flow rate. Residual substrate concentrations and intermediates were analysed by HPLC and LCMS. The organic substrate concentration and ozone flow rate were established based on preliminary experimental data designed to ensure that the reaction process is within a time frame suitable for study (60 minutes). Raising the flow-rate or reducing the substrate concentration reduced the reaction time and thus was undesirable for studying comparative reaction kinetics and catalysis.

3.7.2. Heterogeneous catalysis: Determination of catalytic property of β-FeOOH and composites

For catalytic experiments, 0.01g of β-FeOOH was equilibrated with 100 mL of the desired substrate (4-chlorophenol) for 1 hour to ensure maximum adsorption was achieved. The solution was subsequently sonicated to disperse catalyst and the mixture ozonated. For catalytic experiments, ozonation was done at an oxygen flow-rate of 10 mL/min. Aliquots were drawn from the reactor, filtered through 0.22 µm GHP Acrodisc syringe filters and analysed by HPLC and LCMS. Investigation of catalytic property of β-FeOOH bonded nanomaterial was conducted in a similar manner. Residual substrate (4CP) in solution was plotted as a function of time and the removal efficiency was evaluated assuming first order kinetic data of 4CP.

3.7.3. Determination of Chemical Oxygen Demand (COD)

Chemical oxygen demand measurements were conducted using the closed reflux colorimetric method (ASTM, 1995). Samples and standards were digested using potassium dichromate solution. The digestion process converts the hexavalent chromium (VI) ion to the trivalent chromium (III) ion. The hexavalent dichromate and the chromic ions were quantified at 400 nm and 600 nm, respectively. The digestion solution and samples were prepared as described in Standard methods for the examination of water and wastewater (Eaton et al., 1998). Calibration standards were prepared using potassium hydrogen phthalate (KHP) (stock solution 1 g/L equivalent to 1000 mg O_2/L) in a matrix similar to the one employed in the samples. 2.5 mL of each standard and sample where digested for 2 hours and set aside to cool overnight. The calibration function of the PerkinElmer Spectrum 1000 UV/VIS was used to plot a calibration curve with the monitoring wavelength set at 600 nm. Samples were read off the calibration curve and results presented as mg O_2/L. The digestion of the samples and standards was carried out at the same time to avoid instrumental drifts in standard readings.

3.7.4. Determination of Hydroxy radicals by coumarin experiments

Hydroxyl radicals generated during catalytic experiments were measured using coumarin experiments (Xiang et al., 2011). Coumarin (COU) is highly selective and reactive toward hydroxyl radicals in solution to form 7-hydroxycoumarin (7HC) - a highly fluorescent compound (456 nm)(Xiang et al., 2011). A set of working standards of concentration 0, 0.01, 0.05, 0.1 and 0.2 mg/L 7HC were prepared by serial dilution of a 10 mg/L 7HC stock solution. Dilutions were achieved using similar solution matrix as the sample set i.e. milliQ water. The calibration curve was then plotted using the calibration function of the luminescence spectrometer (PerkinElmer 2565 luminescence spectrometer). A 100 mL of a 1×10^{-2} M solution of COU was treated with ozone at a flow rate of 10 mL/min in the absence of any other reactant with 4 mL samples collected at t = 0, 5, 10, 20, 30 and 40 minutes. Samples where then subsequently analyzed by luminescence spectrometry within an hour of collection. Samples and standards where run on a PerkinElmer 2565 luminescence spectrometer at an excitation and emission wavelength of 350 nm and 456 nm, respectively, with the emission and excitation slit set at 2.5 nm.

3.7.5. Sampling of wastewater

For the purpose of testing the efficiency of prepared composite catalyst (β-FeOOH-NiO), wastewater samples were collected from two companies. Based on a signed disclosure agreement the companies are herein and furthermore referred to as ‘company 1’ and ‘company 2’, both located in Cape Town. The former is a printing mill with wastewater effluent from washing off ink and the latter is a typical Kraft mill producing cardboards and utility paper.

Company 1 had an onsite wastewater treatment installation, which served to reduce colour and maintain pH of their wastewater at permissible disposal levels. pH control was achieved by dosing acidic waste with NaOH while polymeric chelates were used to coagulate large organic molecules, which are filtered off via a compressing system.

Company 2 did not have an on-site treatment facility but sends their wastewater to the Cape Town municipality for treatment after preliminary sedimentation. The treated water is then purchased back by the company as industrial water, which is cheaper than domestic potable water.

Two different water samples were collected from each company. A total of four (4) samples in all.

Company 1: Raw untreated wastewater and onsite-treated wastewater. Two samples collected on the 22nd July 2015.

Company 2: Raw wastewater sent to Cape Town municipality and industrial water received from Cape Town municipality. Two samples collected on 22nd July 2015.

About two and half litres of each sample were collected in pre-labelled glass bottles, stored in an icebox and transferred to the laboratory for treatment. Physicochemical parameters; turbidity, pH, temperature, conductivity and total dissolved solids (TDS) were measured onsite using a multi-parameter meter. Wastewater treatment by ozone and heterogeneous ozonation was conducted according to method described in Section 3.7.2 with an increased ozone flow rate from 10 mL/min to 50 mL/min. The increased flow-rate was necessary as the chemical oxygen demand (COD) levels of the wastewater was 12 times higher than the COD of 4-chlorophenol concentrations applied thus far in earlier sections. Aliquot samples were drawn at regular intervals from the reactor and analysed for COD (ASTM, 1995)

CHAPTER 4

4. RESULTS AND DISCUSSION

4.1. Optimization of ozonation set-up

4.1.1. Calibration of ozone generator

Ozone output from the ozone generator was quantified at various oxygen flow rates adjusted using a mass flow meter. Results of duplicate ozone measurements are presented in Table 4.1. The quantity of ozone produced by the corona discharge generator increased steadily as the oxygen flow rate is increased, reaching a maximum at 50 mL/min O_2 flow after which it dropped by 11.7 % as O_2 flow increased to 100 mL/min. Ozone gas was produced by the generator when O_2 gas passed in-between the corona discharge plates held at a constant current. At low flow rate, ozone dose produced is low. However, increasing flow over a critical maximum leads to a shorter lifetime of the oxygen gas in-between the corona discharge plates and therefore, ozone gas produced reduced. The percentage O_3/O_2 mixture reduced with an increase in flow rate because the ozone generator does not sufficiently convert the increased O_2 molecules into ozone by the factor of the amount by which the O_2 molecules are raised. This further buttress the point that the residence time of the gas between the discharge plates was a determining factor for the efficiency of a corona discharge ozone generator.

Table 4.1: Ozone concentrations as a function of oxygen flow rate.

O_2 flow-rate (mL/min)	Conc. O_3(mg/L)	Conc. O_3(mg/L)	AVG O_3(mg/L)	O_3 (mg/min)	Gas phase O_2(mg/min)	Conc (%) O_3/O_2
5	19,91	18,98	19,45	0,10	2,08	4,68
10	28,24	26,96	27,60	0,14	4,16	3,32
20	32,2	31,76	31,98	0,16	8,31	1,92
50	36,56	35,34	35,95	0,18	20,79	0,86
100	30,36	33,14	31,75	0,16	41,57	0,38
200	21,75	23,99	22,87	0,11	83,14	0,14

4.1.2. Evaluation of reactor mass-transfer efficiency of reactor

The solubility of ozone in a bubble reactor set-up is determined by several factors: operating pressure, temperature, gas-contacting device, and gas flow rate. When ozone gas is introduced into a solution (or reactor set-up), a high concentration zone is momentarily established. Aqueous ozone then disperses throughout the solution till an equilibrium state where the rate of ozone breakdown by natural process is equal to the rate at which the reactor set-up replenishes it. The time taken by a

contacting device to establish equilibrium ozone concentration is taken as a measure of the mass transfer efficiency of the gas-contacting device at specified conditions (Huang and Shu, 1995). In-order to evaluate the mass transfer efficiency of the reactor set-up; aqueous ozone concentrations were determined in aliquots as described in methods section (3.1.1). Results of aqueous ozone concentrations at various O_2 flow rates taken with respect to time are shown in Table 4.2 and Figure 4.1.

Table 4.2: Showing variation of ozone (mg/L) in reactor with time (minutes) at different oxygen flow rates (mL/min). Temperature 20°C

Time (min)	O_2 flow rate (mL/min)				
	10	20	50	100	200
0	0.00	0.00	0.00	0.00	0.00
1	0.00	0.00	6.45	15.46	18.66
5	1.63	19.81	26.51	27.13	19.53
10	15.16	23.74	28.19	29.38	19.91
20	18.16	27.34	29.78	27.32	19.13
30	19.76	27.96	29.78	27.43	19.00
40	20.41	28.62	29.6	25.62	19.41
50	20.45	28.66	29.81	25.21	18.94
60	20.55	28.52	29.48	25.41	18.54

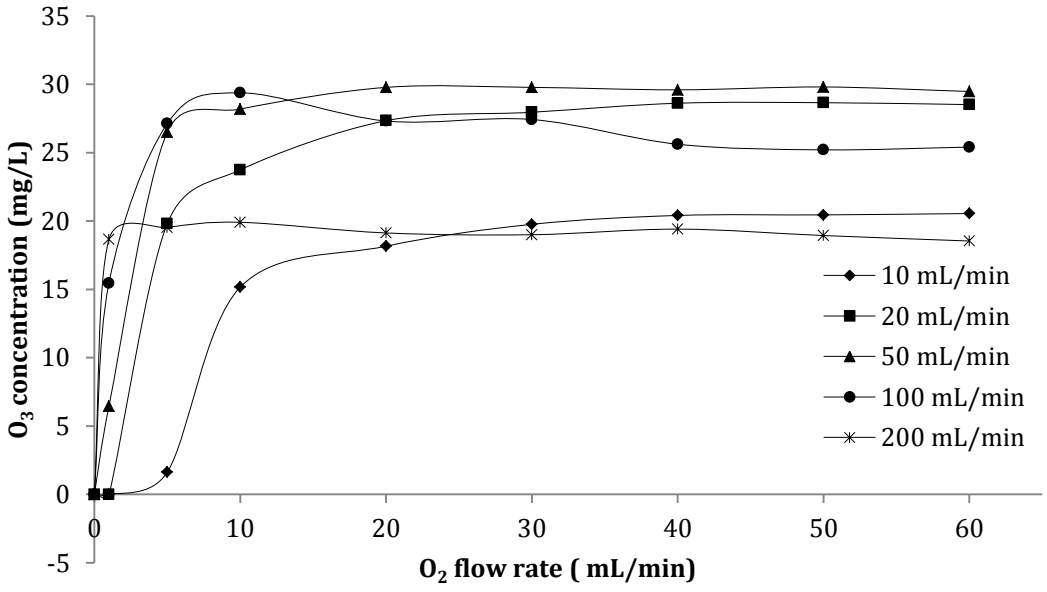

Figure 4.1: Effect of oxygen flow rate on reactor ozone concentration and time

Figure 4.1 illustrates the effect of oxygen flow rate on the reactor ozone concentration and equilibration time. At high flow rate, equilibration time is short, almost instantaneous at 200 mL O_2/min. However, as earlier discussed, above 50

mL O_2/min, efficiency of ozone generator reduces significantly. For that reason, the measured concentrations at 100 mL O_2/min and 200 mL O_2/min were always lower than those measured at 50 mL/min.

The effect of temperature on ozone solubility was evaluated by comparing experiments conducted at 293K and 300K. Results presented in Table 4.3 and Figure 4.2 clearly depicts the role played by temperature on aqueous ozone concentrations in the reactor set-up. Aqueous ozone concentrations reduced by as much as 44 % when flow rate was 200 mL O_2/min over a 7K rise in temperature. Temperature effects are however lower than low flow rates effects. All ozonation experiments were, therefore, carried out in a controlled temperature environment to eliminate fluctuations in results due to changes in laboratory temperature.

Table 4.3: Ozone concentration at 293K and 300K at different flow rates

O2 flow rate (mL/min)	293K	300K	% Reduction
5		14,93	
10	21,37	17,56	18
20	27,89	19,58	30
50	32,84	24,88	24
100	31,61	21,53	32
200	30,96	17,18	44

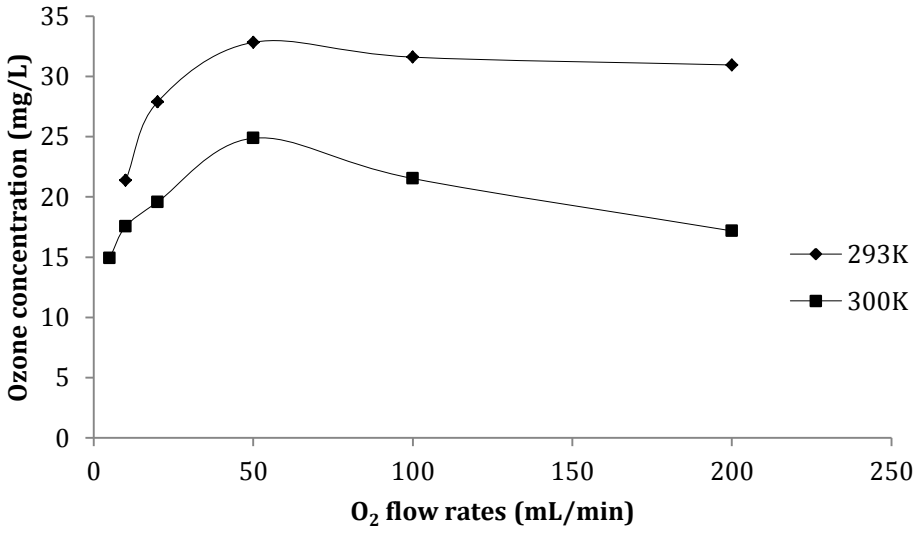

Figure 4.2: Effect of operating temperature on reactor ozone concentration

4.1.3. Optimizing gas flow and substrate concentration

In order to ascertain what ozone gas flow was suitable for a study experiment, phenol was used as substrate at 500 mg/L (≈ 5.3 x 10^{-3}M) concentration at varying ozone gas flow (5 mL/min, 10 mL/min and 50 mL/min). At very low flow rate (5 mL/min), phenol concentration was above 80 mg/L after 180 minutes, while at 50 mL/min phenol concentration was at 20 mg/L at 30 minutes. These flow rates served as undesirable for a systematic study on comparative rates and possible catalysis. 10 mL/min which gave a reaction time of 150 minutes for 500 mg/L phenol (Figure 4.3) was selected for the rest of the study with the starting concentration reduced by half. For the rest of this study, unless otherwise stated, the concentrations of phenol and chlorophenol prepared and tested was 2.5 x10^{-3}M. This concentration combined with an ozone flow of 10 mL/min gave reaction times just under 60 minutes and was thus considered suitable for study.

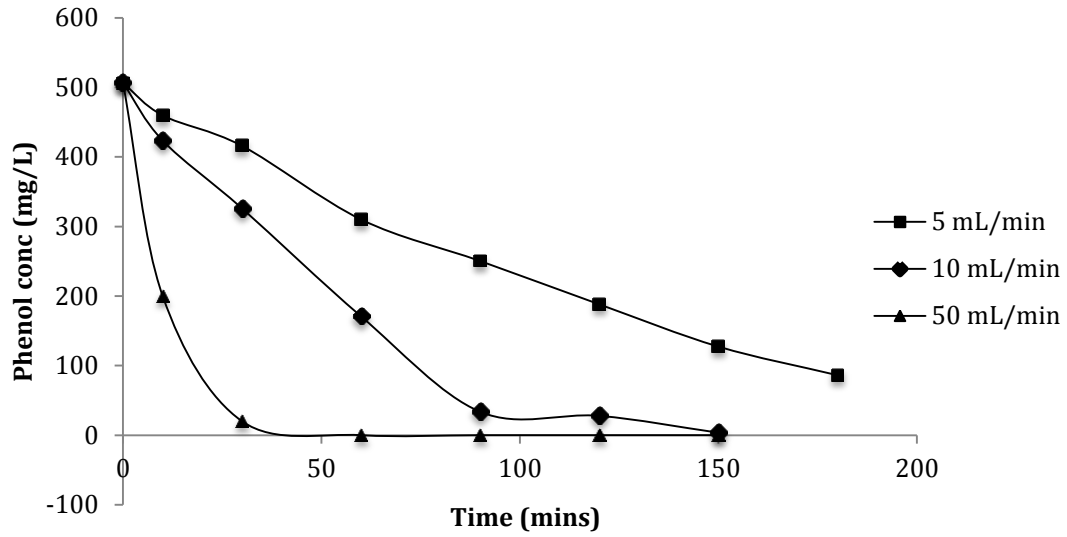

Figure 4.3 Effect of flow rate on phenol ozonation

4.1.4. Optimization of quenching agent for ozone

Aqueous ozone occurs as transient species with a short lifetime of approximately 20 minutes at 20°C (Hoigné, 1998). To preserve the integrity of sampled aliquots for kinetic studies, ozone reactions in samples were quenched with a quenching agent. Two of the more reported quenching agents were tested; bovine catalase (from bovine liver) and sodium thiosulfate. Figure 4.4a shows UV scans for bovine in milliQ at concentrations from 10 mg/L to 1000 mg/L. As shown in Figure 4.4a, bovine concentration above 10 mg/L impacted a significant absorbance at 280 nm. The absorbance of bovine obscured the absorbance for ozone at 254 nm (compare ozone absorbance in ozonated water in Figure 4.4b). Quenching test using bovine

catalase (ratio 1:1 with ozonated solution) presented in Figure 4.4b showed that below 100 mg/L bovine concentration [green plot], ozone species were still active in solution - the catalase did not completely quench ozone present in ozonated solution. Above 100 mg/L bovine concentration (as seen using 250 mg/L [yellow plot], 500 mg/L [black plot] and 1000 mg/L [bluish-green plot] bovine catalase solution), the bovine peak obscured the detection and determination of ozone. Further testing using bovine catalase as possible quenching agent was therefore discontinued.

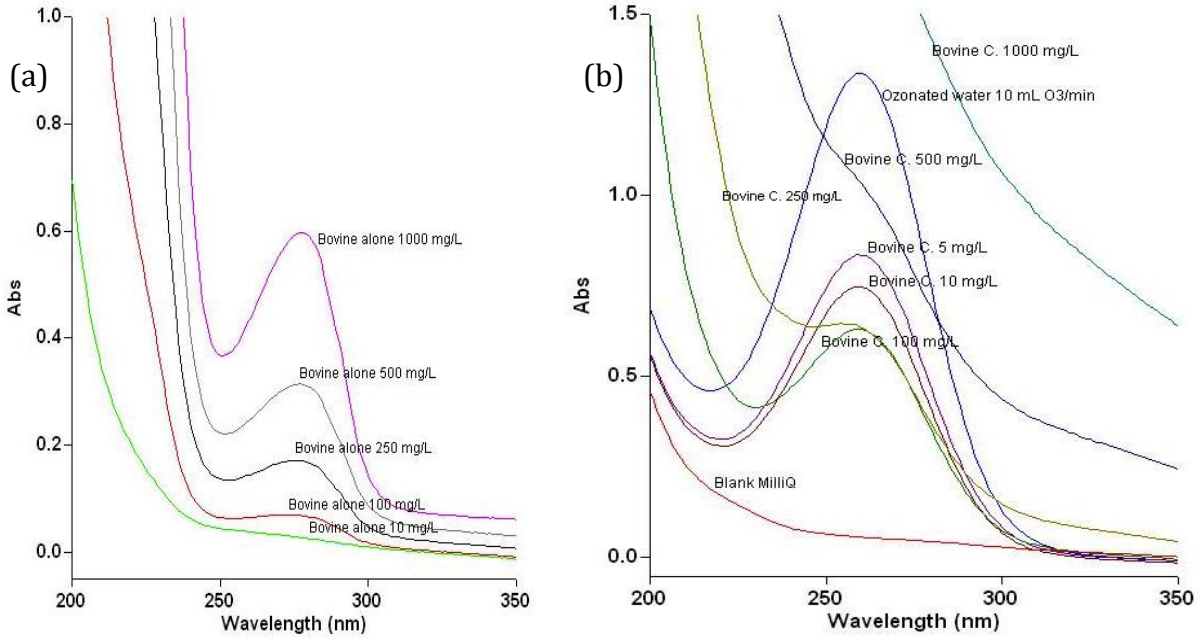

Figure 4.4 (a) UV absorption patterns of bovine catalase at different concentrations (b) ozone quenching experiments using varying concentrations of bovine catalase

Ozone quenching experiments using thiosulphate is presented in Figure 4.5. Figure 4.5a shows ozonated solutions when mixed with equal volumes (ratio 1:1) of thiosulphate solutions at different concentrations vis: 0.0005 M, 0,001 M and 0.005 M. As shown in the figure, thiosulphate concentration at 0.0005 M was sufficient to instantaneously quench aqueous ozone at 27.6 mg/L. The optimized ratio of thiosulphate and ozone solution is presented in Figure 4.5b. Below ratio 1:1, thiosulphate at concentration of 0.0005 M was insufficient for quenching ozone in ozonated solutions. For subsequent kinetic experiments, aqueous ozone in 1 mL aliquots drawn from reactor was therefore quenched with 1 mL 0.0005 M thiosulphate before analysis.

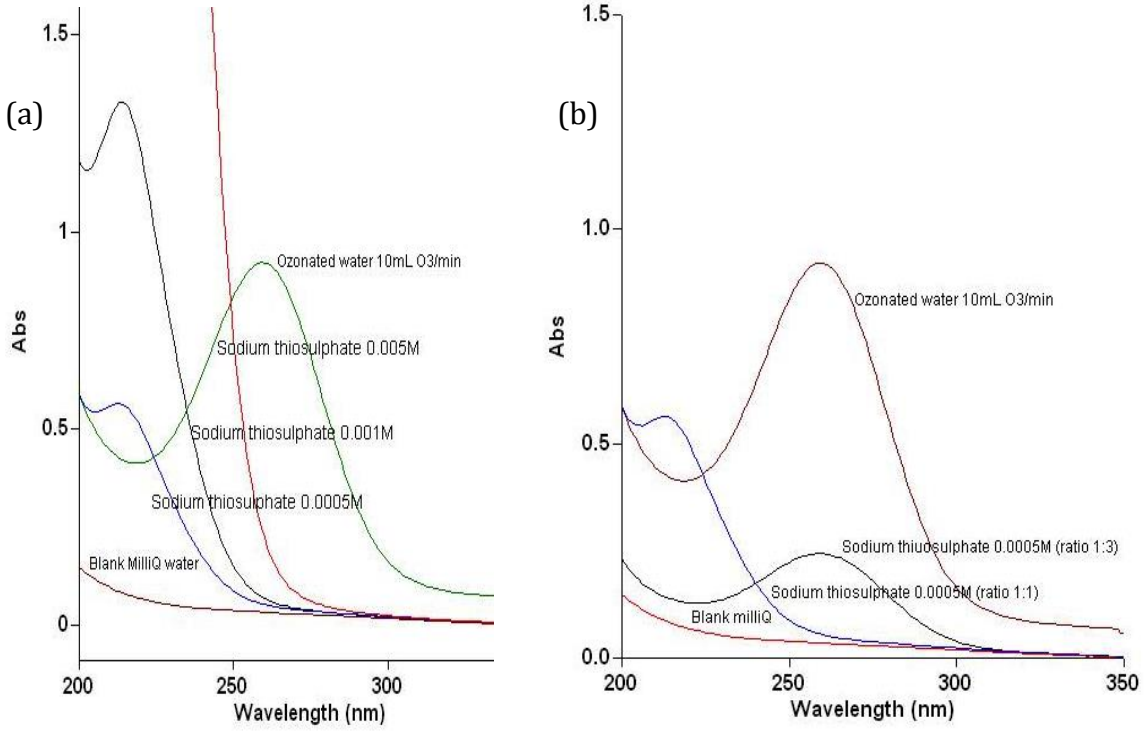

Figure 4.5 (a) ozone quenching experiment using varying concentration of sodium thiosulphate (b) ozone quenching experiment at varying ration of ozonated solution and sodium thiosulphate (0.0005 M)

4.2. Characterization of β-FeOOH, NiO and β-FeOOH-NIO composite

The characterization of pure β-FeOOH, NiO and β-FeOOH-NiO composite are presented here from a comparative point of view. FTIR spectrum of pure material and the composite is presented in Figure 4.6. The broad band appearing at 3550 and 1650 cm^{-1} are related to the stretching and bending vibrations of the water molecules absorbed by the sample or KBr in all cases. The band at 1384.19 and 428 in the commercially purchased pure NiO is attributed to the bending vibration of ionic CO_3^{2-} and Ni-O stretching of the octahedral NiO_6 groups respectively (Bahari Molla Mahaleh et al., 2008). For the pure β-FeOOH the absorptions peak at 851 and 681 cm^{-1} is attributed to the Fe-O vibrational modes (Chowdhury et al., 2015a). Fe-O vibration modes of β-FeOOH diminished in β-FeOOH/NiO composite material. This phenomenon is attributed to the existence of Fe-O-Ni bond in the composite and further implies that the β-FeOOH material is highly dispersed in the NiO lattice.

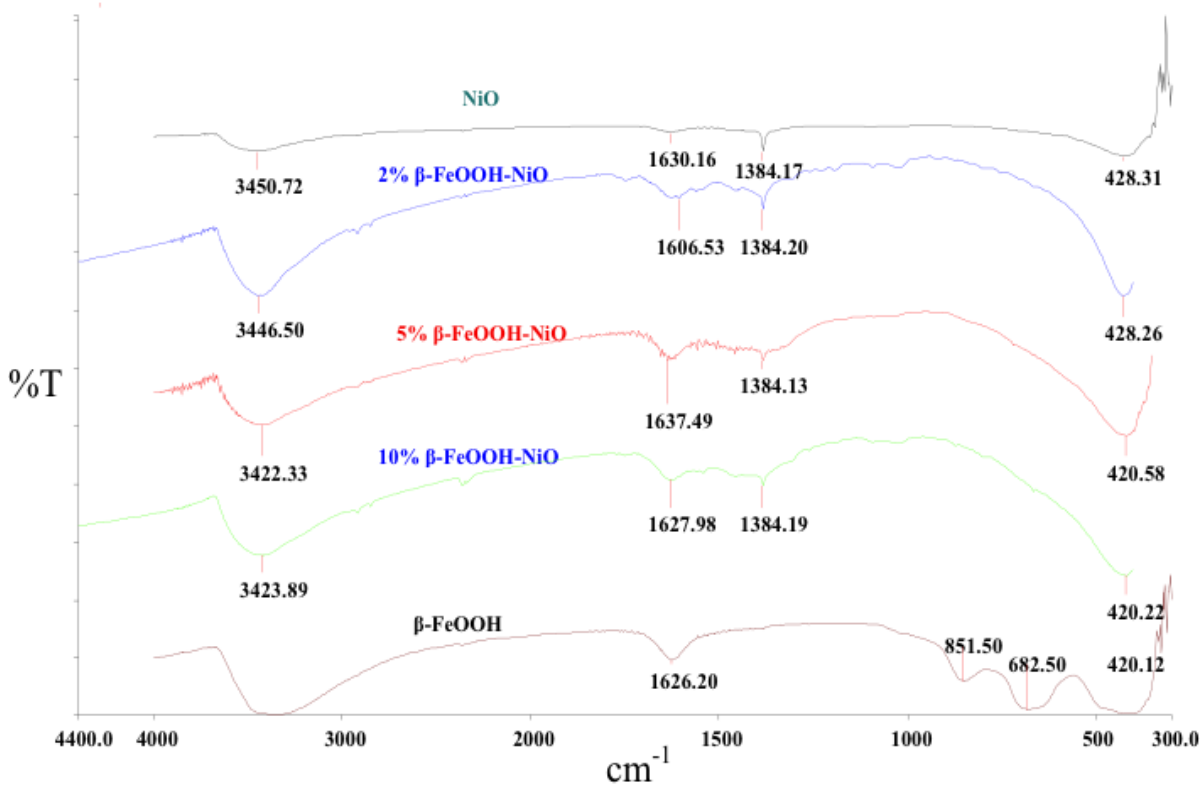

Figure 4.6: FTIR spectrum of β-FeOOH, NiO, and 2%, 5% and 10% β-FeOOH –NiO composite

X-ray diffraction of pure β-FeOOH (JCPDS: No. 42-1315); NiO (JCPDS: No. 071-1179) and composite material (bonded with 2, 5 and 10 %) are shown in Figure 4.7. Important planes on β-FeOOH and NiO based on the JCPDS card numbers are also shown in the presented figure. Despite the absence of β-FeOOH diffraction planes in XRD spectrum for the composites, the increasing full width at half maximum (FWHM) with an increase in β-FeOOH for the observed peaks is an indication of increasing crystal size of the composite and would infer the incorporation of β-FeOOH into NiO. The absence of β-FeOOH planes in the composite may, therefore, be attributed to low loading of β-FeOOH and its high dispersion on NiO.

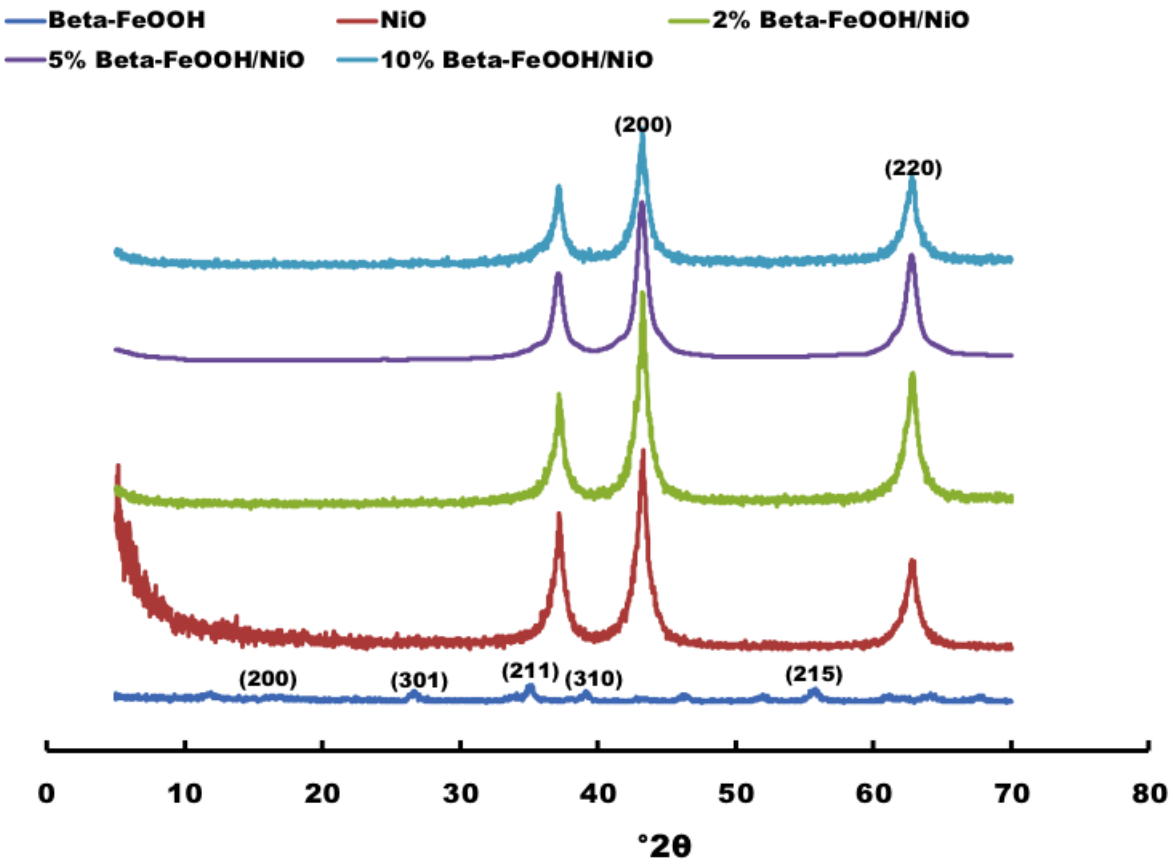

Figure 4.7: XRD spectrum of β-FeOOH, NiO, 2 %, 5 % and 10 % β-FeOOH –NiO composite

Transmission electron microscopy (TEM) images for prepared β-FeOOH and NiO are presented in Figure 4.8(a) and Figure 4.8(b), respectively. The selected area electron diffraction pattern (SAED) for β-FeOOH is presented –inset in Figure 4.8(a). D-spacing calculated to be 5.30 Å from SAED corresponds to the [200] diffraction planes of β-FeOOH. TEM images obtained in bright field mode of 2% and 5% β-FeOOH-NiO composite along with their corresponding energy dispersive spectrums (EDS) are shown in Figure 4.9(a-d). In both images, highlighted areas of interest shown in boxes (Figure 4.9a and Figure 4.9c). The EDS evidence the presence of Fe and Ni. The copper mesh upon which the samples are supported is also shown in the EDS. The d-spacing of β-FeOOH-NiO was measured using the image-J software and are highlighted in Figure 4.10(b). The [200] plane of NiO is seen here to overlap with the [310] plane of β-FeOOH indicating the formation of a chemically bonded interface/hetero-junction.

Dark field scanning TEM (STEM) micrograph of a single β-FeOOH-NiO composite material was collected with a high angular annular dark field (HAADF) detector at an electron probe size of 0.7 nm for elemental mapping purposes and are presented in

Figure 4.11(a, b and c). Figure 4.11(a) shows the STEM image of the composite, while Figure 4.11(b) shows the drift corrected STEM-EDS spectrum image of the highlighted section (yellow box) in the orange window. The HAADF intensity of the highlighted section in in Figure 4.11(b) was collected and elemental maps are presented in Figure 4.11(c). As shown by the elemental mapping, the identified composite contains Fe, Ni and O atoms. A hetero-joining of the two metals was therefore supported.

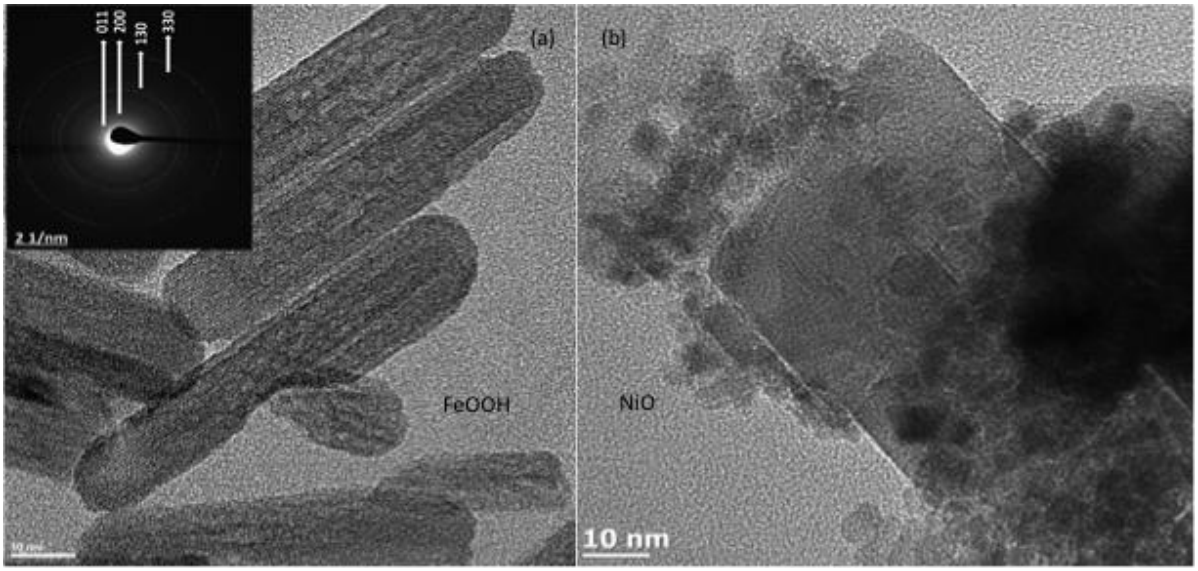

Figure 4.8: Bright field electron transmission images of (a) β- FeOOH and (b) NiO at 10 nm Inset: SAED showing diffraction planes

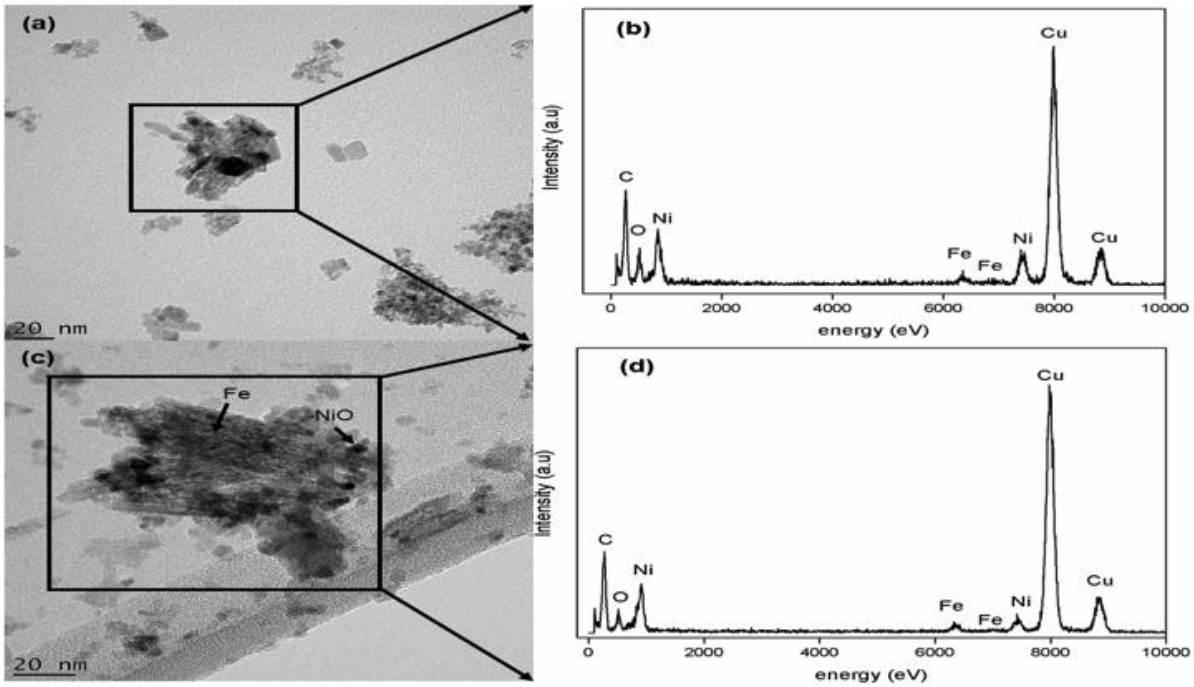

Figure 4.9 (a) Bright-field TEM micrograph of 2 % FeOOH-NiO, (b) corresponding EDS spectrum of area of interest, (c) Bright-field TEM micrograph of 5% FeOOH-NiO, (d) corresponding EDS spectrum

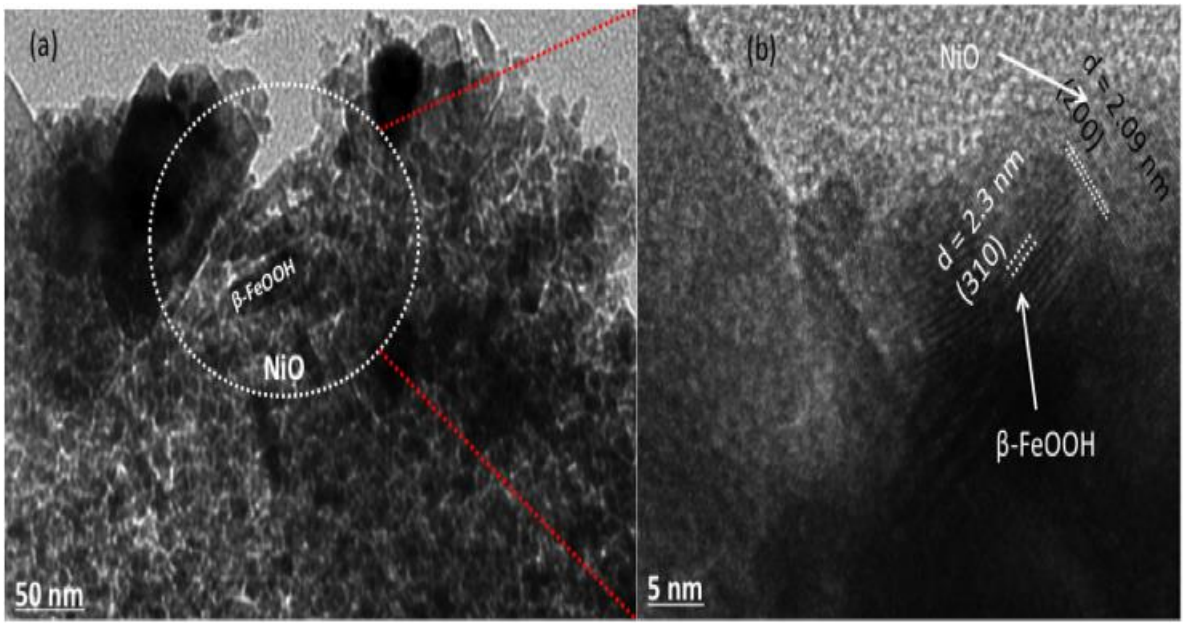

Figure 4.10: (a) TEM image of composite, (b) HRTEM image with characteristic d-spacing

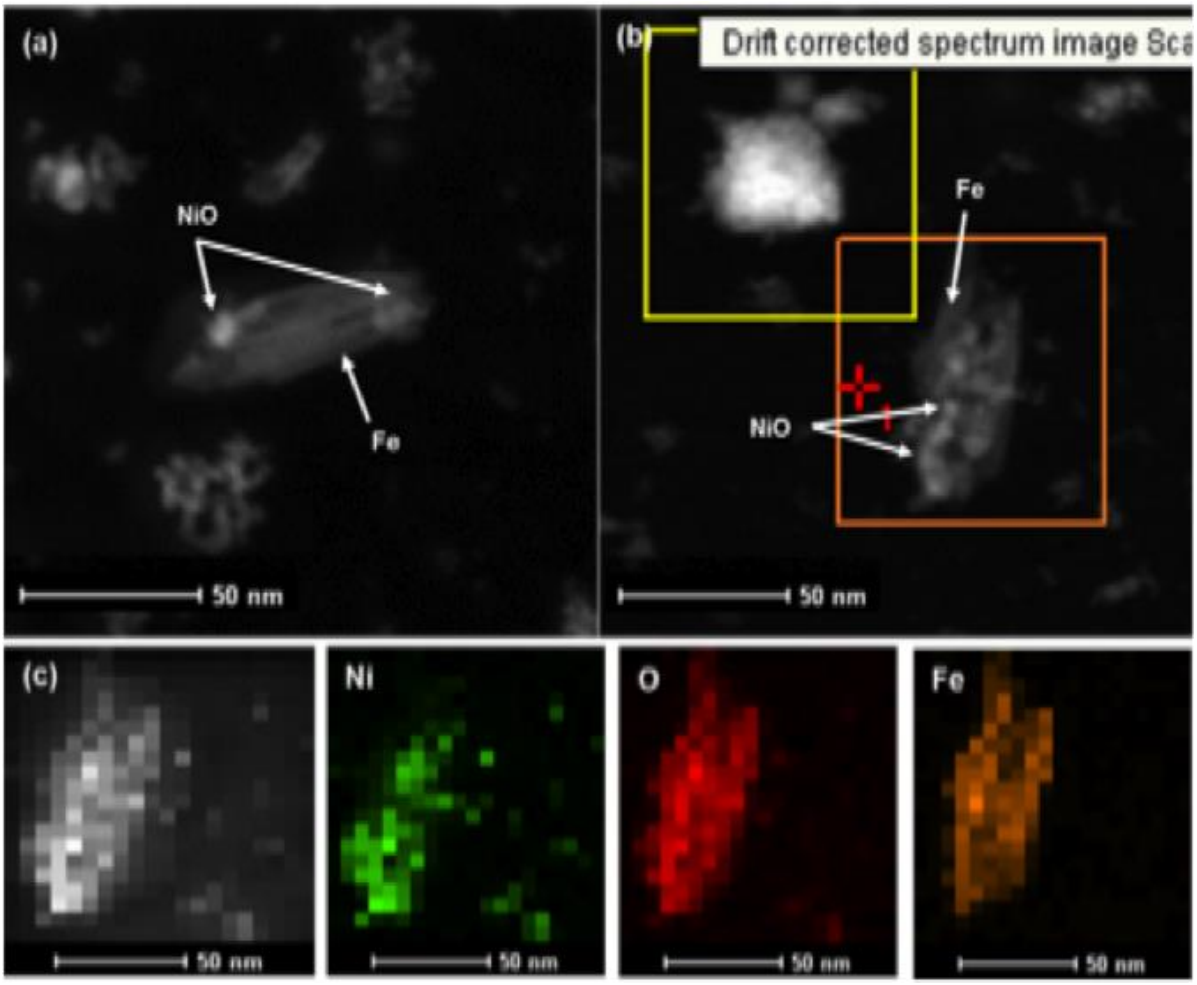

Figure 4.11: (a) Dark-field scanning TEM (STEM) micrograph of the 5 wt% Fe-NiO, (b) area of interest in the yellow window was used to correct for sample drift. (c) extracted elemental maps.

4.3. Effect of pH on kinetics and intermediates of phenol and chlorophenols ozonation

4.3.1. Effect of pH on kinetics

Ozone is widely applied for treatment of drinking water to remove taste, colour and improve biodegradability of impurities. Increasing interest in ozone is based on its stronger oxidizing power compared to chlorine, as well as its avoidance of chlorinated by-products. Ozone is a selective oxidant and many of its generated by-products during oxidation are only further removed upon prolonged oxidation. In order to assess the advantage and potential risks posed by an ozonation process, kinetic data are needed to predict what organics would be left upon ozonation of a single compound or mixture, and/or when it is suitable to halt an ozonation process.

The rate of ozone breakdown, and thus its reaction rate with aqueous organic is strongly dependent on reaction pH. While molecular ozone [-reactions] predominates at low pH, the conversion of ozone to hydroxyl radicals and the reactions of hydroxyl radicals occur at higher pH. The pH of the reaction mixture therefore, plays a role in determining the reaction rate as well as possible intermediates that would be generated during aqueous ozone reaction.

The effect of pH (2.5, 4, 7 and 10) on the reaction rates and intermediates of phenol and chlorophenols (2CP, 4CP, 24DCP) was studied. For each reaction, 100 mL, 2.0 x 10^{-3} M of substrate was adjusted to desired pH and fed into the reactor. Ozone gas supply into the rector was constant at 10 mL /min. Aliquot samples were drawn at regular intervals, quenched with sodium thiosulfate and analysed by HPLC.

The effect of initial pH solution on reaction rates of phenol, 2-chlorophenol, 4-chlorophenol and 2,4-dichlorophenol are presented in Figure 4.12– Figure 4.15. Due to low solubility of 2,4,6-trichlorophenol, equivalent solutions corresponding to 2.0 x 10^{-3} M could not be accurately and reproducibly prepared and are therefore not presented here.

The effect of starting solution pH is clearly visible upon inspection of the reaction rates obtained for the four compounds at the presented pH values. In all cases, the order of rate (refer to Table 4.4) was pH 10> pH 7> pH 4 > pH 2.5. This is in line with literature expected trend for rate measurements at varying pH (Ni and Chen, 2001). At high pH, ozone reacts with hydroxyl ions, decomposing quickly to generate non-selective hydroxyl radicals whose oxidizing power is superior to that of ozone [relative oxidizing power: •OH= 2.05, O_3= 1.53 and Cl_2= 1.00] (Munter, 2001, Glaze et al., 1987, Staehelin and Hoigne, 1982). The consequence of this is that organic removal at high pH is attributed to oxidation by both ozone and hydroxyl radicals. Conversely, at low pH, organic removal is primarily due to ozone alone, and is therefore slower.

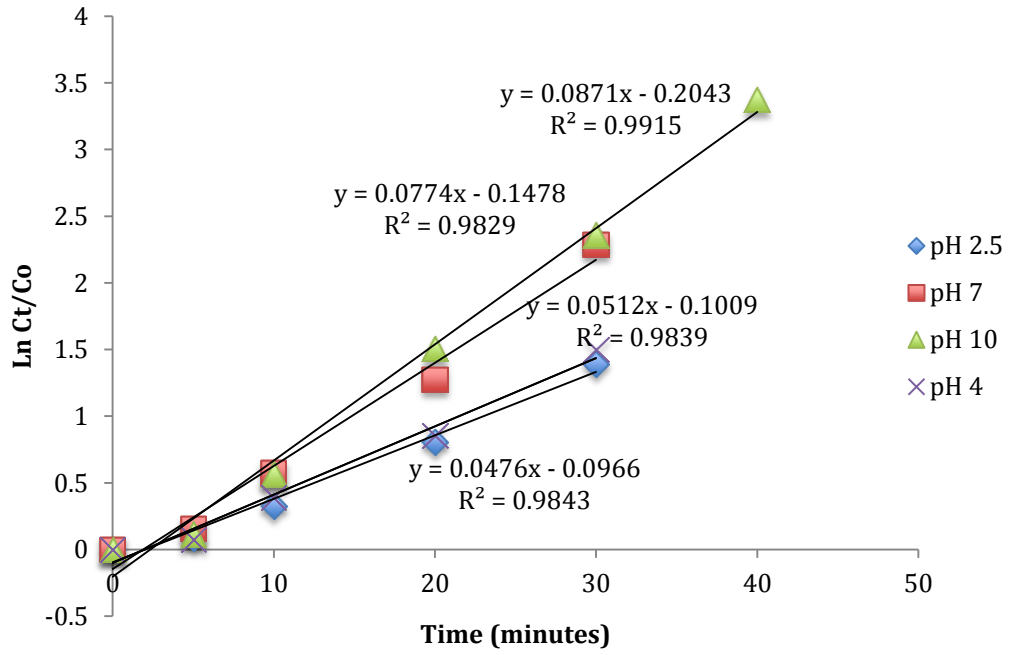

Figure 4.12: Pseudo first order plots for ozonation of phenol and varying pH (2.5, 4, 7, 10)

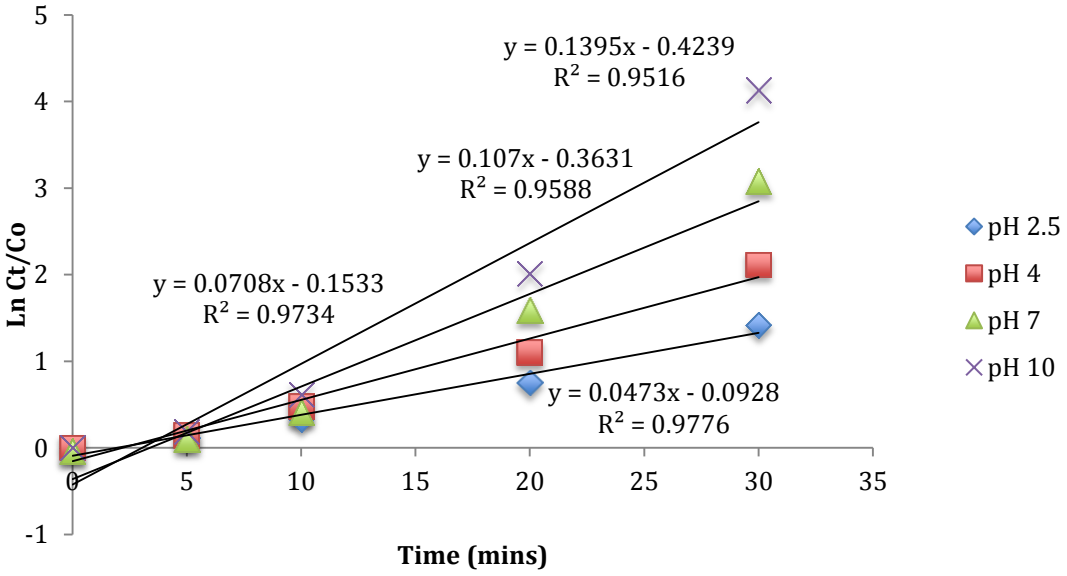

Figure 4.13: Pseudo first order plots for ozonation of 2-chorophenol and varying pH (2.5, 4, 7, 10)

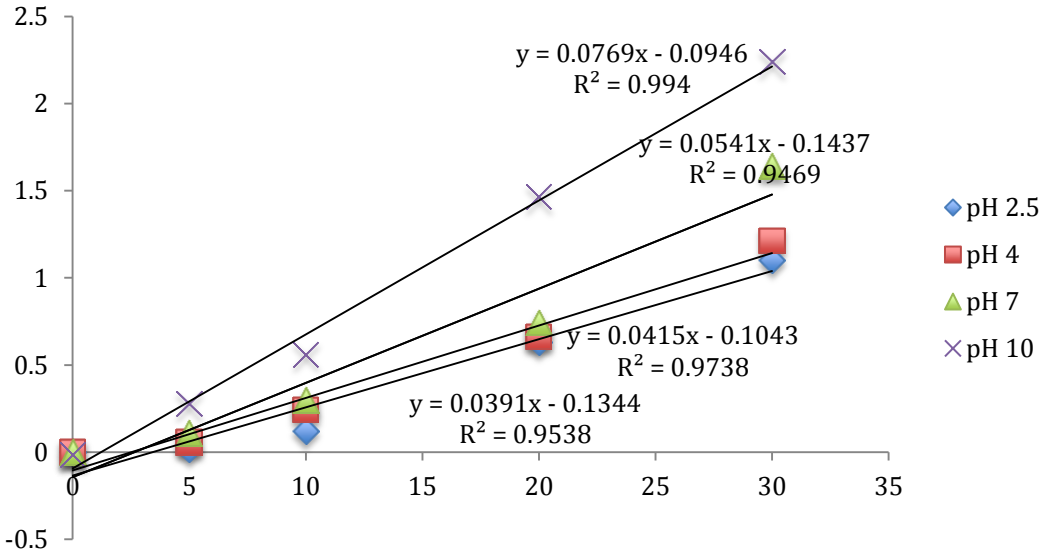

Figure 4.14: Pseudo first order plots for ozonation of 4-chorophenol and varying pH (2.5, 4, 7, 10)

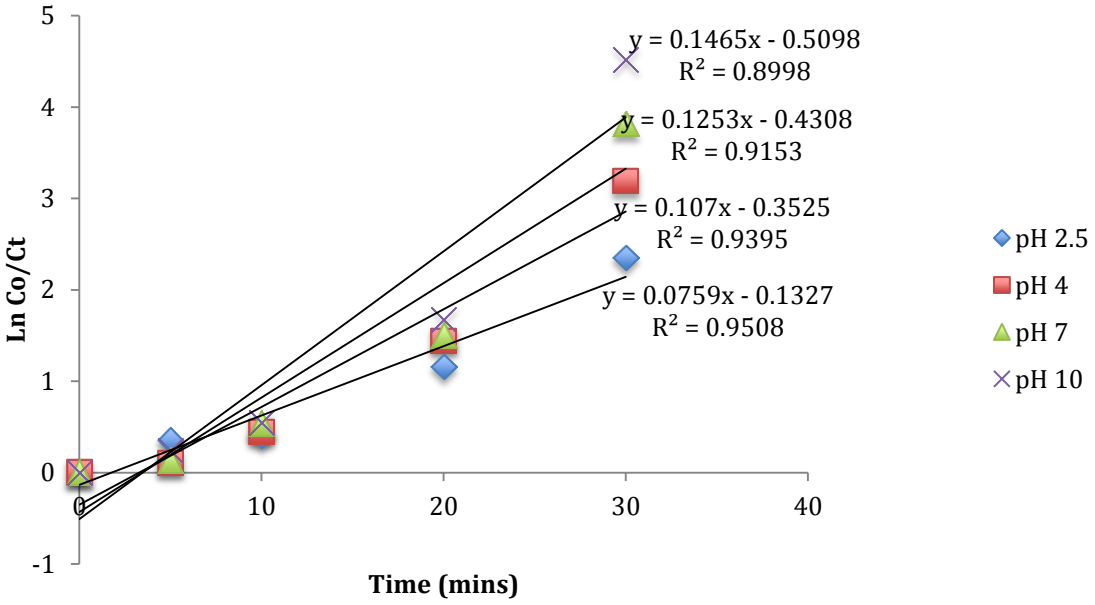

Figure 4.15: Pseudo first order plots for ozonation of 2,4-dichlorphenol at varying pH (2.5, 4, 7 and 10)

The apparent oxidation rates presented for phenol, 2CP, 4CP and 24DCP in Figure 4.12– Figure 4.15, all determined in a solution of dynamic pH (unbuffered) are summarized in Table 4.4. The trend of these results depicts that the order of ozonation rate is 24DCP > 2CP > Phenol > 4CP. Several differing opinions have been published to explain the apparent and absolute rate constants published for substituted phenols in same-study experiments. One point of view has proposed that the observed rate of ozonation is a direct consequence of ozonation mechanism which proceeds via hydroxylation, dechlorination and finally ring cleavage (Ni and

Chen, 2001, Benitez et al., 2000a, Arslan-Alaton and Koyunluoglu, 2007). In this manner, Benitez and co-workers explained the observed order in their study as 2,3,4,6-tetrachlorophenol > 2,4,6-trichlorophenol > 2,4-dichlorophenol > 4-chlorophenol. Another argument anchored on the electron withdrawing nature of chlorine atom suggested that the reduction of “active sites” on a phenolic ring by an attached chlorine atom would reduce the reactivity of chlorophenols with electrophilic species such as ozone. This formed the basis for explaining the order: phenol > 4-chlorophenol (similar to this study) observed by Fontanier and co-workers. (Fontanier et al., 2005). In explaining the high rate of ozonation of 2,4,6-trichorophenol containing three chlorine atoms, the authors argued that the presence of three chlorine atoms in ortho-, meta- and para- positions causes a strong destabilization of electron flow due to a combined electron withdrawing effect. This destabilization outweighs the resonance effect to produce a pseudo-olefinic structure and would thus account for the higher reaction rate of poly substituted phenols (Fontanier et al., 2005). While the arguments presented in the above discussion so far adequately account for the higher ozonation rate of 2,4-dichlorophenol compared to the monologues (2- and 4- chlorophenols), it does not explain why ozonation of 2-chlorophenol was faster than that of 4-chlorophenol and phenol.

At this juncture, it is important to highlight the report of Kuo and Huang (1995) on the relative rates of ozonation of 2-, 3- and 4-chlorophenols. The workers identified 3-chlorophenol as the least reactive, and 4-chlorophenol as the most reactive of the three. Based on thermodynamic experiments, the slower reactivity of 3-cholophenol towards ozone was attributed to its lower activation energy by the meta-Cl. While this meta- deactivation of a phenyl ring is essentially true, its application here would imply that a further substitution on position 5- of 3-chlorophenol ring by a chlorine atom would reduce the rate of ozonation of 3,5-dichlorophenol when compared to 3,4-dichlorphenol. Later publications by the same authors established that the rate of ozonation of 3,5-dichlorphenol was indeed higher than that of 3,4-dichlorophenol at several-experimental pHs and was closely related to the degree of dissociation of the compounds themselves (Qiu et al., 2004, Qiu et al., 2002). The increased rate of 4-cholrophenol ozonation over 2-chlorophenol was explained based on differing mechanism taken by the ortho- and para- substituents to aliphatic carboxylic acids (Kuo and Huang, 1995). The trend of chlorophenol oxidation obtained in this study

does not agree with that published by the authors (i.e. ozonation rate for 4-chlorophenol was not higher than that of 2-chlorophenol).

In an extensive work to elucidate the absolute rate constants of various organics, Hoigné and Bader reported the order of ozonation of phenol and chlorophenol as: 2,4,6-trichlorophenol > 2,4,5-trichlorophenol > 2,3-dichlorophenol > 2,4-dichlorophenol > 2-chlorophenol ≈ phenol > 4-chlorophenol (Hoigné and Bader, 1983b, Hoigné and Bader, 1983a, Hoigné et al., 1985). According to the workers, the acidity of a chlorophenol increases with increasing chlorine atom as evidenced from the pK values of the non-dissociated form. Therefore, at any given pH value (keeping concentration constant), the population of dissociated chlorophenol would increase with increasing chlorine atom. Since the reactivity of the dissociated chloro-phenolate ions approach values for diffusion-controlled reactions, the consequence is a faster rate for these compounds. This argument would imply that the rate of ozonation of chlorophenols is directly dependent on (and inversely related to) their pK_a values [phenol = 9.9; 2-chlorophenol = 8.3; 4-chlorophenol = 9.2; 2,4-dichlorophenol = 7.8]. The experimental data obtained in this study are in agreement with those by the authors. The proposed explanation also accounts for 2-chlorophenol reaction rates being higher than the isomer, 4-chlorophenol. It however does not explain why 4-chlorophenol rates are lower than those obtained for phenol even though it has a lower pK_a value.

From the foregoing, it is clear that current existing explanations provided by different researchers have been largely insufficient in accounting for observed trends of chlorophenol ozonation. It is most probable that more than one explanation applied simultaneously holds true for the ozonation process. For examples, the high oxidation rates observed at high pH could be ascribed to an increased fraction of the phenolate ion, in addition to a faster breakdown of ozone to hydroxyl radicals by hydroxide ions. An increased dissociation can account for the order of the mono-substituted chlorophenols 2-chlrophenol > 4- chlorophenol (pK_a = 8.3 and 9.2, respectively), but cannot account for the order: phenol > 4-chlorophenol (pK_a = 9.9 and 9.2, respectively). The chlorine atoms, which increase acidity and therefore increase the concentration of phenolate ions, can play a different (-or dual) role when positioned differently on the molecule. A more radical approach to the matter would be to consider the individual chlorine atoms as distinct in behaviour with respect to their positions and also by using frontier models. Based on such a

hypothesis the chlorine atom at the ortho position may be regarded as being a site of high electron density, thus serving as a candidate site for electrophilic attack, while the chlorine at the para position may appear as a site of low electron density. The existence of a positive chlorine atom in an aromatic ring is not new (Morrison and Boyd, 1992); and may serve an additional explanation for the behaviour of the isomers.

The apparent rate constant for phenol and the chlorophenols are summarized in Table 4.4. Rates calculations were restricted to the first 30 minutes of the reaction where the pH had a significant effect on the pH. Beyond 30 minutes, the pH had dropped well into the acidic region for all experiments. If we consider the apparent rate constants of the phenols to be the sum of the rate of oxidation of the acid (HB) and its ionized forms (phenolate ions) B-, then

Equation 4.1

$$Rate = K_{HB}[HB] + K_{B^-}[B^-]$$

The contribution of K_{B^-} to the rate increases with pH due to increased ionization of HB and Equation 4.2 proposed by Hoigné and Bader (1983b) holds.

Equation 4.2

$$\log K_{tot} = \log K_{HB} + pH - pK_{B^-}$$

A logarithmic plot of total apparent rate would rise linearly with pH (Figure 4. 16), which is in agreement with literature.

Table 4.4: Apparent rate constants for ozonation of phenol and chlorophenols at varying pH

pH	Phenol		2chlorophenol		4-chlorophenol		2,4dichlorophenol	
	K	R^2	K	R^2	K	R^2	K	R^2
2,5	0,0476	0,98	0,0437	0,98	0,0391	0,95	0,0759	0,95
4	0,0512	0,98	0,0766	0,97	0,0415	0,97	0,107	0,94
7	0,0774	0,98	0,0899	0,96	0,0553	0,99	0,1253	0,92
10	0,0828	0,99	0,1208	0,95	0,0769	0,99	0,1424	0,9

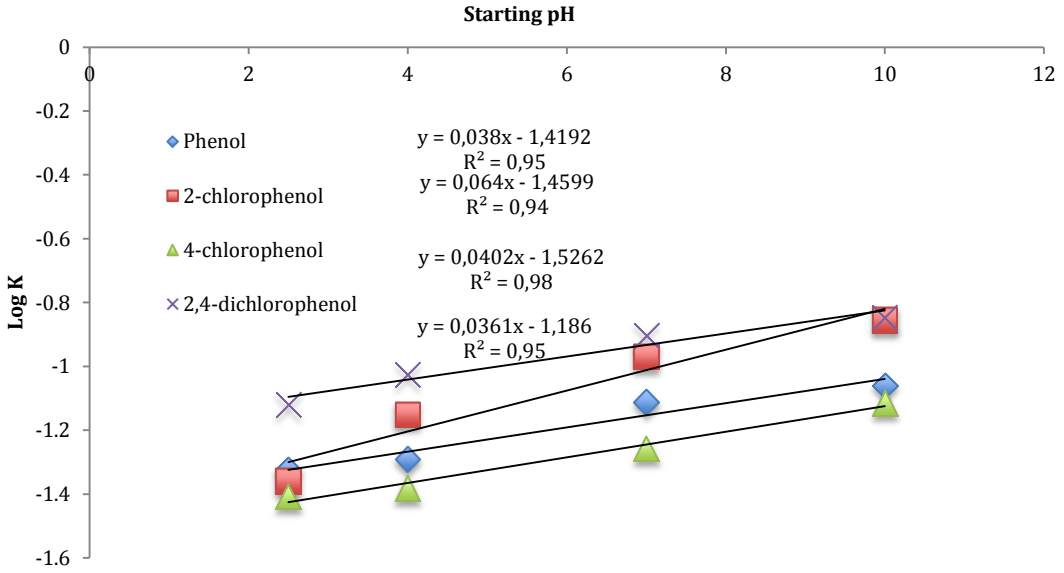

Figure 4.16: Logarithmic plot of total apparent rate versus starting pH of solution

4.3.2. Effect of pH on intermediates

The process of oxidation of an aromatic ring (organic molecules in general), involves the infusion of one or more oxygen atoms into the molecule (either on the ring, or as a hetero-atom in the ring), followed by elimination of small atoms [-moieties] or ring rupture. The products of such ring opening reactions are low molecular weight carboxylic acid as identified by several workers. While a lot of research have been devoted to studying the removal of organics from aqueous media by various oxidation processes, fewer workers have devoted studies to the breakdown products of aromatic rings, and far less concerns have been given to the actual intermediates taken to the final products as well as the mechanisms involved in the reaction processes themselves. Some of the intermediates and by-products of ozonation (and oxidations in general) are less reactive to further oxidation and therefore slow down the oxidation process as they accumulate in solution. Furthermore, the possibility of secondary reactions between two or more generated intermediates in a reaction cannot be ruled out.

In order to identify real time intermediates generated during ozonation of phenol and chlorophenols, aliquot samples drawn from the reactor at varying time intervals were analysed by LC-MS. By varying the pH of the starting solution, the effect of pH on the intermediates was monitored. Phenol and chlorophenols were ozonated in acidic (pH 3), in alkaline (pH 10) and in solution without pH adjustments furthermore

referred to as ‘dissolution pH’ (pH 6). The pH of starting solutions in acidic and alkaline experiments was adjusted to pH 3 and pH 10 using aliquots of H_3PO_4 and NaOH, respectively. A fourth experiment was conducted at pH 10 where the pH was held constant by continuous introduction of small does of NaOH as the ozonation process progressed. By keeping the pH constantly in the high alkaline region, the reactions of the ionized phenolics as well as radical mechanisms would be promoted ahead of direct ozonation reactions, which would predominate at lower pH values. In experiments to identify intermediates, the use of sodium thiosulphate was avoided. Preliminary experimental runs revealed that the intermediates were labile (some lasting only about 6 hours in solution). All samples for identification of intermediates were therefore analysed immediately.

4.3.2.1 Intermediates of phenol ozonation

Figure 4.17(a) and (b) show the DAD (280 nm) and total ion chromatogram (TIC) of phenol based on the LC-MS method applied in this study. Due to the weak ionization of phenol, an extracted ion chromatogram could not be obtained. Breakdown intermediates were sought based on the molecular features of phenol. Algorithm for formula assignments was C=30, H=60, O=10. This allowed for possible ring coupling or side reactions with other intermediate products. Based on literature guidance, a list of possible expected intermediates (catechol, hydroquinone, resorcinol, benzoquinone and 2,5-dihydroxybenzoquinone) obtained as pure standards were analysed alongside samples (Figure 4.18- Figure 4.22). A time-based study of intermediates identified during the ozonation of phenol in acidic pH (3.5), dissolution pH (6), alkaline pH (10) and constant-alkaline pH (10) experiments are summarily presented in Table 4.5. For the purpose of this discuss, the results presented are limited to time t= 30mins. Results on further oxidation intermediates after this time are presented in Appendix 7.A. Important compounds which form the basis of discuss in this section are highlighted in the Table. Other compounds identified by molecular formula search (MFE) are presented with relevant supporting MFE spectrums in Appendix 7.B - Appendix 7.H.

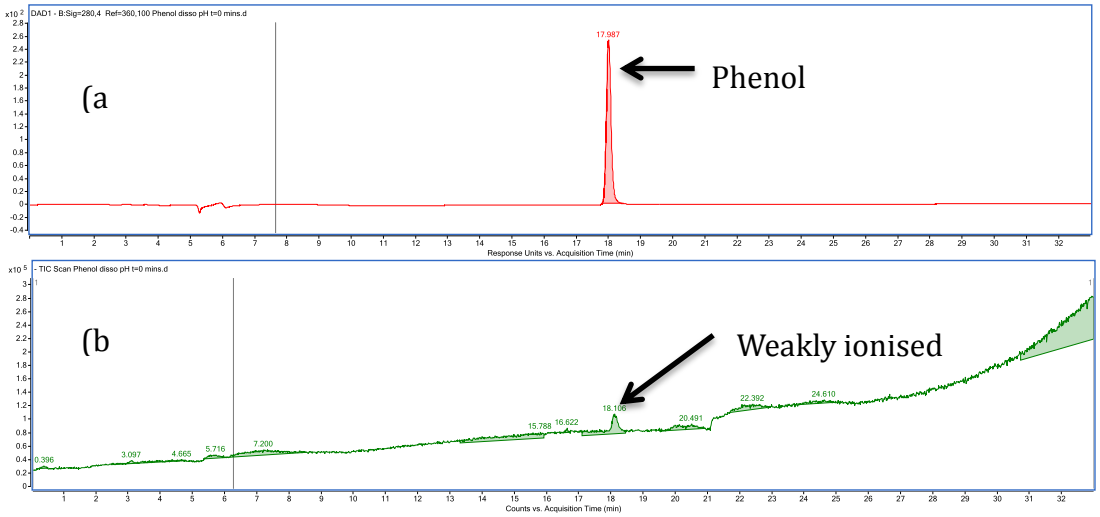

Figure 4.17: (a) DAD [280 nm] and (b) TIC chromatograms of phenol (C_6H_6O) RT = 17.897 min

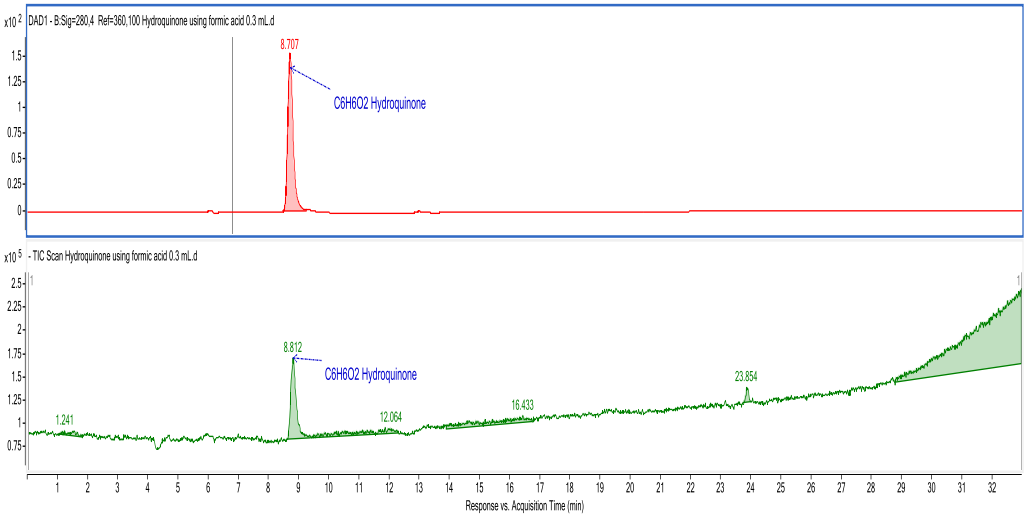

Figure 4.18: DAD and TIC chromatograms for hydroquinone ($C_6H_6O_2$) RT = 8.707 min

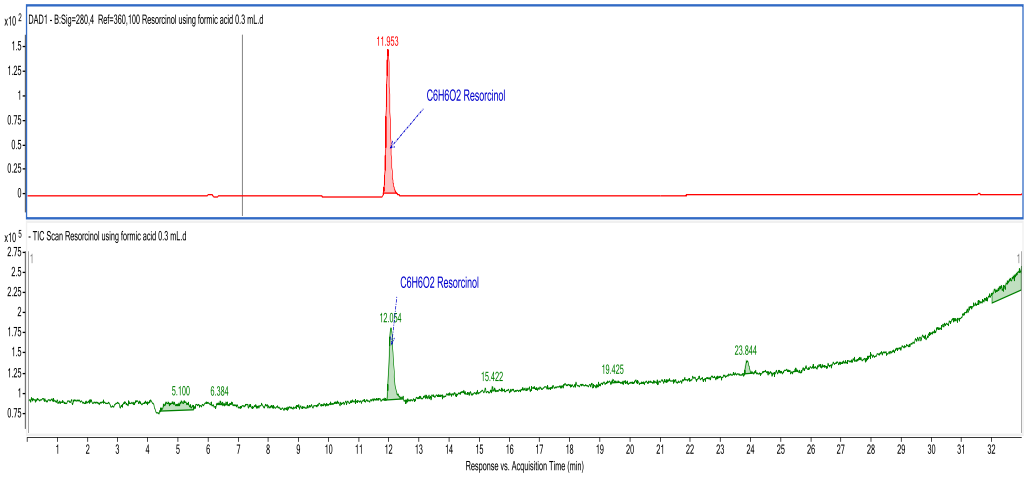

Figure 4.19: DAD and TIC chromatograms for resorcinol ($C_6H_6O_2$) RT= 11.963 min

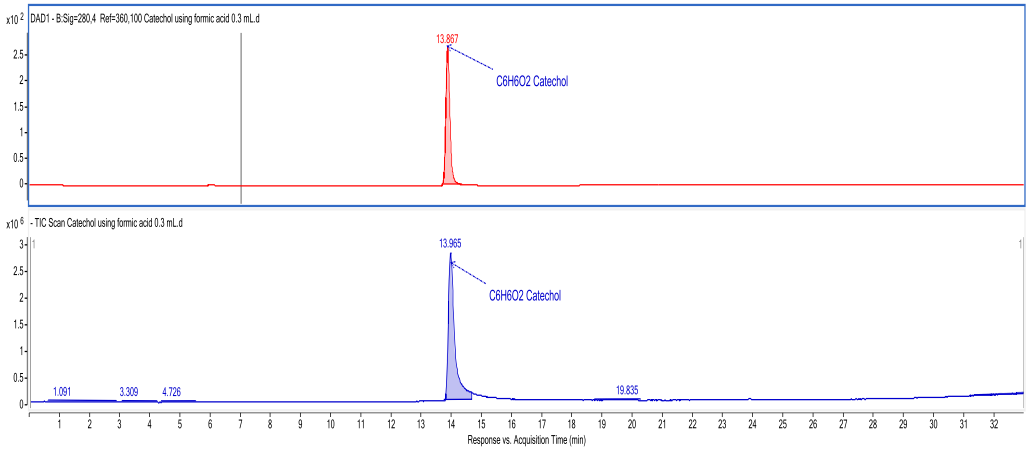

Figure 4.20: DAD and TIC chromatograms for catechol ($C_6H_6O_2$) RT= 13.867 min

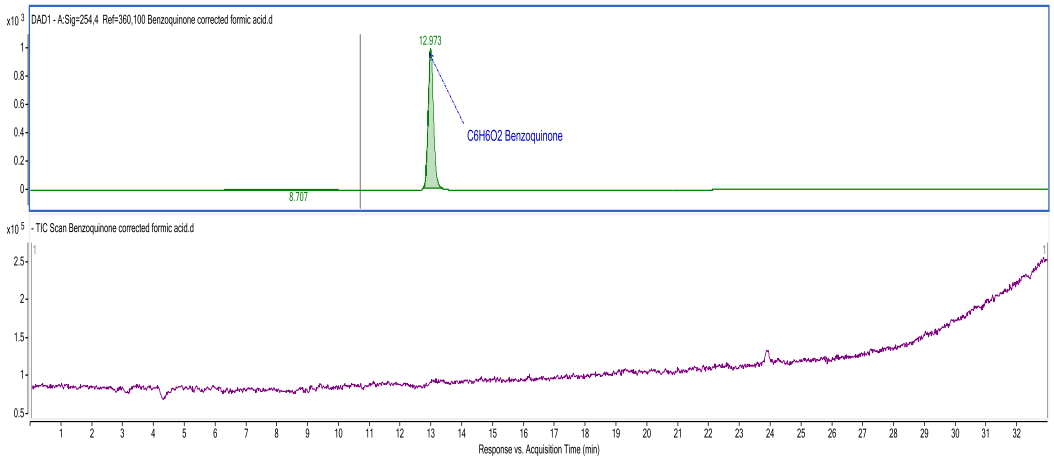

Figure 4.21: DAD and TIC chromatograms for benzoquinone ($C_6H_4O_2$) RT = 12.973 min

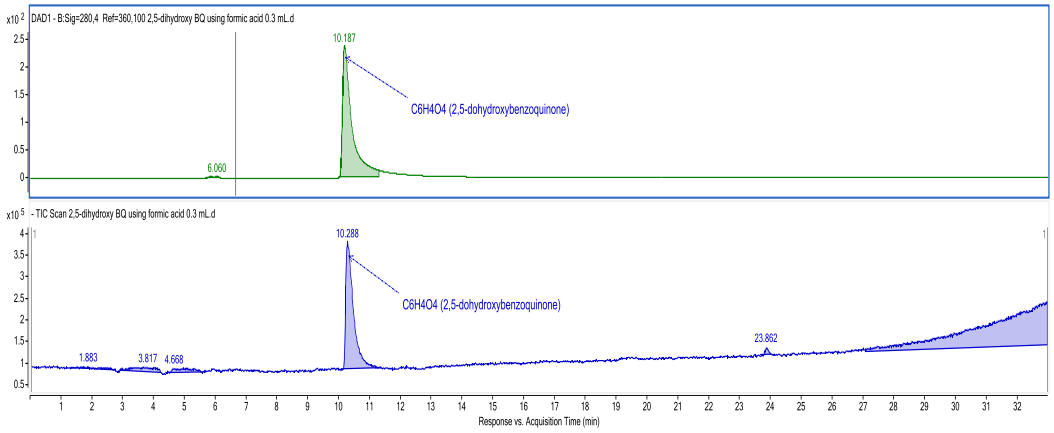

Figure 4.22: DAD and TIC chromatogram of 2,5-dihydroxybenzoquinone ($C_6H_6O_4$) RT = 10.187 min

Table 4.5: Intermediates of phenol ozonation at varying pH as followed by LCMS

Time (min)		Acidic pH (3)			Dissolution pH 6			Alkaline pH (10) [not held constant]			Constant alkaline pH (10)		
		RT	mass	Formula	RT	mass	Formula	RT	mass	Formula	RT	mass	Formula
0		17,987		C6H6O	17,987		C6H6O	17,987		C6H6O	17,987		C6H6O
10	1	13,996	110,03721	C6H6O2	13,998	110,03759	C6H6O2	12,8	72,02096	C3H4O2	3,153	113,99286	C4H2O4
	2							14,003	110,03625	C6H6O2	21,13	186,06842	C12H10O2
	3							20,812	110,03676	C6H6O2	23,044	186,06852	C12H10O2
	4							20,814	136,0525	C8H8O2			
	5							21,134	186,06903	C12H10O2			
	6							22,888	94,04237	C6H6O			
	7							23,047	186,0691	C12H10O2			
20	1	12,797	72,02222	C3H4O2	13,995	13,99500	C6H6O2	13,995	110,03725	C6H6O2	3,177	113,99286	C4 H2 O4
	2	13,996	110,03721	C6H6O2				19,749	110,03712	C6H6O2	4,512	140,01121	C6 H4 O4
	3							22,881	94,04284	C6H6O	4,563	178,04825	C6 H10 O6
	4										5,717	146,02211	C5 H6 O5
	5										5,721	88,01662	C3 H4 O3
	6										8,026	220,03786	C11 H8 O5
	7										8,971	222,05347	C11 H10 O5
	8										12,505	138,03221	C7 H6 O3
	9										12,755	72,02145	C3 H4 O2
	10										13,995	110,03656	C6 H6 O2
	11										14,772	164,04707	C9 H8 O3
	12										20,81	110,03697	C6 H6 O2
	13										20,812	136,05279	C8 H8 O2
	14										21,129	186,06892	C12 H10 O2
	15										22,883	96,02153	C5 H4 O2
	16										22,884	124,01611	C6 H4 O3
	17										22,884	94,04247	C6 H6 O
	18										23,043	186,06892	C12 H10 O2
	19										27,573	278,09535	C18 H14 O3

Time (min)		Acidic pH (3)			Dissolution pH 6			Alkaline pH (10) [not held constant]			Constant alkaline pH (10)		
		RT	mass	Formula	RT	mass	Formula	RT	mass	Formula	RT	mass	Formula
30	1	12,797	72,02222	C3H4O2	12,807	72,02235	C3H4O2	12,749	72,01976	C3H4O2	3,2	113,99286	C4 H2 O4
	2	13,996	110,03721	C6H6O2	13,998	110,03763	C6H6O2	14,008	110,03447	C6H6O2	4,508	140,01152	C6 H4 O4
	3							22,892	94,04244	C6H6O	4,561	178,04877	C6 H10 O6
	4										4,649	134,02187	C4 H6 O5
	5										4,657	72,02182	C3 H4 O2
	6										5,48	176,03098	C6 H8 O6
	7										5,717	146,02046	C5 H6 O5
	8										5,721	192,02596	C6 H8 O7
	9										5,726	88,01532	C3 H4 O3
	10										5,729	150,01516	C4 H6 O6
	11										7,002	96,02034	C5 H4 O2
	12										7,25	96,02031	C5 H4 O2
	13										8,026	220,03632	C11 H8 O5
	14										8,441	114,03057	C5 H6 O3
	15										8,97	222,05216	C11 H10 O5
	16										12,501	138,03162	C7 H6 O3
	17										12,721	116,01021	C4 H4 O4
	18										12,725	72,02178	C3 H4 O2
	19										13,998	110,03719	C6 H6 O2
	20										14,774	164,04757	C9 H8 O3
	21										20,807	136,05298	C8 H8 O2
	22										20,807	110,03703	C6 H6 O2
	23										21,128	186,0692	C12 H10 O2
	24										22,884	94,04251	C6 H6 O
	25										22,884	96,02147	C5 H4 O2
	26										22,885	124,01622	C6 H4 O3
	27										23,043	186,06916	C12 H10 O2
	28										27,579	278,09543	C18 H14 O3

In general, the ozonation of phenol **1** is observed to proceed via the formation of catechol **2** ($C_6H_6O_2$, RT= 13.996 confirmed against pure standard: Figure 4.8) and yields acrylic acid **3** ($C_3H_4O_2$) as a low molecular weight product. Catechol is a product of ortho hydroxylation of phenol and its formation is favoured at acidic pH where it is seen as the only intermediate product after 10 minutes, and together with acrylic acid constitute the only identified intermediates after 30 minutes.

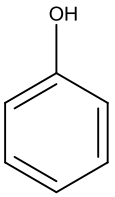

phenol

Structure 1: Phenol

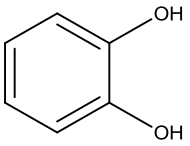

catechol

Structure 2: Catechol

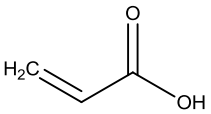

acrylic acid

Structure 3: Acrylic acid

At higher pH10, the breakdown, however, proceeded via the formation of other major intermediates. Important amongst these intermediates is an isomer of catechol ($C_6H_6O_2$, RT= 20.812), the dimerised isomers $C_{12}H_{10}O_2$ (RT= 21.134 and 23.047), the trimer $C_{18}H_{14}O_3$ (RT = 27.573) and an isomer of phenol (C_6H_6O, RT = 22.888) produced when the solution pH was either started from pH 10, or held constant at pH 10. The mass spectrums (MFE) of these compounds showing the isotope abundance and spacing used for identification were acquired from their individual extracted ion chromatograms (EIC) and are presented in the appendix section. The trimer was observed within 20 minutes when the reaction was kept constant at pH 10. The compound C_6H_6O at RT=22.888 identified only in the alkaline experiment is clearly different from the starting phenol (RT= 17.987) which does not ionize appreciable to be detected by the method applied in this study (Figure 4.17b). The pKa for phenol (9.9) allows for majority of the phenol molecules to exist as phenolate ions at pH 10. The reactions of the phenolate ion with ozone may well account for the presence of the higher dimers, trimer, isomeric phenol and two differing hydroxylated phenols observed at high pH. There is little or no information regarding the ozonation of phenol to generate the dimers, trimer. Structures presented here were arrived at based on searches conducted on the Royal Society of Chemistry's ChemSpider, taking into account the molecular features of phenol and in other cases, literature guidance.

C_6H_6O RT= 22.888 minutes: there are 57 possible structures for this formula. Only isomers where the six-membered ring framework is preserved are considered here. **4** and **5** are neutral isomers produced upon phenol tautomerism to a keto-structure. Unlike in aliphatic structures, the aromaticity of phenol **1** renders the enol tautomer more stable than its keto counterparts (Bertrand and Bouchoux, 1998). The conversion of **1** to **4** (or **5)** is therefore not energetically favourable. Of the three ionized forms, **6** is the more stable isomer, having energies 133 and 146 $kJmol^{-1}$ lower than **7** and **8**, respectively (Turecek and Cramer, 1995, Smith et al., 1991). Structure **6** (the ionized isomer of phenol) is therefore proposed as the possible compound with RT= 23.888. Despite the selection of structure **6** here based on stability and ionizing possibility of phenol **1** at pH 10, it should be noted that the ketones **4** and **5** has been identified as crucial intermediates during phenol decomposition (Capponi et al., 1986, Gadosy and McClelland, 1996) and mechanisms of conversion of **6** to **7** have been proposed (Turecek et al., 1989, Le et al., 2001).

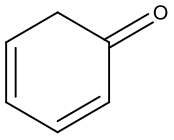

cyclohexadieneone

Structure 4: cyclohexadieneone

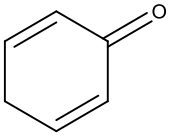

2,5-cyclohexadieneone

Structure 5: 2,5-cyclohexadieneone

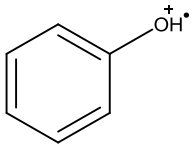

phenol radical cation

Structure 6: phenol radical ion

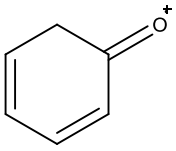

cyclohexadieneone radical cation

Structure 7: cyclohexadieneone radical ion

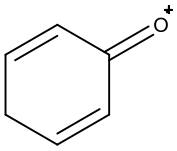

2,5-cyclohexadieneone radical cation

Structure 8: 2,5-cyclohexadieneone radical ion

$C_6H_6O_2$ (RT: 20.812, MFE Appendix 7.C): Based on a search results of 115 compounds, compound **9** and **10** were selected as most probable. The other hydroxylated phenols were eluted at; resorcinol **12** (RT= 11.953) and hydroquinone **13** (RT=8.707) and were therefore excluded. Literature evidence of an ionized catechol **11** is scarce and has only being recently proposed as an intermediate of catechol reactions (Yin et al., 2015). It is important to highlight that this isomer at RT

= 20.812 minutes cease to exist in experiments conducted at pH 10 as the solution pH dropped despite catechol being the major intermediate identified. Compound **10**, 1-(3-furyl)ethanone been the more stable of the furan structures is here considered as most probable structure for $C_6H_6O_2$ RT= 20.812.

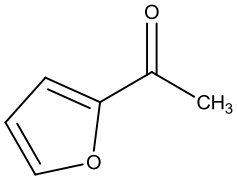

2-acetylfuran

Structure 9: 2-Acetylfuran

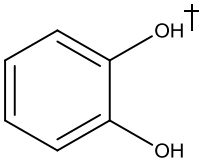

catechol radical

Structure 11: Catechol radical

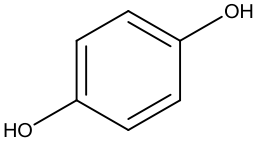

hydroquinone

Structure 13: Hydroquinone

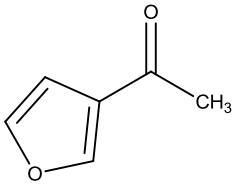

1-(3-furyl)ethanone

Structure 10: 1-(3-furyl)ethanone

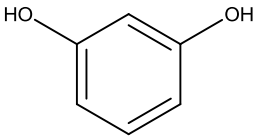

resorcinol

Structure 12: Resorcinol

$C_{12}H_{10}O_2$: Experiments conducted at pH 10 showed two isomers for $C_{12}H_{10}O_2$ with retention times RT= 21.134 and 23.047 (Respective mass spectrums Appendix 7.D and Appendix 7.E). These compounds are possible products of reactions of ionized phenolate ions initiated by ozone in alkaline medium. Earlier reports have identified $C_{12}H_{10}O_2$ as an intermediate during ozonation (Huang and Shu, 1995) and peroxidase catalysed oxidation of phenol (Yu et al., 1994). Structures **14**, **15**, **16**, **17** and **18,** selected based on the molecular features of phenol from a list of 331 compounds, are five stable intermediates of phenol coupling. Structures **15** and **18** which contain a phenoxy group better represent the expected coupled dimers of ionic reactions which predominate at pH 10, and are thus selected as probable structures for the two compounds with RT= 21.134 and 23.047. These compounds may be generated by the attack of a phenolate ion or phenoxy radical on a para (**15**) and ortho (**18**) position of a phenol molecule.

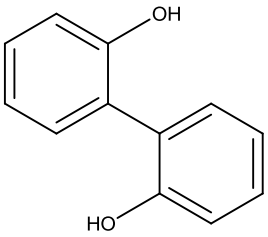

o,o-biphenol

Structure 14: o,o-biphenol

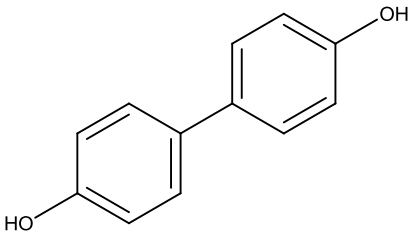

p,p-biphenol

Structure 17: p,p-biphenol

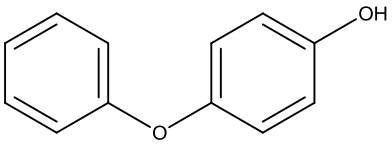

p-phenoxyphenol

Structure 15: p-phenoxyphenol

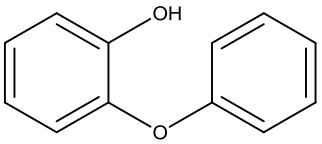

o-phenoxyphenol

Structure 18: o-phenoxyphenol

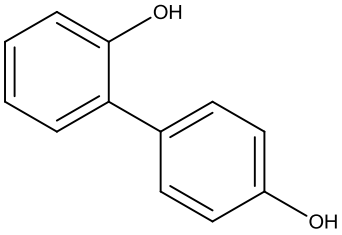

o,p-biphenol

Structure 16: o,p-biphenol

$C_{18}H_{14}O_3$ (RT=27.573, Mass spectrum Appendix 7.F) $C_{18}H_{14}O_3$ was identified only in experiments where the pH was held constant at pH10 and is possibly generated by a further attack of the dimer by a phenolate ion/radical with a concomitant loss of a hydrogen molecule. There are two possible structures arising from a further attack of either **15** or **18** by a phenoxy radical. While ortho-attacks leading to **19** are preferentially supported by theory, 4-(4- phenoxyphenoxy)phenol **20** arising from para- phenoxy attacks has been identified as a trimeric product during phenol oxidation (Yu et al., 1994). **20** which is supported by literature is therefore accepted as most probable structure for $C_{18}H_{14}O_3$.

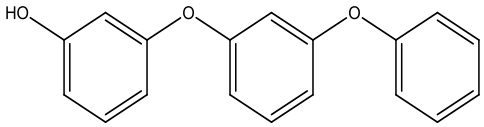

3-(3-phenoxyphenoxy)phenol

Structure 19: 3-(3-phenoxyphenoxy)phenol

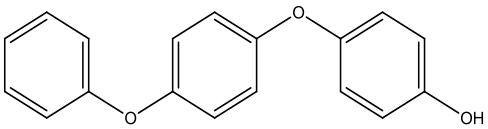

4-(4-phenoxyphenoxy)phenol

Structure 20: 4-(4-phenoxyphenoxy)phenol

An evaluation of the final breakdown products of an ozonation reaction is important as the overall assessment of the process itself is based on its ability to remove target organics (of known toxicity), compared with the by-products left behind. In this regard, the final intermediates after phenol removal (time t=60 minutes) were compared and are comparatively discussed pari-passu their existence in literature.

1.3.2.1.1 Residual three carbon (C3) compounds:

Residual C3 compounds identified in solution after 60 minutes included the ubiquitous acrylic acid **3** to the highly oxygenated tartronic acid **24**. **21** and **23** were identified in experiments conducted at high pH and are supported by existing literature (Pimentel et al., 2008, Devlin and Harris, 1984). Compound **3** was common to all experiments and has been worked out as a product of phenol breakdown and the precursor to compounds **21, 22, 23** and **24**. (Devlin and Harris, 1984). Oxidation of C2 on acrylic acid **3** gives pyruvic acid **21** and further oxidation on C3 gives **22**. Malonic acid **23** is readily converted to tartronic acid **24** by radical hydroxylation of C2.

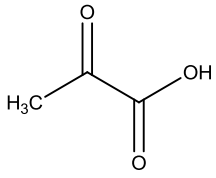

pyruvic acid

Structure 21: Pyruvic acid

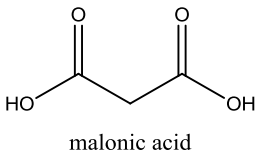

malonic acid

Structure 23: Malonic acid

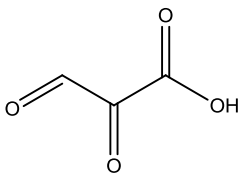

2,3-dioxypropanoic acid

Structure 22: 2,3-dioxypropanoic acid

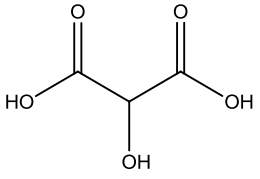

tartronic acid

Structure 24: Tartronic acid

1.3.2.1.2 Residual four carbon (C4) compounds

Residual C4 compounds are products of ring opening of a 1-4-quinone system. Despite the absence of hydroquinone **13** in analysed samples, the presence of these 4-carbon breakdown products supports its existence as a transient compound during the ozonation of phenol. **25** is a di-oxo product of ring opening of hydroquinone at position 1 and position 4 of the phenyl ring. Oxidation of carbon one (C1) on **25** gives **26**, which undergoes further oxidation on carbon four (C4) to give **27** and **28**. **27** and **28** are generally reported in any of two isomeric forms (fumaric or maleic acids) and were not observed in any experiments conducted in the alkaline pH. Both isomers were detected in this study. Malic acid **29** is a product of hydroxylation of carbon 2 (C2) on **27**. Further hydroxylation on C3 gives tartaric acid **30**. Compounds **25**, **26**, **29** and **30** were identified as break down products in all experiments when the pH was not held constant in the alkaline region. These break down products are supported by literature (Devlin and Harris, 1984, Eisenhower, 1968, Bauch et al., 1970, Pimentel et al., 2008).

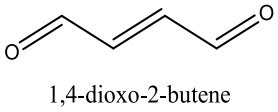

1,4-dioxo-2-butene

Structure 25: 1,4-dioxo-2-butene

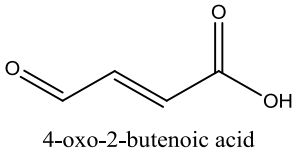

4-oxo-2-butenoic acid

Structure 26: 4-oxo-2-butenoic acid

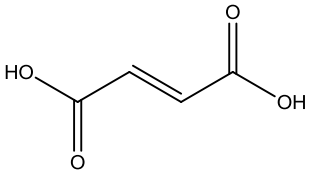

fumaric acid

Structure 27: Fumaric acid

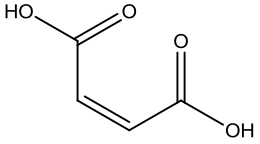

cis-butenedioic acid

Structure 28: Maleic acid

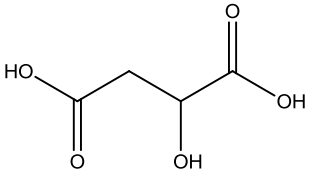

malic acid

Structure 29: Malic acid

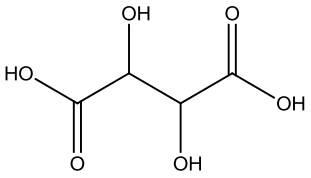

tartaric acid

Structure 30: Tartaric acid

4.3.2.1.3 *Residual five carbon (C5) compounds*

Literature on five carbon compounds obtained as breakdown products of phenol is scarce. Structures presented here are therefore hypothetical. Two C5 intermediates identified were $C_5H_4O_2$ and $C_5H_6O_5$, assigned structures **31** and **32**, respectively. Catechol is an established intermediate of phenol breakdown. A loss of methylene – CH2 group may yield **31**, which may undergo ring opening after C2 hydroxylation to give **32**.

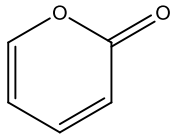

pyrone

Structure 31: Pyrone

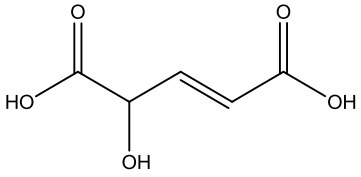

4-hydroxy-2-pentendioic acid

Structure 32: 4-hydroxy-2-pentendioic acid

4.3.2.1.4 *Residual six carbon (C6) compounds*

Two C6 compounds, $C_6H_4O_4$ and $C_6H_6O_4$ were detected in solution during and after the degradation of phenol. $C_6H_4O_4$ may be represented by one of structures **33**, **34**, **35** or **36**. The ortho hydroxylation of catechol supports structure **36**.

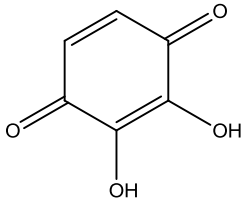

2,3-dihydroxy-1,4-benzoquinone

Structure 33: 2,3-dihydroxy-1,4-benzoquinone

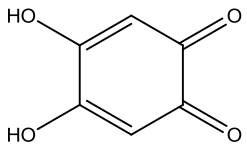

4,5-dihydroxy-1,2-benzoquinone

Structure 34: 4,5-dihydroxy-1,2-benzoquinone

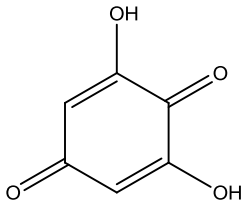

2,6-dihydroxybenzoquinone

Structure 35: 2,6-dihydroxybenzoquinone

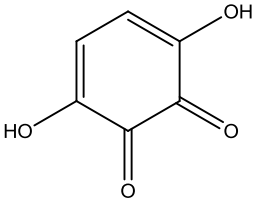

3,6-dihydroxy-1,2-benzoquinone

Structure 36: 3,6-dihydroxy-1,2-benzoquinone

Two isomers of $C_6H_6O_4$ were identified with RT= 4.575 and 11.745 minutes. The lower retention time of the first isomer is suggestive of a carboxylic acid. Muconic acid **37** is most probable candidate acid and is supported by early literature (Eisenhower, 1968). The other less polar isomer may be represented by one of **38**, **39** or **40**. Compound $C_6H_4O_3$ may be represented by one of **41**, **42** or **43**.

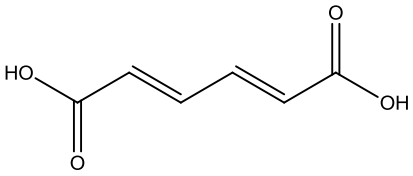

muconic acid

Structure 37: muconic acid

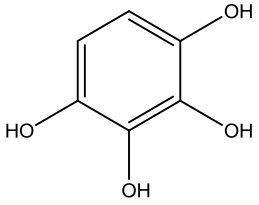

2,3-dihydroxy hydroquinone

Structure 38: 2,3-dihydroxyhydroquinone

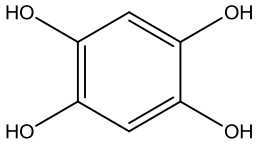

2,5-dihydroxy hydroquinone

Structure 39: 2,5-dihydroxyhydroquinone

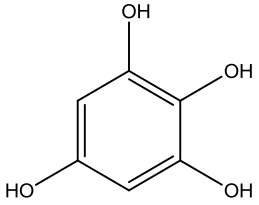

2,6-dihydroxy hydroquinone

Structure 40: 2,6-dihydroxyhydroquinone

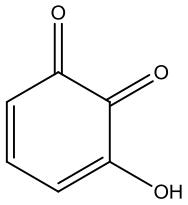

3-hydroxy-1,2-benzoquinone

Structure 41: 3-hydroxy-1,2-benzoquinone

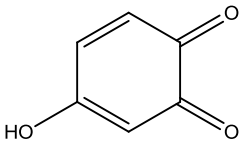

4-hydroxy-1,2-benzoquinone

Structure 42: 4-hydroxy-1,2-benzoquinone

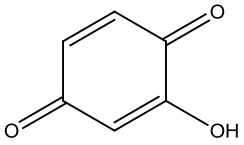

2-hydroxy-1,4-benzoquinone

Structure 43: 2-hydroxy-1,4-benzoquinone

Other compounds identified during ozonation reaction are summarily presented in Table 4.6 along with earlier studies that have reported the same compounds. As a basis for comparison, compounds previously identified by other workers not

identified in this study, were also added. Based on the compounds identified, a scheme for phenol breakdown is presented in Figure 4.23. It is interesting to note that literature reports have identified hydroquinone (and its dehydrogenated derivative: benzoquinone) as intermediates for phenol oxidation, which are not reported here. While the method of intermediate identification used here is capable of identifying these compounds, their existence in a highly oxidizing environment is expected to be short-lived. This was evidenced from the short shelf life of laboratory prepared standards used for intermediate identifications. Despite this, it should be mentioned that several workers have identified hydroquinone in their studies – mostly by HPLC-DAD method - and hence it is largely regarded as a breakdown product of phenol (Huang and Shu, 1995, Mallevialle, 1975, Pimentel et al., 2008, Dong et al., 2008). The presence of **27**, **28**, **29** and **30** as four-carbon chain ozonation products supports the existence of the -1,4-quinone during the ozonation process.

Table 4.6: Other intermediates reported during oxidation of phenol. In bold are intermediates also identified in this study.

Compound	Formula	Structure	Identification	References
Catechol	$C_6H_6O_2$	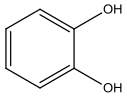	GCMS, HPLC-DAD	(Pimentel et al., 2008, Dong et al., 2010)+ **current study**
P-quinone	$C_6H_4O_2$	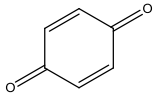	HPLC-DAD	(Pimentel et al., 2008, Prato-Garcia et al., 2009)
Muconic acid	$C_6H_6O_4$	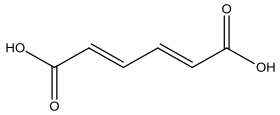		(Eisenhower, 1968) + **current study**
Fumaric acid	$C_4H_4O_2$	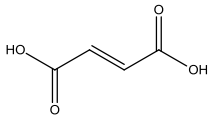	HPLC-DAD	(Eisenhower, 1968, Pimentel et al., 2008) + **current study**
Oxalic acid	$C_2H_2O_4$	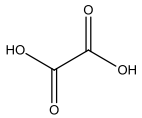	HPLC-DAD	(Pimentel et al., 2008, Prato-Garcia et al., 2009, Gould and Weber, 1976)
Maleic acid	$C_4H_4O_4$	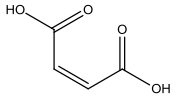	HPLC-DAD	(Bauch et al., 1970) + **current study**
Tartaric acid	$C_4H_6O_6$	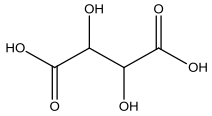	HPLC-DAD	(Bauch et al., 1970) + **current study**
Glyoxylic acid	$C_2H_2O_3$	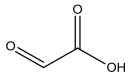	HPLC-DAD	(Bauch et al., 1970, Gould and Weber, 1976, Pimentel et al., 2008)
O-quinone	$C_6H_4O_2$	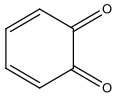	HPLC-DAD	(Mallevialle, 1975)

Hydroquinone	$C_6H_6O_2$	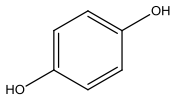	HPLC-DAD	(Mallevialle, 1975, Gould and Weber, 1976, Pimentel et al., 2008, Dong et al., 2008, Huang and Shu, 1995)
Resorcinol	$C_6H_6O_2$	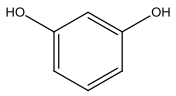	HPLC-DAD	(Spanggord and McClurg, 1978)
Malonic acid	$C_3H_4O_4$	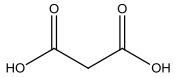	HPLC-DAD	(Pimentel et al., 2008) + **current study**
Pyruvic acid	$C_3H_4O_3$	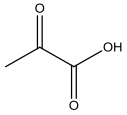	HPLC-DAD	(Pimentel et al., 2008) + **current study**
Succinic acid	$C_4H_6O_4$	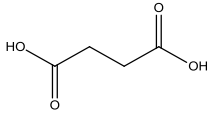	HPL-DAD	(Prato-Garcia et al., 2009)
Dimer	$C_{12}H_{10}O_2$		GCMS	(Huang and Shu, 1995)

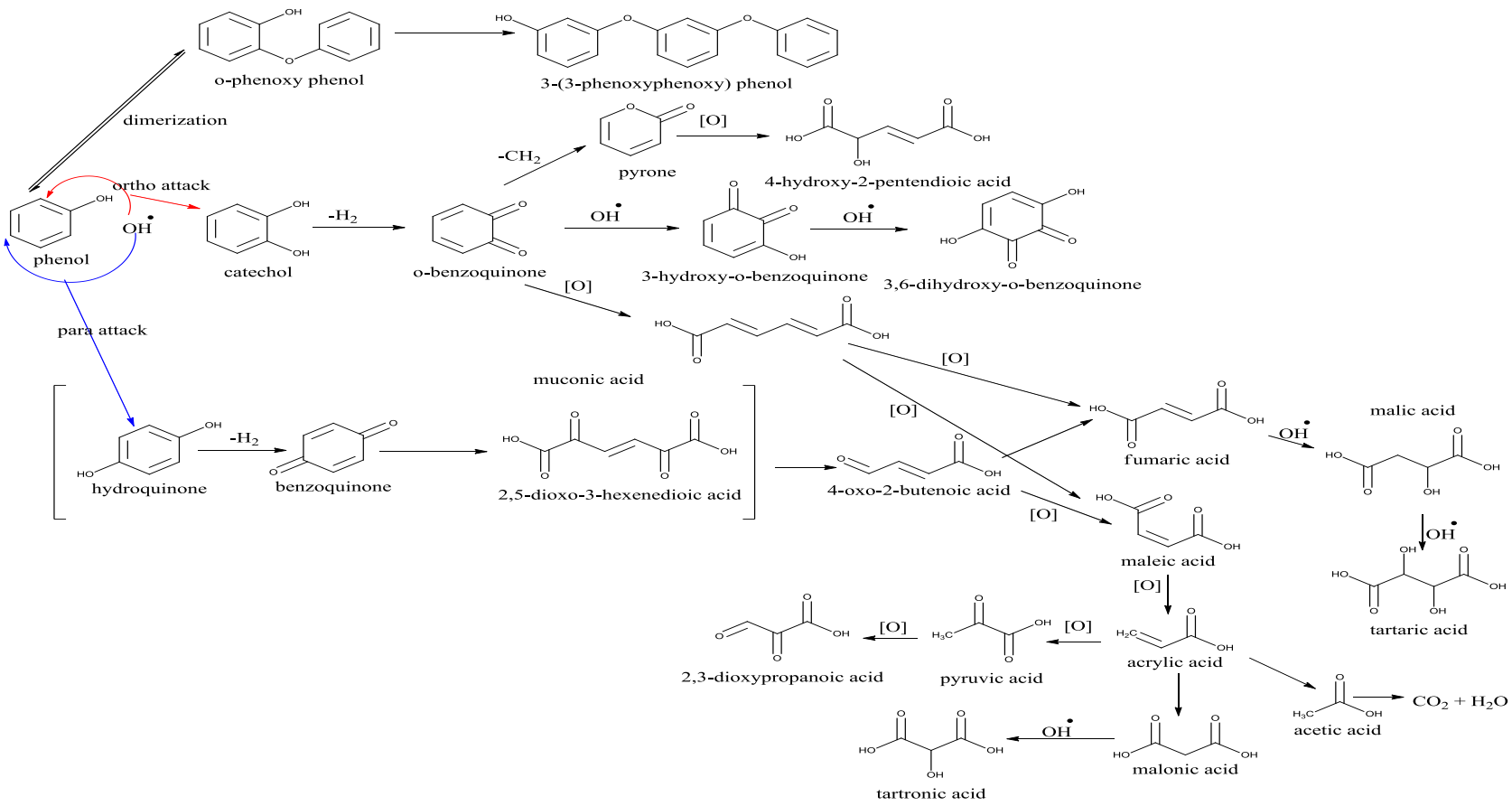

Figure 4.23: Proposed scheme for phenol degradation based on results from this study. Structures in parentheses are assumed/inferred from literature.

4.3.2.2 Intermediates of 2-chlorophenol ozonation

The ozonation of 2-chlorophenol was conducted in a similar manner to phenol. The pH of 100 mL $2x10^{-3}$ M, 2-chlorophenol was set at acidic pH (3) and alkaline pH (10) using H_3PO_4 and NaOH, respectively. A constant-alkaline pH (10) experiment was conducted by injecting 10µL, 1 M NaOH at regular intervals during ozonation using a glass syringe to keep the pH of 2-chlorophenol in the reactor fixed at pH 10. A final experiment was conducted without pH adjustment (pH 6), hereinafter referred to as dissolution pH. A representative chromatogram for 2-chlorophenol is shown in Figure 4.24. Figure 4.25 to Figure 4.28 are illustrative chromatograms (t= 20 minutes) for experiments conducted at pH 3, without pH control, alkaline and constant alkaline, respectively. A comparative summary of **major** compounds identified based on the molecular features of 2-chlorophenol are presented in Table 4.7 (important compounds are highlighted). Molecular search algorithm was set at C=18, H=16, O=15 and Cl = 6. This allowed for identification of possible ring coupled products and highly oxygenated compounds.

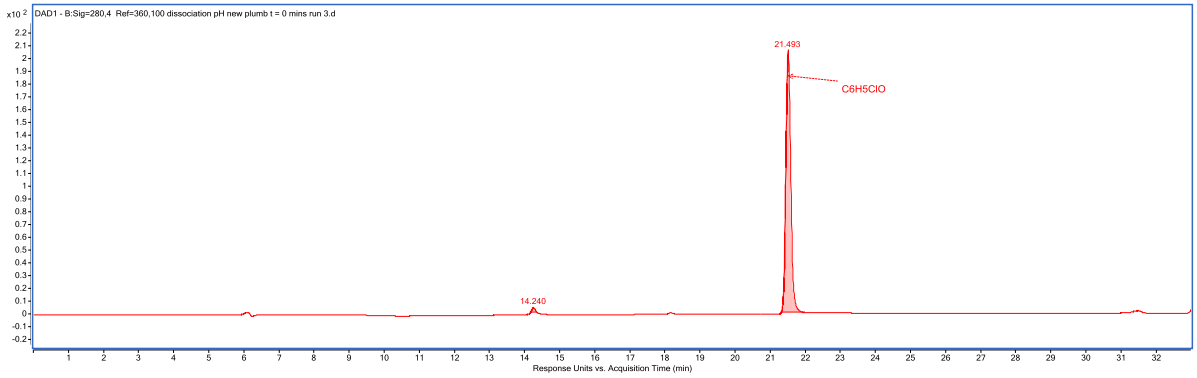

Figure 4.24: Representative chromatogram for 2-chlorophenol RT= 21.493

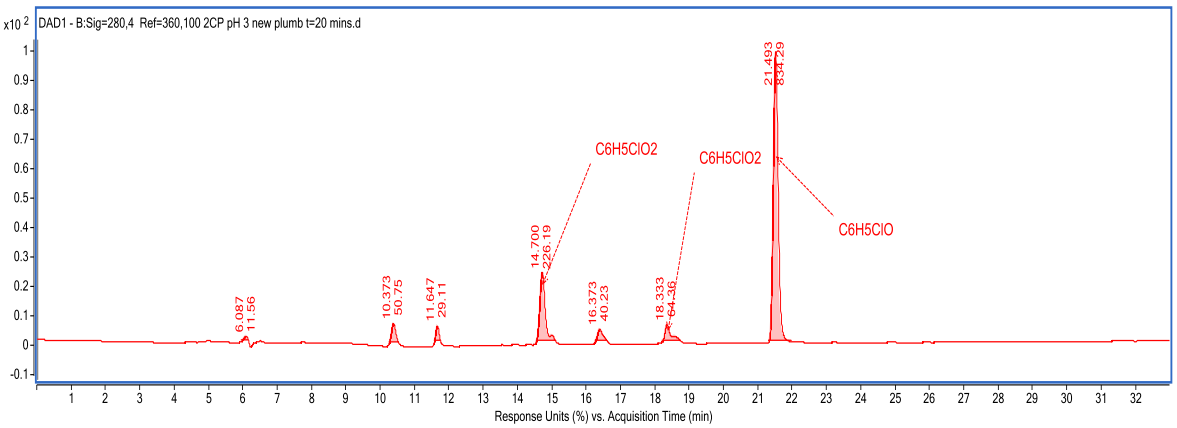

Figure 4.25: DAD (280 nm) chromatogram for 2-chlorophenol ozonation in acidic media (pH 3) t=20mins

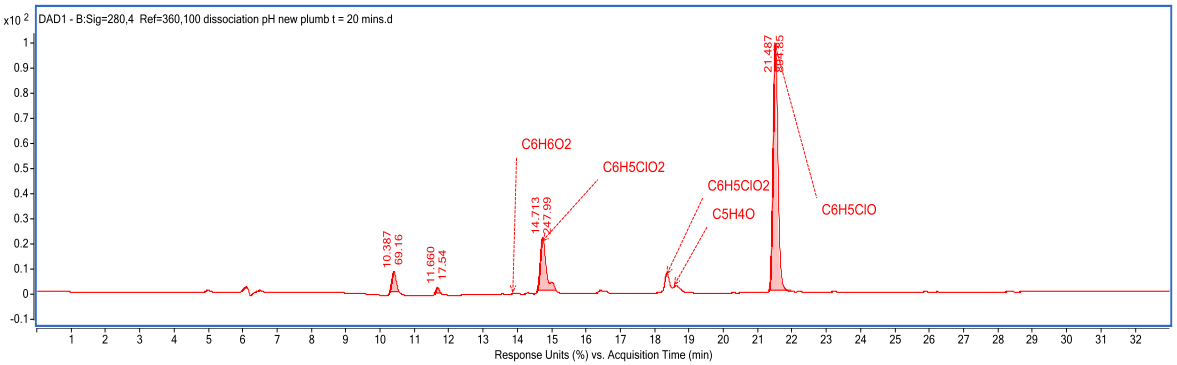

Figure 4.26: DAD (280 nm) chromatogram for 2-chlorophenol ozonation without pH control t=20mins

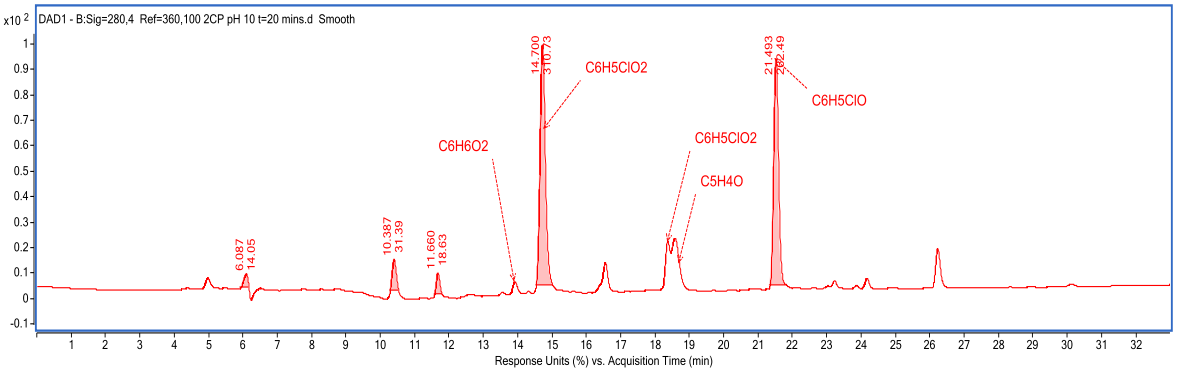

Figure 4.27: DAD (280 nm) chromatogram for 2-chlorophenol ozonation in alkaline media (pH 10) t=20mins

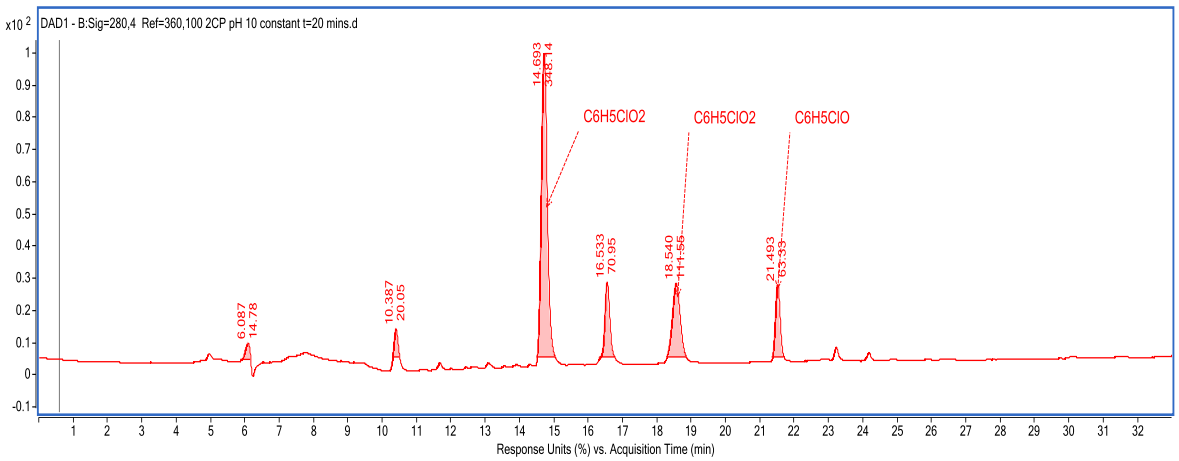

Figure 4.28: DAD (280 nm) chromatogram for 2-chlorophenol ozonation constant alkaline media (pH 10) t=20mins

Table 4.7: Intermediates for 2-chlorophenol ozonation at varying pH as followed by LCMS

Time mins		Acidic pH (3)			Dissolution pH 6			Alkaline pH (10) [not held constant]			Constant-alkaline pH (10)		
		RT	Mass	Formula	RT	Mass	Formula	RT	Mass	Formula	RT	Mass	Formula
0		21,493		C6H5ClO	21,493		C6H5ClO	21,493		C6H5ClO	21,493		C6H5ClO
10	1	18,440	142,9918	C6 H5Cl O2	14,003	110,03693	C6 H6 O2	14,003	110,03741	C6 H6 O2	7,035	96,0216	C5 H4 O2
	2				18,429	142,9918	C6 H5Cl O2	18,434	142,9918	C6 H5Cl O2	12,803	72,02222	C3 H4 O2
	3				18,43	80,02719	C5 H4 O	24,232	128,00299	C6 H5 Cl O	14,004	110,037	C6 H6 O2
	4							26,294	128,00297	C6 H5 Cl O	18,436	142,9918	C6 H5Cl O2
	5										26,66	253,99058	C12 H8 Cl2 O2
20	1	18,433	142,9918	C6 H5Cl O2	4,461	140,01119	C6 H4 O4	4,462	140,01118	C6 H4 O4	12,781	72,02226	C3 H4 O2
	2				13,999	110,03704	C6 H6 O2	12,811	72,02213	C3 H4 O2	18,435	142,9918	C6 H5Cl O2
	3				18,432	142,9918	C6 H5Cl O2	13,998	110,03714	C6 H6 O2			
	4				18,433	80,02711	C5 H4 O	18,434	142,9918	C6 H5Cl O2			
	5							18,436	80,02699	C5 H4 O			
	6							26,296	128,00312	C6 H5 Cl O			
30	1	18,440	142,9918	C6 H5Cl O2	4,457	140,01109	C6 H4 O4	5,416	101,99576	C3 H2 O4	5,464	180,02731	C5 H8 O7
	2				13,993	142,9918	C6 H5Cl O2	3,132	113,99286	C4 H2 O4	5,727	150,01689	C4 H6 O6
	3				18,429	108,02134	C6 H4 O2	4,461	140,01117	C6 H4 O4			
40	1				4,455	140,01104	C6 H4 O4	3,131	113,99286	C4 H2 O4			
	2				12,848	72,02218	C3 H4 O2	5,416	101,99576	C3 H2 O4			
	3				18,436	108,02128	C6 H4 O2						
60	1	5,414	101,99547	C3 H2 O4	4,238	88,01637	C3 H4 O3	5,397	150,01669	C4 H6 O6			
	2				5,416	101,99572	C3 H2 O4	5,416	101,99576	C3 H2 O4			
	3				5,418	120,00582	C3 H4 O5						

Generally, the degradation of 2-chlorophenol C_6H_5ClO **44** produced catechol $C_6H_6O_2$ **2** (RT=14.001), which was confirmed from the retention time of pure standard. Since catechol is a major product of phenol degradation, it may be inferred that both phenol **1** and 2-chlorophenol **44** would degrade via identical reaction routes. The conversion of 2-chlorophenol to catechol involves cleavage (hydroxylative dechlorination) of the ortho chlorine atom with a simultaneous attack by a hydroxyl group in a manner similar to electrophilic aromatic substitution reactions.

Compounds $C_3H_2O_4$ (RT=5.414) and $C_6H_5ClO_2$ (RT= 18.434) were intermediates ubiquitous to all experiments and may therefore be suggested as pH independent compounds of 2-chlorophenol break down by ozone. The most probable structure from a list of five suggestions available on ChemSpider database with the molecular formula $C_3H_2O_4$ is 2,3-dioxopropanoic acid **45** and is possibly generated from oxidation of acrylic acid **3**. This compound was also identified in this study as a by-product of phenol break down. $C_6H_5ClO_2$ is the product of hydroxylation of 2-chlorophenol and is highlighted in presented chromatograms (Figure 4.25 - Figure 4.28). Formula search revealed that two isomers of the hydroxylated 2-chlorophenol are produced. Extracted ion chromatogram showing both isomers is presented in Appendix 7.I. The corresponding mass spectrums are presented in Appendix 7.J. and Appendix 7.K, respectively. Both isomers are produced by the hydroxylation of **44** at position 4 and 6 to give **46** and **47**, respectively. The existence of both isomers during the oxidation of 2-chlorphenol is sustained in literature (Sung and Huang, 2007). The presence of these intermediates suggests that hydroxylation takes place before dechlorination as a route for degradation of chlorophenol.

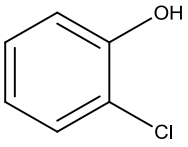

2-chlorophenol

Structure 44: 2-chlorophenol

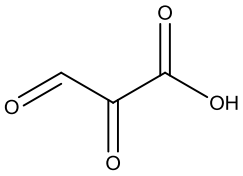

2,3-dioxopropanoic acid

Structure 45: 2,3dioxopropanoic acid

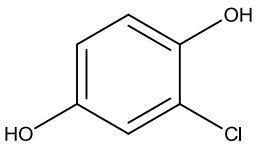

chlorohydroquinone

Structure 46: chlorohydroquinone

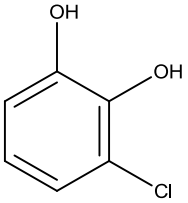

chlorocatechol

Structure 47: chlorocatechol

$C_{12}H_8Cl_2O_2$ (RT= 26.660) is a dimerised 2-chlorophenol that was only observed in alkaline experiments. This compound is analogous to the ring coupled dimers produced by phenol and is supported by literature (Hirvonen et al., 2000, Chrostowski et al., 1983). There are 101 possible isomers for $C_{12}H_8ClO_2$ on ChemSpider database search. Based on the symmetry and ortho-position of the attached groups in 2-chlorophenol, 4,4'-dichloro-3,3'-biphenyldiol **48** and 2,2'-dichloro-3,3'-biphenyldiol **49** are the most probable structures for $C_{12}H_8ClO_2$.

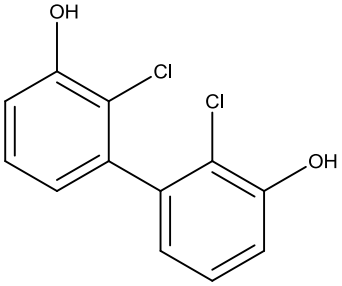

2,2'-dichloro-3,3'-biphenyldiol

Structure 48: 2,2'-3,3'-biphenyldiol

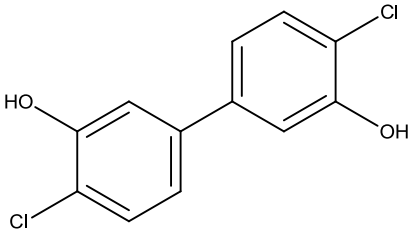

4,4'-dichloro-3,3'-biphenyldiol

Structure 49: 4,4'-dichloro-3,3'-biphenyldiol

A summary of compounds reported by the two available studies on intermediates of ozonation/oxidation of 2-chlorophenol is presented in Table 4.8. The majority of the low molecular weight acids presented by Hirvonen et al. (2000) and Sung and Huang (2007) -Table 4.8- were not identified in this study. Both researchers utilized GC-MS method of analysis, which required a preliminary sample preparation step to make the compounds thermally labile for GC separation as opposed to direct analysis by the LC-MS method applied in this study. It is therefore possible that the sample treatment step brought about changes to transient oxidized compounds, consequently leading to differences in observed breakdown products between earlier referenced reports and findings from this study. Several other compounds identified as minor breakdown products of 2-chlorophenol (Figure 4.29) are novel at

this point and probable structures could not be presented based on the molecular features of 2-cholorphenol or any of its known intermediates. A scheme depicting a proposed ozonation pathway is presented in Figure 4.30.

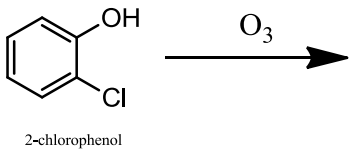

2-chlorophenol

C_2 : $C_2H_2O_3$

C_3 : $C_3H_4O_2$

C_4 : $C_4H_2O_4$, $C_4H_4O_3$, $C_4H_6O_6$

C_5 : C_5H_4O, $C_5H_4O_3$, $C_5H_4O_3$,$C_5H_6O_5$

C_6 : $C_6H_4O_2$, $C_6H_4O_4$, $C_6H_2O_6$, $C_6H_6O_6$, $C_6H_4O_5$

C_{18} : $C_{18}H_{34}O_5$, $C_{18}H_{36}O_4$

C_{11} : $C_{11}H_6O_5$

Figure 4.29: Novel break down products of ozonation of 2-chlorophenol identified by LC-MS

Table 4.8: Intermediates reported in the literature during ozonation of 2-chlorophenol. In bold are intermediates also identified in this study.

Compound	Formula	Structure	Method	References
Phenol	C_6H_6O	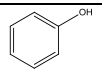	GCMS	(Hirvonen et al., 2000)
Propenoic acid	$C_3H_4O_2$		GCMS	(Hirvonen et al., 2000)
Dichloro-dihydroxybiphenyl	$C_{12}H_8Cl_2O_2$	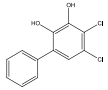	GCMS	(Hirvonen et al., 2000) + **Current study**
Succinic	$C_4H_6O_4$	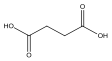	GCMS	(Sung and Huang, 2007)
Mono-chlorodihydroxybiphenyl	$C_{12}H_9ClO_2$	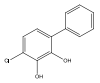	GCMS	(Sung and Huang, 2007)
3-Chlorocatechol	$C_6H_5ClO_2$		GCMS	(Sung and Huang, 2007)
Chlorohydroquinone	$C_6H_5ClO_2$	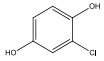	GCMS	(Sung and Huang, 2007)
Tartaric acid	$C_4H_6O_6$	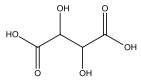	GCMS	(Sung and Huang, 2007)
Oxalic acid	$C_2H_2O_4$		GCMS	(Sung and Huang, 2007)

Compound	Formula	Structure	Method	References
Muconic acid	$C_6H_6O_4$	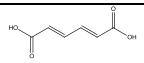	GCMS	(Sung and Huang, 2007)
Malonic acid	$C_3H_4O_4$	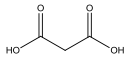	GCMS	(Sung and Huang, 2007)
Acetic acid	$C_2H_4O_2$		GCMS	(Sung and Huang, 2007)
Valeric acid	$C_5H_{10}O_2$	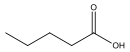	GCMS	(Sung and Huang, 2007)
2-propenoic acid	$C_3H_4O_2$	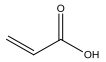	GCMS	(Sung and Huang, 2007)
Maleic acid	$C_4H_4O_4$	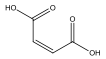	GCMS	(Sung and Huang, 2007)
Dihydroxymaleic acid	$C_4H_4O_6$	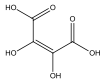	GCMS	(Sung and Huang, 2007)

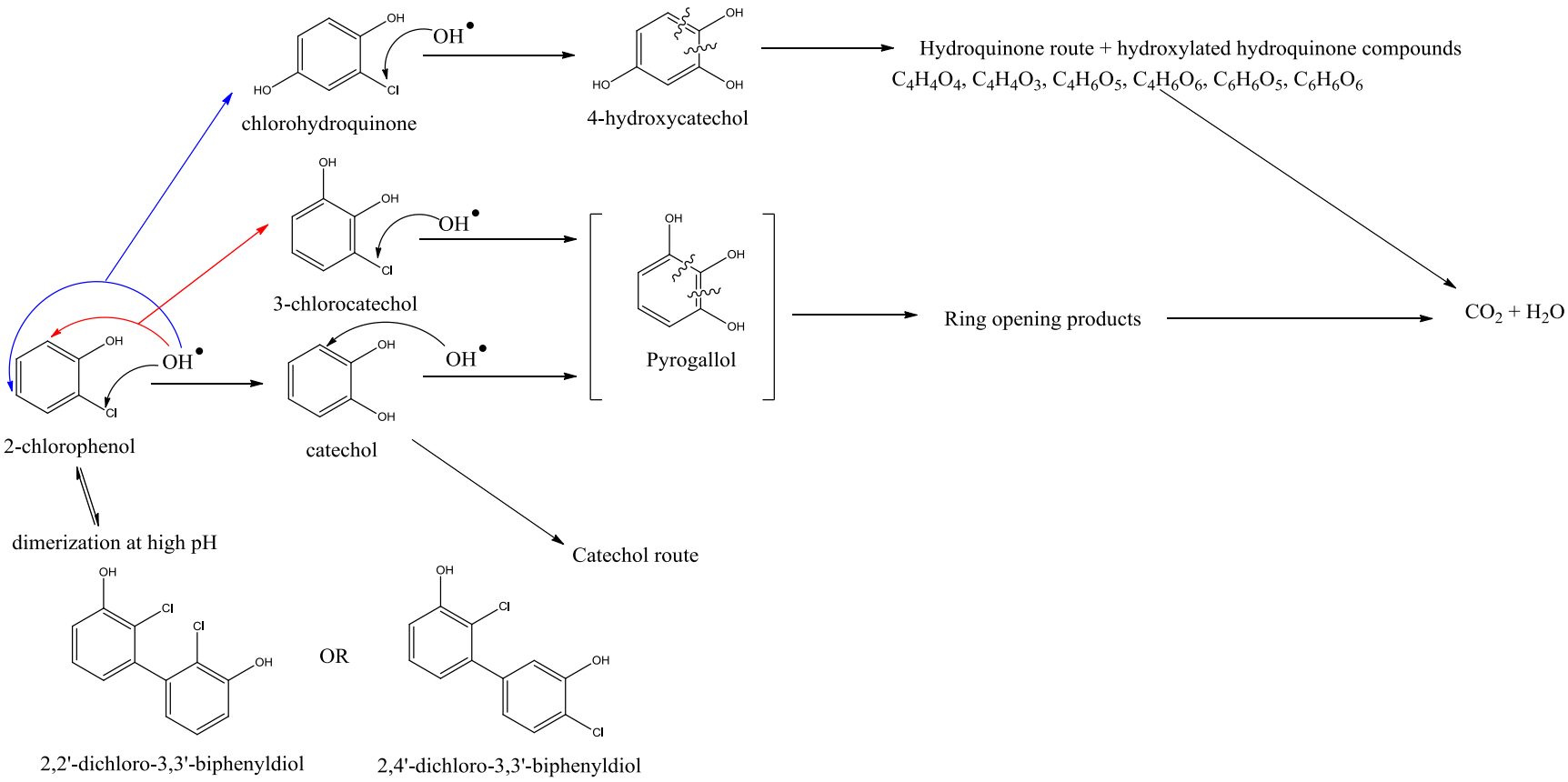

Figure 4.30: Proposed scheme for 2-chlorophenol degradation and polymerization based on results from this study.

4.3.2.3 Intermediates of 4-chlorophenol ozonation

The ozonation of 4-chlorophenol was conducted in a similar manner as described above for phenol and 2-chlorophenol. The pH of separate 4-chlorophenol solutions was set at acidic pH 3 and alkaline pH 10 using H_3PO_4 and NaOH, respectively. An experiment was conducted where the pH was held constant in the alkaline region (pH 10) by continuously dosing the reactor with 10 µL, 1M NaOH at regular intervals during the ozonation process. A final experiment was conducted without pH adjustment (pH 6), furthermore referred to as dissolution pH 6. A representative chromatogram for 4-chlorophenol (Figure 4.31) showed that unlike phenol and 2-chlorophenol, 4-chlorophenol ionizes sufficiently to be monitored by its total ion.

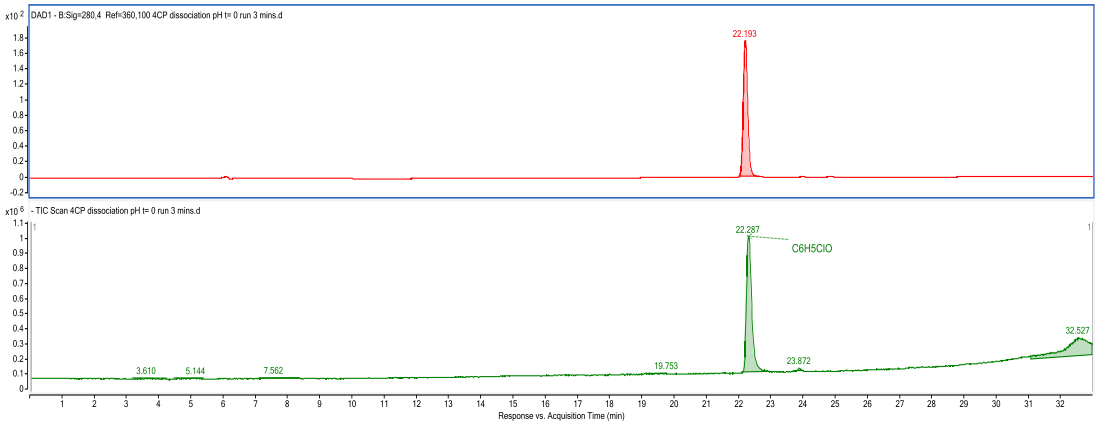

Figure 4.31: Representative chromatogram of 4-chlorophenol (RT=22,287). Top DAD. Bottom TIC.

Total ion chromatograms for samples collected at 20 minutes from each experiment are presented in Figure 4.32 - Figure 4.35. A summary of **major** compounds identified during the course of each pH experiment is presented in Table 4.9.

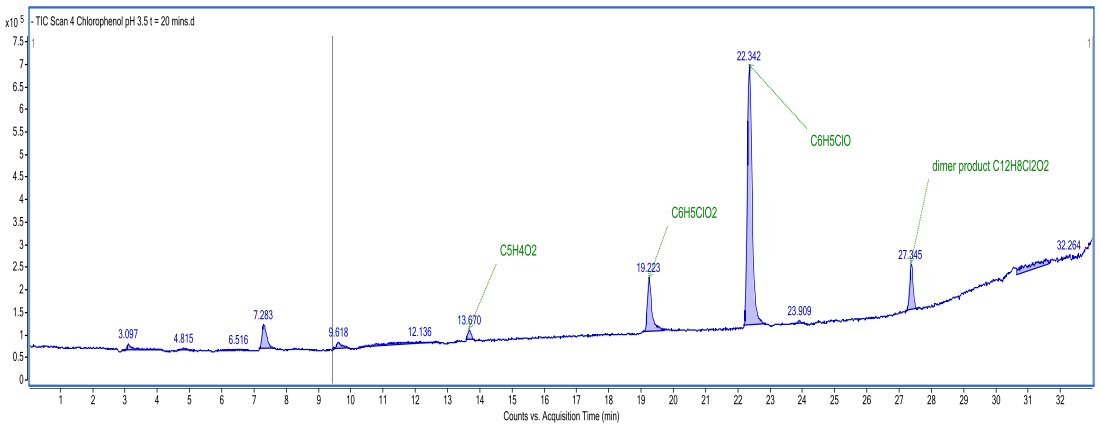

Figure 4.32: Total ion chromatogram (TIC) for 4-chlorophenol ozonation in acidic medium. Starting pH 3.5, t=20 minutes

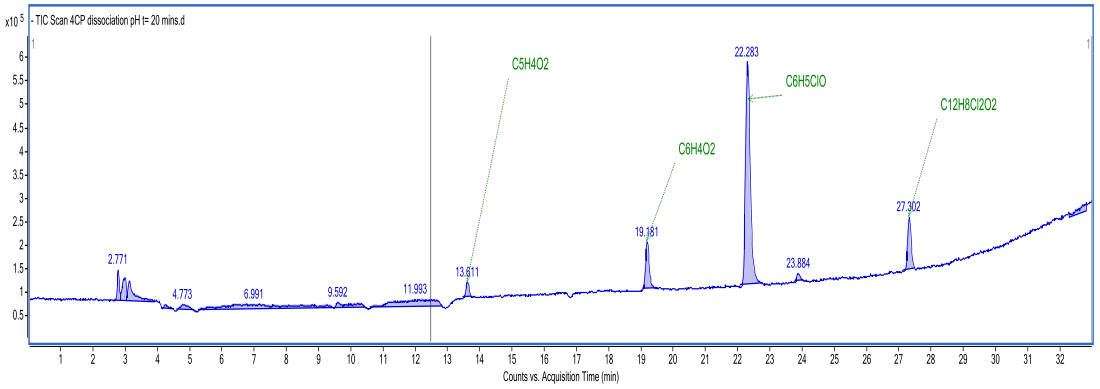

Figure 4.33 Total ion chromatogram (TIC) for 4-chlorophenol ozonation at dissolution pH 6 t=20 minutes

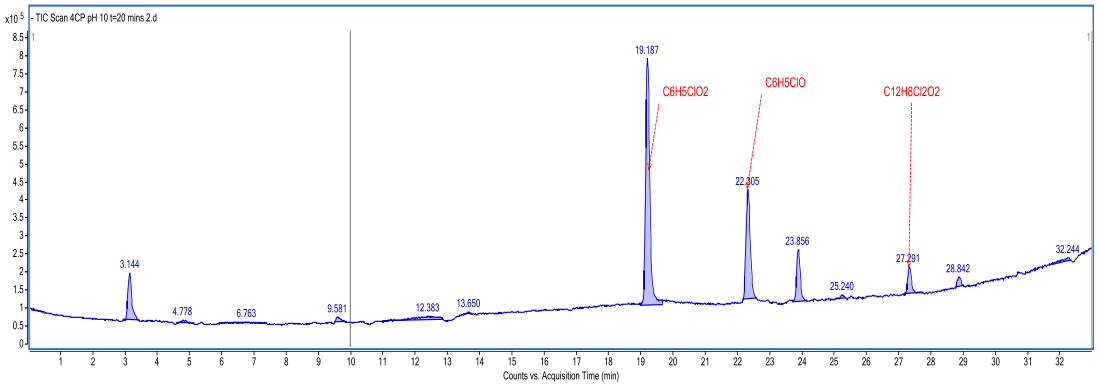

Figure 4.34: Total ion chromatogram (TIC) for 4-chlorophenol ozonation in alkaline medium. Starting pH 10, t=20 minutes

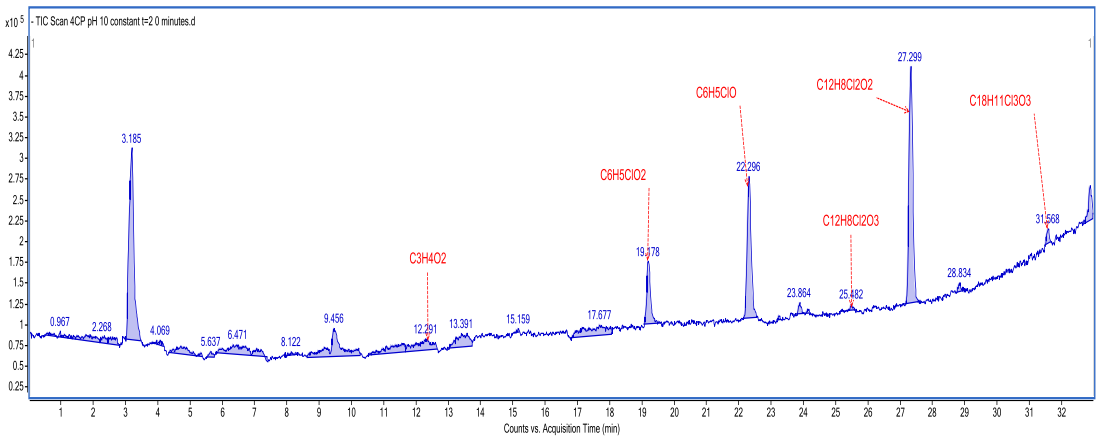

Figure 4.35 Total ion chromatogram (TIC) for 4-chlorophenol ozonation with pH held constant at pH 10. Time =20 minutes

Table 4.9: Intermediates for 4-chlorophenol ozonation at varying pH as followed by LCMS

		Acidic pH (3)			Dissolution pH (6)			Alkaline pH (10) [not held constant]			Constant alkaline pH (10)		
Time mins		RT	mass	Formula	RT	mass	Formula	RT	mass	Formula	RT	mass	Formula
0	1	22,349	128,00341	C6 H5 Cl O	22,349	128,00341	C6 H5 Cl O	22,306	128,00306	C6 H5 Cl O	3,131	113,99286	C4 H2 O4
	2										22,299	128,00338	C6 H5 Cl O
10	1	19,233	143,99792	C6H5ClO2	19,179	145,99495	**C5H6O5**	3,156	155,98109	**C6H4O5**	3,145	113,99286	C4 H2 O4
	2	22,339	128,00338	C6 H5 Cl O	19,18	143,99808	C6H5ClO2	22,287	128,00317	C6 H5 Cl O	22,298	128,00329	C6 H5 Cl O
	3	27,358	253,99058	C12H8Cl2O2	22,295	128,00336	C6 H5 Cl O	27,301	253,9908	C12 H8 Cl2 O2	27,306	253,99099	C12 H8 Cl2 O2
	4				27,304	253,99087	C12 H8 Cl2 O2						
20	1	13,659	96,02137	C5 H4 O2	13,605	96,02141	C5 H4 O2	19,189	143,99823	C6 H5 Cl O2	3,167	113,99286	C4 H2 O4
	2	19,234	145,99472	**C5H6O5**	19,179	145,99495	**C5H6O5**	22,305	128,00321	C6 H5 Cl O	12,813	72,02164	**C3 H4 O2**
	3	19,234	143,99787	C6 H5 Cl O2	19,179	108,02088	C6 H4 O2	27,312	253,99059	C12 H8 Cl2 O2	19,182	145,99491	C5H6O5
	4	22,341	128,00331	C6 H5 Cl O	22,293	128,00331	C6 H5 Cl O				19,182	108,02078	C6 H4 O2
	5	27,354	253,99058	C12H8Cl2O2	27,305	253,99083	C12 H8 Cl2 O2				22,297	128,00304	**C6 H5Cl O**
	6										25,48	269,98515	C12 H8 Cl2 O3
	7										27,304	253,99106	C12 H8 Cl2 O2

	8										31,547	379,97781	C18 H11 Cl3 O3
30	1	13,65	96,02148	C5 H4 O2	12,889	72,02191	C3 H4 O2				3,184	113,99286	C4 H2 O4
	2	19,229	108,02107	C6 H4 O2	13,601	96,02142	C5 H4 O2				12,808	72,02165	C3 H4 O2
	3	27,355	253,99041	C12 H8 Cl2 O2	19,181	108,02067	C6 H4 O2				19,178	145,99486	**C5H6O5**
	4				27,305	253,99069	C12 H8 Cl2 O2				19,178	108,02063	C6 H4 O2
	5										22,299	128,00274	C6 H5 Cl O
40	1	12,848	72,02202	C3 H4 O2	13,601	96,02137	C5 H4 O2	3,134	113,99286	C4 H2 O4	3,199	113,99285	C4 H2 O4
	2	13,648	96,02138	C5 H4 O2	19,184	143,99780	C6 H5 Cl O2	12,884	72,02159	C3 H4 O2	5,749	150,01641	C4 H6 O6
	3	19,228	108,02079	C6 H4 O2	27,304	253,99038	C12 H8 Cl2 O2	13,606	96,02114	C5 H4 O2	12,807	72,02163	C3 H4 O2
	4	22,338	128,00317	**C6H5ClO**				19,187	143,99774	**C6H5ClO2**			
	5	27,353	253,99055	**C12H8Cl2O2**				22,292	128,00275	**C6H5ClO**			
60	1				4,249	113,99286	C4 H2 O4	3,133	113,99286	C4 H2 O4	3,221	113,99286	C4 H2 O4
	2										5,747	150,01642	C4 H6 O6

The presence of a hydroxylated 4-chlorophenol, $C_6H_5ClO_2$ (RT= 19.180) strongly supports the accepted theory that hydroxylation occurs before dechlorination (Ni and Chen, 2001). Similar hydroxylated compounds (**46** and **47**) were observed for 2-chlorophenol. However, unlike in the case with 2-chlorophenol, catechol was not identified as an intermediate product in any of the pH experiments conducted for 4-chlorophenol. This would further imply that the dechlorination step does not generate phenol as suggested by earlier studies (Hirvonen et al., 2000), as catechol is a major product of phenol oxidation. There are four (4) possible points of hydroxylation on 2-chlorophenol (position 3, 4, 5 and 6), each generating an un-identical dihydroxyl-system. If we exclude the meta-positions due to aromatic deactivation, then hydroxylation would take place at position 4 and 6. In line with such argument, two hydroxylated 2-chlorophenol compounds (**46** and **47**) have being reported (Sung and Huang, 2007) and were identified in this study. 4-chlorophenol **50** on the other had posses only one point of hydroxylation –both ortho positions give identical products and the meta position is deactivated for electrophilic aromatic substitutions. Only one hydroxylated 4-chlorophenol was detected in solution using several search algorithms. Structure **51** (4-chlorocatechol) was, therefore, assigned as the most probable compound for the detected hydroxylated 4-chlorophenol. The absence of catechol in 4-chlorophenol oxidation intermediates clearly suggest that the dechlorination at position 4 is less likely to occur, when compared to dechlorination at position 3 on the catechol ring. This may be a likely reason why 4-chlorophenol is less amenable to oxidation reactions compared to 2-chlorophenol as shown by the kinetics of their oxidation by ozone. More so, the fact that 2-chlorophenol possess two hydroxylation points compared to 4-chlorophenol may further increase its susceptibility to hydroxylation reactions and therefore its degradation during aqueous ozonation reactions.

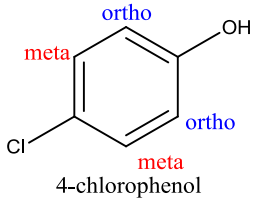

Structure 50: 4-chlorophenol

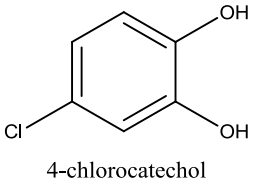

Structure 51: 4-chlorocatechol

A common compound observed across all pH studied during the ozonation of 4-chlorophenol is the dimerised compound $C_{12}H_8Cl_2O_2$ (RT= 27.306). Similar to the

dimerised products obtained with phenol and 2-chlorophenol, this dimer is the product of ionic reaction of two 4-chlorophenol molecules. In contrast to experiments for phenol and 2-chlorophenol, this dimer was detected in acidic solutions. According to Hirvonen and co-workers, the dimer is one of two isomers of dichloro-dihydroxylbiphenyl (Hirvonen et al., 2000). There are 101 existing structures corresponding to the formula $C_{12}H_8ClO_2$ in the chemical structure database ChemSpider. Based on the symmetry of 4-chlorophenol, there are two probable isomers possible: 4-chloro-3-(4-chlorophenoxy)phenol **52** and 5,5'-dichloro-2,2'-diphenyldiol **53**. These structures are isomeric to **48** and **49** proposed for 2-chlorophenol, differing only in the ortho- and para- positioning of the hydroxyl and chlorine atoms in the dimers. The most likely compound based on ionic reaction is **52**. Also, **53** is less likely to occur since it would require one 4-chlorophenol molecule reacting via the deactivated meta position.

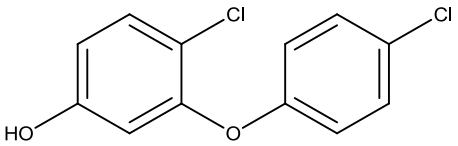

4-chloro-3-(4-chlorophenoxy)phenol

Structure 52: 4-chloro-3-(4-chlorophenoxy)phenol

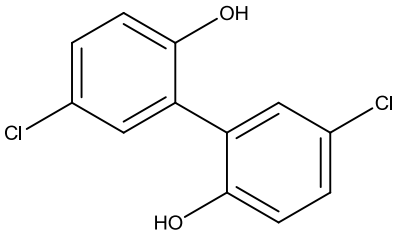

5,5'-dichloro-2,2'-biphenyldiol

Structure 53: 5,5'-dichloro-2,2'-biphenyldiol

Acrylic acid **3**, $C_3H_4O_2$ (RT=12.813) was also detected in all pH experiments. This acid was identified as a major breakdown acid for phenol and 2-chlrophenol. It may therefore be inferred that all three compounds follow identical breakdown schemes.

An important compound only detected after 20 minutes in experiments when the pH was kept constant in the alkaline is $C_{18}H_{11}Cl_3O_3$, which is a trimeric product of 4-chlorophenol analogous to $C_{12}H_{14}O_3$ for phenol. As highlighted in previous section, an alkaline pH favours ionization of the phenols and hence promotes ionic reactions. The trimer is possibly a product of such ionic reactions initiated in the presence of ozone. The oxidation of the dimer $C_{12}H_8Cl_2O_2$ (RT= 27.306) to a higher oxidation product, $C_{12}H_8Cl_2O_3$ (RT= 25.480) was also obtained in experiments conducted at constant alkaline pH. Compound 4-chloro-3-(4-chlorophenoxy)phenol **54** and

5,5’,6’’-trichloro-[1,1’:4,1’’-terphenyl]-2,2’,3’’-triol **55** are proposed for $C_{18}H_{11}Cl_3O_3$ based on structure of **52** and **53**.

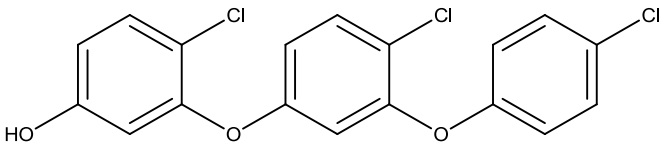

4-chloro-3-(4-chloro-3-(4-chlorophenoxy)phenoxy) phenol

Structure 54: 4-chloro-3-(4-chloro-3-(4-chlorophenoxy)phenol

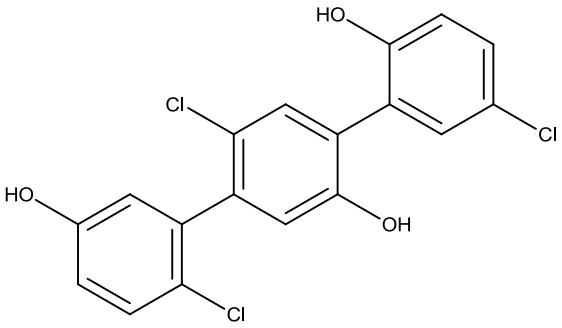

5,5',6"-trichloro-[1,1':4',1"-terphenyl]-2,2',3"-triol

Structure 55: 5,5’,6’’-trichloro-[1,1’:4’,1’’-terphenyl]-2,2’3’’-triol

Residual low molecular weight compounds in solution after the degradation of 4-chlorophenol are presented in Figure 4.36. A summary of compounds earlier identified during the ozonation of 4-chlorophenol is presented in Table 4.10, while a proposed pathway for degradation based on intermediates identified in this study is presented in Figure 4.37.

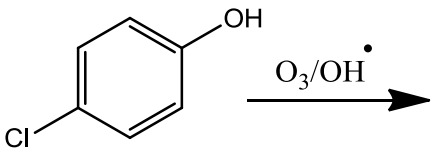

4-chlorophenol

C_3 : $C_3H_4O_2$, $C_3H_4O_3$, $C_3H_2O_4$

C_4 : $C_4H_4O_2$, $C_4H_4O_4$, $C_4H_6O_6$, C_4H_3ClO

C_5 : $C_5H_4O_2$, $C_5H_4O_4$,$C_5H_6O_5$

C_6 : $C_6H_4O_4$

C_{18} : $C_{18}H_{34}O_5$

Figure 4.36: Residual compounds of 4-chlorophenol degradation

Table 4.10: Intermediates reported in the literature during ozonation of 4-chlorophenol. In bold are intermediates also identified in this study

Compound	Formula	Structure	Method of identification	References
Formic acid	CH_2O_2	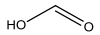	IC	(Xu et al., 2005)
Oxalic acid	$C_2H_4O_2$	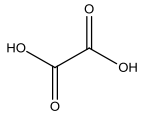	IC	(Sauleda and Brillas, 2001, Xu et al., 2005)
Phenol	C_6H_6O	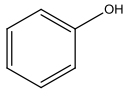	GCMS	(Hirvonen et al., 2000)
Dichloro-dihydroxybiphenyl	$C_{12}H_{11}Cl_2O_2$	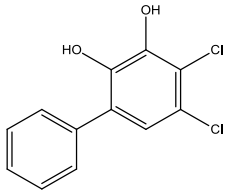	GCMS	(Hirvonen et al., 2000)
Mono-chloro-dihydroxybiphenyl	$C_{12}H_{12}ClO_2$	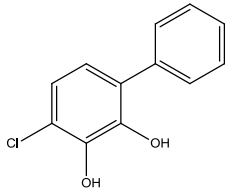	GCMS	(Hirvonen et al., 2000)
Catechol	$C_6H_6O_2$	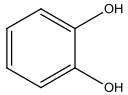	GCMS	(Xu et al., 2005)

Hydroquinone	$C_6H_6O_2$	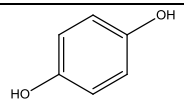	HPLC	(Xu et al., 2005)
p-benzoquinone	$C_6H_4O_2$	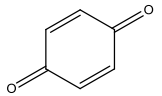	HPLC	(Xu et al., 2005)
Fumaric acid	**$C_4H_4O_4$**	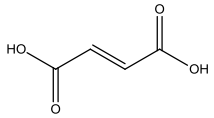	HPLC	(Xu et al., 2005, Sauleda and Brillas, 2001)
4-chloro-1-3-dihydroxybenzene	**$C_6H_5ClO_2$**	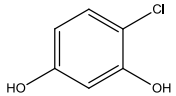	HPLC	(Sauleda and Brillas, 2001)
4-chlorocatechol	**$C_6H_5ClO_2$**	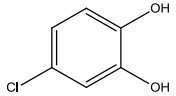	HPLC	(Sauleda and Brillas, 2001)

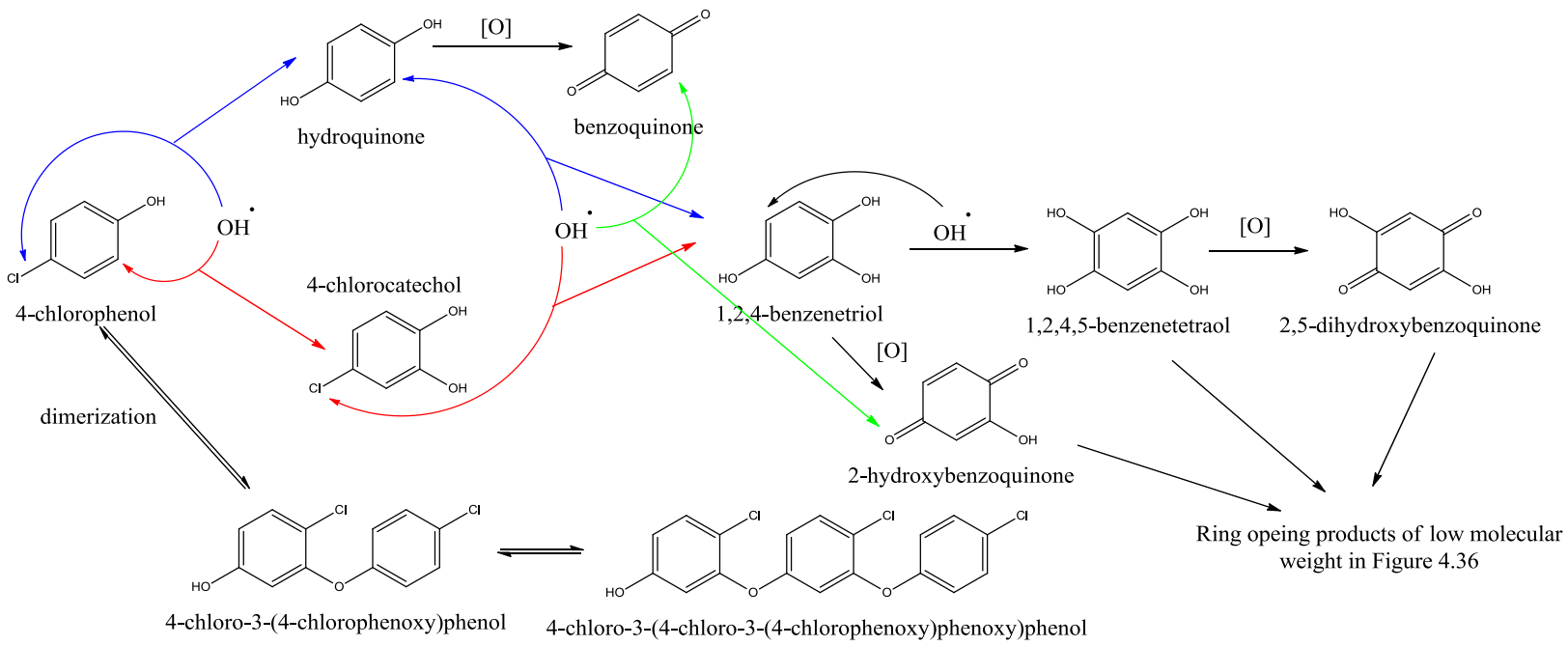

Figure 4.37: Proposed scheme for 4-chlorophenol degradation and polymerization based on results from this study

4.3.2.4. Intermediates of 2,4-dichlorophenol ozonation

Ozonation of 2,4-dichlorophenol was carried out in a similar manner as described for ozonation other phenolics earlier discussed. Intermediates were monitored at various pH regimes: acidic (pH 3), uncontrolled (pH 6), alkaline (pH 10) and another experiment where the pH was held constant by careful dosing of reactor solution with NaOH (1M). LCMS elution flow-rate was raised from 0.3 mL/min to 0.4 mL/min to accommodate less polar dimeric and trimeric by-products. All other parameters were kept constant.

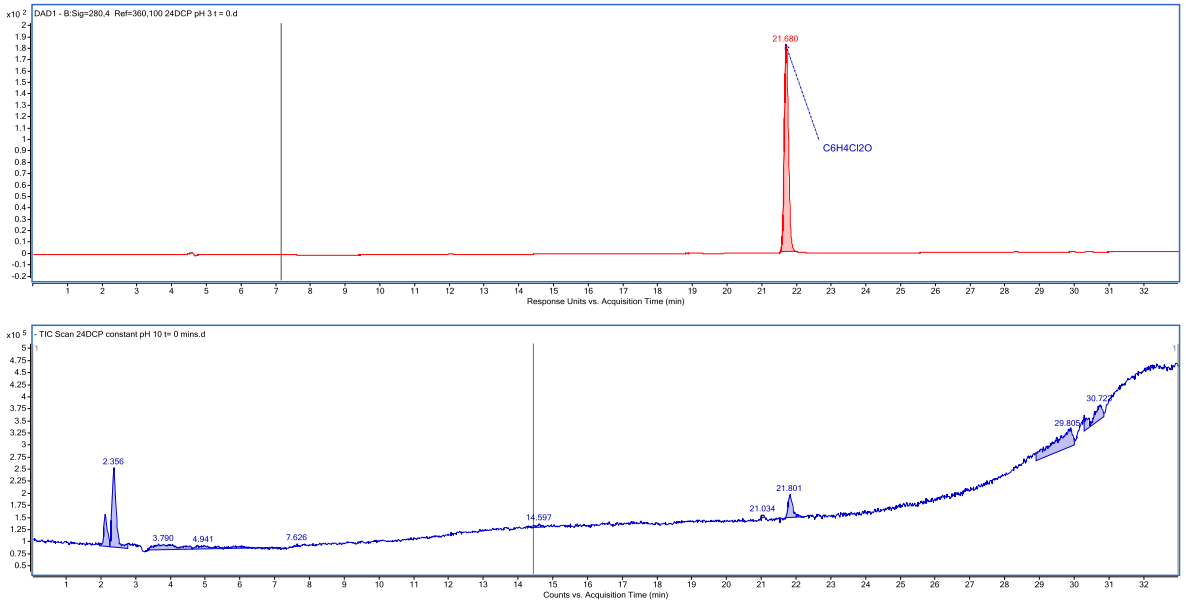

Figure 4.38: Representative DAD and TIC chromatogram for 2,4-dichlorophenol at the start of each experiment. RT= 21.680 minutes.

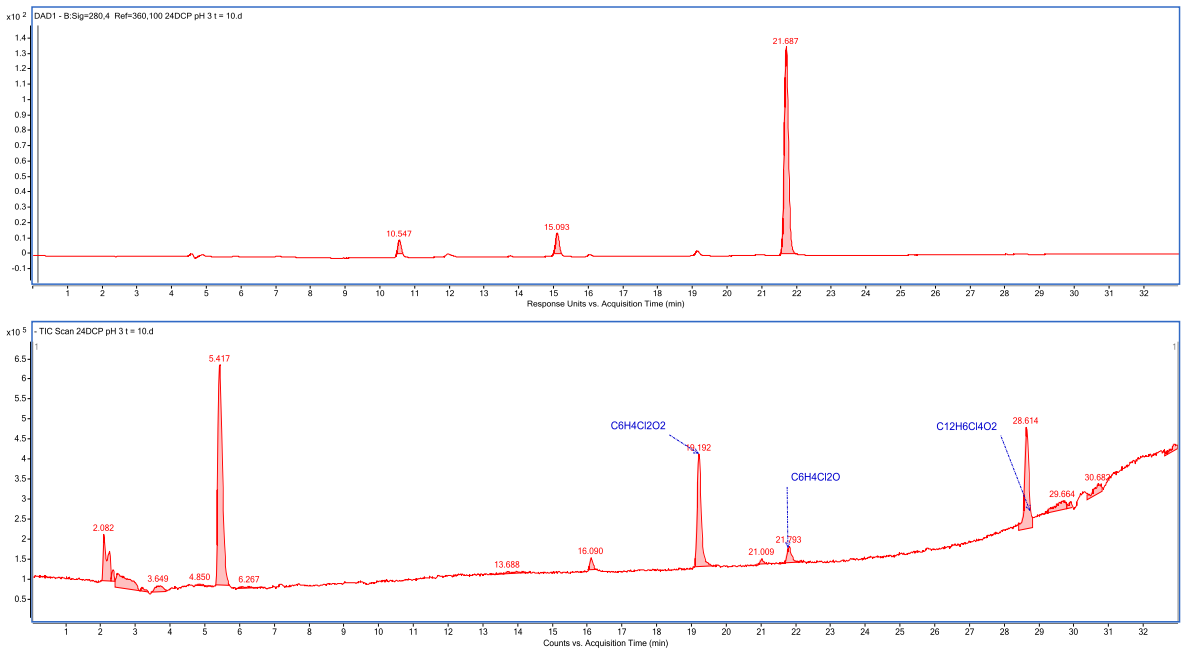

Figure 4.39: DAD (280 nm) and TIC chromatogram for 2,4-dichlorophenol at t= 10 minutes in acidic media. pH 3

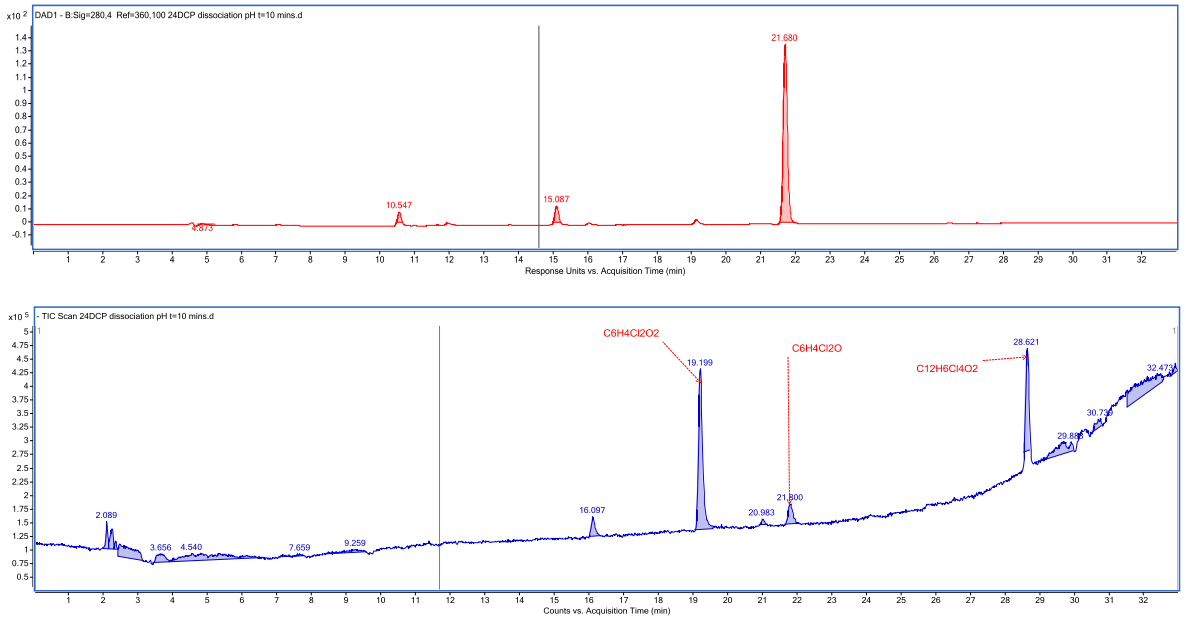

Figure 4.40: DAD (280 nm) and TIC chromatogram for 2,4-dichlorophenol at t= 10 minutes without pH control.

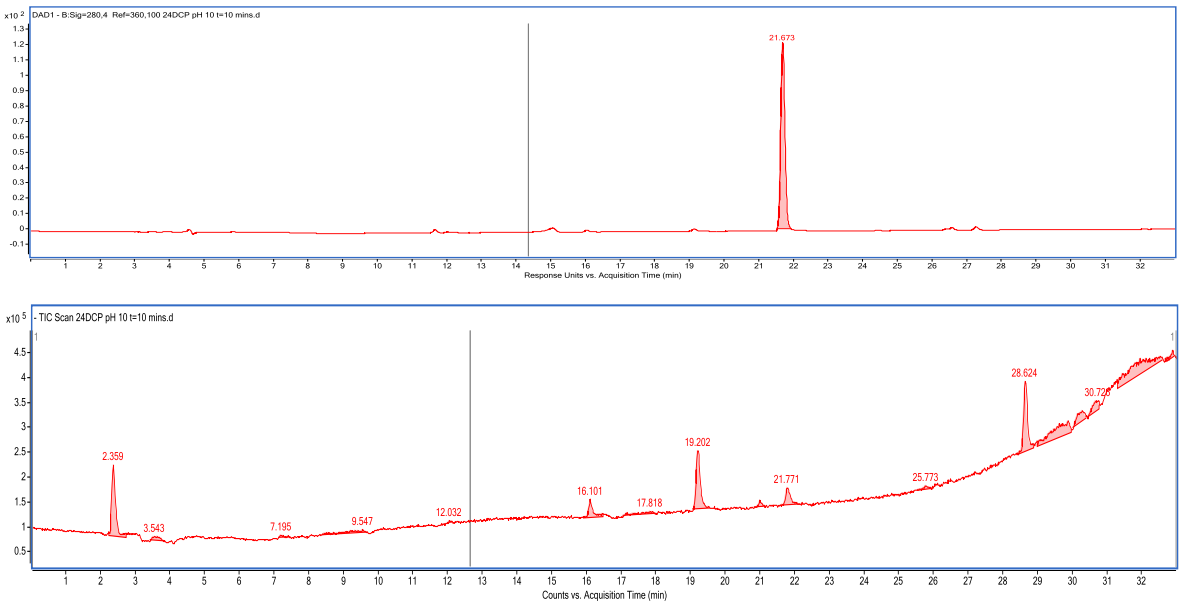

Figure 4.41: DAD (280 nm) and TIC chromatogram for 2,4-dichlorophenol at t= 10 minutes in alkaline medium. pH 10.

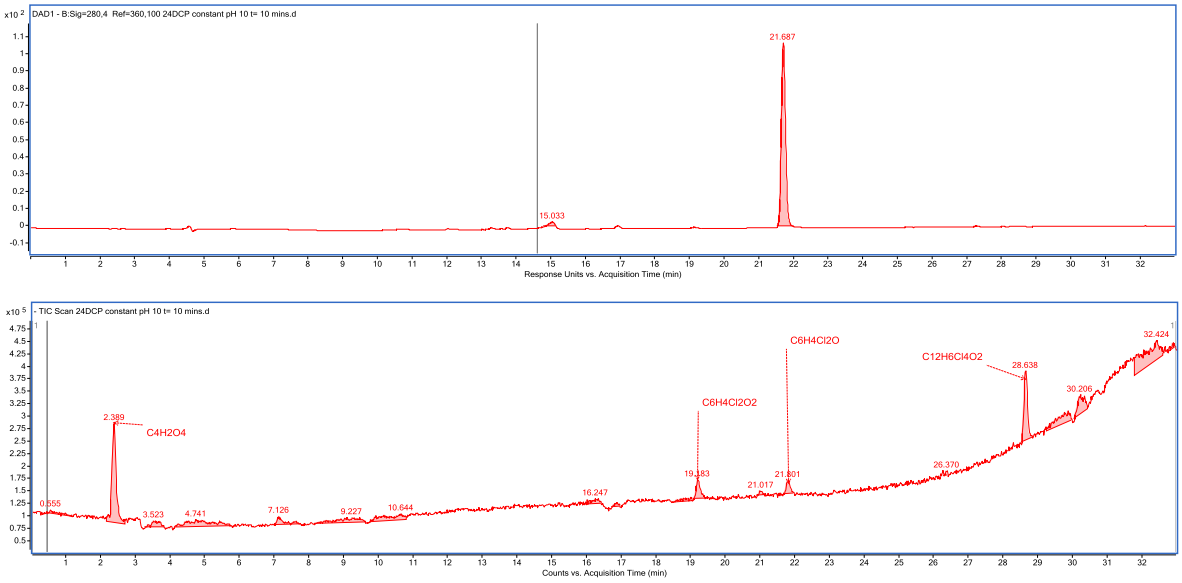

Figure 4.42: DAD (280 nm) and TIC chromatogram for 2,4-dichlorophenol at t= 10 minutes. pH held constant in alkaline medium (pH 10).

The **major** ions identified by LCMS in the course of various experiments are summarized in Table 4.11. Compounds common to all experiments are highlighted in yellow and those unique to specific experiments are highlighted in green.

Table 4.11: Intermediates for 2,4-dichlorophenol ozonation at varying pH as followed by LCMS

Time mins		Acidic pH (3)			Dissolution pH 6			Alkaline pH (10) [not held constant]			Constant alkaline pH (10)		
		RT	mass	Formula	RT	mass	Formula	RT	mass	Formula	RT	mass	Formula
0		21,795	161,96385	C6 H4 Cl2 O	21,795	161,96385	C6 H4 Cl2 O	21,769	161,96397	C6 H4 Cl2 O	21,803	161,96397	C6 H4 Cl2 O
10	1	5,418	97,97711	**C4H2O3**	16,1	143,99046	C6 H5 Cl O2	2,362	113,99286	C4 H2 O4	2,375	113,99286	C4 H2 O4
	2	16,101	143,99046	C6 H5 Cl O2	19,196	177,95917	C6 H4 Cl2 O2	16,1	143,99046	C6 H5 Cl O2	19,201	177,95893	C6 H4 Cl2 O2
	3	19,197	177,95921	C6 H4 Cl2 O2	21,789	161,96385	C6 H4 Cl2 O	19,199	177,95901	C6 H4 Cl2 O2	21,794	161,96385	C6 H4 Cl2 O
	4	21,789	161,96385	C6 H4 Cl2 O	28,617	321,91325	C12 H6 Cl4 O2	21,784	161,96385	C6 H4Cl2 O	28,632	321,91312	C12 H6 Cl4 O2
	5	28,62	321,91330	C12 H6 Cl4 O2				28,628	321,91318	C12 H6 Cl4 O2			
20	1	5,435	97,97689	**C4H2O3**	16,102	143,99046	C6 H5 Cl O2	2,361	113,99286	C4 H2 O4	2,402	113,99286	C4 H2 O4
	2	16,11	143,99046	C6 H5 Cl O2	19,197	177,95929	C6 H4 Cl2 O2	16,12	143,99046	C6 H5 Cl O2	7,037	113,99286	C4 H2 O4
	3	19,21	177,95926	C6 H4 Cl2 O2	21,792	161,96385	C6 H4 Cl2 O	19,223	177,95926	C6 H4 Cl2 O2	19,203	177,959	C6 H4 Cl2 O2
	4	21,8	161,96387	C6 H4 Cl2 O	28,616	321,91300	C12 H6 Cl4 O2	21,819	161,9638	C6 H4 Cl2 O	28,624	321,91321	C12 H6 Cl4 O2
	5	28,624	321,91299	C12 H6 Cl4 O2				28,655	321,91285	C12 H6 Cl4 O2	32,389	447,89976	C18 H9 Cl5 O3
30	1	5,404	97,97706	**C4H2O3**	16,102	143,99046	C6 H5 Cl O2	2,355	113,99286	C4 H2 O4	2,42	113,99286	C4 H2 O4
	2	7,04	113,99286	C4 H2 O4	19,197	177,95922	C6 H4 Cl2 O2	7,086	113,99286	C4 H2 O4	6,989	113,99286	C4 H2 O4
	3	16,1	143,99046	C6 H5 Cl O2	28,615	321,91275	C12 H6 Cl4 O2						
	4	19,198	177,95920	C6 H4 Cl2 O2									
	5	21,796	161,96376	C6 H4 Cl2 O									
	6	28,618	321,91280	C12 H6 Cl4 O2									
40	1	5,397	97,97705	**C4H2O3**				2,358	113,99286	C4 H2 O4	2,435	113,99286	C4 H2 O4
	2	5,402	159,93484	**C5H4O6**				7,024	113,99286	C4 H2 O4	6,966	113,99286	C4 H2 O4
	3	7,008	113,99286	C4 H2 O4									
	4	19,203	177,95902	C6 H4 Cl2 O2									

In general, the ozonation of 2,4-dichlorophenol $C_6H_4Cl_2O$ (Rt= 21.789) produced $C_6H_4Cl_2O_2$ (RT=19.97), $C_{12}H_6Cl_4O_2$ (RT=28.620) and $C_6H_5ClO_2$ (RT= 16.101) at all experimented pH regions within 20 minutes of reaction.

$C_6H_4Cl_2O_2$ is the product of direct hydroxylation 2,4-dichlorophenol **56**. There are 25 possible structures for the compound $C_6H_4Cl_2O_2$ based on ChemSpider data base search, however, only one isomer for the formula $C_6H_4Cl_2O_2$ was detected in analyzed aliquots (MS Appendix 7.T). Probable structures based on a meta-positioning of the two chlorine atoms are **57**, **58** or **59** which correspond to hydroxylation of **56** on one of positions 3, 5 or 6, respectively.

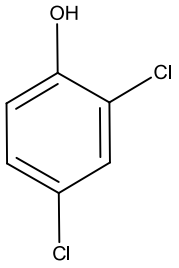

2,4-dichlorophenol

Structure 56: 2,4-dichlorophenol

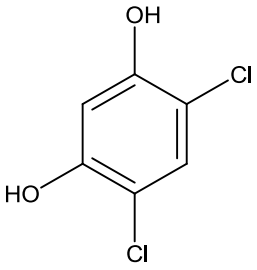

4,6-dichlororesorcinol

Structure 58: 4,6-dichlororesorcinol

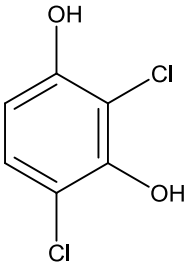

2,4-dichlororesorcinol

Structure 57: 2,4-dichlororesorcinol

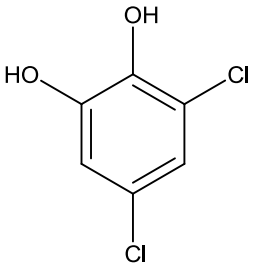

3,5-dichlorocatechol

Structure 59: 3,5-dichlorocatechol

Position 3 and 5 on structure **56** are deactivated sites for electrophilic attack on the phenyl ring. Also, position 3 is especially sterically hindered when compared to 5 and 6 since this would require hydroxylation of a carbon between two carbons carrying chlorine atoms. Structure **57** is therefore an unlikely candidate of hydroxylation of **56**. **58** have been previously proposed as hydroxylation product in Fenton (Xu and Wang, 2012) and pulse high voltage discharge (Zhang et al., 2012) oxidation of **56**, while **59** was proposed structure in photo-catalytic oxidation of **56** (Gaya et al., 2010) and hydroxylation reaction (Radjendirane et al., 1991, Ren et al.,

2014). The exact rationale for the choice of proposed structures are not discussed in some of these studies. Supporting MS masses presented by Zhang et al. (2012) may be considered inconclusive evidence as the mass may correspond to any of the isomers. Despite the perceived visual symmetry of structure **58**, **59** is selected as the most plausible structure for the compound $C_6H_4Cl_2O_2$ due to the steric hindrance posed by hydroxylation of other positions. Furthermore, the -1,2-postioning of hydroxyl groups as in catechol is more favorable for ring opening as opposed to -1,3- positioning as in resorcinol, supporting **59** as a better intermediate for ring opening reactions. It is noteworthy to mention that Radjendirane et al. (1991) compared the spectra qualities of their hydroxylated product with that of authentic samples which may be considered compelling evidence supporting **59**.

$C_{12}H_6Cl_4O_2$ (Mass spectrum Appendix 7.U) is the product of ring coupling leading to dimers similar to those of phenol and chlorophenols earlier discussed. It is one of two dimers identified during the ozonation of 2,4-dichlorophenol. There are 21 isomers of $C_{12}H_6Cl_4O_2$ based on ChemSpider data base search. Taking into account the meta- positioning of the chlorine atoms, only two compounds; **60** and **61** are plausible. Dimerised molecules are promoted by ionic reactions, supporting structure **61**. Thermodynamic calculations presented by Burcat et al. (2003) questioned the stability of this structure but further proposed that it may be a possible transition state intermediate in chemical reactions. **61** is proposed as the most plausible structure for $C_{12}H_6Cl_4O_2$.

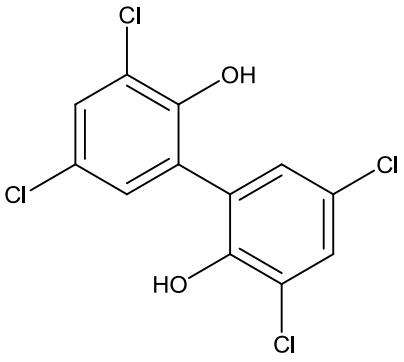

4,4',6,6'-tetrachloro-o,o'-biphenol

Structure 60: 4,4'6,6'-tetra-o-o'biphenol

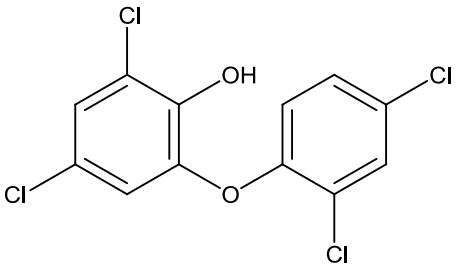

2,4-dichloro-6-(2,4-dichlorophenoxy)phenol

Structure 61: 2,4-dichloro-6-(2,4-dichlorophenoxy)phenol

$C_6H_5ClO_2$ (RT= 16.101, Mass spectrum Appendix 7.W) is the product of hydroxylative dechlorination of 2,4-dichlorophenol. The choice of dechlorinated

chlorine atom is of particular importance because two different products **62** and **63** are possible for the ortho and para substituted chlorine atoms, respectively. Wang and co-workers had previously reported both isomers are intermediates during electrochemical degradation of 2,4-dichlorophenol over chitosan catalyst (Wang et al., 2010b). A subsequent report identified structure only **63** (4-chlorocatechol) as intermediates in high voltage pulse discharged degradation of 2,4-dichlorphenol (Zhang et al., 2012). Since both intermediates would necessarily be formed from hydroxylation of either 2-chlorophenol or 4-chlorophenol, respectively, aliquot samples were further analyzed using both 2-chlorophenol and 4-chlorophenol methods. The retention time for the compound $C_6H_5ClO_2$ produced upon hydroxylative dechlorination of 2,4-dichlorophenol when analyzed at a flow rate of 0.3 mL/min was 19.172 minutes. Based on the retention time, the compound was therefore confirmed to be 4-chlorocatechol **63**, which is the product of hydroxylation of 4-chlorophenol. This observation is in line with previous reports, which suggested that hydroxylation- in this case, hydroxylative dechlorination - on a phenyl ring preferentially occurs at the ortho- position compared to the para- position, leading to a catechol derivative rather than a hydroquinone derivative (Matsuura and Omura, 1966).

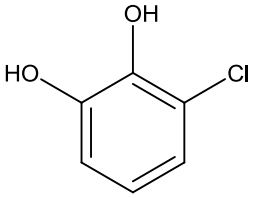

3-chlorocatechol

Structure 62: 3-chlorocatechol

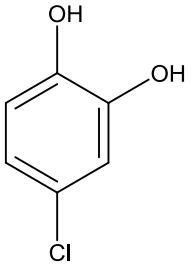

4-chlorocatechol

Structure 63: 4-chlorocatechol

$C_{12}H_7Cl_3O_3$ (RT= 24.828, Mass spectrum Appendix 7.V) is the second of two dimeric compounds detected during the ozonation of 2,4-dichlorophenol. This trichlorinated dimer has been identified in an earlier study and was suggested as **64** trichlorotrihydroxybiphenyl (Hirvonen et al., 2000). Due to the relative positions of the hydroxyl and chloro groups on the phenyl rings, **64** is a highly unlikely structure for $C_{12}H_7Cl_3O_3$. $C_{12}H_7Cl_3O_3$ may be better rationalized as a hydroxylative dechlorinated product of **61** or a product of ionic reaction between 2,4-dichlorophenol **56** and 4-chlorocatechol **63**. Hypothetically, both routes should give

66, which is the most plausible structure for $C_{12}H_7Cl_3O_3$ as **65**, which is the only other possible isomer is less probable from ionic reactions.

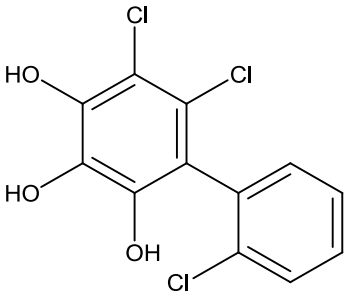

trichlorotrihydroxybiphenyl

Structure 64: trichlorotrihydroxybiphenyl

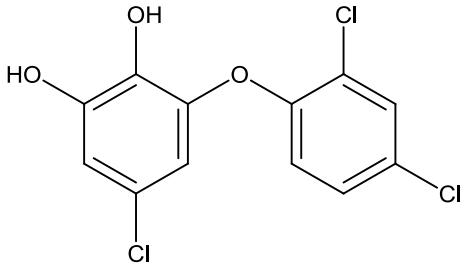

5-chloro-3-(2,4-dichlorophenoxy)benzene-1,2-diol

Structure 66: 5-chloro-3-(2,4-dichlorophenoxy)benzene-1,2-diol

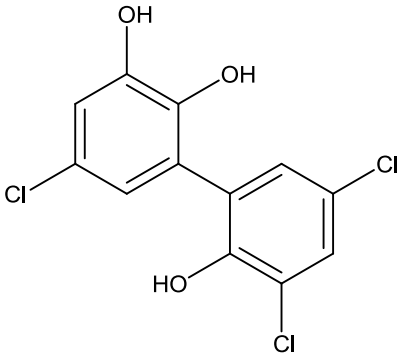

3',5,5',trichloro-2,2'-3-biphenyltriol

Structure 65: 3',5,5'-trichloro-2,2'-3-biphenyltriol

$C_{18}H_9Cl_5O_3$ (RT= 32.389) is a trimeric-coupled compound only observed in experiments where the pH was held constant in the alkaline region. There is no record of this compound in the literature and it may be classified as novel at this point. **67** is a proposed trimer based on ionic reactions at alkaline pH. **67** is a product of reaction between 66 and another molecule of 2,4-dichlorophenol **56** via an ionic pathway under oxidizing conditions.

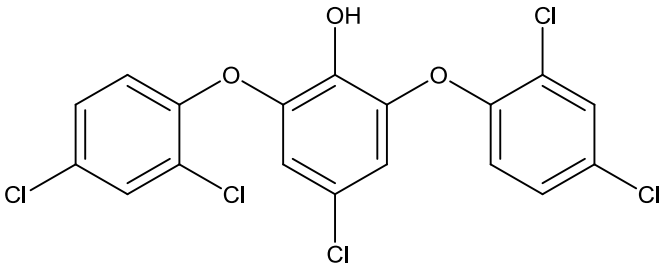

4-chloro-2,6-bis(2,4-dichlorophenoxy)phenol

Structure 67: 4-chloro-2,6-bis(2,4-dichlorophenoxy)phenol

$C_4H_2O_3$ (RT=5.418) detected in acidic pH is maleic anhydride **68**, which is a precursor to maleic and fumaric acid identified as oxidation products of 2,4-dichlorophenol (Wang et al., 2010b).

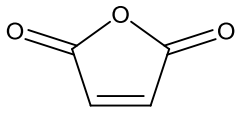

maleic anhydride

Structure 68: maleic anhydride

Other compounds determined in this study as minor products during the ozonation process are summarized in Figure 4.43.

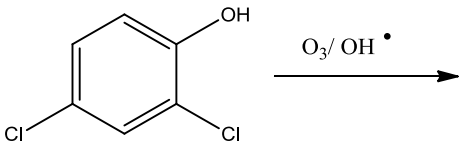

2,4-dichlorophenol

C3: $C_3H_2O_4$, $C_3H_4O_2$, $C_3H_4O_3$

C4: $C_4H_2O_4$, $C_4H_6O_6$, $C_4H_2O_3$, C_4H_3ClO

C5: $C_5H_4O_3$, $C_5H_4O_6$, $C_5H_6O_5$, $C_5H_4O_2$, $C_5H_4O_4$, $C_5H_2O_3$, $C_5H_2O_4$

C6: $C_6H_4O_4$

C8: C_8H_3ClO4

Figure 4.43: Residual compounds of 2,4-dichlorophenol degradation

A summary of compounds (earlier) identified during the ozonation of 2,4-dichlorophenol is presented in Table 4.12 while a proposed pathway for degradation based on intermediates identified in this study is presented in Figure 4.44.

Table 4.12: Intermediates reported during ozonation/oxidation of 2,4-dichlorophenol. In bold are intermediates also identified in this study

Compound	Formula	Structure	Method of identification	References
Phenol	C_6H_6O	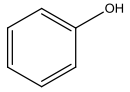	HPLC-UV, GC-MS	(Liu et al., 2009, Wang et al., 2010b)
2-chlorophenol	C_6H_5ClO	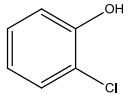	GC-MS	(Liu et al., 2009, Wang et al., 2010b)
4-chlorophenol	C_6H_5ClO	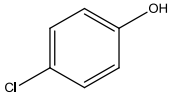	GC-MS	(Liu et al., 2009, Zhang et al., 2012, Wang et al., 2010b)
4-chloro-1,2-benzenediol	$C_6H_5ClO_2$	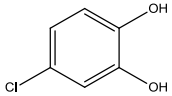	GC-MS	(Wang et al., 2010b)
Maleic acid	$C_4H_4O_4$	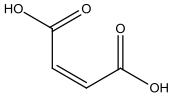	GC-MS	(Wang et al., 2010b)
Fumaric acid	$C_4H_4O_4$	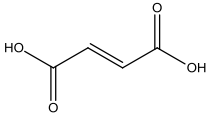	GC-MS	(Wang et al., 2010b)
2,3-dihydroxyl-succinic acid	$C_4H_4O_6$	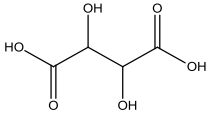	GC-MS	(Wang et al., 2010b)
Propanedioic acid	$C_3H_4O_4$	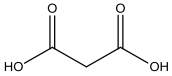	GC-MS	(Wang et al., 2010b)

Compound	Formula	Structure	Method of identification	References
Oxalic acid	$C_2H_2O_4$	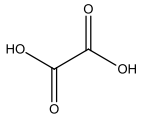	NB, GC-MS	(Wang et al., 2010b, Li et al., 2015, Zhang et al., 2012)
Formic acid	CH_2O_2	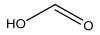	GC-MS, HPLC and IC	(Wang et al., 2010b, Xu and Wang, 2012)
Acetic acid	$C_2H_4O_2$		GC-MS, HPLC and IC	(Li et al., 2015, Wang et al., 2010b, Xu and Wang, 2012, Zhang et al., 2012)
2-chlorohydroquinone	$C_6H_5ClO_2$	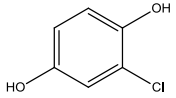	GC-MS; HPLC and IC	(Gaya et al., 2010, Xu and Wang, 2012, Zhang et al., 2012, Wang et al., 2010a)
3,5-dichlorocatechol	$C_6H_4Cl_2O_2$	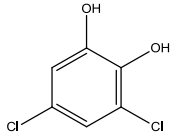	GC-MS	(Gaya et al., 2010)
4,6-dichloreresorcinol	$C_6H_4Cl_2O_2$	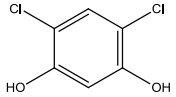	HPLC and IC	(Xu and Wang, 2012)
Trichlorinated dimer (trichlorotrihydroxybiphenyl)	$C_{12}H_7Cl_3O_3$	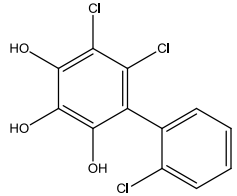	GC-MS	(Hirvonen et al., 2000)
Tetrachlorinated dimer (tetrachlorotrihydroxybiphenyl)	$C_{12}H_6Cl_4O_3$	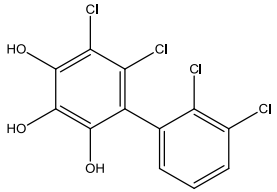	GC-MS	(Hirvonen et al., 2000)

Compound	Formula	Structure	Method of identification	References
Tetrachlorinated dimer (tetrachlorotetrahydroxybiphenyl)	$C_{12}H_6Cl_4O_4$	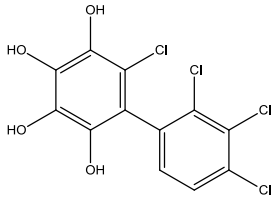	GC-MS	(Hirvonen et al., 2000)
2,6-dichlorophenol	$C_6H_4Cl_2O$	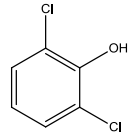	GC-MS	(Zhang et al., 2012)
4,6-dichloro-1,3-benzenediol	$C_6H_4Cl_2O_2$	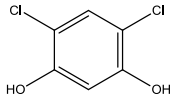	GC-MS	(Zhang et al., 2012)
3,5-dichloro-1,2-benzenediol	$C_6H_4Cl_2O_2$	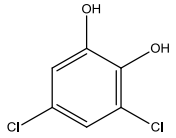	GC-MS	(Zhang et al., 2012)
4-chlorocatechol	$C_6H_5ClO_2$	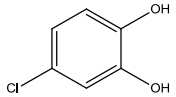	GC-MS	(Zhang et al., 2012)
Hydroquinone	$C_6H_6O_2$	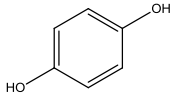	GC-MS	(Li et al., 2015)

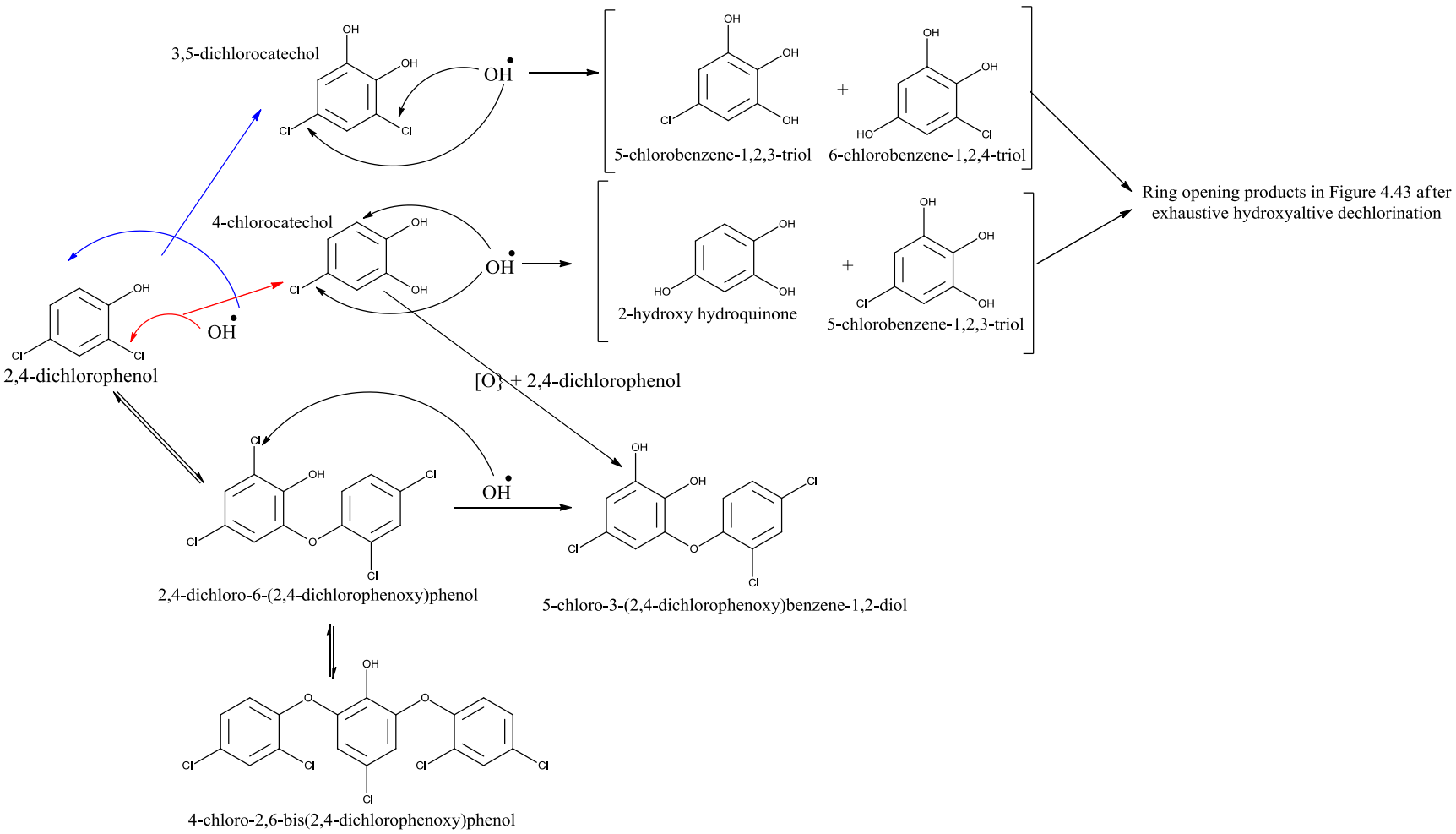

Figure 4.44: Proposed scheme for 2,4-dichlorophenol degradation and polymerization based on results from this study. Compounds in parenthesis are inferred based on reactions

4.4. Heterogeneous catalysis of 4-chlorophenol ozonation by β-FeOOH

Results on kinetics for the degradation of phenol, 2-chlorophenol, 4-chlorophenol and 2,4-dichlorophenol by ozone presented in Section 4.3.1 showed that the order of reactivity of the four substrates at all tested pH was 2,4-dichlorophenol> 2-chlorophenol> phenol> 4-chlorophenol. A summary of observed apparent rate constants was presented in Table 4.4. Possible reasons for the observed trend were discussed in line with literature. The observed trend firmly established that 4-chlorophenol with a lower rate constant at all tested pH was the most recalcitrant of the four substrates.

In this section, we present results on catalytic ozonation of 4-chlorophenol using beta-FeOOH as a heterogeneous catalyst. Method of preparation of catalyst and experimentation has been outlined in section 3.4 and 3.7.2, respectively. Results were interpreted by comparing the efficiency of catalysed and uncatalyzed systems in oxidizing aqueous substrate. At attempt is made at interpreting the mode of operation of the catalyst based on experimental data, drawing inferences from literature where similar cases exist. 4-chlorophenol was selected as probe organic for testing catalytic efficiency of β-FeOOH because it was the most recalcitrant amongst the tested chlorophenols to ozone oxidation. Figure 4.45 illustrates the efficiency of β-FeOOH in promoting 4-CP degradation. In the presence of β-FeOOH nano particles and ozone, 99% of 4-CP was removed after 40 min, whereas, 67% of 4-CP was removed when ozone only was used. In the absence of ozone (in the presence of β-FeOOH only) negligible amount of 4-CP (3%) was removed, indicating that the amount of 4-chlorophenol removed by adsorption was negligible. Therefore, the prepared β-FeOOH nano-rods exhibit good catalytic behaviour for the ozonation degradation of 4-CP.

Tert-butanol is regarded as scavenger for hydroxyl radicals and when added to a system containing hydroxyl radicals, would suppress their activity (Dong et al., 2008, Benitez et al., 2000b). For this purpose, a separate experiment was conducted in which t-butanol (0.1 g/L) was added to the reactor mixture. The suppressing effect of t-butanol is also shown in Figure 4.46. In the presence of t-butanol, the degradation of 4-chlorophenol was 67% after 40 minutes of reaction as compared to 99% degradation in the absence of the radical scavenger. The suppressing effect highlights the mechanism of operation of FeOOH, i.e., to generate hydroxyl radical thereby accelerating the degradation process. Variables such as pH, catalyst load

and 4-chlorophenol concentrations were systematically studied in order to elucidate the working mechanisms of the catalyst.

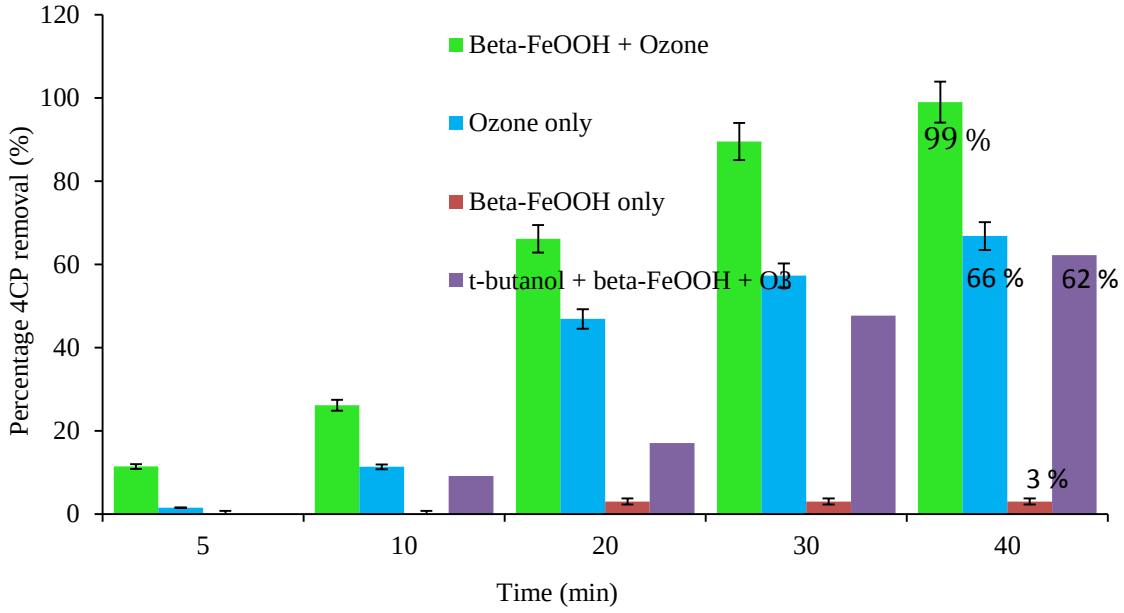

Figure 4.45: Degradation efficiency of 4-chlorophenol (4-CP) by catalytic ozonation (catalyst dose 0.01 %, 4-CP = $2x10^{-3}$M)

4.4.1. Effect of initial pH on the degradation efficiency of 4-CP

The pH of the bulk solution affects the rate of oxidation organics by ozone. At high pH, ozone reacts with hydroxyl ions to generate, among other species, the highly reactive and non-selective hydroxyl radicals as explained in Section 2.3.1.1. Experiments were conducted at varying initial pH (3.5, 7 and 10) to evaluate the contribution of the catalyst to the degradation process at various pH. The rate of degradation of 4-chlorophenol using ozone and β-FeOOH analysed using first order kinetic model is presented in Figure 4.46. By comparing the rate of degradation of ozone alone to that in the presence of β-FeOOH, the contributions of catalyst was calculated and are summarized in Table 4.13. The rate constants were observed to increase with an increase in pH of the solution in neutral and alkaline experiments. This is due to production of hydroxyl radicals by ozone reaction with hydroxyl ions, plus an increased production of hydroxyl radicals due to ozone breakdown on the surface of β-FeOOH. The surface site on FeOOH are related to their equilibrium constants according to Equation 4.3 and Equation 4.4 below (Park et al., 2004)

Equation 4.3

$$\equiv FeOH_2^+ \leftrightarrow \equiv FeOH + H^+ \; pK_{a1}^s = 6.4$$

Equation 4.4

$$\equiv FeOH \leftrightarrow \equiv FeO^- + H^+ \; pK_{a2}^s = 9.2$$

At high pH, ozone breakdown on catalyst surface is due to the reaction of electrophilic ozone molecules with the negatively charged $\equiv FeO^-$ sites on FeOOH (Park et al., 2004). At lower acidic pH where $\equiv FeOH_2^+$ species predominate, contributions of the catalyst to ozone breakdown would be due to interactions with $\equiv FeOH_2^+$. Since ozone is electrophilic in nature, breakdown on FeOOH due to $\equiv FeOH_2^+$ sites would be expected to be slower. As shown in Figure 4.46, the first order kinetic model appropriately described the reaction at pH 7 and pH 10 (R^2= 0.99 and 0.98, respectively), but fails at acidic pH where it deviates largely from first order (R^2=0.87). This deviation from first order kinetics suggested the existence of a secondary mechanism at low pH. The existence of an undefined order during the Fe^{2+} catalysed ozonation of aniline was also identified by Sauleda and Brillas (2001). While the authors provided no explanations for their observations, they went on to show that a limiting concentration for the Fe^{2+} ions exist, above which, they react with ozone, reducing ozone to oxygen.

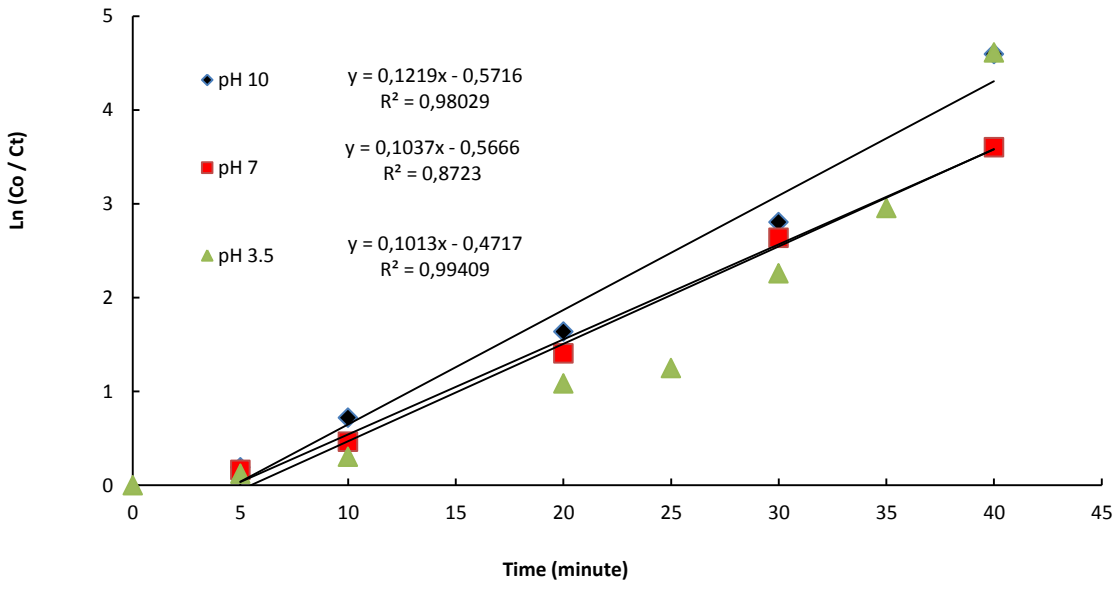

Figure 4.46: Effect of β-FeOOH on rate of 4-chlorophenol degradation

Table 4.13: Effect of pH on contribution of B-FeOOH to kinetic of 4-chlorophenol degradation

K (mol- min-)	pH 3.5	pH 7	pH 10
O_3 alone	0,0418	0,0541	0,0769
O_3 + β-FeOOH	0,1037	0,1013	0,1219
% increase in K	148	87	56

In explaining the observed behaviour of β-FeOOH in acidic media, inferences can be drawn from the work of Chou and Huang (1999). While using supported iron oxyhydroxide as heterogeneous catalyst in Fenton reaction, the workers observed that reduced iron at low pH generated Fe^{2+}, which further catalysed the reaction process in a homogeneous manner. The two stage kinetic model proposed by the worker was applied to the kinetic data at acidic pH and is presented in Figure 4.47. As observed in the presented figure, the two stage kinetic model appropriately described the oxidation process. The reaction within the first 28 minutes is defined by a rate constant 0.0545 min^{-} that is determined by heterogeneous catalysis while the reaction afterwards is defined by the presence of Fe-ions in solution. The concentration of Fe-ions in solution as monitored by atomic absorption spectroscopy is presented in Figure 4.48 (pH 2.4 at start of second stage is indicated). Interestingly, the pH at the start of the second stage coincides with the pH applied for Fenton reactions using Fe^{2+} and H_2O_2.

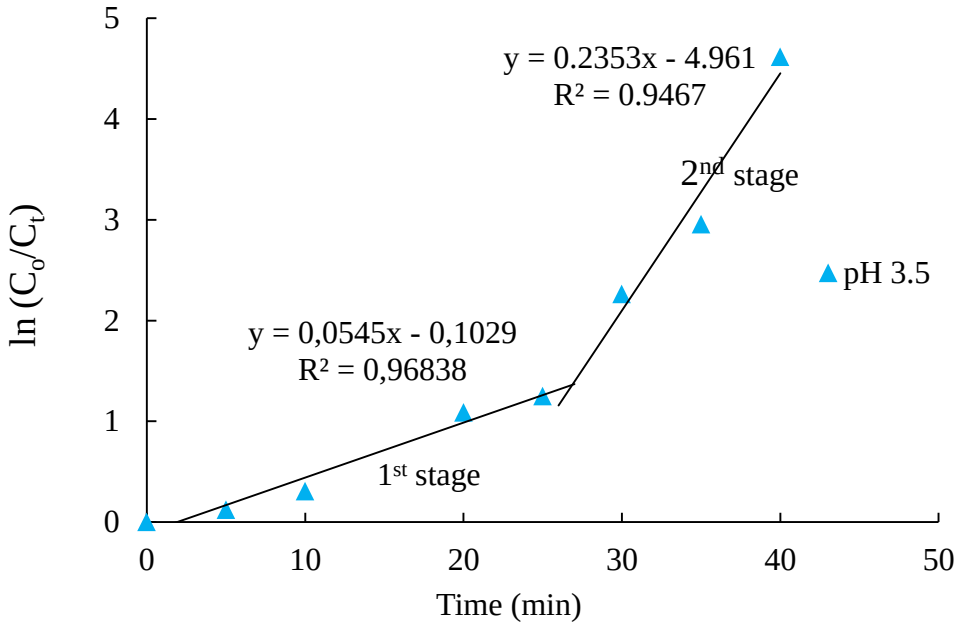

Figure 4.47: Two stage reaction kinetics of β-FeOOH at low pH 3.5

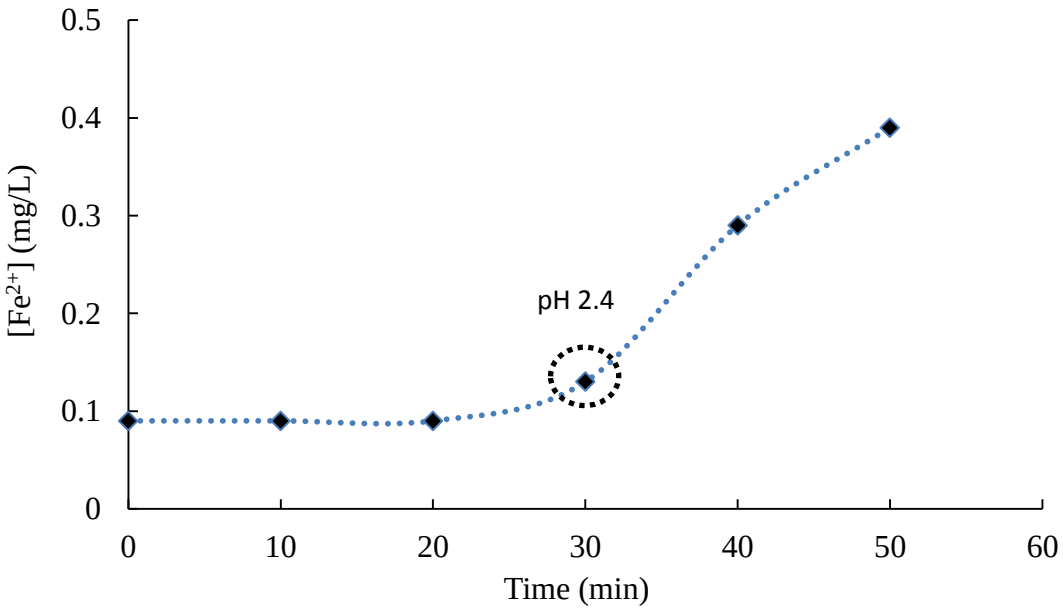

Figure 4.48: Fe-ions in solution in β -FeOOH experiment at low pH 3.5

The mechanism of ozone breakdown in acidic pH may, therefore, be described according to Equations 4.5-4.7. Even though this two stage kinetic model has never being applied to ozonation experiments, the data obtained in this study clearly supports this mechanism at low pH. The high degradation efficiency of β-FeOOH-O_3 at pH 3.5 compared to ozone alone is, therefore, attributed to contributions from direct ozonation, heterogeneous catalysis and homogeneous catalysis initiated by reductive dissolution of β-FeOOH. The organic substrate was the reductant, and thus serves as the source of e^- in Equation 4.5.

Equation 4.5

$$\beta - FeOOH + 3H^+ + e^- \rightarrow Fe^{2+} + 2H_2O$$

Equation 4.6

$$O_3 + Fe^{2+} \rightarrow FeO^{2+} + O_2$$

Equation 4.7

$$FeO^{2+} + H_2O \rightarrow Fe^{3+} + OH^{\bullet} + OH^-$$

4.4.2. Effect of β-FeOOH dose on degradation efficiency of 4-chlorophenol

Ideal catalyst loading for an ozonation reaction is usually kept at 1.0 g catalyst per litre substrate solution, corresponding to 0.1 % catalyst load (Rosal et al., 2008,

Huang et al., 2012). Catalyst tests presented thus far for previous experiments were kept at 0.01 %. Further tests were conducted at increasing catalyst dose to investigate the contribution of this variable to catalyst efficiency. For this purpose, repeat experiments were conducted with 0,05 g and 0.1 g per 100 mL 4-chlorophenpol solution corresponding to 0.05 and 0.1 %, respectively. Based on the highlighted mode of operation of β-FeOOH, it is expected that increasing the catalyst dose would increase the amount of Fe-ions at the onset of homogeneous catalytic stage of the degradation process and therefore increase mineralization. Figure 4.49 (a) and (b) illustrate the percentage 4-chlorophenol and COD removal, respectively with increasing catalyst load.

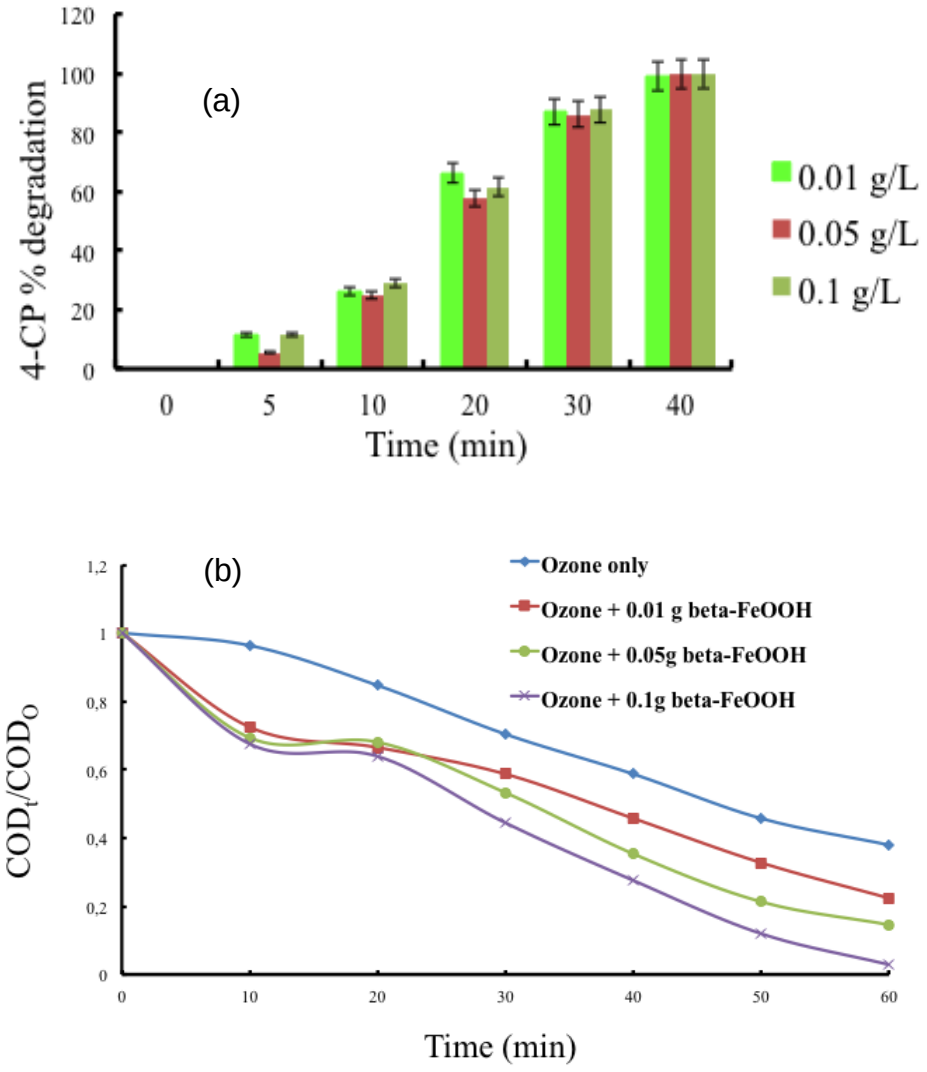

Figure 4.49: (a) 4-CP removal efficiency at increasing catalyst load, (b) COD removal ratio at different catalyst load.

The difference in 4-chlorophenol removals with increasing catalyst load is insignificant as shown by the identical bars after 40 minutes in Figure 4.49 (a). The generated radicals are non-selective in removing 4-chlorophenol and therefore produce identical results. COD removal is however higher in the systems containing more hydroxyl radicals as show in Figure 4.49 (b). It is also important to point out that the rate of mineralization is higher in the catalytic system (78%, 86% and 97%) after 40 minutes, compared to that using ozone alone (62%). It may therefore be inferred that the β-FeOOH significantly enhances the mineralization of the substrate, which is highly important from an environmental point of view. Figure 4.50 (a) illustrates the raising concentration of Fe-ion in solution as measured by atomic absorption spectrometry. In all three experiments, the Fe-ions in solution start to increase rapidly as the experiment exceeds the 20 minutes mark, signalling the start of the homogeneous phase of the reaction mechanism. The kinetic plots for 4-chlorophenol removals, presented as pseudo first order plots are presented in Figure 4.50 (b). All three plots clearly follow a two stage kinetic model as explained earlier. The first stage of the reaction involves heterogeneous catalysis where ozone breakdown is on the surface of β-FeOOH, and in the second stage, ozone breakdown is catalysed by homogeneous Fe-ions in solution.

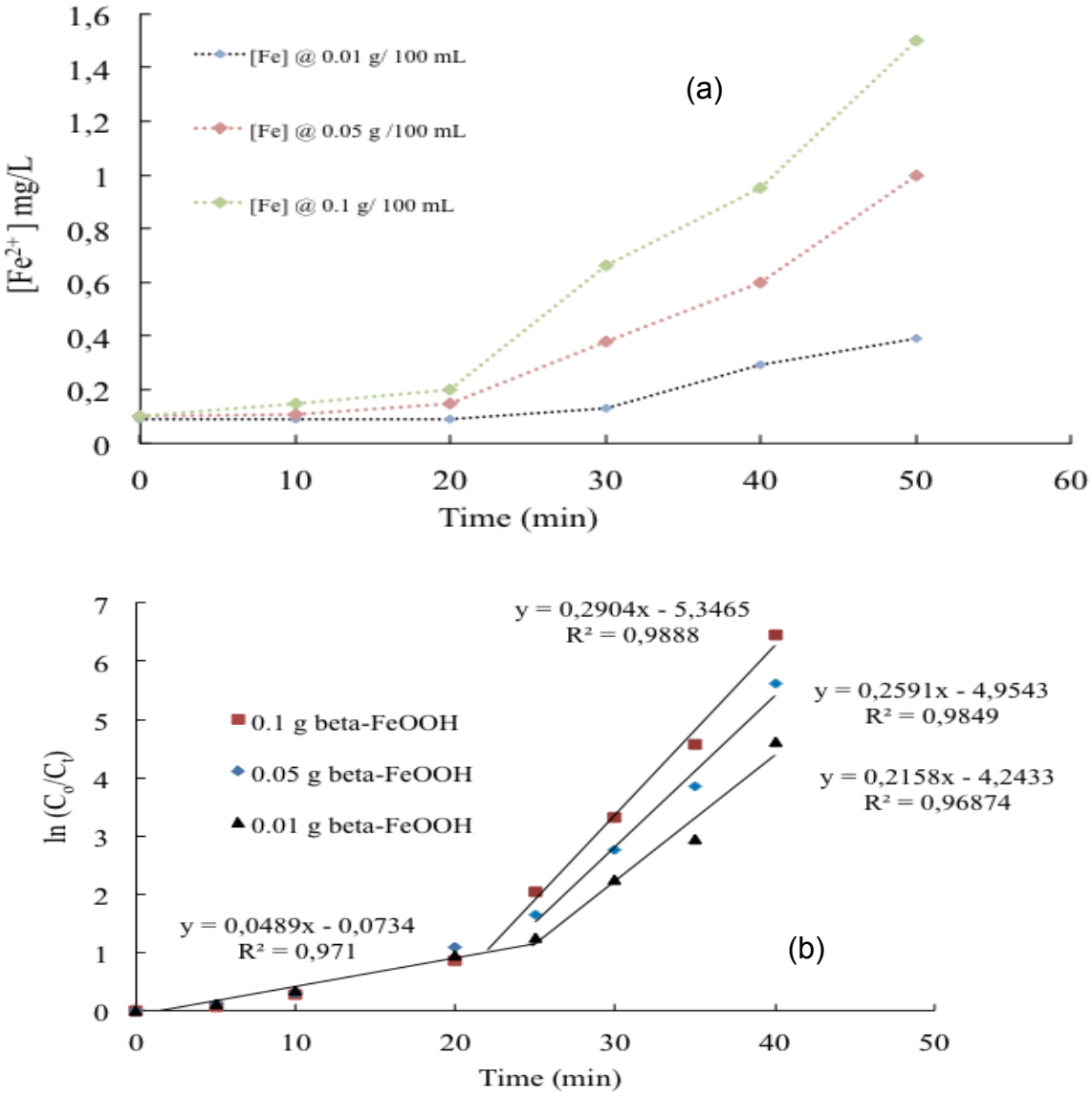

Figure 4.50: (a) Concentration of Fe-ions in solution at increasing β-FeOOH dose, (b) Pseudo first order rate plots for 4-chlorophenol at increasing β-FeOOH dose.

4.4.3. Effect of 4-chlorophenol concentration

Experiments conducted at varying concentrations of 4-chlorophenol also showed two-stage degradation kinetics (Figure 4.51 a). Figure 4.51 (b) shows that below 2 mM 4-chloeophenol concentration both rate constants i.e. first and second stage; increases with increasing 4-chlorophenol concentrations. This suggests that the initial concentration of 4-chlorophenol is not the rate-limiting step below 2 mM. In both cases the second stage rate constants are larger than the first stage rate constants implying faster degradation of 4-chlorophenol during homogenous catalysis.

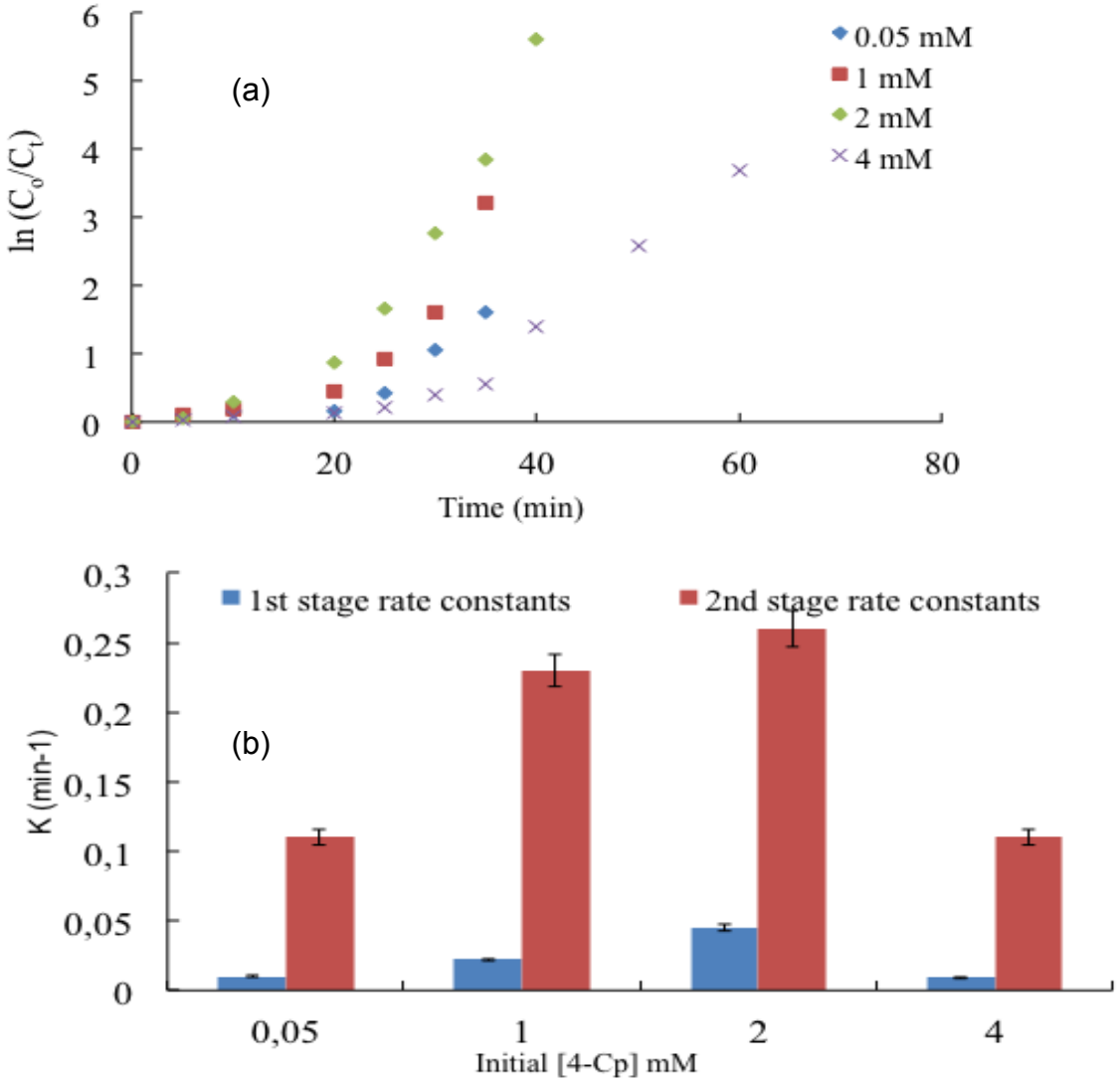

Figure 4.51: (a) Kinetic study under different 4-chlorpphenol concentrations and (b) dependence of rate constants (k) on initial 4-chlorophenol concentrations

4.5. Heterogeneous catalysis of 4-chlorophenol ozonation using β-FeOOH-NiO composite

In an attempt to resolve the instability of β-FeOOH and its subsequent dissolution in acidic pH, which invariably leads to catalyst loss, β-FeOOH was bonded on several metal oxide supports vis: Al_2O_3, TiO_2 and NiO. This method of catalyst enhancement has been reported by several workers (Kasprzyk-Hordern et al., 2003, Dong et al., 2014, Zhao et al., 2015). β-FeOOH composites were prepared according to method describes in Section 3.5. For the purpose of screening, 2%, 5% and 10 % bonded β-FeOOH on Al_2O_3, TiO_2 and NiO was prepared. The respective rates of 4-chlorophenol degradation in the presence of the pristine support and β-FeOOH

bonded supports are presented in Figure 4.52 to Figure 4.54. A summary of apparent rate for the catalytic processes is presented in Table 4.14.

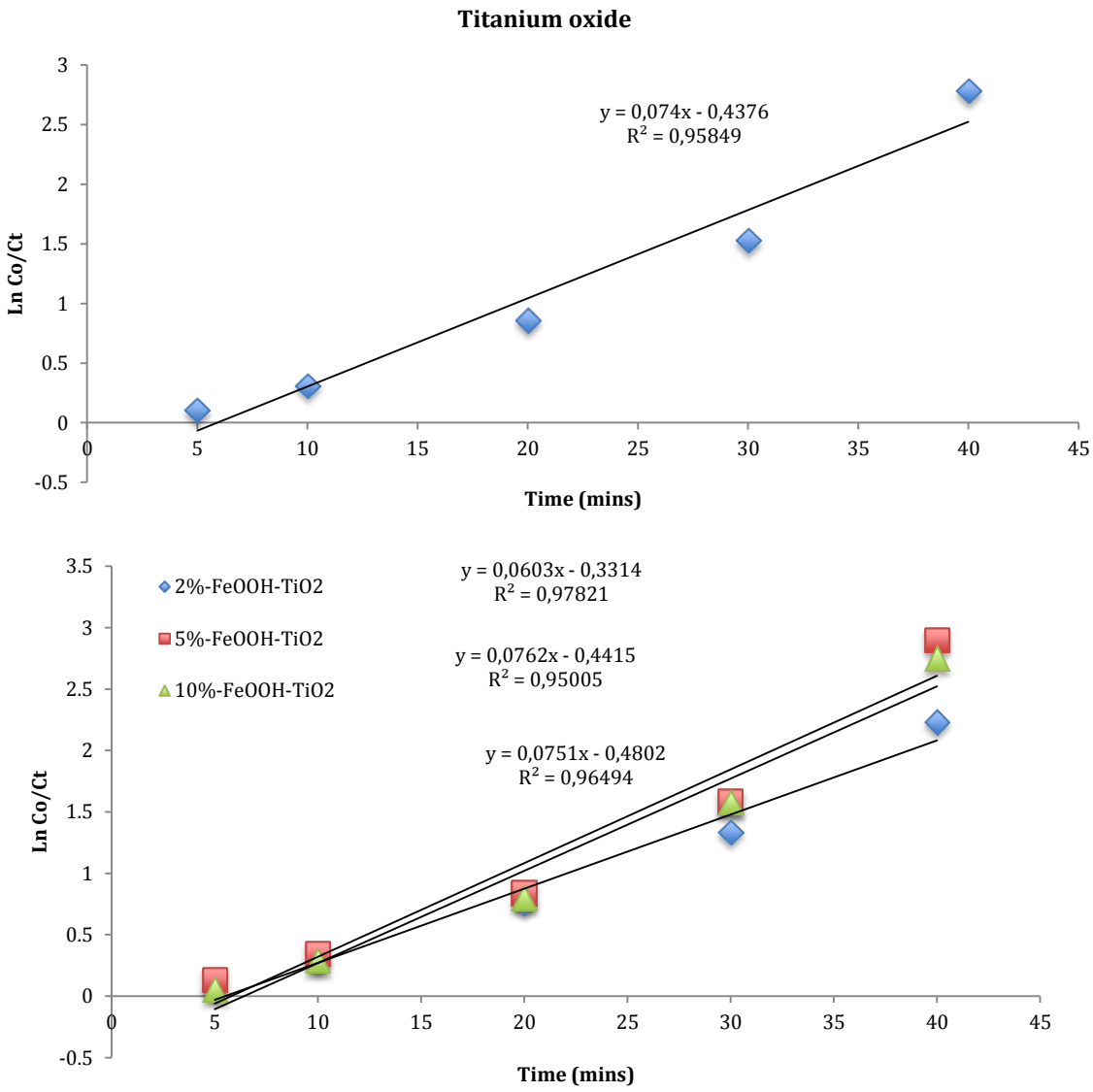

Figure 4.52: Degradation rate (in bold) of 4-chlorophenol by ozonation in the presence of titanium oxide (TiO_2) and β-FeOOH supported on TiO2.

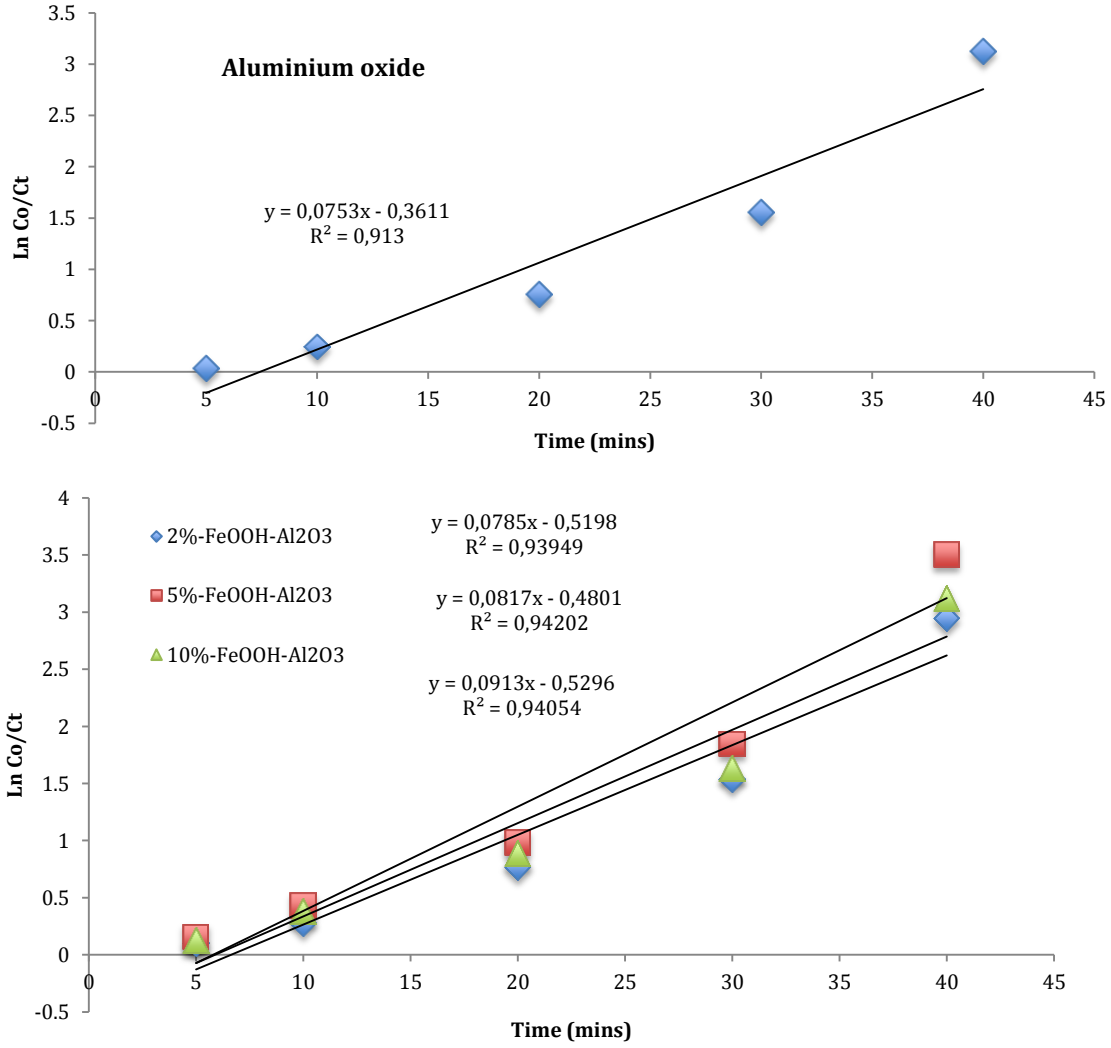

Figure 4.53: Degradation rate (in bold) of 4-chlorophenol by ozonation in the presence of Aluminium oxide (Al_2O_3) and β-FeOOH supported on Al_2O_3.

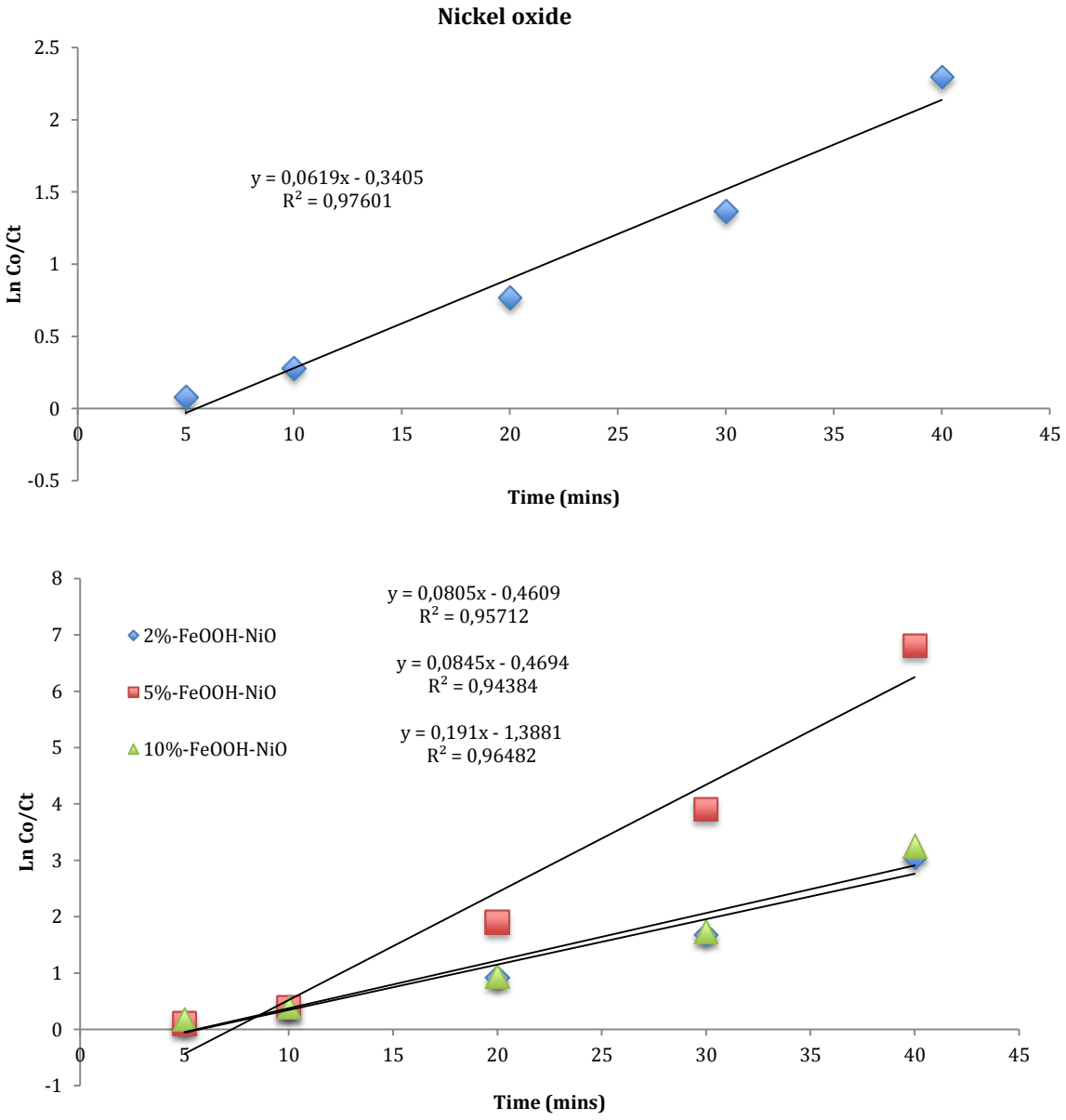

Figure 4.54: Degradation rate (in bold) of 4-chlorophenol by ozonation in the presence of nickel oxide (NiO) and β-FeOOH supported on NiO.

Table 4.14: Apparent rate constants for catalytic ozonation processes. Rates in min^{-1}

	TiO_2		Al_2O_3		NiO	
% dopping	Rate	R^2	Rate	R^2	Rate	R^2
0	0,074	0,96	0,0753	0,91	0,0619	0,98
2,5	0,0603	0,98	0,0785	0,94	0,0805	0,96
5	0,0762	0,95	0,913	0,94	0,191	0,96
10	0,0751	0,96	0,0817	0,94	0,0845	0,94

When compared to the rate of degradation of 4-chlorophenol by ozone alone (0.0541 min^{-} at neutral pH), it is clear that all the pristine supports improve the ozonation process by varying degree. Pure Al_2O_3 (0 % doping) had the highest contribution to 4-chlorophenol removal with a rate of 0,0753 min^{-1} while pristine NiO had the least contribution with k= 0.0619 min^{-1}. The rates for β-FeOOH bonded to supports presented in Table 4.14 also showed varying degrees of improvements of the rate of 4-chlorophenol removals. NiO was selected as suitable support based on the best 4-chlorophenol-degradation rate presented by the 5% doped NiO when compared to NiO alone and with other supported material.

The characterization of β-FeOOH-NiO doped material has being presented in section 4.2. It is interesting to note that for all the supports tested, the 5% doping of β-FeOOH gave the better results compared to the 2% and 10% doped materials. It has previously being reported that excessive or too little dopant can decrease catalytic activity of a nanomaterial (Dai et al., 2014). This may well be the case observed in the current study. Ni in the +II state is classified as borderline Lewis acid while aluminium (+III) and titanium (+IV) are both hard Lewis acids (Kasprzyk-Hordern et al., 2003). The inter-conversion between the two states of iron (reduced +II and oxidized +III) is the basis for stability of iron when stabilized on supports (Bandara et al., 2007). A plausible reason for Ni (II) presenting a better support for iron may be that unlike aluminium and titanium, its boarder –line properties allow for better redox charge transfers between the two states of iron during the ozonation process.

4.5.1. 7-Hydroxycoumarin (7HC) and tert-butanol testing

In order to understand the mode of operation of β-FeOOH-NiO, coumarin was used as probe molecule to verify the presence of hydroxyl radicals and compare the radicals generated by the catalytic system compared to ozone alone. The method for measuring 7HC is described in 3.7.4. Figure 4.55 illustrates 7HC profile in the reactor at varying time. The measured concentrations of 7-HC obtained from a calibration are presented in Figure 4.55 (b). As shown in Figure 4.55 (b), the composite system generates more hydroxyl radicals when compared to the ozone, ozone-NiO and ozone- β-FeOOH systems. It is important to mention that the 7HC method only measures the free hydroxyl radicals in a system and does not measure

those bound on a catalyst surface (Xiang et al., 2011). It may therefore be inferred that the actual hydroxyl radicals generated by the catalytic system is underestimated.

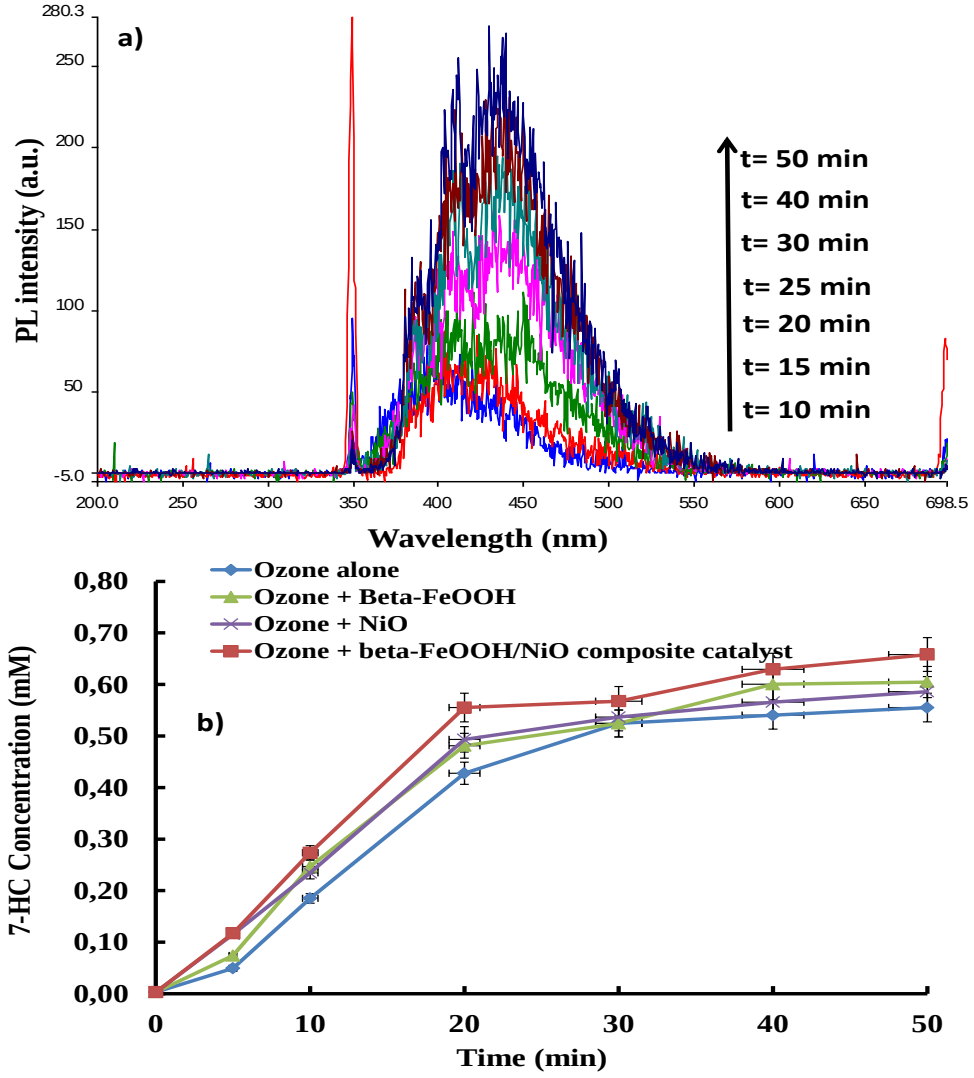

Figure 4.55 (a) Photoluminescence changes observed during reaction in the presence of composite, (b) 7-hydroxycoumarin produced during the reactions.

The presence of hydroxyl radicals as the major contribution to catalytic oxidation of 4-chlorophenol was affirmed by control experiments using tert-butanol as a radical scavenger. Typical catalytic experiments were conducted in the presence of tert-butanol (2 x 10^{-3}M). Experiments were conducted in identical manner describe in Section 3.7.2 with the inclusion of t-butanol at equivalent concentration to 4-chlorophenol. The results in Figure 4.56 shows that the removal efficiency for 4-chlorophenol drops from 85% to 50% in the first 20 minutes when tert-butanol is used to scavenge hydroxyl radicals. This further supports the 7-HC experiments that

the generated radicals are the active mechanism for 4-chlorophenol degradation by the catalytic process.

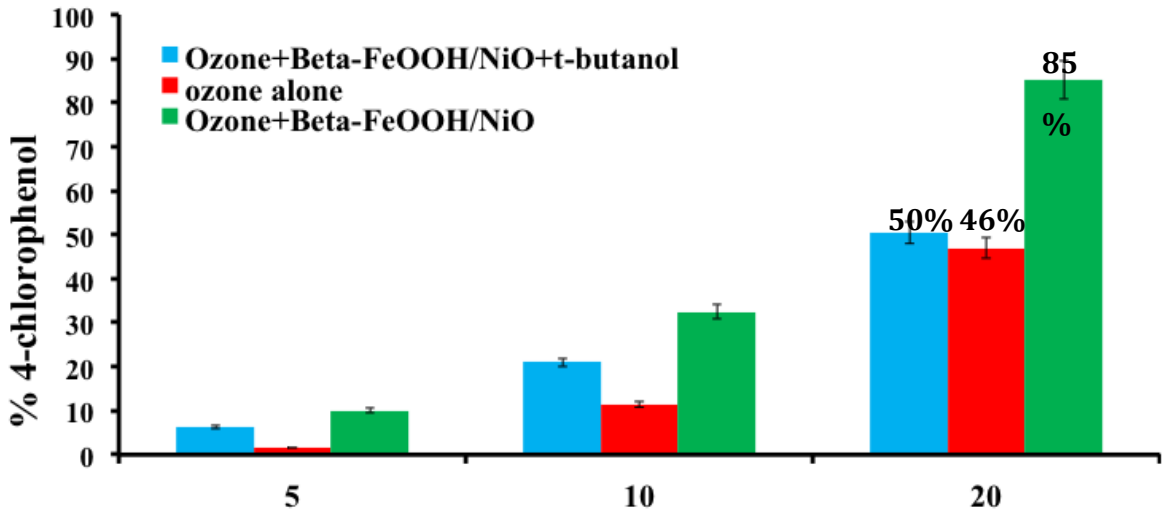

Figure 4.56: Role of hydroxyl radicals on the degradation of 4-chlorophenol

In general degradation of organic compounds during catalytic ozonation occurs via adsorption, direct oxidative reaction by ozone and oxidative reaction by powerful non-selective hydroxyl radical, $OH^{\bullet}$. The total removal of organic compound is the sum of those by these three pathways. The composite material only adsorbed 3% of the 4-CP after 50 minutes in the absence of ozone. Hence, the role of adsorptive mechanism for the degradation of 4-CP was considered negligible. Enhanced degradation of 4-CP in the catalytic ozonation process is clearly attributed to the presence of $OH^{\bullet}$. Generation of hydroxyl radical occurs due to interaction between ozone and hydroxide ions Equation 2.1 - Equation 2.8 and via ozone-metal oxides interactions (Equation 4.8 - Equation 4.10.)

Equation 4.8

$$NiO + O_3 \rightarrow NiO(h^+) + O_3^{\cdot -}$$

Equation 4.9

$$O_3^{\cdot -} + H^+ \rightarrow HO_3^{\cdot -}$$

Equation 4.10

$$HO_3^{\cdot -} \rightarrow O_2 + OH^{\bullet}$$

Equations 4.8 - 4.10 which is supported by several studies is attributed to the electrophilic nature of ozone (Gracia et al., 2000, Dhandapani and Oyama, 1997, Imamura et al., 1991). Also, the presence of iron has been reported to

enhance ozone reactions with organics (Sauleda and Brillas, 2001, Ruppert et al., 1994, Villaseñor et al., 2002). The role of Fe can firstly be related to the ability to accept valence band holes (in a hetero-junction structure) and finally formation of FeO_2^+ species (From the interaction with O_3), which can produce $OH^\bullet$ from water. The valence band edge potential of NiO and β-FeOOH are reported to be 3 and 2.5 eV, respectively (Xu and Schoonen, 2000, Chowdhury et al., 2015a). Generated NiO valence band hole (Equation 4.8; due to the electrophilic nature of O_3) can be transferred to the valence band of the β-FeOOH material (via the hetero-junction) due to difference in valence band edge potentials. The transferred holes can react with water to generate $OH^\bullet$ (Equation 4.11). The presence of too little Fe can hinder efficient hole transfer between NiO and β-FeOOH and excessive Fe can act as a hole trapping site (Nishikawa et al., 2012, Zhu et al., 2006). This phenomenon can be speculated to be the reason for lower catalytic activity of 2% and 10% composite material. However, this subject requires further investigation. Formation of $OH^\bullet$ from β-FeOOH is also possible via (Equation 4.12 - Equation 4.14):

Equation 4.11

$$NiO(h^+) + H_2O \rightarrow OH^\bullet + H^+$$

Equation 4.12

$$\beta - FeOOH + 3H^+ + e^- \rightarrow Fe^{2+} + 2H_2O$$

Equation 4.13

$$O_3 + Fe^{2+} \rightarrow FeO^{2+} + O_2$$

Equation 4.14

$$FeO^{2+} + H_2O \rightarrow Fe^{3+} + OH^\bullet + OH^-$$

Equation 4.12 is a common phenomenon for iron oxy-hydroxides type materials during oxidation of phenolic compounds and has been reported in literature (Chou and Huang, 1999, Stumm and Sulzberger, 1992, Vértes and Czakó-Nagy, 1989, Stone, 1987, Stumm and Morgan, 1981), which normally leads to catalyst dissolution. The rate of reductive dissolution is dependent on the solution pH and organic reductant concentration (Stone, 1987). Note that the organic substrate -4-chlorophenol in this case- serves as the source or required e^- in Equation 4.12 (Stone, 1987). The dissolution of pristine β-FeOOH as Fe^{2+} was explained in section

4.4. Once Fe^{2+} is generated it either reacts with O_3 or detaches from the oxide surface, which leaves a vacancy on the oxide surface i.e. surface dissolution. Fe^{2+} react with O_3 via Equation 4.13 and Equation 4.14 to generate $OH^{\bullet}$ radicals.

Atomic absorption spectroscopy results for Fe and Ni ions in solution are presented in Figure 4.57. As shown by the plots, no measureable Fe or Ni ions were present in solution during the ozonation period. This therefore suggests that Equation 4.13 and Equation 4.14 does not hold with regards to the composite material. It is therefore proposed that the reaction between Fe^{2+} and O_3 is kinetically faster than the rate of Fe^{2+} dissolution reaction. A consequence of this is an inter-conversion between the two oxidation states of Fe in the presence of an oxidant such as ozone. This concept has been previously suggested by Bandara and co-authors (Bandara et al., 2007).

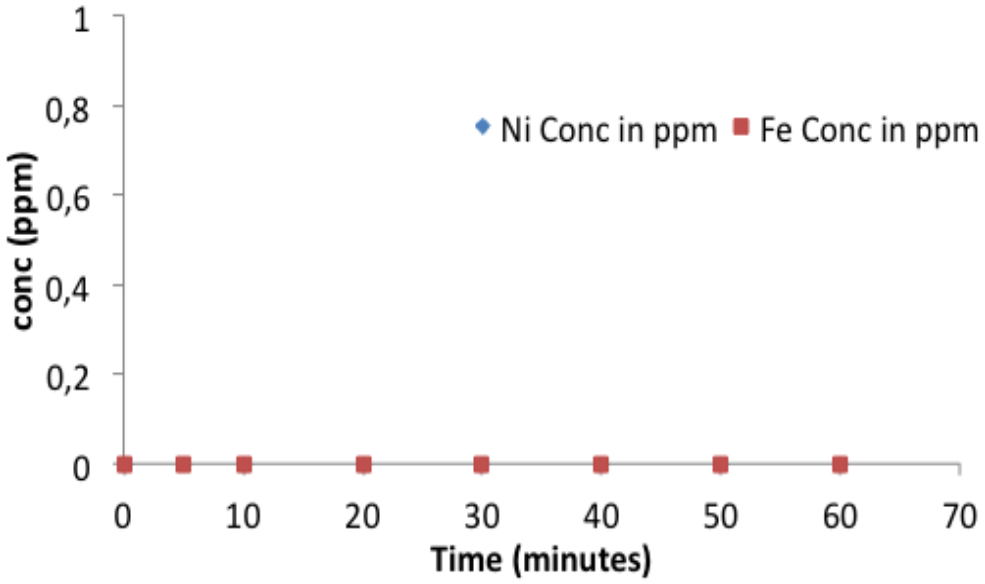

Figure 4.57: Fe and Ni ions in solution during heterogeneous catalysis using β-FeOOH-NiO

4.5.2. Recovery and reuse of catalyst

From an economic point of view, a suitable catalyst must be easily recoverable from solution and capable of being reused in recycle runs. For this purpose, settling and recycle experiments were conducted using β-FeOOH-NiO composite. The settling rate of β-FeOOH-NiO measured as a function of turbidity is compared along side β-FeOOH in Figure 4.58 (a). Pictorial view of reactor post ozonation using both catalysts is presented in Figure 4.58 (b). The composite material settles quickly – within 10 hours - and is easily recovered from solution for reuse. Under the same condition, less than 3% of β-FeOOH had settled. The composite did not require a

filtration process and was collected by simply decanting off the treated 4-chlorophenol solutions. This posses an advantage (compared to β-FeOOH) in view of possible industrial applications. It must however be mentioned that this advantage comes at a compromise. The fact that the composite settles far quicker than β-FeOOH implies that it would need to be kept in suspension via a mechanical means during use. While this would require an additional energy in the economics of the entire process, the cost may be far less than recovering the catalyst via an expensive filtration processes.

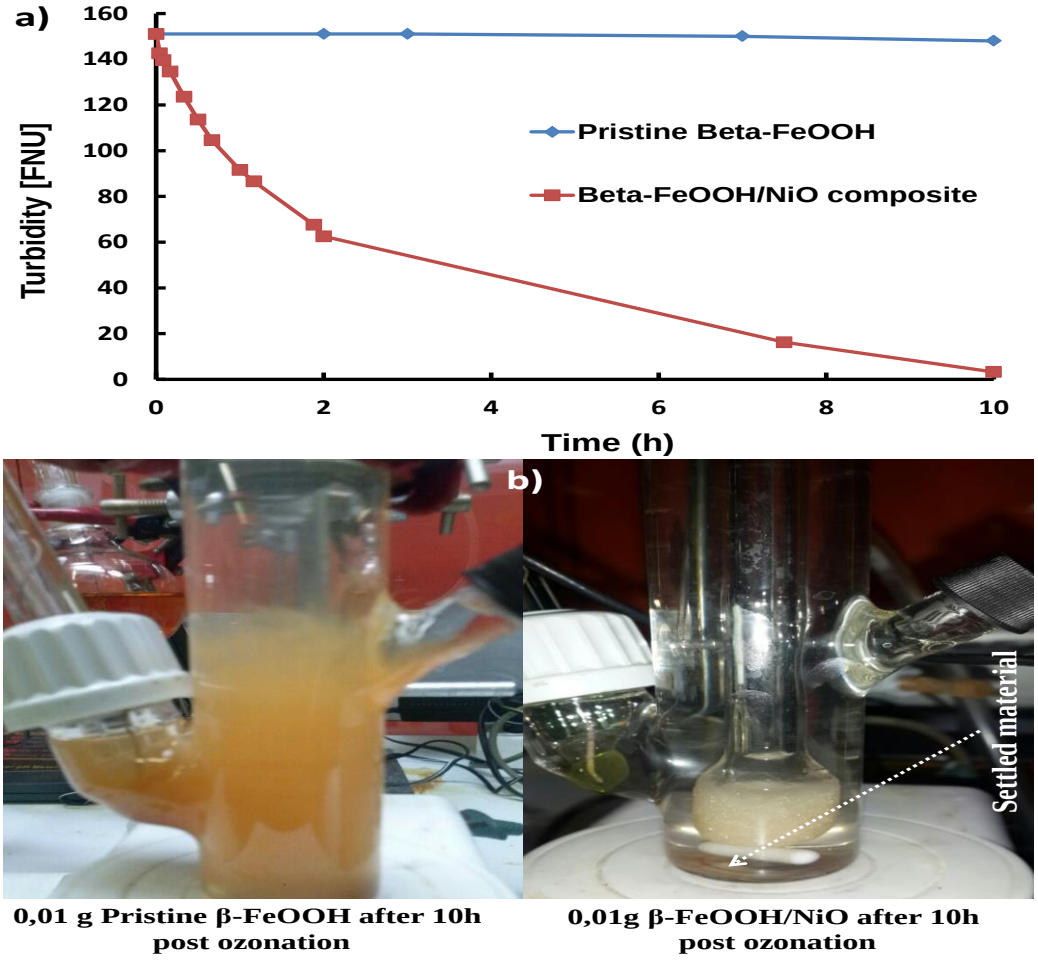

Figure 4.58 (a) Settling rate of β-FeOOH and β-FeOOH-NiO composite over a 10 hour period, (b) reactor conditions after 10 hours post 4-chlorophenol ozonation.

The recovered composite material after decanting was filtered, air-dried and reused for catalytic ozonation in repeated experiments. The entire recycling process was repeated three times, with the catalyst air-dried and reused each time. As shown in Figure 4.59 the removal efficiency of the composite reduced with each cycle. The poisoning of ozonation catalyst has being recently documented (Zhao et al., 2014). The authors proved that the accumulation of low molecular weight acids generated

during the breakdown of the substrate (phenol) led to the poisoning and thus reduction in efficiency of their catalyst-$NiFe_2O_4$ in reuse experiments. Based on such findings, a fourth reuse experiment was conducted after thermal treatment of t β-FeOOH-NiO composite. The objective of the thermal treatment was to burn off low molecular acids, which accumulated on the surface of the composite and thus led to its poisoning. As illustrated in Figure 4.59, the composite is rejuvenated to 92% of its original catalytic activity. We may conclude that the composite may be restored to its original capacity if a preliminary pre-treatment step, necessary to burn off organic poisons, is incorporated in-between recycle applications. The working operation of this novel catalyst has recently been reported (Oputu et al., 2015a)

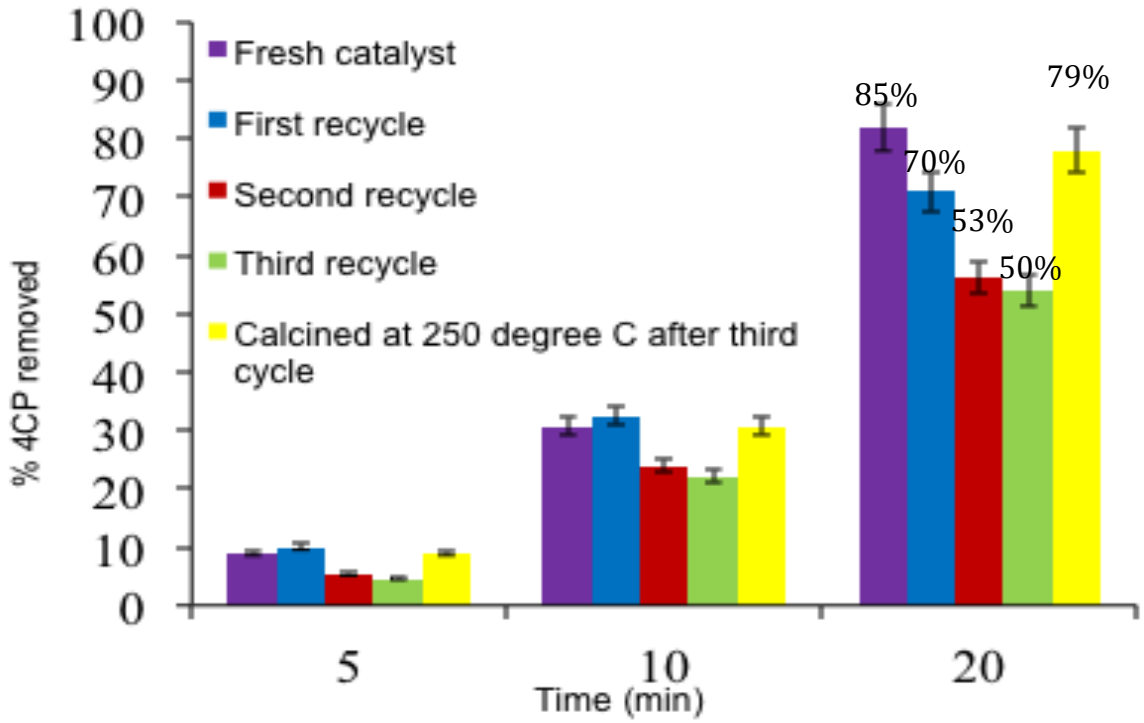

Figure 4.59: Percentage 4-chlorophenol removal using recycled composite

4.6. Testing of composite on wastewater

The paper and pulp industry manages water in the context of a regulatory environment: this requires that all mills must treat water in accordance with the environmental permit. Current treatment protocols applied in the paper industries include sedimentation (in holding tanks) and compacting of alkaline treated wastewater to remove precipitated/coagulated dyes. Sedimentation removes sludge (containing polymers and resins) but does not remove dissolved organics and suspended fibres. Milling plants in Cape Town send their wastewater to the Cape

Town municipality for treatment and purchase the treated water – as industrial water- at a rate lower than domestic water, from the municipality. The process is considered cost effective for the industries due to the expensive process required to treat their wastewater to acceptable surface disposal standards.

Table 4.15 presents the respective physicochemical character of the water samples collected from the companies (NB: COD was measured in-lab). The onsite treatment process of Company 1 is capable of reducing the turbidity and COD of their wastewater by 41% and 17%, respectively. The process however does not completely remove the pink colour from the wastewater. The municipal industrial water had a COD concentration 2000 units below the wastewater generated by Company 2. Results of ozonation of wastewater and municipal industrial water are presented in Figure 4.60 - Figure 4.63. The catalytic ozonation process is capable reducing the COD of wastewater from company 1 by 45% compared to 31% removed by ozonation alone (Figure 4.60) after a three-hour treatment. Similarly, the catalytic process reduces COD of Company 1's onsite treated water by 35% compared to 25% removed by ozonation alone. In both cases, the processes were able to completely remove the pink colour from the solution.

The COD of raw wastewater from Company 2 was reduced by 33% using the catalytic ozonation process compared to 14% removed by simple ozonation alone (Figure 4.62). The higher removal efficiency of the catalytic process may be attributed to the increased generation of hydroxyl radicals in quantities that effect water purification. Industrial water obtained from the municipality was less amenable to both ozonation and catalytic ozonation as shown from the lower COD removals compared to the other wastewater samples. In all cases, the rates of COD removal by catalytic ozonation were higher than that of simple ozonation alone. The higher COD removal efficiency when using the composite as a catalyst in ozonation technology highlights the potential application of the catalyst in industrial water treatment processes. Experiments reported here could not be pursued to complete COD removals, as the stipulated running time of the laboratory ozone generator utilized for this study is 200 minutes. All experiments where therefore halted after 180 minutes.

Table 4.15: Physicochemical character of sampled wastewater and municipal industrial water.* Not determined onsite.

	Company 1		Company 2	
	Waste water	Onsite-treated water	Waste water	Municipal industrial water
Turbidity	13.83	8.12	456	27.48
pH	5.24	5.36	5.79	6.39
Temperature (°C)	18.6	18.5	24.1	17.7
Conductivity (µs)	1.947	2.14	1547	733
TSD (ppt)	1.38	1.50	1.1	0.516
*COD mg O_2/L	2843	2409	2900	1980

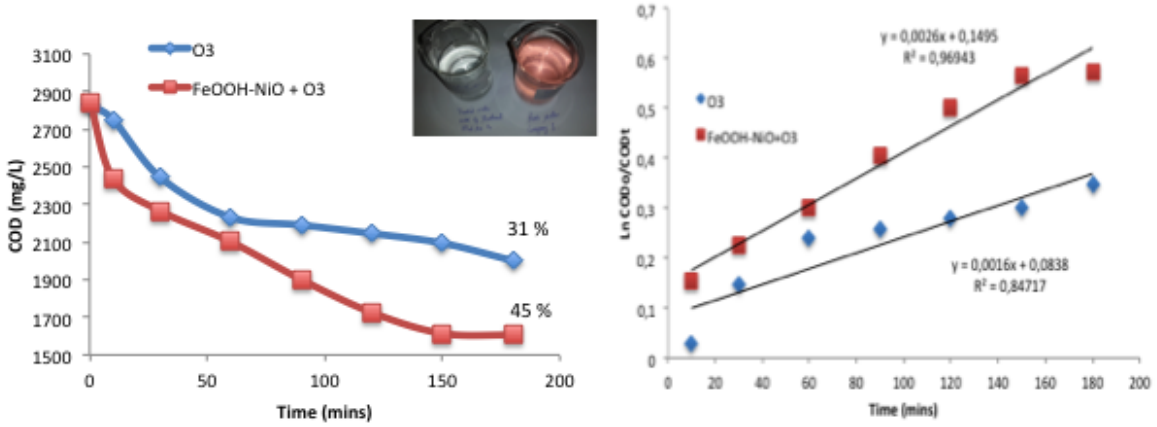

Figure 4.60: COD removal from untreated wastewater from Company 1 by catalysed and uncatalyzed ozonation (inset: picture of raw and ozone treated wastewater). Left: corresponding COD removal rates by both processes

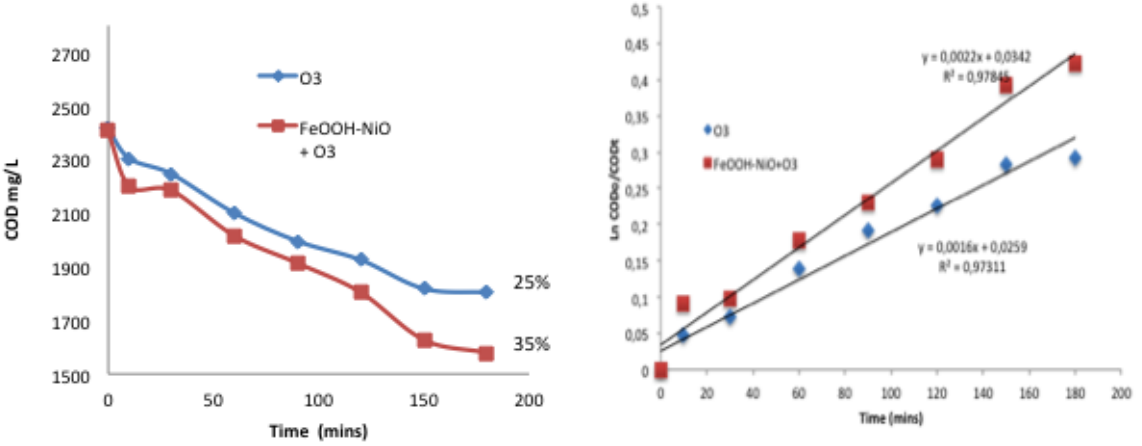

Figure 4.61: COD removal from onsite-treated-wastewater from Company 1 by catalysed and uncatalyzed ozonation. Left: corresponding COD removal rates by both processes

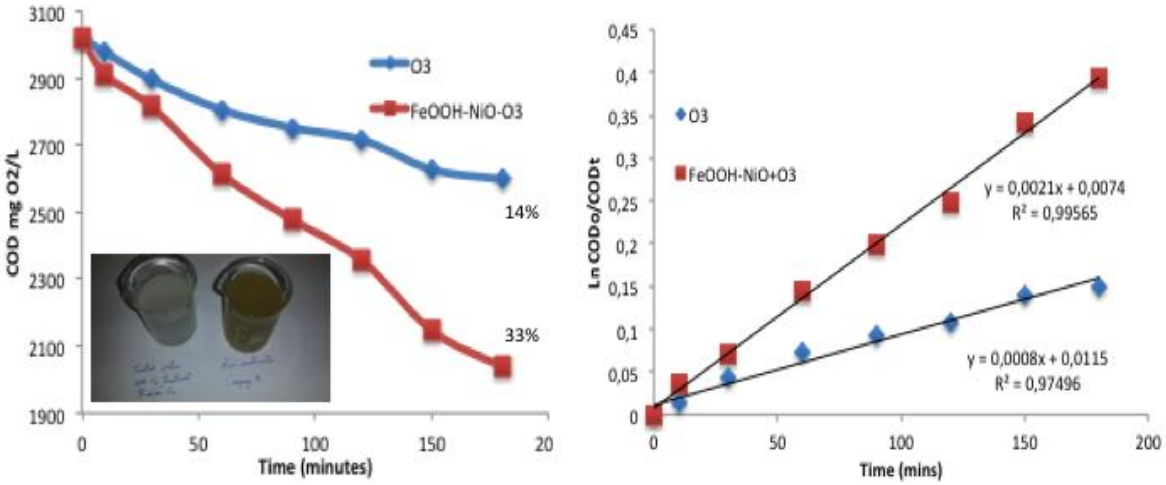

Figure 4.62: COD removal from wastewater from Company 2 by catalysed and uncatalyzed ozonation (inset: picture of raw and ozone treated wastewater). Left: corresponding COD removal rates by both processes

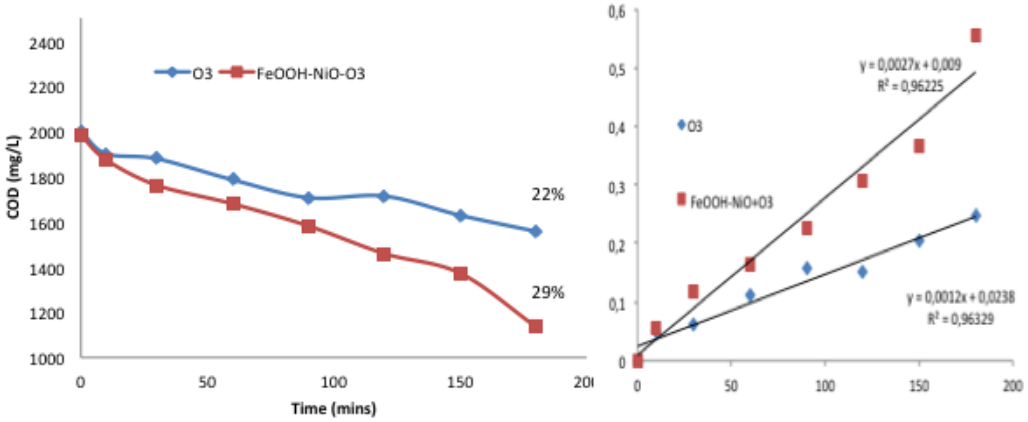

Figure 4.63: COD removal from municipal industrial water collected from Company 1 by catalysed and uncatalyzed ozonation. Left: corresponding COD removal rates by both processes

CHAPTER 5

5. CONCLUSION AND RECOMMENDATION

5.1. CONCLUSION

The amelioration of aqueous solutions of phenol, 2-chlorophenol (2-CP), 4-chlorophenol (4-CP) and 2,4-dichlorophenol (2,4-DCP) by ozone based AOP presented a clear selectivity of the process for the aqueous organic substrate. Compared with some other wastewater technologies, such as chlorination and adsorption on biomass or activated carbon, the method provides a superior procedure for disinfection and removal of organics in water/wastewater. Firstly, the ozonation process followed a first order kinetic pathway for the phenols and chlorophenols, and this increased with increasing pH. Secondly, for all tested pH, the higher chlorinated phenol was more susceptible to degradation by ozone compared to the lower chlorinated phenols. It may, therefore, be inferred that the dechlorination step was crucial in determining the rate of removal of the target chlorophenol. However, the order of selectivity towards ozonation, interpreted from the observed apparent rate constants presented the order: 2,4-DCP > 2-CP > Phenol > 4CP.

Findings from ozonation study as well as arguments from cited literature revealed the rate dependence of the ozonation process on dechlorination of chlorine atoms. Information on the relative contributions of the ortho and para chlorinated atoms on 2CP and 4CP towards the rate of ozonation of mono-chlorinated phenols are scarce in literature. A review of the intermediates obtained during the degradation of phenol and the chlorophenols from this study revealed that catechol and its ring opening products (mechanisms), leading to acrylic acid was a major pathway for phenol and 2-CP while 4-CP followed 4-chlorocatechol pathway (mechanism). Despite the position 2 and position 4 chlorine atoms being on activated points on the phenyl ring, kinetic results from this study showed that the position 2 chlorine atom was more susceptible to hydroxylative dechlorination than the position 4 chlorine atom. This may explain the relative stability of 4-chlorophenol towards ozonation when compared to the ortho isomer, 2-chlorophenol.

Hydrothermally synthesized β-FeOOH nano-rods are presented as suitable catalyst for ozone based degradation of organic substrate. Under optimized conditions, a catalyst load of 0.1 g/L (corresponding to 0.01 % w/w) brought about a 32 % reduction in degradation time, increasing the reaction rate by 148 % in acidic

medium and 56 % in alkaline medium. While the catalyst showed little adsorption characteristics, the increased catalytic behavior is based on its reductive dissolution at acidic pH generating free Fe ions, which initiate homogeneous catalytic break down of ozone to hydroxyl radicals. The kinetic data for the catalytic process was best modeled using a two stage kinetic model with the first and second stage corresponding to heterogeneous and homogeneous catalytic stages, respectively. This novel interpretation of the exact working mechanism of β-oxy-hydroxy-iron during catalytic ozonation is analogous to its behavior in Fenton reactions and may very well be extended to other iron oxide species currently tested as catalyst in ozonation processes.

Three metal oxides were tested as suitable supports for β-FeOOH with a view of suppressing the dissolution of Fe and eventual loss of the catalyst.

Bonding of β-FeOOH on metal oxide supports was done via an organic binder mediated hetero-junction method. An increased bonding concentration of β-FeOOH above 5 % on the support brought about a reduction in catalytic property of the composite material. Hetero-junction support from NiO (β-FeOOH-NiO) gave superior catalytic property when compared to β-FeOOH-TiO_2 and β-FeOOH-Al_2O_3. The catalytic mechanism for bonded iron on metal oxide surface is based on an inter-conversion of iron (II) and iron (III) species. The higher catalytic property of the β-FeOOH-NiO composites may be adduced to the better inter-conversion of the two iron states on nickel (a border-line Lewis acid metal) as opposed to the higher states aluminum and titanium (hard Lewis acid metals). β-FeOOH-NiO composite showed good stability for catalytic ozonation as shown by recycle experiments and was regenerated upon thermal treatment, making it an economically viable catalyst from the practical standpoint.

The composite material presented superior mineralization rates for total organics (measured as COD) when compared to simple ozonation thereby justifying its practical application for water purification purposes. The composite is adduced to function via generation of hydroxyl radicals in quantities superior to ozonation alone, thus effecting a faster water purification process.

Thus the objectives set out for this research project were met.

5.2. RECOMMENDATION

β-FeOOH applied in this study has demonstrated an efficacy in accelerating the kinetics of phenolic compound removal from aqueous solution by promoting the conversion of ozone to hydroxy radicals during the ozonation process. The only apparent drawback for its industrial application was the reductive dissolution of Fe, which was addressed by doping of β-FeOOH on metal oxide supports of which NiO was the most efficient. While the doped catalyst in itself is proposed for possible industrial application in ozonation systems, the recovery of the catalyst still presents an avoidable delay time necessary for catalyst settling. The possibility of filtration for recycling purposes is expensive. It is therefore recommended that more robust supports for the active β-FeOOH be pursued with a view of achieving quick catalyst recovery and shorten recovery times. In this regard, several polymeric supports, which would serve to chelate Fe, while at the same time concentrate organics, would prove advantageous.

6. BIBLIOGRAPHY/REFERENCES

Abdessalem, A. K., Oturan, M. A., Oturan, N., Bellakhal, N. & Dachraoui, M. 2010. Treatment of an aqueous pesticides mixture solution by direct and indirect electrochemical advanced oxidation processes. *International Journal of Environmental Analytical Chemistry,* 90**,** 468-477.

Agilent. 2014. Agilent 6200 Series TOF and 6500 Series Q-TOF LC/MS System; Concepts guide. The big picture. *USA* [Online]. Available: http://cn.agilent.com/cs/library/usermanuals/public/G3335-90173_TOF_Q-TOF_Concepts.pdf.

Ahmed, S., Rasul, M. G., Brown, R. & Hashib, M. A. 2011. Influence of parameters on the heterogeneous photocatalytic degradation of pesticides and phenolic contaminants in wastewater: A short review. *Journal of Environmental Management,* 92**,** 311-330.

Ahmed, S., Rasul, M. G., Martens, W. N., Brown, R. & Hashib, M. A. 2010. Heterogeneous photocatalytic degradation of phenols in wastewater: A review on current status and developments. *Desalination,* 261**,** 3-18.

Akyurtlu, J. F., Akyurtlu, A. & Kovenklioglu, S. 1998. Catalytic oxidation of phenol in aqueous solutions. *Catalysis Today,* 40**,** 343-352.

Al Momani, F. 2007. Degradation of cyanobacteria anatoxin-a by advanced oxidation processes. *Separation and Purification Technology,* 57**,** 85-93.

Alaton, I. A., Balcioglu, I. A. & Bahnemann, D. W. 2002. Advanced oxidation of a reactive dyebath effluent: comparison of O3, H2O2/UV-C and TiO2/UV-A processes. *Water Research,* 36**,** 1143-1154.

An, T., Yang, H., Li, G., Song, W., Cooper, W. J. & Nie, X. 2010. Kinetics and mechanism of advanced oxidation processes (AOPs) in degradation of ciprofloxacin in water. *Applied Catalysis B: Environmental,* 94**,** 288-294.

Andreozzi, R., Caprio, V., Marotta, R. & Radovnikovic, A. 2003. Ozonation and H2O2/UV treatment of clofibric acid in water: a kinetic investigation. *Journal of Hazardous Materials,* 103**,** 233-246.

Arena, F., Italiano, C., Raneri, A. & Saja, C. 2010. Mechanistic and kinetic insights into the wet air oxidation of phenol with oxygen (CWAO) by homogeneous and heterogeneous transition-metal catalysts. *Applied Catalysis B: Environmental,* 99**,** 321-328.

Arslan-Alaton, I. & Koyunluoglu, S. 2007. Ozonation of Two Commercially Important Biocidal Finishing Agents. *Ozone: Science and Engineering,* 29**,** 335-342.

Astm, A. S. F. T. a. M. 1995. *Standard test methods for chemical oxygen demand (dichromate oxygen demand) of water,* Philadelphia, Pa, American Soc. Testing & Materials.

Atkins, P. & De Paula, J. 2006. Atkins' physical chemistry. *Oxford University Press, Oxford*.

Ayoub, K., Van Hullebusch, E. D., Cassir, M. & Bermond, A. 2010. Application of advanced oxidation processes for TNT removal: A review. *Journal of Hazardous Materials,* 178**,** 10-28.

Bader, H. & Hoigné, J. 1981. Determination of ozone in water by the indigo method. *Water Research,* 15**,** 449-456.

Badger, R. M. 1934. A Relation Between Internuclear Distances and Bond Force Constants. *The Journal of Chemical Physics,* 2**,** 128-131.

Bahari Molla Mahaleh, Y., Sadrnezhaad, S. K. & Hosseini, D. 2008. NiO Nanoparticles Synthesis by Chemical Precipitation and Effect of Applied Surfactant on Distribution of Particle Size. *Journal of Nanomaterials,* 2008**,** 4.

Ball, S. L. 2015. The use of phenol as a topical anaesthetic for the tympanic membrane. *Clinical Otolaryngology,* 40**,** 506-506.

Ballesteros Martín, M. M., Sánchez Pérez, J. A., Casas López, J. L., Oller, I. & Malato Rodríguez, S. 2009. Degradation of a four-pesticide mixture by combined photo-Fenton and biological oxidation. *Water Research,* 43**,** 653-660.

Ballesteros Martín, M. M., Sánchez Pérez, J. A., García Sánchez, J. L., Montes De Oca, L., Casas López, J. L., Oller, I. & Malato Rodríguez, S. 2008. Degradation of alachlor and pyrimethanil by combined photo-Fenton and biological oxidation. *Journal of Hazardous Materials,* 155**,** 342-349.

Bandala, E. R., Brito, L. & Pelaez, M. 2009. Degradation of domoic acid toxin by UV-promoted Fenton-like processes in seawater. *Desalination,* 245**,** 135-145.

Bandala, E. R., Peláez, M. A., Salgado, M. J. & Torres, L. 2008. Degradation of sodium dodecyl sulphate in water using solar driven Fenton-like advanced oxidation processes. *Journal of Hazardous Materials,* 151**,** 578-584.

Bandara, J., Klehm, U. & Kiwi, J. 2007. Raschig rings-Fe2O3 composite photocatalyst activate in the degradation of 4-chlorophenol and Orange II under daylight irradiation. *Applied Catalysis B: Environmental,* 76**,** 73-81.

Bauch, H., Burchard, H. & Arsovic, H. M. 1970. Ozone as an Oxidative Disintegrant for Phenols in Aqueous Solutions. *Gesundheit Ingenieur,* 91**,** 258-262.

Beltrán, F. J., Aguinaco, A. & García-Araya, J. F. 2009. Mechanism and kinetics of sulfamethoxazole photocatalytic ozonation in water. *Water Research,* 43**,** 1359-1369.

Beltrán, F. J., Aguinaco, A. & García-Araya, J. F. 2010. Kinetic modelling of TOC removal in the photocatalytic ozonation of diclofenac aqueous solutions. *Applied Catalysis B: Environmental,* 100**,** 289-298.

Benitez, F. J., Acero, J. L., Real, F. J., Roldan, G. & Casas, F. 2011. Comparison of different chemical oxidation treatments for the removal of selected pharmaceuticals in water matrices. *Chemical Engineering Journal,* 168**,** 1149-1156.

Benitez, F. J., Beltran-Heredia, J., Acero, J. L. & Rubio, F. J. 2000a. Contribution of free radicals to chlorophenols decomposition by several advanced oxidation processes. *Chemosphere,* 41**,** 1271-1277.

Benitez, F. J., Beltrán-Heredia, J., Acero, J. L. & Rubio, F. J. 2000b. Rate constants for the reactions of ozone with chlorophenols in aqueous solutions. *Journal of Hazardous Materials,* 79**,** 271-285.

Bertrand, W. & Bouchoux, G. 1998. Keto–enol tautomerism and dissociation of ionized acetaldehyde and vinyl alcohol. A G2 Molecular Orbital Study. *Rapid communications in mass spectrometry,* 12**,** 1697-1700.

Bragg, W. H. & Bragg, W. L. 1913. The Reflection of X-rays by Crystals. Proceedings of the Royal Society A. Mathematical, Physical & Engineering Sciences, 1913. The Royal Society of London.

Brown, J. F., Kulius, J., Thomson, B., Chapman, T. H. & Mawhinney, D. B. 2006. Occurrence of antibiotics in hospital, residential and dairy effluent, municipal wastewater and the Rio Grande in New Mexico. *Science of the Total Environment,* 366**,** 772-783.

Brown, K. & Donnelly, K. 1988. An estimation of the risk associated with the organic constituents of hazardous and municipal waste landfill leachates. *Hazardous waste and hazardous materials,* 5**,** 1-30.

Budavari, S., O'neil, M. J., Smith, A. & Heckelman, P. E. 1989. *The merck index*, Merck Rahway, NJ.

Burcat, A., Khachatryan, L. & Dellinger, B. L. 2003. Thermodynamics of chlorinated phenols, polychlorinated dibenzo-p-dioxins, polychlorinated dibenzofurans, derived radicals, and intermediate species. *Journal of Physical and Chemical Reference Data,* 32**,** 443-518.

Cañizares, P., Paz, R., Sáez, C. & Rodrigo, M. A. 2008. Electrochemical oxidation of alcohols and carboxylic acids with diamond anodes: A comparison with other advanced oxidation processes. *Electrochimica Acta,* 53**,** 2144-2153.

Capponi, M., Gut, I. & Wirz, J. 1986. The Phenol⇌ 2, 4- Cyclohexadienone Equilibrium in Aqueous Solution. *Angewandte Chemie International Edition in English,* 25**,** 344-345.

Castiglioni, S. R., Fanelli, D., Calamari, R. & Bagnati, Z., E. 2004. Methodological approaches for studying pharmaceuticals in the environment by comparing predicted and measured concentrations in river Po, Italy. *Regul. Toxicol. Pharmacol,* 39**,** 25-32.

Catalkaya, E. C. & Kargi, F. 2007. Color, TOC and AOX removals from pulp mill effluent by advanced oxidation processes: A comparative study. *Journal of Hazardous Materials,* 139**,** 244-253.

Çatalkaya, E. Ç. & Sengül, F. 2006. Application of Box-Wilson experimental design method for the photodegradation of bakery's yeast industry with UV/H2O2 and UV/H2O2/Fe(II) process. *Journal of Hazardous Materials,* 128**,** 201-207.

Catorceno, L. L. C., Nogueira, K. R. B. & Teixeira, A. C. S. C. 2010. Treatment of Aqueous Effluents Containing Phenol by the O3, O3-UV, and O3-H2O2 Processes: Experimental Study and Neural Network Modeling. *Separation Science and Technology,* 45**,** 1521-1528.

Centi, G. & Perathoner, S. 2008. Catalysis by layered materials: A review. *Microporous and Mesoporous Materials,* 107**,** 3-15.

Cernigoj, U., Stangar, U. L. & Trebse, P. 2007. Degradation of neonicotinoid insecticides by different advanced oxidation processes and studying the effect of ozone on TiO2 photocatalysis. *Applied Catalysis B: Environmental,* 75**,** 229-238.

Chelme-Ayala, P., El-Din, M. G. & Smith, D. W. 2010. Treatability Study on Membrane Concentrate Containing Pesticides Using Advanced Oxidation Processes. *Ozone: Science & Engineering,* 32**,** 16-24.

Chen, J., Liu, X., Li, G., Nie, X., An, T., Zhang, S. & Zhao, H. 2011. Synthesis and characterization of novel SiO2 and TiO2 co-pillared montmorillonite composite for adsorption and photocatalytic degradation of hydrophobic organic pollutants in water. *Catalysis Today,* 164**,** 364-369.

Chen, X. M., Da Silva, D. R. & Martínez-Huitle, C. A. 2010. Application of advanced oxidation processes for removing salicylic acid from synthetic wastewaters. *Chinese Chemical Letters,* 21**,** 101-104.

Chin, A. & Bérubé, P. R. 2005. Removal of disinfection by-product precursors with ozone-UV advanced oxidation process. *Water Research,* 39**,** 2136-2144.

Choi, K. J., Kim, S. G., Kim, C. W. & Kim, S. H. 2005. Effect of activated carbon types and service life on the removal of endocrine disrupting chemicals: amitrol, nonyphenol and bisphenol A. *Chemosphere.,* 58**,** 1535-1545.

Chou, M.-S. & Chang, K.-L. 2007. Oxidation of Aqueous Dimethyl Sulfoxide (DMSO) Using UV, O3, and UV/O3. *Ozone: Science & Engineering,* 29**,** 391-397.

Chou, S. & Huang, C. 1999. Application of a supported iron oxyhydroxide catalyst in oxidation of benzoic acid by hydrogen peroxide. *Chemosphere,* 38**,** 2719-2731.

Chowdhury, M., Ntiribinyange, M., Nyamayaro, K. & Fester, V. 2015a. Photocatalytic activities of ultra-small β-FeOOH and TiO2 heterojunction structure under simulated solar irradiation. *Materials Research Bulletin,* 68**,** 133-141.

Chowdhury, M., Oputu, O., Kebede, M., Cummings, F., Cespedes, O., Maelsand, A. & Fester, V. 2015b. Rapid and large-scale synthesis of Co3O4 octahedron particles with very high catalytic activity, good supercapacitance and unique magnetic properties. *RSC Advances,* 5**,** 104991-105002.

Chrostowski, P. C., Dietrich, A. M. & Suffet, I. H. 1983. Ozone and oxygen induced oxidative coupling of aqueous phenolics. *Water Research,* 17**,** 1627-1633.

Cmr 2005. PEOPLE & PROFILE - Chemical Profile: Phenol. *Chemical market reporter.,* 267**,** 34.

Coca, M., Peña, M. & González, G. 2005. Chemical Oxidation Processes for Decolorization of Brown-Colored Molasses Wastewater. *Ozone: Science & Engineering,* 27**,** 365-369.

Coca, M., Peña, M. & González, G. 2007. Kinetic study of ozonation of molasses fermentation wastewater. *Journal of Hazardous Materials,* 149**,** 364-370.

Coct. 2006. Water services development plan for City of Cape Town 2006/07. City of Cape Town.

Coct. 2007. Treated effluent re-uses strategy and master planning within the City of Cape Town. BVi Consulting Engineers. BVi Report No. C1500/1.1.

Consejo, C., Ormad, M. P., Sarasa, J. & Ovelleiro, J. L. 2005. Treatment of Wastewater Coming from Painting Processes: Application of Conventional and Advanced Oxidation Technologies. *Ozone: Science & Engineering,* 27**,** 279-286.

Correia, V. M., Stephenson, T. & Judd, S. J. 1994. Characterization of textile wastewater-A review. *Environ. Technol.,* 15**,** 917-929.

Cortés, S., Sarasa, J., Ormad, P., Gracia, R. & Ovelleiro, J. L. 2000. Comparative Efficiency of the Systems O3/High pH And 03/catalyst for the Oxidation of Chlorobenzenes in Water. *Ozone: Science & Engineering,* 22**,** 415-426.

Cortez, S., Teixeira, P., Oliveira, R. & Mota, M. 2011. Evaluation of Fenton and ozone-based advanced oxidation processes as mature landfill leachate pre-treatments. *Journal of Environmental Management,* 92**,** 749-755.

Cowley, J. M. 1995. *Diffraction physics*, Elsevier.

Dai, Q., Wang, J., Chen, J. & Chen, J. 2014. Ozonation catalyzed by cerium supported on activated carbon for the degradation of typical pharmaceutical wastewater. *Separation and Purification Technology,* 127**,** 112-120.

Daughton, C. G. & Ternes, T. A. 1999. Pharmaceutical and personal care products in the environment: agents of subtle change? *Environ. Health Perspect. Suppl.,* 107**,** 907-938.

Debecker, D., Gaigneaux, E. & Busca, G. 2009. Exploring, Tuning, and Exploiting the Basicity of Hydrotalcites for Applications in Heterogeneous Catalysis. *Chemistry--A European Journal,* 15**,** 3920–3935.

Debellefontaine, H. & Foussard, J. N. 2000. Wet air oxidation for the treatment of industrial wastes. Chemical aspects, reactor design and industrial applications in Europe. *Waste Manage.,* 20**,** 15-25.

Devlin, H. R. & Harris, I. J. 1984. Mechanism of the oxidation of aqueous phenol with dissolved oxygen. *Industrial & engineering chemistry fundamentals,* 23**,** 387-392.

Dhandapani, B. & Oyama, S. T. 1997. Gas phase ozone decomposition catalysts. *Applied Catalysis B: Environmental,* 11**,** 129-166.

Dombi, A., Ilisz, I., László, Z. & Wittmann, G. 2002. Comparison of Ozone-based and other (VUV and TiO2/UV) Radical Generation Methods in Phenol Decomposition. *Ozone: Science & Engineering,* 24**,** 49-54.

Dong, S., Zhou, D. & Bi, X. 2010. Liquid phase heterogeneous photocatalytic ozonation of phenol in liquid-solid fluidized bed: Simplified kinetic modeling. *Particuology,* 8**,** 60-66.

Dong, Y., Gao, Z.-L., Li, R.-S., Hu, Y.-M., Dong, H.-S. & Xiea, Z.-X. 2014. RSC Advances.

Dong, Y., Yang, H., He, K., Wu, X. & Zhang, A. 2008. Catalytic activity and stability of Y zeolite for phenol degradation in the presence of ozone. *Applied Catalysis B: Environmental,* 82**,** 163-168.

Doocey, D. J. & Sharratt, P. N. 2004. Zeolite-Mediated Advanced Oxidation of Model Chlorinated Phenolic Aqueous Waste: Part 1: Aqueous Phase Fenton Catalysis. *Process Safety and Environmental Protection,* 82**,** 352-358.

Dore, M. H. 2005. Forecasting the economic costs of desalination technology. *Desalination,* 172**,** 207-214.
Dore, M. H. 2014. *Global Drinking Water Management and Conservation: Optimal Decision-Making*, Springer International Publishing.
Dussert, B. & Van Stone, G. 2000. The biological activation process for water purification. Water and Wastes Digest. Available: http://www.wwdmag.com/desalination/biological-activated-carbon-process-water-purification [Accessed 21 July 2016].
Dwaf. 2004. National water resource strategy. Pretoria: Department of Water Affairs and Forestry.
Eaton, A. D., Clesceri, L. S., Greenberg, A. E., Franson, M. a. H., American Public Health, A., American Water Works, A. & Water Environment, F. 1998. *Standard methods for the examination of water and wastewater,* Washington, DC, American Public Health Association.
Ec 2003. Technical guidance document on risk assessment: Part II. EUR 20418 EN/2. http://publications.jrc.ec.europa.eu/repository/bitstream/111111111/5619/2/EUR 20418 EN-2.pdf. Accessed 11 August 2011.
Eisenhower, H. R. 1968. The Ozonization of Phenolic Wastes. *Journal of the Water Pollution Control Federation,* 40**,** 1887-1899.
Erickson, B. E. 2002. Analyzing the ignored environmental contaminants. *Environ. Sci. Technol.,* 36**,** 140A-145A.
Faludi, T., Balogh, C., Serfőző, Z. & Molnár-Perl, I. 2015. Analysis of phenolic compounds in the dissolved and suspended phases of Lake Balaton water by gas chromatography-tandem mass spectrometry. *Environmental Science and Pollution Research,* 22**,** 11966-11974.
Faouzi, M., Cañizares, P., Gadri, A., Lobato, J., Nasr, B., Paz, R., Rodrigo, M. A. & Saez, C. 2006. Advanced oxidation processes for the treatment of wastes polluted with azoic dyes. *Electrochimica Acta,* 52**,** 325-331.
Fatimah, I., Wang, S., Narsito & Wijaya, K. 2010. Composites of TiO2-aluminum pillared montmorillonite: Synthesis, characterization and photocatalytic degradation of methylene blue. *Applied Clay Science,* 50**,** 588-593.
Fatoki, O. & Opeolu, B. 2009. Studies on the occurrence and quantification of phenolic endocrine disruptors in water. *Scientific Research and Essays,* 4**,** 1415-1422.
Feng, F., Xu, Z., Li, X., You, W. & Zhen, Y. 2010. Advanced treatment of dyeing wastewater towards reuse by the combined Fenton oxidation and membrane bioreactor process. *Journal of Environmental Sciences,* 22**,** 1657-1665.
File, P. D. 1967. Joint committee on powder diffraction standards. *ASTM, Philadelphia, Pa***,** 9-185.
Focazio, M. J., Kolpin, D. W., Barnes, K. K., Furlong, E. T., Meyer, M. T., Zaugg, S. D., Barber, L. B. & Thurman, M. E. 2008. A national reconnaissance for pharmaceuticals and other organic wastewater contaminants in the United States -- II) Untreated drinking water sources. *Science of The Total Environment,* 402**,** 201-216.
Fontanier, V., Farines, V., Albet, J., Baig, S. & Molinier, J. 2005. Oxidation of organic pollutants of water to mineralization by catalytic ozonation. *Ozone: Science and Engineering,* 27**,** 115-128.
Fritzmann, C., Löwenberg, J., Wintgens, T. & Melin, T. 2007. State-of-the-art of reverse osmosis desalination. *Desalination,* 216**,** 1-76.
Fukuhara, T., Iwasaki, S., Kawashima, M., Shinohara, O. & Abe, I. 2006. Adsorbility of estrone and 17-β estradiol in water onto activated carbon. *Water Research,* 40**,** 241-248.
Gadosy, T. A. & Mcclelland, R. A. 1996. The keto/enol equilibrium of phenol. An ab initio investigation. *Journal of Molecular Structure: THEOCHEM,* 369**,** 1-8.

Garcia, J., Gomes, H. T., Serp, P., Kalck, P., Figueiredo, J. L. & Faria, J. L. 2005. Platinum catalysts supported on MWNT for catalytic wet air oxidation of nitrogen containing compounds. *Catalysis Today,* 102-103**,** 101-109.

García-Molina, V., López-Arias, M., Florczyk, M., Chamarro, E. & Esplugas, S. 2005. Wet peroxide oxidation of chlorophenols. *Water Research,* 39**,** 795-802.

Gaya, U. I., Abdullah, A. H., Zainal, Z. & Hussein, M. Z. 2010. Photocatalytic degradation of 2, 4-dichlorophenol in irradiated aqueous ZnO suspension. *International Journal of Chemistry,* 2**,** 180.

Gerrity, D., Stanford, B. D., Trenholm, R. A. & Snyder, S. A. 2010. An evaluation of a pilot-scale nonthermal plasma advanced oxidation process for trace organic compound degradation. *Water Research,* 44**,** 493-504.

Gilliom, R. J., Barbash, J. E., Koplin, D. W. & Larson, S. J. 1999. Testing water quality for pesticide pollution. *Environ. Sci. Technol.,* 33**,** 164-169.

Glaze, W. H., Kang, J.-W. & Chapin, D. H. 1987. The Chemistry of Water Treatment Processes Involving Ozone, Hydrogen Peroxide and Ultraviolet Radiation. *Ozone: Science & Engineering,* 9**,** 335-352.

Goerlitz, D. F., Troutman, D. E., Godsy, E. M. & Franks, B. J. 1985. Migration of wood-preserving chemicals in contaminated groundwater in a sand aquifer at Pensacola, Florida. *Environmental Science & Technology,* 19**,** 955-961.

Gomez, M. J., Bruneau, C., Soyer, N. & Brault, A. 1988. Thermal degradation of chlorophenoxy acid herbicides. *Journal of Agricultural and Food Chemistry,* 36**,** 649-653.

Gould, J. P. & Weber, W. J. 1976. Oxidation of Phenols by Ozone. *Journal of the Water Pollution Control Federation,* 48**,** 47-60.

Gracia, R., Cortes, S., Sarasa, J., Ormad, P. & Ovelleiro, J. 2000. Heterogeneous catalytic ozonation with supported titanium dioxide in model and natural waters. *Ozone: science & engineering,* 22**,** 461-471.

Grafias, P., Xekoukoulotakis, N. P., Mantzavinos, D. & Diamadopoulos, E. 2010. Pilot treatment of olive pomace leachate by vertical-flow constructed wetland and electrochemical oxidation: An efficient hybrid process. *Water Research,* 44**,** 2773-2780.

Gültekin, I. & Ince, N. H. 2007. Synthetic endocrine disruptors in the environment and water remediation by advanced oxidation processes. *Journal of Environmental Management,* 85**,** 816-832.

Guwy, A. J., Buckland, H., Hawkes, F. R. & Hawkes, D. L. 1998. Active biomass in activated sludge: Comparison of respirometry with catalase activity measured using an on-line monitor. *Water Research,* 32**,** 3705-3709.

Guwy, A. J., Martin, S. R., Hawkes, F. R. & Hawkes, D. L. 1999. Catalase activity measurements in suspended aerobic biomass and soil samples. *Enzyme and Microbial Technology,* 25**,** 669-676.

He, Z., Lin, L., Song, S., Xia, M., Xu, L., Ying, H. & Chen, J. 2008. Mineralization of C.I. Reactive Blue 19 by ozonation combined with sonolysis: Performance optimization and degradation mechanism. *Separation and Purification Technology,* 62**,** 376-381.

He, Z., Song, S., Xia, M., Qiu, J., Ying, H., Lü, B., Jiang, Y. & Chen, J. 2007. Mineralization of C.I. Reactive Yellow 84 in aqueous solution by sonolytic ozonation. *Chemosphere,* 69**,** 191-199.

Heller, A. 1995. Chemistry and Applications of Photocatalytic Oxidation of Thin Organic Films. *Accounts of Chemical Research,* 28**,** 503-508.

Hirvonen, A., Trapido, M., Hentunen, J. & Tarhanen, J. 2000. Formation of hydroxylated and dimeric intermediates during oxidation of chlorinated phenols in aqueous solution. *Chemosphere,* 41**,** 1211-1218.

Hoekstra, E. J., De Weerd, H., De Leer, E. W. B. & Brinkman, U. a. T. 1999. Natural Formation of Chlorinated Phenols, Dibenzo-p-dioxins, and Dibenzofurans in Soil of a Douglas Fir Forest. *Environmental Science & Technology,* 33**,** 2543-2549.

Hofmann, J., Freier, U., Wecks, M. & Demund, A. 2005. Degradation of halogenated organic compounds in ground water by heterogeneous catalytic oxidation with hydrogen peroxide. *Topics in Catalysis,* 33**,** 243-247.

Hoigné, J. 1997. Inter-calibration of OH radical sources and water quality parameters. *Water Science and Technology,* 35**,** 1-8.

Hoigné, J. 1998. Chemistry of Aqueous Ozone and Transformation of Pollutants by Ozonation and Advanced Oxidation Processes. *In:* HRUBEC, J. (ed.) *Quality and Treatment of Drinking Water II.* Berlin, Heidelberg: Springer Berlin Heidelberg.

Hoigné, J. & Bader, H. 1983a. Rate constants of reactions of ozone with organic and inorganic compounds in water—I. *Water Research,* 17**,** 173-183.

Hoigné, J. & Bader, H. 1983b. Rate constants of reactions of ozone with organic and inorganic compounds in water—II. *Water Research,* 17**,** 185-194.

Hoigné, J., Bader, H., Haag, W. R. & Staehelin, J. 1985. Rate constants of reactions of ozone with organic and inorganic compounds in water—III. Inorganic compounds and radicals. *Water Research,* 19**,** 993-1004.

Hong, R. Y., Li, J. H., Chen, L. L., Liu, D. Q., Li, H. Z., Zheng, Y. & Ding, J. 2009. Synthesis, surface modification and photocatalytic property of ZnO nanoparticles. *Powder Technology,* 189**,** 426-432.

Hoppin, J. A., Tolbert, P. E., Herrick, R. F., Freedman, D. S., Ragsdale, B. D., Horvat, K. R. & Brann, E. A. 1998. Occupational Chlorophenol Exposure and Soft Tissue Sarcoma Risk among Men Aged 30-60 Years. *American Journal of Epidemiology,* 148**,** 693-703.

Horikoshi, S., Kajitani, M., Sato, S. & Serpone, N. 2007. A novel environmental risk-free microwave discharge electrodeless lamp (MDEL) in advanced oxidation processes: Degradation of the 2,4-D herbicide. *Journal of Photochemistry and Photobiology, A: Chemistry,* 189**,** 355-363.

Huang, C.-R. & Shu, H.-Y. 1995. The reaction kinetics, decomposition pathways and intermediate formations of phenol in ozonation, UV/O3 and UV/H2O2 processes. *Journal of Hazardous Materials,* 41**,** 47-64.

Huang, R., Lan, B., Chen, Z., Yan, H., Zhang, Q., Bing, J. & Li, L. 2012. Catalytic ozonation of p-chlorobenzoic acid over MCM-41 and Fe loaded MCM-41. *Chemical Engineering Journal,* 180**,** 19-24.

Huang, Y.-H., Huang, Y.-F., Chang, P.-S. & Chen, C.-Y. 2008. Comparative study of oxidation of dye-Reactive Black B by different advanced oxidation processes: Fenton, electro-Fenton and photo-Fenton. *Journal of Hazardous Materials,* 154**,** 655-662.

Hugo, W. 1977. Phenols: a review of their history and development as antimicrobial agents. *Microbios,* 23**,** 83-85.

Ikematsu, T., Hayashi, N., Ihara, S., Satoh, S. & Yamabe, C. 2004. Advanced oxidation processes (AOPs) assisted by excimer lamp. *Vacuum,* 73**,** 579-582.

Imamura, S., Ikebata, M., Ito, T. & Ogita, T. 1991. Decomposition of ozone on a silver catalyst. *Industrial & Engineering Chemistry Research,* 30**,** 217-221.

Jamil, T. S., Ghaly, M. Y., El-Seesy, I. E., Souaya, E. R. & Nasr, R. A. 2011. A comparative study among different photochemical oxidation processes to enhance the biodegradability of paper mill wastewater. *Journal of Hazardous Materials,* 185**,** 353-358.

Javier Benitez, F., Acero, J. L. & Real, F. J. 2002. Degradation of carbofuran by using ozone, UV radiation and advanced oxidation processes. *Journal of Hazardous Materials,* 89**,** 51-65.

Jay, K. & Stieglitz, L. 1995. Identification and quantification of volatile organic components in emissions of waste incineration plants. *Chemosphere,* 30**,** 1249-1260.

Jeong, J., Jung, J., Cooper, W. J. & Song, W. 2010a. Degradation mechanisms and kinetic studies for the treatment of X-ray contrast media compounds by advanced oxidation/reduction processes. *Water Research,* 44**,** 4391-4398.

Jeong, J., Song, W., Cooper, W. J., Jung, J. & Greaves, J. 2010b. Degradation of tetracycline antibiotics: Mechanisms and kinetic studies for advanced oxidation/reduction processes. *Chemosphere,* 78**,** 533-540.

Ji, Y., Yang, Z., Ji, X., Huang, W., Feng, X., Liu, C., Lu, L. & Lu, X. 2009. Thermodynamic study on the reactivity of trace organic contaminant with the hydroxyl radicals in waters by advanced oxidation processes. *Fluid Phase Equilibria,* 277**,** 15-19.

Jing, Y., Li, L., Zhang, Q., Lu, P., Liu, P. & Lü, X. 2011. Photocatalytic ozonation of dimethyl phthalate with TiO2 prepared by a hydrothermal method. *Journal of Hazardous Materials,* 189**,** 40-47.

Jonathan, S. Y., Michele, C. H., Gunther, F. C., Vincent, H., Virginia, R., Patricia, A. Y., Lauri, A. H., Nicole, T. A., Rebecca, L. C., Sharon, L. R. & Michael , J. B. 2008. Surveillance for Waterborne Disease and Outbreaks Associated with Recreational Water Use and Other Aquatic Facility-Associated Health Events - United States, 2005-2006. *In:* SERVICES, D. O. H. A. H. (ed.). 1600 Clifton Rd, MailStop E-90, Atlanta, GA 30333, U.S.A: US.Gov.

José, H. J., Gebhardt, W., Moreira, R. F. P. M., Pinnekamp, J. & Schröder, H. F. 2010. Advanced Oxidation Processes for the Elimination of Drugs Resisting Biological Membrane Treatment. *Ozone: Science & Engineering,* 32**,** 305-312.

Julcour Lebigue, C., Andriantsiferana, C., N'guessan, K., Ayral, C., Mohamed, E., Wilhelm, A.-M., Delmas, H., Le Coq, L., Gerente, C., Smith, K. M., Pullket, S., Fowler, G. D. & Graham, N. J. D. 2010. Application of sludge-based carbonaceous materials in a hybrid water treatment process based on adsorption and catalytic wet air oxidation. *Journal of Environmental Management,* 91**,** 2432-2439.

Junk, G. A., Richard, J. J., Avery, M. J., Vick, R. D. & Norton, G. A. 1986. Organic Compounds from Coal Combustion. *Fossil Fuels Utilization.* American Chemical Society.

Kannan, S., Dubey, A. & Knozinger, H. 2005. Synthesis and characterization of CuMgAl ternary hydrotalcites as catalysts for the hydroxylation of phenol. *Journal of Catalysis,* 231**,** 381-392.

Karagiannis, I. C. & Soldatos, P. G. 2008. Water desalination cost literature: review and assessment. *Desalination,* 223**,** 448-456.

Karamanis, D., Ökte, A. N., Vardoulakis, E. & Vaimakis, T. 2011. Water vapor adsorption and photocatalytic pollutant degradation with TiO2-sepiolite nanocomposites. *Applied Clay Science,* 53**,** 181-187.

Kasprzyk-Hordern, B., Ziółek, M. & Nawrocki, J. 2003. Catalytic ozonation and methods of enhancing molecular ozone reactions in water treatment. *Applied Catalysis B: Environmental,* 46**,** 639-669.

Kestioglu, K., Yonar, T. & Azbar, N. 2005. Feasibility of physico-chemical treatment and Advanced Oxidation Processes (AOPs) as a means of pretreatment of olive mill effluent (OME). *Process Biochemistry,* 40**,** 2409-2416.

Kim, K.-H. & Ihm, S.-K. 2011. Heterogeneous catalytic wet air oxidation of refractory organic pollutants in industrial wastewaters: A review. *Journal of Hazardous Materials,* 186**,** 16-34.

Kirkland, E. J. 2010. *Advanced computing in electron microscopy*, Springer Science & Business Media.

Klavarioti, M., Mantzavinos, D. & Kassinos, D. 2009. Removal of residual pharmaceuticals from aqueous systems by advanced oxidation processes. *Environment International,* 35**,** 402-417.

Krijgsheld, K. R. & Van Der Gen, A. 1986. Assessment of the impact of the emission of certain organochlorine compounds on the aquatic environment. *Chemosphere,* 15**,** 825-860.

Kuo, C. & Huang, C. H. 1995. Aqueous phase ozonation of chlorophenols. *Journal of Hazardous Materials,* 41**,** 31-45.

Kusvuran, E. & Erbatur, O. 2004. Degradation of aldrin in adsorbed system using advanced oxidation processes: comparison of the treatment methods. *Journal of Hazardous Materials,* 106**,** 115-125.

Kusvuran, E., Gulnaz, O., Irmak, S., Atanur, O. M., Ibrahim Yavuz, H. & Erbatur, O. 2004. Comparison of several advanced oxidation processes for the decolorization of Reactive Red 120 azo dye in aqueous solution. *Journal of Hazardous Materials,* 109**,** 85-93.

Lachheb, H., Ammar Houas, A. & Herrmann, J. 2008. Photocatalytic Degradation of Polynitrophenols on Various Commercial Suspended or Deposited Titania Catalysts Using Artificial and Solar Light. *International Journal of Photoenergy,* 2008**,** 1-9.

Larachi, F. 2005. Catalytic wet oxidation: micro-meso-macro methodology from catalyst synthesis to reactor design. *Topics in Catalysis,* 33**,** 109-134.

Le, H. T., Flammang, R., Gerbaux, P., Bouchoux, G. & Nguyen, M. T. 2001. Ionized Phenol and Its Isomers in the Gas Phase. *The Journal of Physical Chemistry A,* 105**,** 11582-11592.

Ledakowicz, S., Michniewicz, M., Jagiella, A., Stufka-Olczyk, J. & Martynelis, M. 2006. Elimination of resin acids by advanced oxidation processes and their impact on subsequent biodegradation. *Water Research,* 40**,** 3439-3446.

Ledakowicz, S., Solecka, M. & Zylla, R. 2001. Biodegradation, decolourisation and detoxification of textile wastewater enhanced by advanced oxidation processes. *Journal of Biotechnology,* 89**,** 175-184.

Levec, J. & Pintar, A. 2007. Catalytic wet-air oxidation processes: A review. *Catalysis Today,* 124**,** 172-184.

Li, B. & Cao, H. 2011. ZnO@graphene composite with enhanced performance for the removal of dye from water. *Journal of Materials Chemistry,* 21**,** 3346-3349.

Li, L., Chen, P. & Gloyna, E. F. 1991. Generalized kinetic model for wet oxidation of organic compounds. *AIChE Journal,* 37**,** 1687–1697.

Li, S., Ma, X., Liu, L. & Cao, X. 2015. Degradation of 2, 4-dichlorophenol in wastewater by low temperature plasma coupled with TiO 2 photocatalysis. *RSC Advances,* 5**,** 1902-1909.

Liou, M.-J., Lu, M.-C. & Chen, J.-N. 2003. Oxidation of explosives by Fenton and photo-Fenton processes. *Water Research,* 37**,** 3172-3179.

Liu, L., Chen, F. & Yang, F. 2009. Stable photocatalytic activity of immobilized Fe 0/TiO 2/ACF on composite membrane in degradation of 2, 4-dichlorophenol. *Separation and Purification Technology,* 70**,** 173-178.

Ma, J., Sui, M.-H., Chen, Z.-L. & Wang, L.-N. 2004. Degradation of Refractory Organic Pollutants by Catalytic Ozonation—Activated Carbon and Mn-Loaded Activated Carbon as Catalysts. *Ozone: Science & Engineering,* 26**,** 3-10.

Madhavan, J., Grieser, F. & Ashokkumar, M. 2010a. Degradation of orange-G by advanced oxidation processes. *Ultrasonics Sonochemistry,* 17**,** 338-343.

Madhavan, J., Kumar, P. S. S., Anandan, S., Zhou, M., Grieser, F. & Ashokkumar, M. 2010b. Ultrasound assisted photocatalytic degradation of diclofenac in an aqueous environment. *Chemosphere,* 80**,** 747-752.

Mallevialle, J. 1975. Action of Ozone in the Degradation of Simple and Polymeric Phenolic Compounds-Application to Humic Materials Contained in Waters. *T.S.M. l'Eau,* 70**,** 107-113.

Mandal, T., Maity, S., Dasgupta, D. & Datta, S. 2010. Advanced oxidation process and biotreatment: Their roles in combined industrial wastewater treatment. *Desalination,* 250**,** 87-94.

Mark, G., Tauber, A., Laupert, R., Schuchmann, H.-P., Schulz, D., Mues, A. & Von Sonntag, C. 1998. OH-radical formation by ultrasound in aqueous solution – Part II: Terephthalate and Fricke dosimetry and the influence of various conditions on the sonolytic yield. *Ultrasonics Sonochemistry,* 5**,** 41-52.

Marken, F., Tsai, Y.-C., Coles, B. A., Matthews, S. L. & Compton, R. G. 2000. Microwave activation of electrochemical processes: convection, thermal gradients and hot spot formation at the electrode|solution interface. *New Journal of Chemistry,* 24**,** 653-658.

Mascolo, G., Ciannarella, R., Balest, L. & Lopez, A. 2008. Effectiveness of UV-based advanced oxidation processes for the remediation of hydrocarbon pollution in the groundwater: A laboratory investigation. *Journal of Hazardous Materials,* 152**,** 1138-1145.

Matsuura, T. & Omura, K. 1966. The hydroxylation of phenols by the photolysis of hydrogen peroxide in aqueous media. *Chemical Communications (London)***,** 127-128.

Mcdonnell, G. & Russell, A. D. 1999. Antiseptics and Disinfectants: Activity, Action, and Resistance. *Clinical Microbiology Reviews,* 12**,** 147-179.

Méndez-Arriaga, F., Torres-Palma, R. A., Pétrier, C., Esplugas, S., Gimenez, J. & Pulgarin, C. 2009. Mineralization enhancement of a recalcitrant pharmaceutical pollutant in water by advanced oxidation hybrid processes. *Water Research,* 43**,** 3984-3991.

Michael, E. & St. Louis, M. D. 1988. Water-Related Disease Outbreaks, 1985. *In:* SERVICES, D. O. H. A. H. (ed.). 1600 Clifton Rd, MailStop E-90, Atlanta, GA 30333, U.S.A: US.GOV.

Michałowicz, J. & Duda, W. 2007. Phenols—sources and toxicity. *Polish Journal of Environmental Studies,* 16**,** 347-362.

Mikulová, J., Rossignol, S., Barbier Jr, J., Mesnard, D., Kappenstein, C. & Duprez, D. 2007. Ruthenium and platinum catalysts supported on Ce, Zr, Pr-O mixed oxides prepared by soft chemistry for acetic acid wet air oxidation. *Applied Catalysis B: Environmental,* 72**,** 1-10.

Moreira Dos Santos, C. Y., De Almeida Azevedo, D. & De Aquino Neto, F. R. 2004. Atmospheric distribution of organic compounds from urban areas near a coal-fired power station. *Atmospheric Environment,* 38**,** 1247-1257.

Morrison, R. & Boyd, R. 1992. Organic Chemistry, 6th. Englewood Cliffs, NJ: Prentice Hall.

Mortimer, J. V. Liquid chromatography discussion group session. *In:* LITTLE-WOOD, ed. Gas chromatography 1966 (Rome Symposium), 1967. Institute of Petroleum, London, 414.

Muñoz, I., Rieradevall, J., Torrades, F., Peral, J. & Domènech, X. 2006. Environmental assessment of different advanced oxidation processes applied to a bleaching Kraft mill effluent. *Chemosphere,* 62**,** 9-16.

Munter, R. 2001. Advanced oxidation processes – current status and prospects. *Proceedings of the Estonian Academy of Sciences. Chemistry,* 50**,** 59-80.

Muruganandham, M. & Swaminathan, M. 2007. Solar driven decolourisation of Reactive Yellow 14 by advanced oxidation processes in heterogeneous and homogeneous media. *Dyes and Pigments,* 72**,** 137-143.

Muruganandham, M. & Wu, J. J. 2007. Granular α-FeOOH – A stable and efficient catalyst for the decomposition of dissolved ozone in water. *Catalysis Communications,* 8**,** 668-672.

Ni, C. H. & Chen, J. N. 2001. Heterogeneous catalytic ozonation of 2-chlorophenol queous solution with alumina as a catalyst. *Water Science and Technology,* 43**,** 213-220.

Nishikawa, M., Mitani, Y. & Nosaka, Y. 2012. Photocatalytic Reaction Mechanism of Fe(III)-Grafted TiO2 Studied by Means of ESR Spectroscopy and Chemiluminescence Photometry. *The Journal of Physical Chemistry C,* 116**,** 14900-14907.

Öberg, T., Warman, K. & Bergström, J. 1989. Proceedings of the Eight International Symposium Production of chlorinated aromatics in the post-combustion zone and boiler. *Chemosphere,* 19**,** 317-322.

Ökte, A. N. & Yilmaz, Ö. 2009. La and Ce loaded TiO2-ZSM-5 catalysts: Comparative characterization and photocatalytic activity investigations. *Microporous and Mesoporous Materials,* 126**,** 245-252.

Oller, I., Malato, S. & Sanchez-Perez, J. A. 2010. Combination of advanced oxidation processes and biological treatments for wastewater decontamination- A review. *Science of the Total Environment,* Article in press.

Olmez-Hanci, T., Dalmaz, B., Arslan-Alaton, I., Kabdaşlı, I. & Tünay, O. 2010. Kinetic Modeling and Toxicity Assessment of Diethyl Phthalate Treated by H2O2/UV-C Process. *Ozone: Science & Engineering,* 32**,** 238-243.

Olorundare, O. F., Msagati, T. a. M., Krause, R. W. M., Okonkwo, J. O. & Mamba, B. B. 2015. Preparation and use of maize tassels' activated carbon for the adsorption of phenolic compounds in environmental waste water samples. *Environmental Science and Pollution Research,* 22**,** 5780-5792.

Olujimi, O. O., Fatoki, O. S., Odendaal, J. P. & Daso, A. P. 2012. Chemical monitoring and temporal variation in levels of endocrine disrupting chemicals (priority phenols and phthalate esters) from selected wastewater treatment plant and freshwater systems in Republic of South Africa. *Microchemical Journal,* 101**,** 11-23.

Oputu, O., Chowdhury, M., Nyamayaro, K., Cummings, F., Fester, V. & Fatoki, O. 2015a. A novel [small beta]-FeOOH/NiO composite material as a potential catalyst for catalytic ozonation degradation of 4-chlorophenol. *RSC Advances,* 5**,** 59513-59521.

Oputu, O., Chowdhury, M., Nyamayaro, K., Fatoki, O. & Fester, V. 2015b. Catalytic activities of ultra-small β-FeOOH nanorods in ozonation of 4-chlorophenol. *Journal of Environmental Sciences,* 35**,** 83-90.

Oputu, O. U., Ayanda, O. S., Fatoki, O. S., Akintayo, C. O., Olumayede, E. G. & Amodu, O. S. 2015c. Water Treatment Technologies: Principles, Applications, Successes and Limitations of Bioremediation, Membrane Bioreactor and the Advanced Oxidation Processes. *In:* AYANDA, O. S. (ed.). OMICS ebooks group.

Paasivirta, J., Heinola, K., Humppi, T., Karjalainen, A., Knuutinen, J., Mäntykoski, K., Paukku, R., Piilola, T., Surma-Aho, K. & Tarhanen, J. 1985. Polychlorinated phenols, guaiacols and catechols in environment. *Chemosphere,* 14**,** 469-491.

Pal, B., Sharon, M. & Nogami, G. 1999. Preparation and characterization of TiO2/Fe2O3 binary mixed oxides and its photocatalytic properties. *Materials Chemistry and Physics,* 59**,** 254-261.

Pálfi, T., Wojnárovits, L. & Takács, E. 2011. Mechanism of azo dye degradation in Advanced Oxidation Processes: Degradation of Sulfanilic Acid Azochromotrop and its parent compounds in aqueous solution by ionizing radiation. *Radiation Physics and Chemistry,* 80**,** 462-470.

Papoulis, D., Komarneni, S., Nikolopoulou, A., Tsolis-Katagas, P., Panagiotaras, D., Kacandes, H. G., Zhang, P., Yin, S., Sato, T. & Katsuki, H. 2010. Palygorskite- and Halloysite-TiO2 nanocomposites: Synthesis and photocatalytic activity. *Applied Clay Science,* 50**,** 118-124.

Park, J.-S., Choi, H. & Cho, J. 2004. Kinetic decomposition of ozone and para-chlorobenzoic acid (pCBA) during catalytic ozonation. *Water Research,* 38**,** 2285-2292.

Parkhurst, B., Bradshaw, A., Forte, J. & Wright, G. 1979. An evaluation of the acute toxicity to aquatic biota of a coal conversion effluent and its major components. *Bulletin of Environmental Contamination and Toxicology,* 23**,** 349-356.

Pham, T. T. H., Brar, S. K., Tyagi, R. D. & Surampalli, R. Y. 2010. Optimization of Fenton oxidation pre-treatment for B. thuringiensis - Based production of value added products from wastewater sludge. *Journal of Environmental Management,* 91**,** 1657-1664.

Pimentel, M., Oturan, N., Dezotti, M. & Oturan, M. A. 2008. Phenol degradation by advanced electrochemical oxidation process electro-Fenton using a carbon felt cathode. *Applied Catalysis B: Environmental,* 83**,** 140-149.

Pistonesi, M. F., Di Nezio, M. S., Centurión, M. E., Palomeque, M. E., Lista, A. G. & Fernández Band, B. S. 2006. Determination of phenol, resorcinol and hydroquinone in air samples by synchronous fluorescence using partial least-squares (PLS). *Talanta,* 69**,** 1265-1268.

Poyatos, J., Muñio, M., Almecija, M., Torres, J., Hontoria, E. & Osorio, F. 2010. Advanced Oxidation Processes for Wastewater Treatment: State of the Art. *Water, Air, & Soil Pollution,* 205**,** 187-204.

Prado, J. & Esplugas, S. 1999. Comparison of Different Advanced Oxidation Processes Involving Ozone to Eliminate Atrazine. *Ozone: Science & Engineering,* 21**,** 39-52.

Prato-Garcia, D., Vasquez-Medrano, R. & Hernandez-Esparza, M. 2009. Solar photoassisted advanced oxidation of synthetic phenolic wastewaters using ferrioxalate complexes. *Solar Energy,* 83**,** 306-315.

Qiu, Y., Kuo, C.-H. & Zappi, M. E. 2002. Ozonation kinetics of six dichlorophenol isomers. *Ozone: science & engineering,* 24**,** 123-131.

Qiu, Y., Kuo, C.-H., Zappi, M. E. & Fleming, E. C. 2004. Ozonation of 2, 6-, 3, 4-, and 3, 5-dichlorophenol isomers within aqueous solutions. *Journal of Environmental Engineering,* 130**,** 408-416.

Radjendirane, V., Bhat, M. A. & Vaidyanathan, C. S. 1991. Affinity purification and characterization of 2,4-dichlorophenol hydroxylase from Pseudomonas cepacia. *Archives of Biochemistry and Biophysics,* 288**,** 169-176.

Rahman, M. F., Jasim, S. Y., Yanful, E. K., Ndiongue, S. & Borikar, D. 2010a. Advanced Oxidation Treatment of Drinking Water: Part II. Turbidity, Particles and Organics Removal from Lake Huron Water. *Ozone: Science & Engineering,* 32**,** 295-304.

Rahman, M. F., Yanful, E. K., Jasim, S. Y., Bragg, L. M., Servos, M. R., Ndiongue, S. & Borikar, D. 2010b. Advanced Oxidation Treatment of Drinking Water: Part I. Occurrence and Removal of Pharmaceuticals and Endocrine-Disrupting Compounds from Lake Huron Water. *Ozone: Science & Engineering,* 32**,** 217-229.

Rajeswari, R. & Kanmani, S. 2009. A study on synergistic effect of photocatalytic ozonation for carbaryl degradation. *Desalination,* 242**,** 277-285.

Rawal, S., Chakraboty, A. & Lee, W. 2009. Heterojunction of FeOOH and TiO[2] for the Formation of Visible Light Photocatalyst. *Bulletin of the Korean Chemical Society,* 30**,** 4.

Razavi, B., Song, W., Santoke, H. & Cooper, W. J. 2011. Treatment of statin compounds by advanced oxidation processes: Kinetic considerations and destruction mechanisms. *Radiation Physics and Chemistry,* 80**,** 453-461.

Ren, H., Zhan, Y., Fang, X. & Yu, D. 2014. Enhanced catalytic activity and thermal stability of 2,4-dichlorophenol hydroxylase by using microwave irradiation and imidazolium ionic liquid for 2,4-dichlorophenol removal. *RSC Advances,* 4**,** 62631-62638.

Rivera-Utrilla, J., Sánchez-Polo, M., Méndez-Díaz, J. D., Ferro-García, M. A. & Bautista-Toledo, M. I. 2008. Behavior of two different constituents of natural organic matter in the removal of sodium dodecylbenzenesulfonate by O3 and O3-based advanced oxidation processes. *Journal of Colloid and Interface Science,* 325**,** 432-439.

Rodriguez-Mozaz, S., De Alda, M. J. L. & Barceló, D. 2004. Monitoring of estrogens, pesticides and bisphenol A in natural waters and drinking water treatment plants by solid-phase extraction–liquid chromatography–mass spectrometry. *Journal of Chromatography A,* 1045**,** 85-92.

Rosal, R., Rodríguez, A., Gonzalo, M. S. & García-Calvo, E. 2008. Catalytic ozonation of naproxen and carbamazepine on titanium dioxide. *Applied Catalysis B: Environmental,* 84**,** 48-57.

Rosenfeldt, E. J., Chen, P. J., Kullman, S. & Linden, K. G. 2007. Destruction of estrogenic activity in water using UV advanced oxidation. *Science of The Total Environment,* 377**,** 105-113.

Ruppert, G., Bauer, R. & Heisler, G. 1994. UV-O3, UV-H2O2, UV-TiO2 and the photo-Fenton reaction - comparison of advanced oxidation processes for wastewater treatment. *Chemosphere,* 28**,** 1447-1454.

Sadik, W. A., Sadek, O. M. & El-Demerdash, A. M. 2004. The Use of Heterogeneous Advanced Oxidation Processes to Degrade Neutral Red Dye in Aqueous Solution. *Polymer-Plastics Technology and Engineering,* 43**,** 1675-1686.

Sánchez-Polo, M., Rivera-Utrilla, J., Méndez-Díaz, J. D., Canonica, S. & Von Gunten, U. 2007. Photooxidation of naphthalenesulfonic acids: Comparison between processes based on O3, O3/activated carbon and UV/H2O2. *Chemosphere,* 68**,** 1814-1820.

Sánchez-Polo, M., Salhi, E., Rivera-Utrilla, J. & Von Gunten, U. 2006. Combination of Ozone with Activated Carbon as an Alternative to Conventional Advanced Oxidation Processes. *Ozone: Science & Engineering,* 28**,** 237-245.

Sánchez-Polo, M., Von Gunten, U. & Rivera-Utrilla, J. 2005. Efficiency of activated carbon to transform ozone into OH radicals: Influence of operational parameters. *Water Research,* 39**,** 3189-3198.

Saritha, P., Aparna, C., Himabindu, V. & Anjaneyulu, Y. 2007. Comparison of various advanced oxidation processes for the degradation of 4-chloro-2 nitrophenol. *Journal of Hazardous Materials,* 149**,** 609-614.

Sauer, T. P., Casaril, L., Oberziner, A. L. B., José, H. J. & Moreira, R. D. F. P. M. 2006. Advanced oxidation processes applied to tannery wastewater containing Direct Black 38--Elimination and degradation kinetics. *Journal of Hazardous Materials,* 135**,** 274-279.

Sauleda, R. & Brillas, E. 2001. Mineralization of aniline and 4-chlorophenol in acidic solution by ozonation catalyzed with Fe 2+ and UVA light. *Applied Catalysis B: Environmental,* 29**,** 135-145.

Schröder, H. F. & Meesters, R. J. W. 2005. Stability of fluorinated surfactants in advanced oxidation processes--A follow up of degradation products using flow injection-mass spectrometry, liquid chromatography-mass spectrometry and liquid chromatography-multiple stage mass spectrometry. *Journal of Chromatography, A,* 1082**,** 110-119.

Scow, K. & Et Al. 1982. *EXPOSURE AND RISK ASSESSMENT FOR CHLORINATED PHENOLS: 2-CHLOROPHENOL, 2,4-DICHLOROPHENOL, 2,4,6-TRICHLOROPHENOL*, U.S. EPA OFFICE OF WATER REGULATIONS AND STANDARDS, WASHINGTON, D.C. 1982.

Shehata, M., Durner, J., Thiessen, D., Shirin, M., Lottner, S., Van Landuyt, K., Furche, S., Hickel, R. & Reichl, F. X. 2012. Induction of DNA double-strand breaks by monochlorophenol isomers and ChKM in human gingival fibroblasts. *Archives of Toxicology,* 86**,** 1423-1429.

Shemer, H. & Narkis, N. 2005. Trihalomethanes aqueous solutions sono-oxidation. *Water Research,* 39**,** 2704-2710.

Skoumal, M., Cabot, P. L., Centellas, F., Arias, C., Rodríguez, R. M. & Garrido, J. A. 2006. Mineralization of paracetamol by ozonation catalyzed with Fe^{2+}, Cu^{2+} and UVA light. *Applied Catalysis B: Environmental,* 66**,** 228-240.

Smith, B. J., Tho, N. M., Bouma, W. J. & Radom, L. 1991. Unimolecular rearrangements connecting hydroxyethylidene (CH3-C-OH), acetaldehyde (CH3-CH: O), and vinyl alcohol (CH2: CH-OH). *Journal of the American Chemical Society,* 113**,** 6452-6458.

Spanggord, R. J. & Mcclurg, V. J. 1978. Ozone Methods and Ozone- Chemistry of Selected Organics in Water. *In:* RICE, R. G. & COTRUVO, J. A. (eds.) *Ozone/Chlorine Dioxide Oxidation Products of Organic Materials.* Cleveland: Intl. Ozone Assoc.

Stackelberg, P. E., Gibbs, J., Furlong, E. T., Meyer, M. T., Zangg, S. D. & Lippincott, R. L. 2007. Efficiency of conventional drinking water treatment process in the removal of pharmarceuticals and other organic compounds. *Science of the Total Environment,* 377**,** 255-272.

Staehelin, J. & Hoigne, J. 1982. Decomposition of ozone in water: rate of initiation by hydroxide ions and hydrogen peroxide. *Environmental Science & Technology,* 16**,** 676-681.

Stone, A. T. 1987. Reductive Dissolution of Manganese(III/Iv) Oxides by Substituted Phenols. *Environmental Science & Technology,* 21**,** 979-988.

Stumm, W. & Morgan, J. 1981. *Aquatic Chemistry,* New york, Wiley-Interscience.

Stumm, W. & Sulzberger, B. 1992. The cycling of iron in natural environments: Considerations based on laboratory studies of heterogeneous redox processes. *Geochimica et Cosmochimica Acta,* 56**,** 3233-3257.

Sun, J., Li, X., Feng, J. & Tian, X. 2009. Oxone/Co2+ oxidation as an advanced oxidation process: Comparison with traditional Fenton oxidation for treatment of landfill leachate. *Water Research,* 43**,** 4363-4369.

Sun, J.-H., Sun, S.-P., Fan, M.-H., Guo, H.-Q., Lee, Y.-F. & Sun, R.-X. 2008. Oxidative decomposition of p-nitroaniline in water by solar photo-Fenton advanced oxidation process. *Journal of Hazardous Materials,* 153**,** 187-193.

Sung, M. & Huang, C. P. 2007. Kinetics of the degradation of 2-chlorophenol by ozonation at pH 3. *Journal of Hazardous Materials,* 141**,** 140-147.

Tambosi, J. L., De Sena, R. F., Gebhardt, W., Moreira, R. F. P. M., José, H. J. & Schröder, H. F. 2009. Physicochemical and Advanced Oxidation Processes – A Comparison of Elimination Results of Antibiotic Compounds Following an MBR Treatment. *Ozone: Science & Engineering,* 31**,** 428-435.

Tanaka, K., Abe, K. & Hisanaga, T. 1996. Photocatalytic water treatment on immobilized TiO2 combined with ozonation. *Journal of Photochemistry and Photobiology A: Chemistry,* 101**,** 85-87.

Tanaka, K., Padermpole, K. & Hisanaga, T. 2000. Photocatalytic degradation of commercial azo dyes. *Water Research,* 34**,** 327-333.

Teh, C. M. & Mohamed, A. R. 2011. Roles of titanium dioxide and ion-doped titanium dioxide on photocatalytic degradation of organic pollutants (phenolic compounds and dyes) in aqueous solutions: A review. *Journal of Alloys and Compounds,* 509**,** 1648-1660.

Thiruvenkatachari, R., Kwon, T. O., Jun, J. C., Balaji, S., Matheswaran, M. & Moon, I. S. 2007. Application of several advanced oxidation processes for the destruction of terephthalic acid (TPA). *Journal of Hazardous Materials,* 142**,** 308-314.

Turecek, F. & Cramer, C. J. 1995. Thermochemistry of simple enols and enol cation radicals revisited. A G2 (MP2) ab initio study. *Journal of the American Chemical Society,* 117**,** 12243-12253.

Turecek, F., Drinkwater, D. E., Maquestiau, A. & Mclafferty, F. W. 1989. Neutralization-reionization study of C6H6O isomers. *Organic mass spectrometry,* 24**,** 669-672.

Usepa. 2016. Toxic and Priority Pollutants Under the Clean Water Act. Available: https://http://www.epa.gov/eg/toxic-and-priority-pollutants-under-clean-water-act - priority [Accessed 04/07/2016].

Vértes, A. & Czakó-Nagy, I. 1989. Mössbauer spectroscopy and its application to corrosion studies. *Electrochimica Acta,* 34**,** 721-758.

Villaseñor, J., Reyes, P. & Pecchi, G. 2002. Catalytic and photocatalytic ozonation of phenol on MnO 2 supported catalysts. *Catalysis Today,* 76**,** 121-131.

Vogelpohl, A. 2007. Applications of AOPs in wastewater treatment. *Water Science and Technology,* 55**,** 207-211.

Walling, C. 1975. Fenton's reagent revisited. *Accounts of Chemical Research,* 8**,** 125-131.

Wang, C., Shi, H., Adams, C. D., Gamagedara, S., Stayton, I., Timmons, T. & Ma, Y. 2011. Investigation of pharmaceuticals in Missouri natural and drinking waer using high performance liquid chromatography-tandem mass spectrometry. *Water Research,* 45**,** 1818-1828.

Wang, D., Bolton, J. R. & Hofmann, R. 2012. Medium pressure UV combined with chlorine advanced oxidation for trichloroethylene destruction in a model water. *Water Research,* 46**,** 4677-4686.

Wang, H., Xiang, X., Li, F., Evans, D. G. & Duan, X. 2009a. Investigation of the structure and surface characteristics of Cu-Ni-M(III) mixed oxides (M = Al, Cr and In) prepared from layered double hydroxide precursors. *Applied Surface Science,* 255**,** 6945-6952.

Wang, K., Guo, J., Yang, M., Junji, H. & Deng, R. 2009b. Decomposition of two haloacetic acids in water using UV radiation, ozone and advanced oxidation processes. *Journal of Hazardous Materials,* 162**,** 1243-1248.

Wang, Y., Shen, Z., Li, Y. & Niu, J. 2010a. Electrochemical properties of the erbium-chitosan-fluorine-modified PbO2 electrode for the degradation of 2,4-dichlorophenol in aqueous solution. *Chemosphere,* 79**,** 987-996.

Wang, Y., Shen, Z., Li, Y. & Niu, J. 2010b. Electrochemical properties of the erbium–chitosan–fluorine–modified PbO 2 electrode for the degradation of 2, 4-dichlorophenol in aqueous solution. *Chemosphere,* 79**,** 987-996.

Wang, Y., Wei, Y. & Liu, J. 2009c. Effect of H2O2 dosing strategy on sludge pretreatment by microwave-H2O2 advanced oxidation process. *Journal of Hazardous Materials,* 169**,** 680-684.

Waters 1996. Determination of EPA Method 604 Phenols by HPLC. *In:* UWE, N. D. (ed.). USA.

Wensing, M., Uhde, E. & Salthammer, T. 2005. Plastics additives in the indoor environment-flame retardants and plasticizers. *Science of The Total Environment.,* 339**,** 19-40.

Wikipedia. 2016. *List of waste-water treatment technologies* [Online]. Available: https://en.wikipedia.org/wiki/List_of_waste-water_treatment_technologies [Accessed 13th January 2017].

Wu, J. J., Wu, C.-C., Ma, H.-W. & Chang, C.-C. 2004. Treatment of landfill leachate by ozone-based advanced oxidation processes. *Chemosphere,* 54**,** 997-1003.

Xiang, Q., Yu, J. & Wong, P. K. 2011. Quantitative characterization of hydroxyl radicals produced by various photocatalysts. *Journal of Colloid and Interface Science,* 357**,** 163-167.

Xiao, M., Zhou, J., Tan, Y., Zhang, A., Xia, Y. & Ji, L. 2006. Treatment of highly-concentrated phenol wastewater with an extractive membrane reactor using silicone rubber. *Desalination,* 195**,** 281-293.

Xing, B., Mcgill, W. B., Dudas, M. J., Maham, Y. & Hepler, L. 1994. Sorption of phenol by selected biopolymers: isotherms, energetics, and polarity. *Environmental Science & Technology,* 28**,** 466-473.

Xu, L. & Wang, J. 2012. Fenton-like degradation of 2, 4-dichlorophenol using Fe 3 O 4 magnetic nanoparticles. *Applied Catalysis B: Environmental,* 123**,** 117-126.

Xu, X.-W., Xu, X.-H., Shi, H.-X. & Wang, D.-H. 2005. Study on US/O3 mechanism in p-chlorophenol decomposition. *Journal of Zhejiang University. Science. B,* 6**,** 553.

Xu, Y. & Schoonen, M. a. A. 2000. The absolute energy positions of conduction and valence bands of selected semiconducting materials. *American mineralogist,* 85**,** 543-556.

Yang, S., Wang, P., Yang, X., Wei, G., Zhang, W. & Shan, L. 2009. A novel advanced oxidation process to degrade organic pollutants in wastewater: Microwave-activated persulfate oxidation. *Journal of Environmental Sciences,* 21**,** 1175-1180.

Yasar, A., Ahmad, N., Latif, H. & Amanat Ali Khan, A. 2007. Pathogen Re-Growth in UASB Effluent Disinfected By UV, O3, H2O2, and Advanced Oxidation Processes. *Ozone: Science & Engineering,* 29**,** 485-492.

Yin, G., Jin, F., Yao, G. & Jing, Z. 2015. Hydrothermal Conversion of Catechol into Four-Carbon Dicarboxylic Acids. *Industrial & Engineering Chemistry Research,* 54**,** 68-75.

Yu, C., Zhao, P., Chen, G. & Hu, B. 2011. Al2O3 supported Ru catalysts prepared by thermolysis of Ru3(CO)12 for catalytic wet air oxidation. *Applied Surface Science,* 257**,** 7727-7731.

Yu, J., Taylor, K. E., Zou, H., Biswas, N. & Bewtra, J. K. 1994. Phenol Conversion and Dimeric Intermediates in Horseradish Peroxidase-Catalyzed Phenol Removal from Water. *Environmental Science & Technology,* 28**,** 2154-2160.

Zhan, Y., Li, H. & Chen, Y. 2010. Copper hydroxyphosphate as catalyst for the wet hydrogen peroxide oxidation of azo dyes. *Journal of Hazardous Materials,* 180**,** 481-485.

Zhang, J., Liu, D., Bian, W. & Chen, X. 2012. Degradation of 2, 4-dichorophenol by pulsed high voltage discharge in water. *Desalination,* 304**,** 49-56.

Zhao, H., Dong, Y., Jiang, P., Wang, G., Zhang, J. & Li, K. 2014. An insight into the kinetics and interface sensitivity for catalytic ozonation: the case of nano-sized NiFe 2 O 4. *Catalysis Science & Technology,* 4**,** 494-501.

Zhao, H., Dong, Y., Jiang, P., Wang, G., Zhang, J. & Zhang, C. 2015. ZnAl 2 O 4 as a novel high-surface-area ozonation catalyst: One-step green synthesis, catalytic performance and mechanism. *Chemical Engineering Journal,* 260**,** 623-630.

Zhao, L., Ma, J. & Sun, Z.-Z. 2008. Oxidation products and pathway of ceramic honeycomb-catalyzed ozonation for the degradation of nitrobenzene in aqueous solution. *Applied Catalysis B: Environmental,* 79**,** 244-253.

Zhou, S., Qian, Z., Sun, T., Xu, J. & Xia, C. 2011. Catalytic wet peroxide oxidation of phenol over Cu–Ni–Al hydrotalcite. *Applied Clay Science,* 53**,** 627-633.

Zhu, J., Chen, F., Zhang, J., Chen, H. & Anpo, M. 2006. Fe3+-TiO2 photocatalysts prepared by combining sol–gel method with hydrothermal treatment and their characterization. *Journal of Photochemistry and Photobiology A: Chemistry,* 180**,** 196-204.

7. APPENDIX

Appendix 7.A: Intermediates of phenol ozonation at varying pH as followed by LCMS t= 40 mins and t=60 mins

		Acidic pH (3)				Neutral pH (7)				Alkaline pH (10) [no pH control]				Constant alkaline pH (10)			
Time		RT	mass	Formula	%	RT	mass	Formula	%	RT	mass	Formula	%	RT	mass	Formula	%
40	1	12,797	72,02222	C3H4O2	79	4,457	140,01087	C6H4O4	87	3,127	112,98559	C4H2O4	56	3,221	113,99286	C4 H2 O4	67,51
	2	13,996	110,03721	C6H6O2	93	4,571	124,16090	C6H4O3	85	12,731	72,02158	C3H4O2	85	4,505	140,0116	C6 H4 O4	87,7
	3					4,575	142,02665	C6H6O4	87	14,002	110,03702	C6H6O2	95	4,513	112,01621	C5 H4 O3	87,39
	4					4,787	128,01090	C5H4O4	87	22,885	94,04234	C6H6O	83	4,559	178,04851	C6 H10 O6	80,92
	5					4,792	84,02170	C4H4O2	85					4,649	134,02194	C4 H6 O5	85,65
	6					7,980	176,03249	C6H8O6	86					4,658	72,02207	C3 H4 O2	81,01
	7					7,890	86,03757	C4H6O2	83					5,403	150,01648	C4 H6 O6	86,55
	8					7,891	132,04247	C5H8O4	87					5,479	176,03231	C6 H8 O6	84,61
	9					11,754	98,03714	C5H6O2	87					5,712	146,0216	C5 H6 O5	85,86
	10					11,754	142,02678	C6H6O4	87					5,718	192,02734	C6 H8 O7	83,78
	11					12,776	72,02241	C3H4O2	75					5,723	150,01658	C4 H6 O6	85,74
	12					12,777	116,01101	C4H4O4	87					5,726	88,0162	C3 H4 O3	87,24
	13					14,000	110,03742	C6H6O2	92					5,734	86,03706	C4 H6 O2	86,99
	14					14,918	164,06752	C9H8O3	86					7	96,02103	C5 H4 O2	86,62
	15													8,014	220,03688	C11 H8 O5	84,95
	16													8,425	114,03075	C5 H6 O3	81,23
	17													8,955	222,05231	C11 H10 O5	79,54
	18													9,334	132,0048	C4 H4 O5	80,57
	19													9,335	88,01547	C3 H4 O3	85,28
	20													12,491	138,03025	C7 H6 O3	72,29
	21													12,692	116,00924	C4 H4 O4	70,78
	22													12,694	72,02095	C3 H4 O2	86,69
	23													13,992	110,03554	C6 H6 O2	73,19
	24													20,798	110,03693	C6 H6 O2	86,45
	25													20,799	136,05273	C8 H8 O2	85,77
	26													22,883	96,02139	C5 H4 O2	87,07

	27														22,884	94,04245	C6 H6 O	82,16
	28														22,885	124,01618	C6 H4 O3	87,11
	29														23,041	186,06906	C12 H10 O2	80,64
60	1	4,234	88,01647	C3H4O3	86	4,23	88,01643	C3H4O3	86	4,233	C3H4O3	88,01653	85		3,247	113,99286	C4 H2 O4	67,33
	2	4,753	72,02213	C3H2O2	80	4,457	140,01108	C6H4O4	87	4,463	C6H4O4	140,01113	87		4,553	178,04862	C6 H10 O6	80,49
	3	5,412	101,99585	C3H2O4	85	4,51	128,01103	C5H4O4	87	4,559	C6H4O3	124,01612	86		4,657	134,02117	C4 H6 O5	85,51
	4	12,699	116,01110	C4H4O4	86	4,575	142,02659	C6H6O4	87	4,561	C6H6O4	142,02678	86		4,668	72,02162	C3 H4 O2	85,76
	5	12,704	72,02251	C3H4O2	85	4,757	72,02209	C3H3O2	81	4,691	C4H6O5	134,02163	87		4,751	210,03745	C6 H10 O8	83,7
	6	13,995	110,03725	C6H6O2	82	4,789	128,01112	C5H4O4	87	4,74	C3H4O2	72,02213	80		4,858	164,03167	C5 H8 O6	84,93
	7					4,793	84,02183	C4H4O2	84	4,789	C5H4O4	128,01124	87		4,931	158,02118	C6 H6 O5	84,59
	8					5,413	101,99556	C3H2O4	87	4,795	C4H4O2	84,02175	85		4,931	140,01051	C6 H4 O4	85,67
	9					7,968	86,03746	C4H6O2	84	5,393	C4H6O6	150,0167	86		5,008	210,0376	C6 H10 O8	95,23
	10					7,969	176,03236	C6H8O6	86	5,408	C3H2O4	101,99564	86		5,399	150,01618	C4 H6 O6	85,4
	11					7,972	132,04239	C5H8O4	87	5,72	C4H6O6	150,01675	86		5,465	180,02665	C5 H8 O7	84,98
	12					10,354	100,01606	C4H4O3	87	6,988	C5H4O2	96,02182	84		5,478	176,03171	C6 H8 O6	84,27
	13					12,732	116,01099	C4H4O4	87	10,306	C3H4O2	72,02255	74		5,714	146,02111	C5 H6 O5	85,53
	14					12,732	72,02243	C3H4O2	87	10,307	C4H4O3	100,01671	84		5,722	150,01627	C4 H6 O6	97,56
	15					13,998	110,03734	C6H6O2	93	11,744	C5H6O2	98,03762	82		5,725	88,01603	C3 H4 O3	87,48
	16					16,382	110,03682	C6H6O2	88	11,745	C6H6O4	142,02741	82		6,983	96,02104	C5 H4 O2	87,21
	17									12,677	C3H4O2	72,02266	83		8,415	114,03128	C5 H6 O3	86,44
	18									12,677	C4H4O4	116,01132	86		9,287	88,01632	C3 H4 O3	86,86
	19									13,991	C6H6O2	110,03756	90		9,288	132,00567	C4 H4 O5	86,5
	20									19,75	C6H6O2	110,03689	87		12,71	72,0224	C3 H4 O2	75,38
	21									22,882	C6H6O	94,04244	84		12,71	116,01101	C4 H4 O4	87,14
	22														22,887	94,04214	C6 H6 O	86,47

Mass spectrums obtained from extracted ion chromatograms (EICs) used for identification of phenol intermediates and breakdown products.

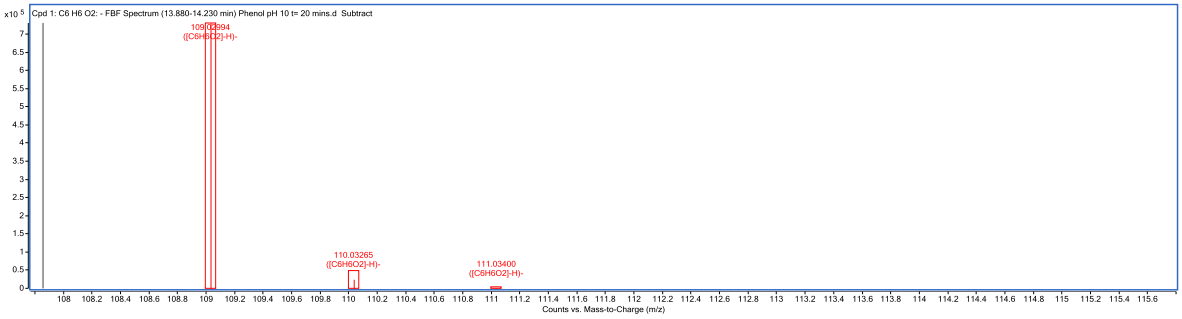

Appendix 7.B: EIC of Catechol $C_6H_6O_2$ produced upon ozonation of phenol

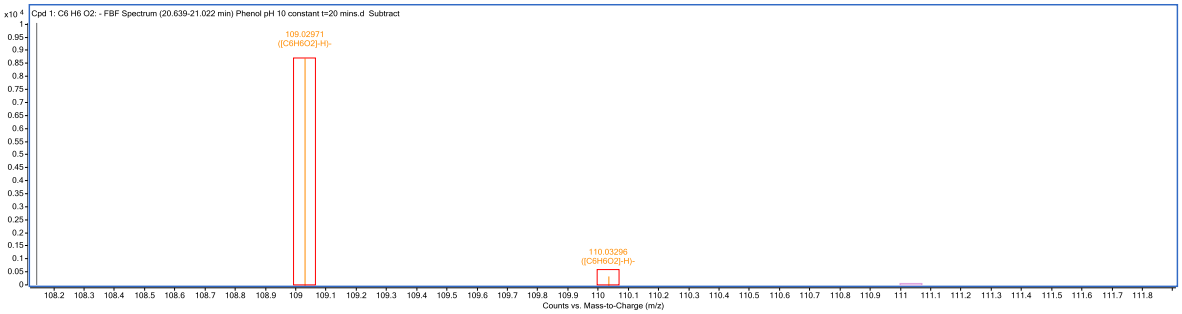

Appendix 7.C: EIC of isomer of Catechol $C_6H_6O_2$ produced upon ozonation of phenol

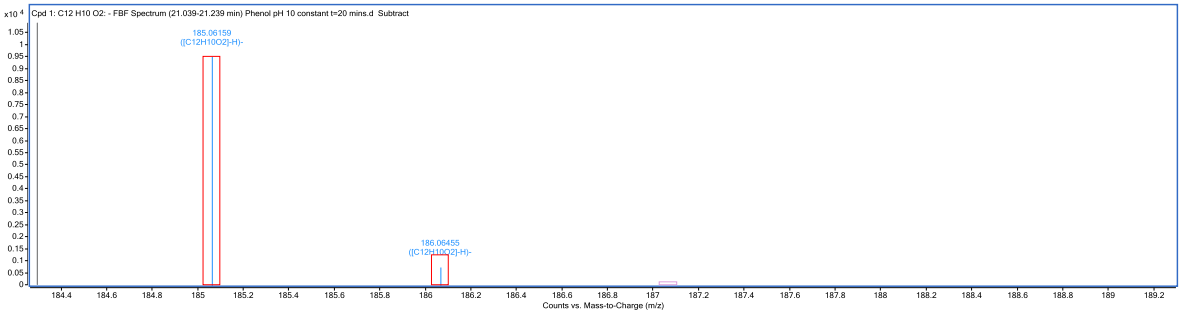

Appendix 7.D: EIC of one of two dimerised compounds of phenol ozonation in alkaline medium $C_{12}H_{10}O_2$

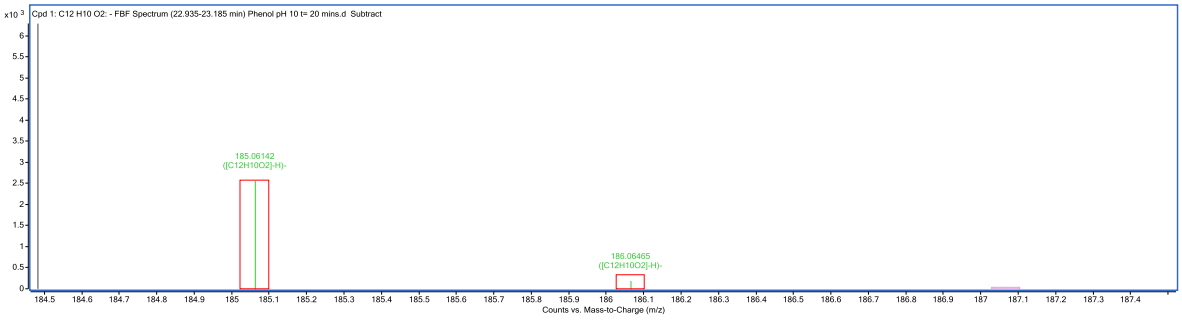

Appendix 7.E: EIC of second dimerization compound of phenol ozonation $C_{12}H_{10}O_2$

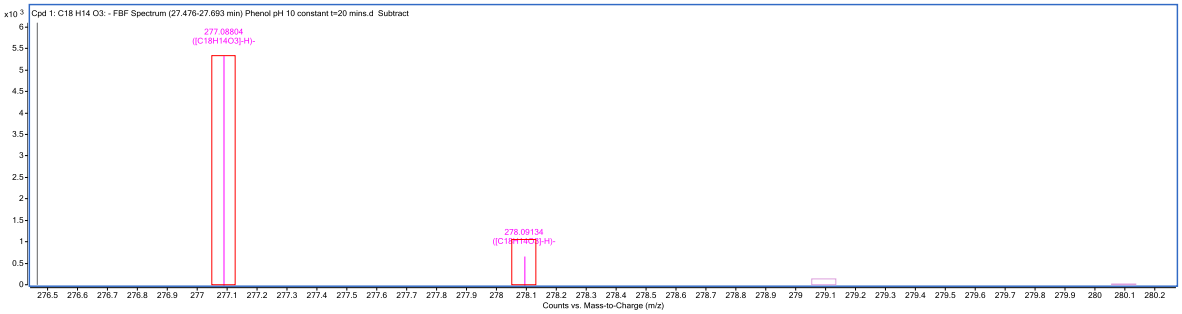

Appendix 7.F: EIC of trimer $C_{18}H_{14}O_3$ produced upon alkaline ozonation of phenol

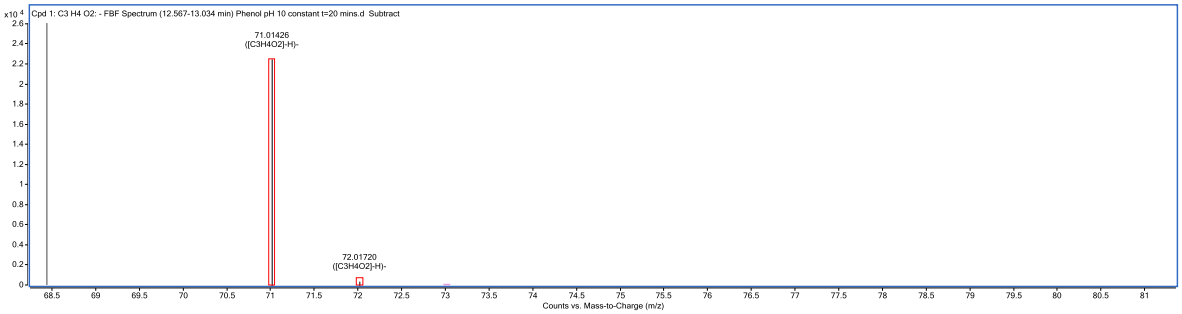

Appendix 7.G: EIC of acrylic acid $C_3H_4O_2$ (compound 21) produced upon ozonation of phenol

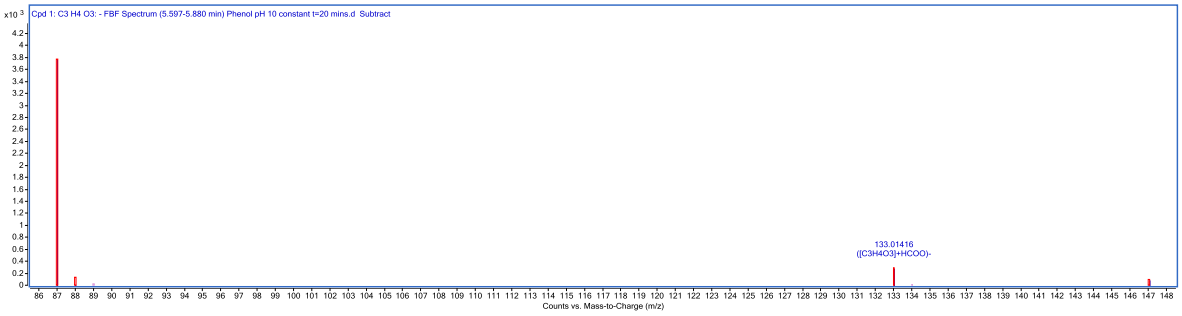

Appendix 7.H: EIC of pyruvic acid $C_3H_4O_3$ (compound 17) produced upon ozonation of phenol

Mass Spectrums (MFE) and extracted ion chromatograms (EIC) used for identification of 2-chlorophenol (2CP) intermediates and breakdown products.

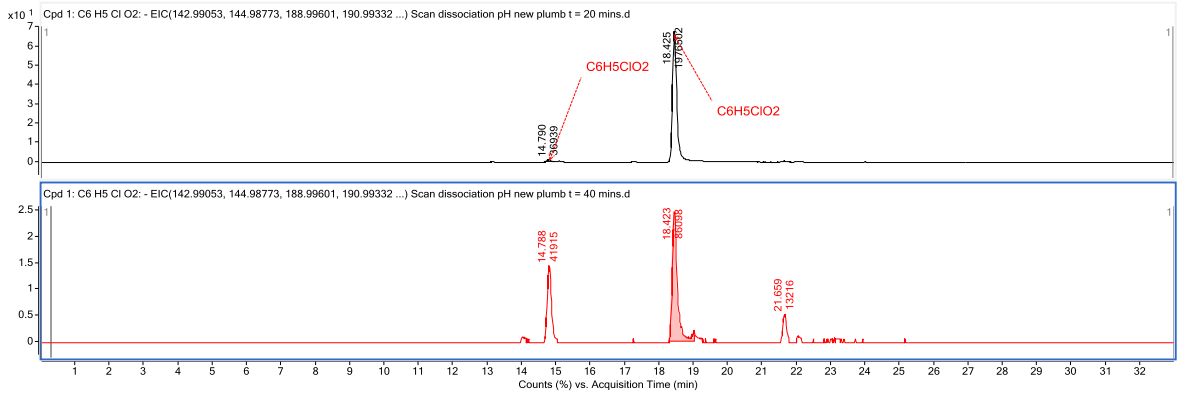

Appendix 7.I: Extracted chromatograms showing two hydroxylation products of 2CP ozonation $C_6H_5ClO_2$ presented as compound 43 and compound 44.

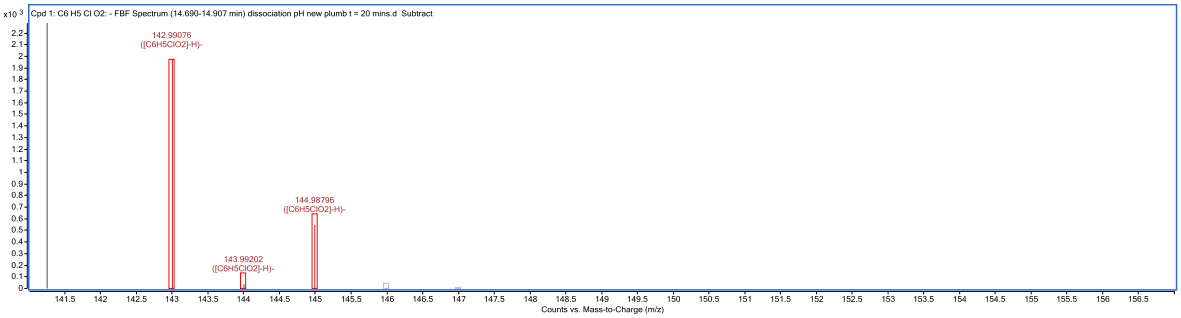

Appendix 7.J: Mass spectrum of first hydroxylation product of 2-chlorophenol $C_6H_5ClO_2$

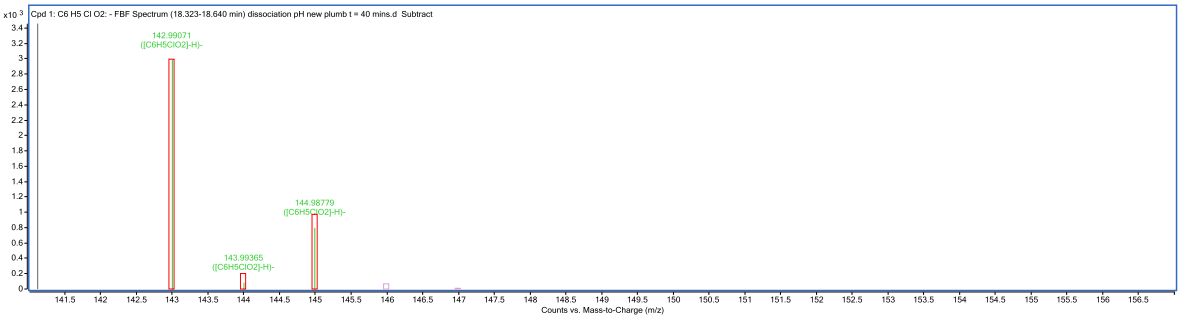

Appendix 7.K: Mass spectrum of second hydroxylation product of 2-chlorophenol ozonation $C_6H_5ClO_2$

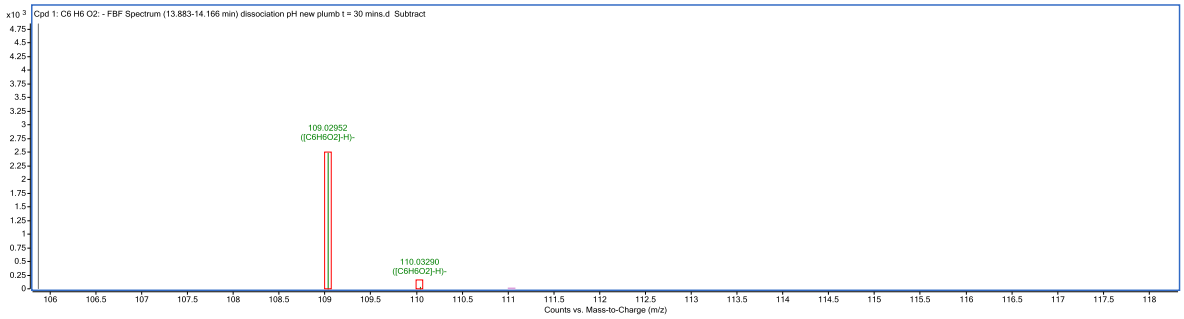

Appendix 7.L: Mass spectrum of catechol $C_6H_6O_2$ produced upon hydroxylation of 2-chlorophenol

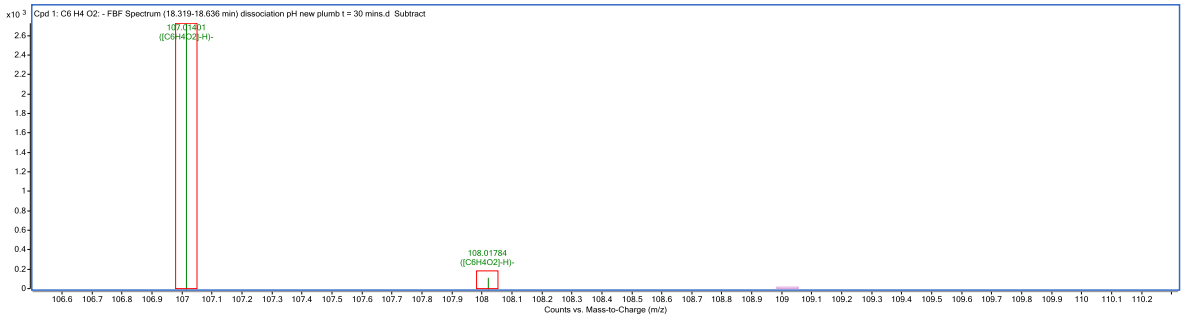

Appendix 7.M: Mass spectrum of quinone produced from catechol $C_6H_4O_2$

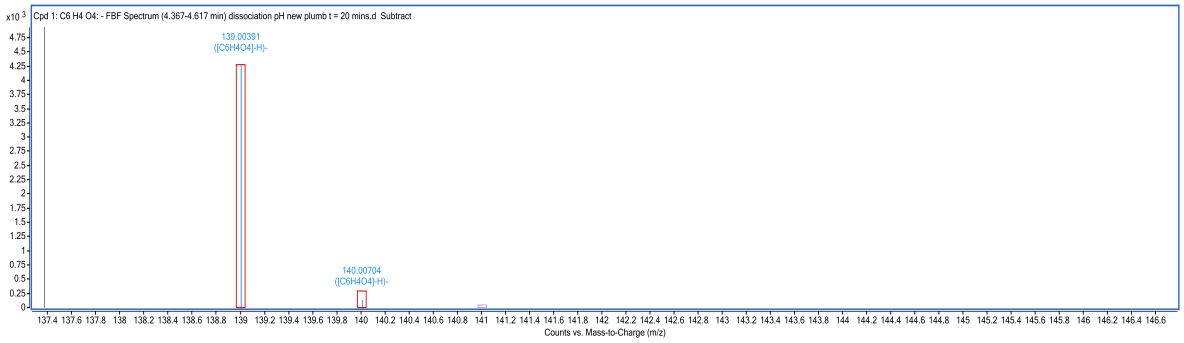

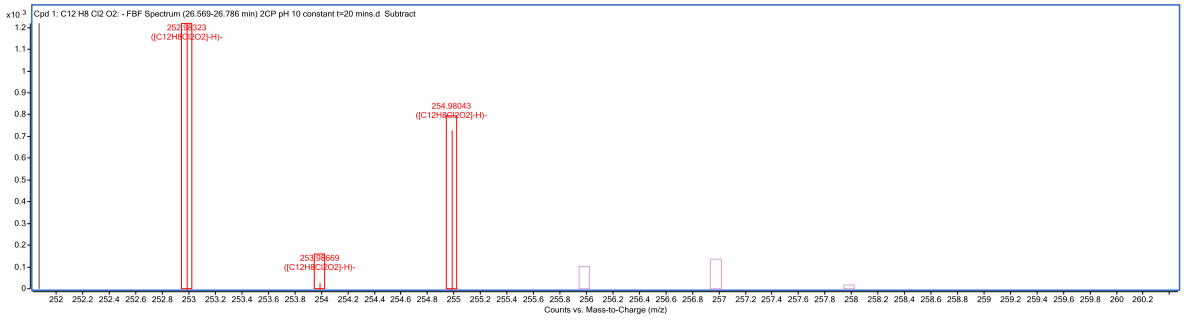

Appendix 7.N: Mass spectrum of dimerization compound of 2-chlorophenol $C_{12}H_8Cl_2O_2$

Mass Spectrums (MFE) and extracted ion chromatograms (EIC) used for identification of 4-chlorophenol (4CP) intermediates and breakdown products.

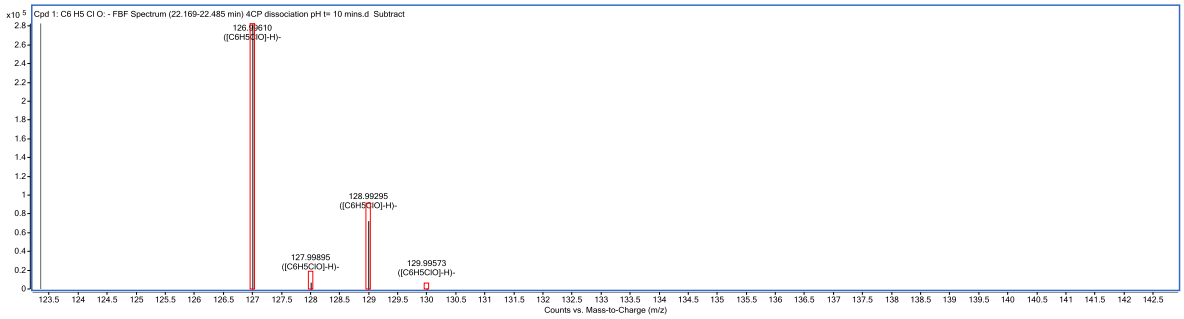

Appendix 7.O: Mass spectrum of 4-chlorophenol showing isotope distributions C_6H_5ClO

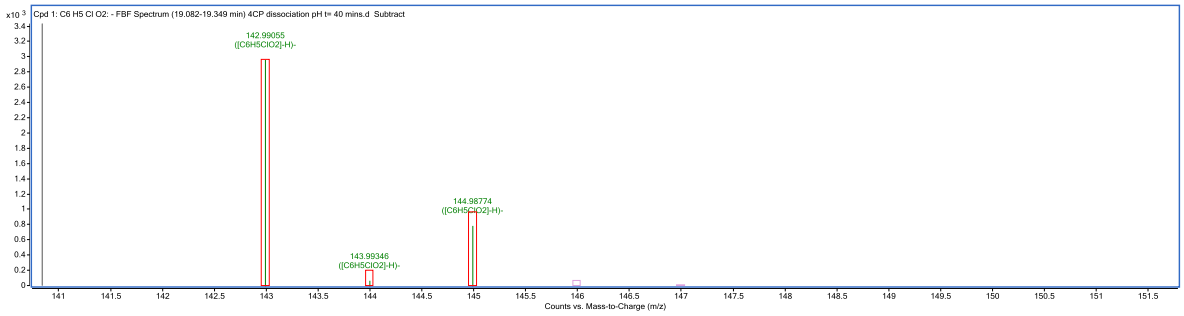

Appendix 7.P: Mass spectrum of single hydroxylation product of 4-chlorophenol ozonation $C_6H_5ClO_2$

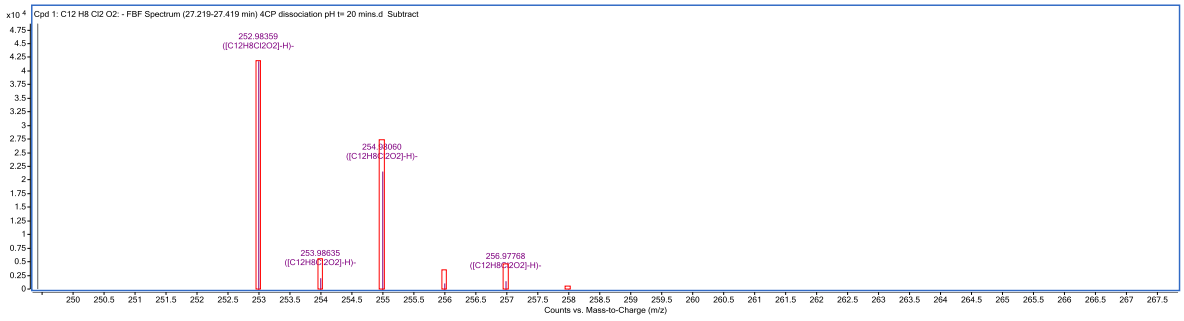

Appendix 7.Q: Mass spectrum of dimerised product of 4-chlorophenol ozonation $C_{12}H_8Cl_2O_2$

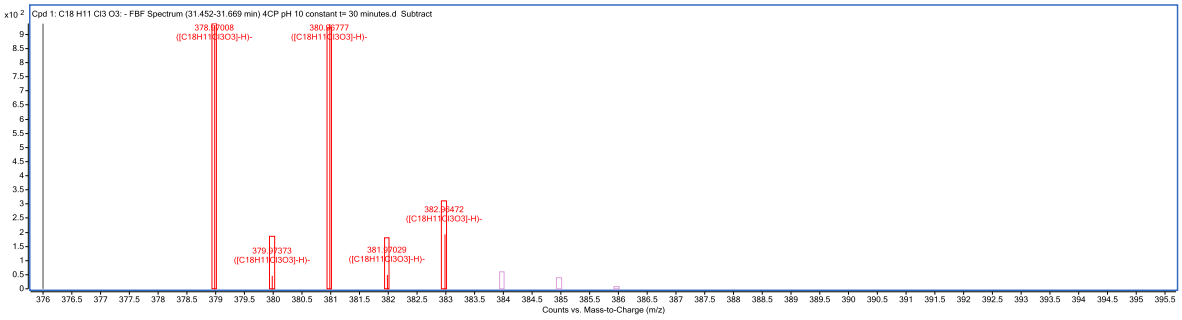

Appendix 7.R: Mass spectrum of trimerised product of 4-chlorophenol ozonation $C_{18}H_{11}Cl_3O_3$

Mass Spectrums (MFE) and extracted ion chromatograms (EIC) used for identification of 2,4-dichlorophenol (24DCP) intermediates and breakdown products.

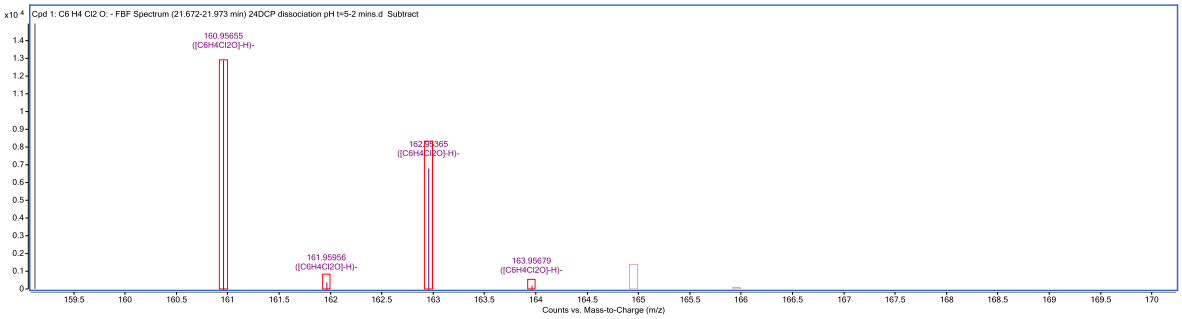

Appendix 7.S: Mass spectrum of 2,4-dichlorophenol showing isotope spacing used for identification $C_6H_4Cl_2O$

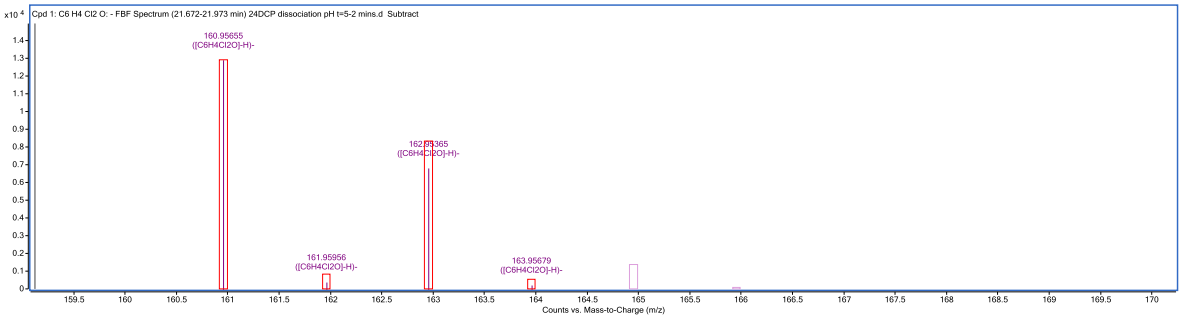

Appendix 7.T: Mass spectrum of hydroxylation product on ozonation of 2,4-dichlorophenol $C_6H_4Cl_2O_2$

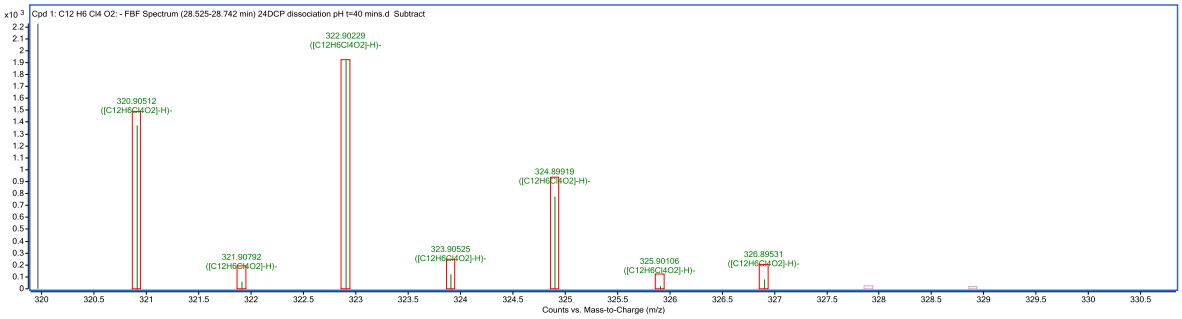

Appendix 7.U: Mass spectrum of first dimerization product of 2,4-dichlorophenol ozonation $C_{12}H_6Cl_4O_2$

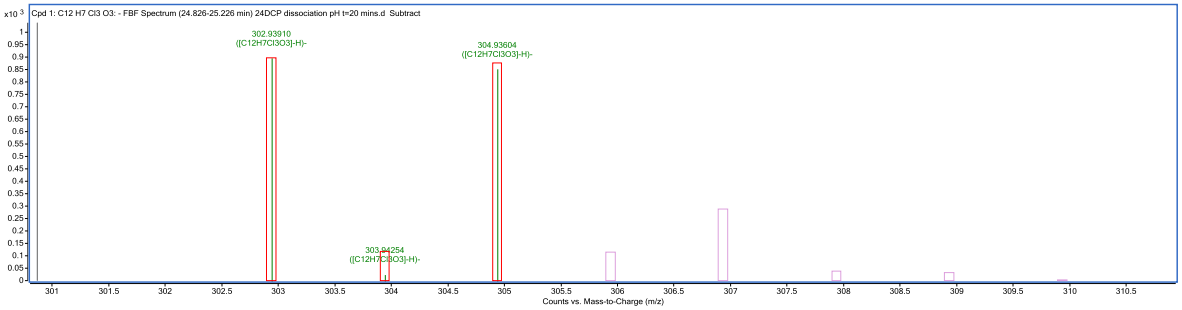

Appendix 7.V: Mass spectrum of second dimerization product of 2,4-dichlorophenol ozonation $C_{12}H_7Cl_3O_3$

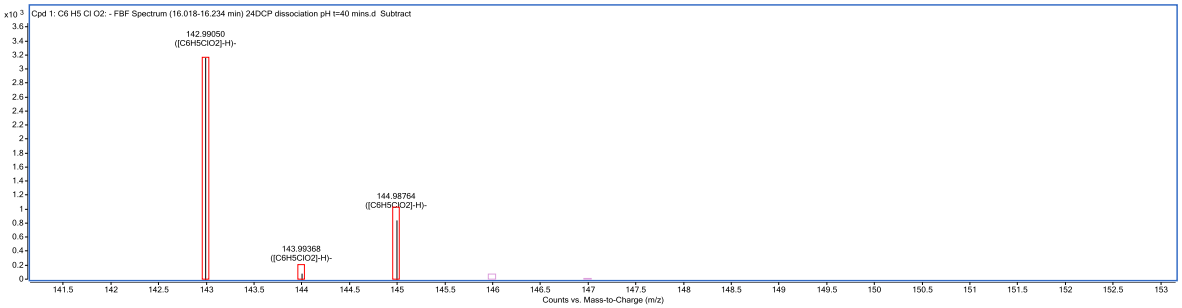

Appendix 7.W: Mass spectrum of dechlorination product of 2,4-dichlorophenol ozonation $C_6H_5ClO_2$